

Defining Peptide Structure with Metathesis

A thesis submitted for the
degree of Doctor of Philosophy

Krystle Chua Chia Hsien, B.Sc. (Hons.)



THE UNIVERSITY

of ADELAIDE

Department of Chemistry
The University of Adelaide
South Australia
January 2013

TABLE OF CONTENTS

ABSTRACT	iv
DECLARATION	vi
ACKNOWLEDGEMENT	vii
ABBREVIATIONS	viii
CHAPTER ONE: INTRODUCTION TO PEPTIDES AND METATHESIS	1
1.1 Importance of Peptide Conformation in Biology/Nature	2
1.1.1 Peptide and Protein Structure	2
1.1.2 Relationship Between Polypeptide Structure and Function	9
1.2 Conformational Manipulation by Olefin Metathesis	11
1.2.1 Ring Closing Metathesis (RCM)	14
1.2.2 Cross Metathesis (CM)	16
1.2.3 Ring Opening Polymerization Metathesis (ROMP)	16
1.3 Overview of Thesis	17
1.4 References for Chapter One	19
CHAPTER TWO: DESIGN AND SYNTHESIS OF PROTEASE INHIBITORS	22
2.1 Introduction: Protease conformation and Inhibitor Design	23
2.1.1 Overview and Classification of Proteases	23
2.1.2 Cysteine and Serine Proteases	23
2.1.3 Current Design of Inhibitors of Cysteine and Serine Proteases	33
2.2 Improved Inhibitor Design for Cysteine and Serine Protease	36
2.2.1 Importance of β -Strand Conformation	36
2.2.2 Importance of the Macrocyclic for Conformational Constraint	38
2.2.3 Methods for Introducing Conformation Restriction	39
2.3 Design and Synthesis of Macrocyclic Protease Inhibitors	41
2.3.1 Molecular Modelling of Macrocyclic Protease Inhibitors	44
2.3.2 Synthesis of 2 nd Generation Macrocycles by Ring Closing Metathesis (RCM)	49
2.3.2.1 Preparation of P ₁ -P ₃ Macrocyclic Protease Inhibitors	60
2.3.2.2 Preparation of P ₂ -P ₄ Macrocyclic Protease Inhibitors	62
2.3.3 Synthesis of 2 nd Generation P ₁ -P ₃ Macrocycles by Huisgen 1,3-Dipolar Cycloaddition	64

2.4	Design and Synthesis of Acyclic Protease Inhibitors	72
2.4.1	Synthesis of P ₁ -P ₃ Acyclic Protease Inhibitors	74
2.4.2	Synthesis of P ₁ -P ₄ Acyclic Protease Inhibitors	75
2.5	Conclusions and Future Directions	76
2.6	References for Chapter Two	78
 CHAPTER THREE: ENZYME ASSAYS AND RESULTS		86
3.1	Introduction: Protease Inhibition Assays	87
3.2	Assay Protocols for Cysteine and Serine Proteases	87
3.2.1	Calpain Inhibition Assay: BODIPY-Casein Fluorescence	87
3.2.2	α -Chymotrypsin Assay	94
3.2.3	Cathepsin L, Cathepsin S, Human Leukocyte Elastase and Bovine Trypsin Assays	96
3.3	Inhibitor Structure-Activity Relationship	96
3.3.1	Structure-Activity of Peptidyl Macrocyclic Alcohols and Aldehydes Against Cysteine Proteases	97
3.3.1.1	Calpain	97
3.3.1.2	Cathepsin L and Cathepsin S	105
3.3.1.3	Inhibitor Selectivity Within the Cysteine Protease Family	108
3.3.2	Structure-Activity of Peptidyl Macrocyclic Alcohols and Aldehydes Against Serine Proteases	110
3.3.2.1	α -Chymotrypsin	110
3.3.2.2	Human Leukocyte Elastase (HLE)	113
3.3.1.3	Inhibitor Selectivity within the Serine Protease Family	115
3.3.3	Summary: Structure-Activity Relationship for Cysteine and Serine Protease Inhibition	117
3.4	Conclusions	119
3.5	References for Chapter Three	121
 CHAPTER FOUR: NEW GELATIN-BASED MATERIALS BY RING OPENING POLYMERIZATION METATHESIS (ROMP)		123
4.1	Introduction	124
4.1.1	Ruthenium-catalyzed Aqueous Olefin Metathesis	124
4.1.2	Hydrogels in Biomedical Applications	125
4.1.3	The Extracellular Matrix	128
4.1.4	Objectives	135
4.2	Synthesis and Characterization of Gelatin Hybrid Materials	136
4.2.1	Investigation of Ideal Reaction Conditions for Aqueous Metathesis	136

4.2.2	Validation of Crosslinking between Gel-GMA and NBE-OH	142
4.2.3	Effect of NBE-OH Concentration on Polymer Gel Characteristics	143
4.2.4	Mechanistic Studies of Aqueous Metathesis Reactions using PEGMA	145
4.2.5	Attempted Polymer Gel Film Formation	148
4.3	Conclusion and Future Directions	150
4.4	References for Chapter Four	152
CHAPTER FIVE: EXPERIMENTAL PROCEDURES		157
5.1	General Methods and Procedures	158
5.1.1	General Practice	158
5.1.2	General Procedures	163
5.2	Experimental Work Described in Chapter Two	168
5.3	Experimental Work Described in Chapter Three	230
5.4	Experimental Work Described in Chapter Four	234
5.5	References for Chapter Five	240
APPENDIX		242
A1	Raw Data for Molecular Modelling	243
A2	Raw Assay Data and IC ₅₀ Calculation Example for Calpain Assay	244
A3	Raw Assay Data and K _i Calculation Example for α-Chymotrypsin Assay	249
A4	Percentage Inhibition of Alcohols Synthesized in Chapter 2	254
A5	Enzyme Assays Data	257

ABSTRACT

Understanding protein structure and function is central for the development of therapeutics for the treatment of diseases and also novel biocompatible materials. Herein describes studies on the control of peptide structure and function through synthetic modifications, for the synthesis of novel enzyme inhibitors and biomaterials, primarily using olefin metathesis chemistry. Metathesis is chosen for the manipulation of peptide structure in order to induce conformational constraint in novel macrocyclic peptidomimetic inhibitors and to develop novel hydrogel matrices, which are of importance in the advancement of the pharmaceutical and medical industries.

The realization that enzymes bind their substrates in an extended β -stranded conformation has led to the development of inhibitors that mimic this bioactive conformation. The controlled organization of secondary structures in peptides by conformational constraint has been utilized to design two novel series of macrocyclic inhibitors, which are constrained by the P₁ and P₃ residues or the P₂ and P₄ residues using ring closing metathesis (RCM). These inhibitors contain a pyrrole group in the peptide backbone, thereby decreasing the peptidic nature of these inhibitors minimising susceptibility to proteolysis, while maintaining the appropriate geometry for inhibitor binding. The corresponding P₁-P₃ and P₁-P₄ acyclic inhibitors are designed and synthesized to provide an insight into the importance of cyclisation on the potency of inhibition against serine and cysteine protease.

The macrocyclic and acyclic inhibitors synthesized are assayed against a series of cysteine (calpain and cathepsin) and serine proteases (α -chymotrypsin, human leukocyte elastase and trypsin). These enzyme assays analyse the efficacy of the inhibitors against the enzymes tested. The potency of the inhibitors against the aforementioned proteases provides an insight into the effect of cyclisation, ring size and introduction of aryl groups into the ring system, as well as trends in selectivity between proteases of the same family (calpain vs. cathepsin and α -chymotrypsin vs. HLE and trypsin) and between the cysteine and serine protease families.

The ability to mimic the natural environment of structural proteins in wound healing, has led to the development of biocompatible materials, such as hydrogels, through the manipulation of natural peptide structure. The controlled organization of the tertiary structure of naturally occurring peptides is investigated by aqueous metathesis in the synthesis of biocompatible hydrogels derived from gelatin. Novel gelatin-gels are obtained by reacting methacrylate-functionalized gelatin and norbornene dicarboxylic acid in the presence of a catalyst in aqueous media. Optimisation of the hydrogel formation is investigated by; i) varying catalyst utilised and ii) varying ratios of starting gelatin and norbornene dicarboxylic acid. These polymer gels exhibited physical and chemical properties that might be useful in regenerative medicine. Mechanistic studies using MALDI is also performed to provide an insight into the mode of hydrogel formation.

DECLARATION

This work contains no material which has been accepted for the award of any other degree or diploma in any university or other tertiary institution and to the best of my knowledge and belief, contains no material previously published or written by another person, except where due reference has been made in the text.

I give consent to this copy of my thesis, when deposited in the University Library, being made available for loan and photocopying, subject to the provisions of the Copyright Act 1968.

I also give permission for the digital version of my thesis to be made available on the web, via the University's digital research repository, the Library catalogue, and also through web search engines, unless permission has been granted by the University to restrict access for a period of time.

.....
Krystle Chua Chia Hsien

.....
Date

ACKNOWLEDGEMENTS

First of all, I would like to thank my supervisor, Prof. Andrew Abell, for the opportunity to undertake a PhD under his guidance and supervision. I really appreciated the freedom to direct my own PhD. I would also like to thank my co-supervisor, Dr. Markus Pietsch, for his guidance in many aspects of my PhD.

Thank you to the many people who provided invaluable assistance throughout my PhD, especially: to the technical staff Philip Clements (NMR & MS), Gino Farese & Graham Bull (instrumentation); the members of the Abell Group; Dr. Daouda Traore and Prof. Matthew Wilce from Monash University for X-ray crystallography. I would like to express my many thanks and gratitude to Dr. Axel Neffe, Prof. Andreas Lendlein and Dr. Benjamin Pierce from the Helmholtz-Zentrum Geesthacht, as well as the members of the Neffe group for their guidance and hospitality during the three months in Germany. I would also like to thank Prof. Michael Gütschow from the University of Bonn for running the enzyme assays for my compounds.

To all my friends, who have gone through the many “ups and downs” throughout my postgraduate journey – thank you. Spending time with all of you have been a huge relieve to my sanity and made this journey a whole lot easier, with many things to look forward to. In particular, I would like to thank Catherine, my fellow PhD comrade; as well as Stephanie and Ivy, who have been there for me through all the complains and the toughest parts of my journey; and also, Monika, who brought lots of fun with our Arashi sessions ☺

To my family - my mother and father; my sister, Joanne and her husband, Robert – Thank you for being there for me constantly, providing support, encouragement and valuable advice throughout my life. I am eternally in dept to you and would not be where I am without your endless support.

And last, but most importantly, to Ondrej – thank you. You have been my greatest source of support. Thank you for your endless patience, love, support and encouragement. Without you, I would not have completed this journey. ♥

ABBREVIATIONS

δ	chemical shift (in NMR)
Å	angstrom
anh.	anhydrous
aq.	aqueous
bCT	bovine α -chymotrypsin
Boc	<i>tert</i> -butoxycarbonyl
BODIBY	4,4-difluoro-5,7-dimethyl-4-bora-3a,4-diaza- <i>s</i> -indacene-3-propionic acid (in assay)
CatL	cathepsin L
CatS	cathepsin S
COSY	H-H correlation spectroscopy
CM	cross metathesis
CM-ROMP	cross metathesis-ring opening metathesis polymerization
DBU	1,8-diazabicyclo[5.4.0]undec-7-ene
DCE	dichloroethane
DIEA	<i>N,N</i> -diisopropylethylamine
4-DMAP	4- <i>N,N</i> -dimethylaminopyridine
DMF	<i>N,N</i> -dimethylformamide
DMSO	dimethyl sulfoxide
ECM	extracellular matrix
EDCI	1-[3-(dimethylamino)propyl]-3-carbodiimide hydrochloride
EDTA	ethylenediaminetetraacetic acid (in assay)
EGTA	ethylene glycol tetraacetic acid (in assay)
EI	electron impact ionization (in mass spectrometry)
equiv	equivalent(s)
ESI	electrospray ionization (in mass spectrometry)
EtOAc	ethyl acetate
Et ₂ O	diethyl ether

gel-GMA	methacrylate-functionalized gelatin
GMA	glycidyl methacrylate
Grubbs 1 st Generation Catalyst (GI)	benzylidene-bis(tricyclohexylphosphine)dichlororuthenium
Grubbs 2 nd Generation Catalyst (GII)	benzylidene[1,3-bis(2,4,6-trimethylphenyl)-2-imidazolidinylidene]dichloro(tricyclohexylphosphine)ruthenium
h	hour(s)
HATU	<i>N,N,N',N'</i> -tetramethyl-O-(7-azabenzotriazol-1-yl)uronium hexafluorophosphate
HLE	human leukocyte elastase
HOBt	1-hydroxybenzotriazole
Hoveyda-Grubbs 1 st Generation Catalyst	dichloro(<i>o</i> -isopropoxyphenylmethylene)(tricyclohexylphosphine)ruthenium(II)
Hoveyda-Grubbs 2 nd Generation Catalyst	(1,3-bis-(2,4,6-trimethylphenyl)-2-imidazolidinylidene)dichloro(<i>o</i> -isopropoxyphenylmethylene)ruthenium
rp-HPLC	reversed phased high performance liquid chromatography
HRMS	high resolution mass spectrometry
Hz	hertz (in NMR)
IC ₅₀	half maximal inhibitory constant
IR	infrared
<i>J</i>	coupling constant (in NMR)
<i>K_i</i>	inhibitor disassociation constant
kDa	kilodalton
LRMS	low resolution mass spectrometry
MALDI	matrix-assisted laser desorption/ionization
MeOH	methanol
min	minute(s)
MOPS	3-(<i>N</i> -morpholino)propanesulfonic acid (in assay)
m.p.	melting point
NaAsc	sodium ascorbate
NBE-OH	norbornene dicarboxylic acid
NMR	nuclear magnetic resonance
o-CAPN1	ovine calpain 1 (μ-calpain)

o-CAPN2	ovine calpain 2 (m-calpain)
PEGMA	polyethylene glycol methacrylate
Pet. ether	petroleum ether (50-70 °C)
Pd/C	palladium on carbon catalyst
ppm	parts per million
rCAPN1	rat calpain 1 (μ -calpain)
rCAPN2	rat calpain 2 (m-calpain)
RCM	ring closing metathesis
ROCM	ring opening cross metathesis
ROMP	ring opening metathesis polymerization
rt	room temperature
SOCl ₂	thionyl chloride
SO ₃ Py	sulfur trioxide-pyridine complex
T _c	helix-to-coil transition temperature
T _m	crystalline melting temperature
<i>t</i> -BuOH	<i>tert</i> -butanol
TBAI	tetrabutylammonium iodide
TFA	trifluoroacetic acid
TGA	thermal gravimetric analysis
THF	tetrahydrofuran
TLC	thin layer chromatography
TMDSC	temperature modulated differential scanning calorimetry
TMS	trimethylsilyl
TNBS	trinitrobenzene sulfonate (colorimetric assay)
TRIS	tris(hydroxymethyl)aminomethane
Yb(OTf) ₃	ytterbium triflate

CHAPTER ONE:
Introduction to
Peptides and Metathesis

1.1 Importance of Peptide Conformation in Biology/Nature

Peptides and proteins are versatile macromolecules that play a crucial role in many biological processes. They are an essential part of life forming the building blocks that give rise to the structure and function of biological entities.^{1,2} A typical mammalian cell contains as many as 10,000 different proteins having a diverse array of functions, including binding, catalysis, operating as molecular switches; and serving as structural components of cells and organisms.³

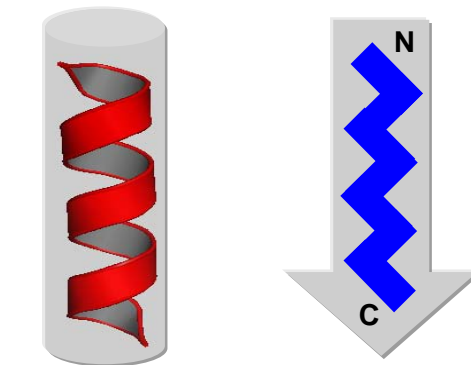
1.1.1 Peptide and Protein Structure

The function of a protein is governed by its amino acid composition and structural organisation.¹⁻³ There are four levels of protein structure: primary, secondary, tertiary and quaternary structure. The *primary structure* (Figure 1.1a) is defined as the linear sequence of amino acids in a protein that is directly determined by the sequence of nucleotides in the genome. The sequence of amino acids within the primary structure determines how the protein folds to form higher-level secondary structures. The *secondary structure* (Figure 1.1b) can take the form of either alpha helices or beta sheets, as defined by hydrogen-bonding interactions between the polypeptide backbone N-H and C=O groups. *Tertiary structure* (Figure 1.1c) refers to the overall three-dimensional shape of the protein resulting from the folding of secondary structure elements (alpha helices and/or beta sheets) linked by loops that have no secondary structure. The *quaternary structure* (Figure 1.1d) of a protein is the further association of two or more folded polypeptides to give rise to a functional unit. The tertiary and quaternary structures are stabilised by various types of amino acid side chain interactions, including hydrophobic interactions, hydrogen bonding, ionic bonding and covalent disulfide bonds (Figure 1.2).⁴⁻⁶

(a) Primary Structure



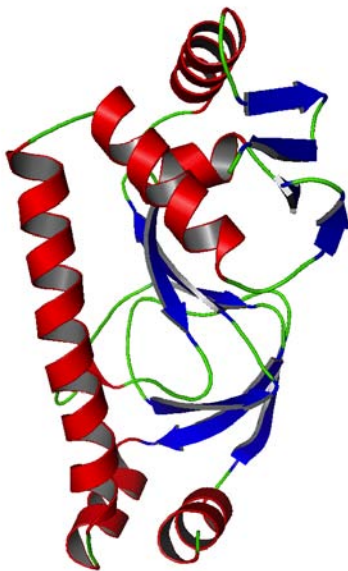
(b) Secondary Structure



alpha helices

beta strands

(c) Tertiary Structure



(d) Quaternary Structure

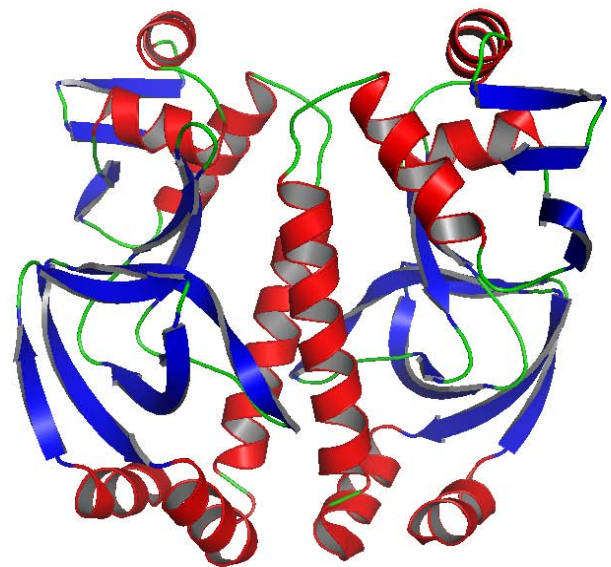


Figure 1.1 Levels of protein structures: (a) Primary structure: the amino acid sequence of a protein; (b) Secondary structure: stabilization of peptide backbones by hydrogen bonds forming alpha helices and beta sheets; (c) Tertiary structure: the overall 3-D structure of the folded polypeptide chains (PDB 2CGP); (d) Quaternary structure: the assembly of two or more polypeptides into a functional unit (PDB 1CGP). Adapted from Petsko and Ringe.³

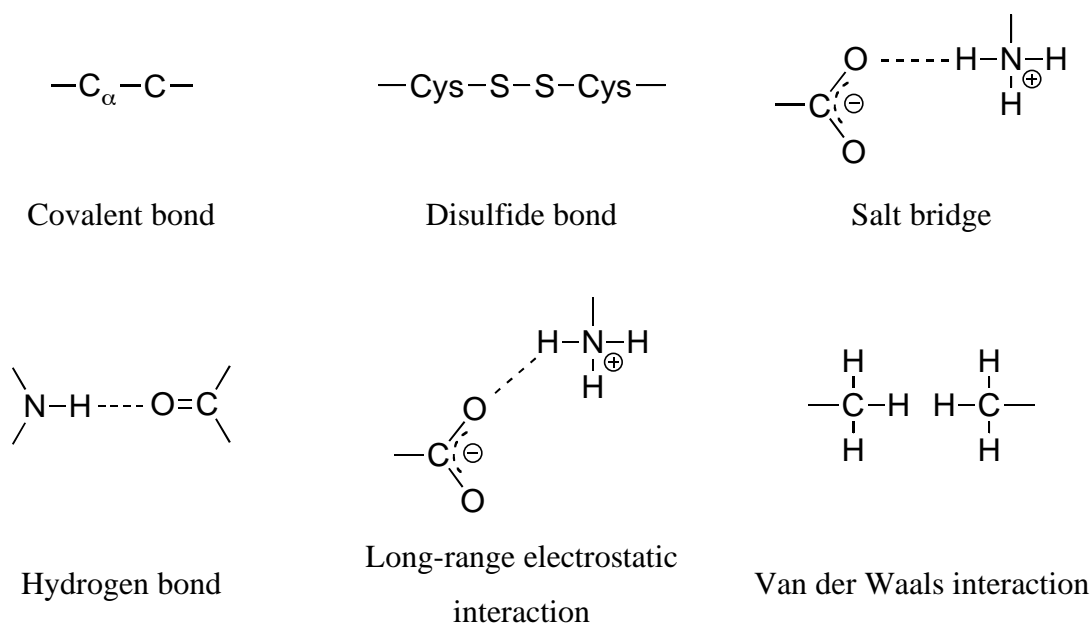


Figure 1.2 Chemical interactions commonly observed in polypeptide stabilization.

Secondary Structure

The secondary structure of peptides and proteins is governed by the sequence of component amino acids, i.e. the primary structure. The sequence and nature of these amino acids result in the formation of regular segments known as the secondary structure. There are three general types of secondary structure: alpha helices, beta sheets and beta turns.

(i) α -helix

An α -helix is a cylindrical structure, composed of a tightly coiled polypeptide chain (Figure 1.3a), where the wall of the cylinder is formed through the hydrogen-bonded polypeptide backbone, with the side residues protruding outwards. Hydrogen bonding interactions between the amide CO and NH groups of amino acids that are four residues apart stabilise the secondary structure (Figure 1.3a). The protruding side chains determine the interactions of the α -helix with other sections of the folded protein chain and with other protein molecules. The α -helix is a compact structure, with phi and psi values of -60° and -50° , respectively and a distance of 1.5\AA between successive residues along the helical axis (Figure 1.3b). This translates to 3.6 residues per turn, corresponding to a rotation of 100° per residue, resulting in the side chains projecting out of the helical axis at 100° intervals (Figure 1.3c).^{7,8}

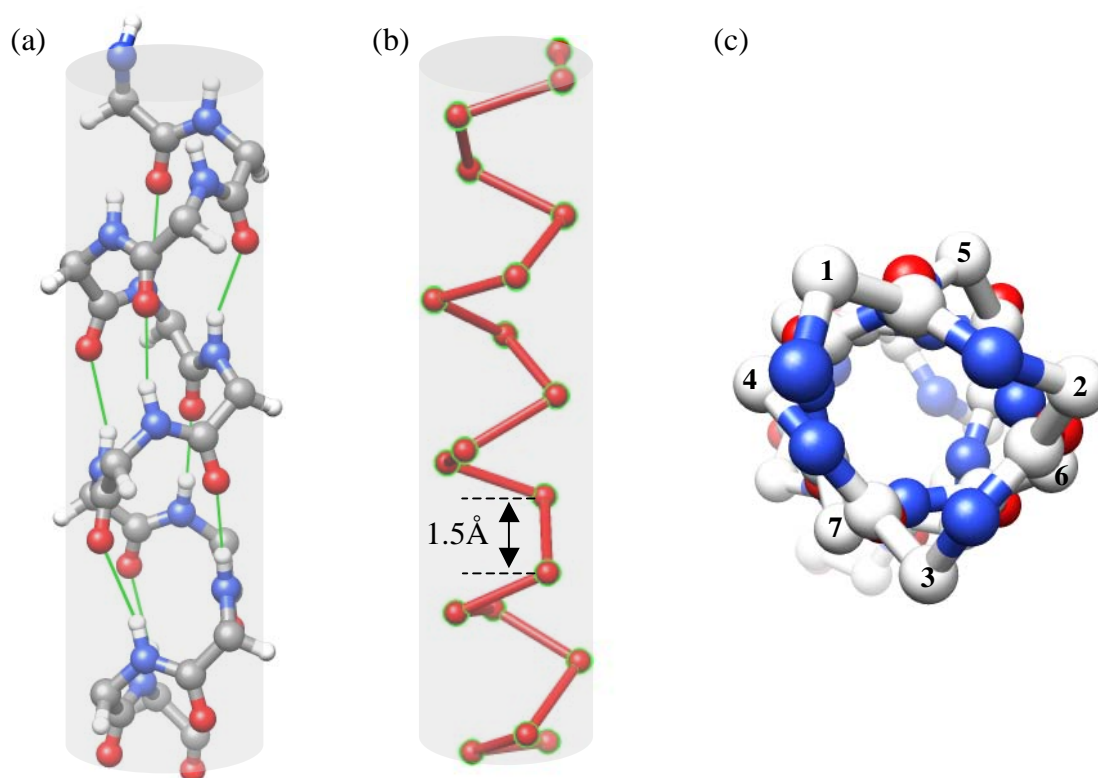


Figure 1.3 The structure of an α -helix [PDB 1B9P]: (a) Hydrogen bonding (green lines) between the carbonyl group of residue n and the amide N-H four residues away ($n+4$); (b) Distance between successive residues along the helical axis; and (c) Side chains projection from the helical axis.

An example of a naturally occurring helical structure formed from amino acid sequences rich in proline is the collagen triple helix.⁹ Collagen, a component of the extracellular matrix, is the main constituent of bones, tendons, ligaments and blood vessels. It consists of a repeating tripeptide in which every third residue is a glycine (GlyXY) $_n$, where X and Y are usually proline residues. Each collagen strand forms a left-handed helical conformation, which coils around each other to form a rope-like structure (Figure 1.4). Further aspects of this are discussed in chapter 4.

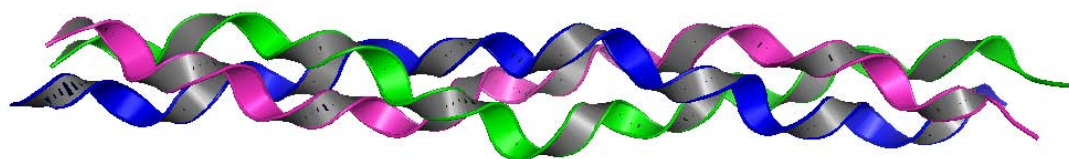


Figure 1.4 The figure of collagen [PDB 1CAG].

(ii) *β -sheets*

The β -sheet is a structural arrangement that has an extended sheet-like conformation. It consists of β -strands that are connected laterally by hydrogen bonds to form a pleated sheet. A β -strand is a stretch of polypeptide composed of 3-10 amino acids, and is represented as an extended or “saw-tooth” arrangement of amino acids, with the amide bonds being almost co-planar. The torsion angles of a classic β -strand is defined by $\phi = 120^\circ$, $\psi = 120^\circ$ and $\omega = 180^\circ$. This results in the amino acid side chains alternating above and below the plane of the peptide backbone (Figure 1.5a).¹⁰ The steric effects of the L-amino acid configurations giving rise to a pronounced right-handed twist. Furthermore, the β -sheet is stabilized by hydrogen bonding interactions between the amide NH and CO groups in the polypeptide chains. These sheets can lie in the same direction (parallel β -sheet) or in the opposite direction (antiparallel β -sheet) (Figure 1.5b).¹¹ The role of a β -strand geometry in the design of protease inhibitors is discussed in chapter 2.

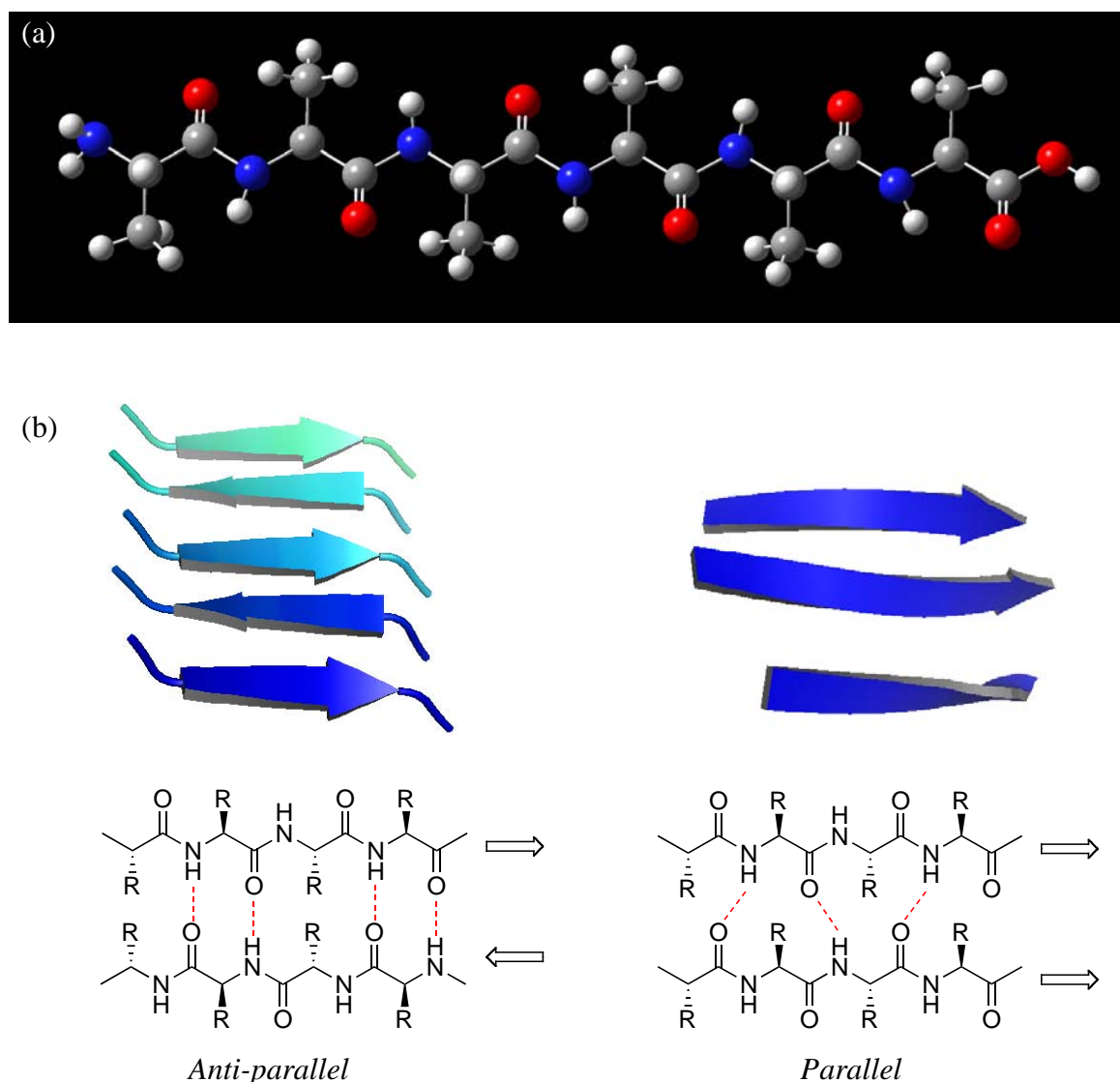


Figure 1.5 (a) “Saw-tooth” arrangement for amino acids for a peptide β -strand; and (b) the structural representation of antiparallel β -sheets (PDB 1SLK) and parallel β -sheets (PDB 2B1L, residues 71-76, 97-104 and 123-128). Hydrogen bonds indicated in red lines.

(iii) β -turn

The β -turn (also known as a reverse turn or hairpin turn) is the simplest form of secondary structure, and usually involves four residues.¹² It consists of an intramolecular hydrogen bond between the carbonyl group oxygen of one residue (n) and the amide N-H of the fourth residue apart ($n+3$), thereby reversing the direction of the peptide chain (Figure 1.6). The torsion angles, ϕ and ψ of residues $n+1$ and $n+2$ are used to classify the different types of β -turns. β -Turns are usually found on the surfaces of folded proteins, where they are in contact with the aqueous environment, allowing stabilization with water molecules. Apart

from its structural role in protein folding, β -turns serve as recognition motifs for protein-protein and protein-ligand interactions.^{12,13}

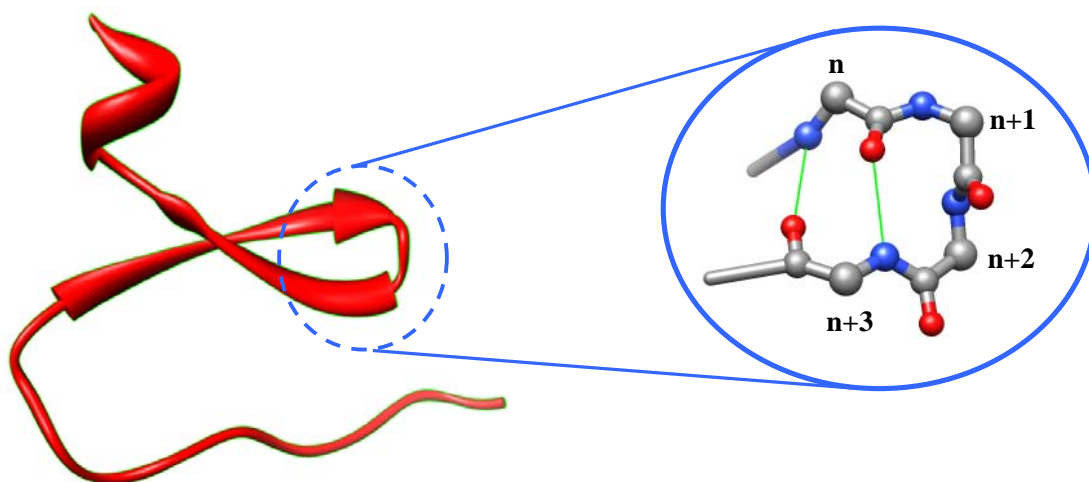


Figure 1.6 Structural representation of a β -turn (PDB 2WW6, chain A), showing the hydrogen bonding (green lines) between the carbonyl of residue n with the amide N-H three residues away ($n+3$).

The secondary structure of a given peptide or protein contributes significantly to the stabilization of the overall structure, through extensive hydrogen bonding networks that provides the enthalpy of stabilization required for the polar backbone groups to exist in the hydrophobic core of a folded protein. As a result, the structures of most proteins are not random, but are globular and have a tightly-packed core, consisting primarily of hydrophobic amino acids, due to the tendency of hydrophobic groups to avoid contact with the aqueous cell environment.¹⁴⁻¹⁶

Tertiary Structure and Quartinary Structure

The tertiary structure of a protein is the three-dimensional structure formed from the folding or grouping of secondary structures into more complex and functional forms. This spatial arrangement is particularly important for protein activity as it brings together activity-specific amino acid residues that may be far apart in the polypeptide chain sequence.¹⁵⁻¹⁷ The tertiary structure of a protein is stabilized by weak interactions (Figure 1.2) and the tight packing of atoms maximizes both the strength and the occurrence of these interactions. Subsequently, this leads to the creation of a complex surface topography, which enables a protein to interact with either small molecules that bind in

clefts, or with other macromolecules that have regions of complementary topology and charge. Further aspects of this are discussed in chapter 2 with regards to the structure and inhibition of proteases.

The complementary nature of protein surfaces enables them to associate with other protein chains or subunits into a closely packed arrangement, which results in the formation of quaternary structures.^{17,18} Each protein subunit of the quaternary structure has its own primary, secondary and tertiary structure. Furthermore, they are able to self-associate to form homodimers (a₂) or associate with other, unrelated proteins to give mixed species such as heterodimers (ab) and heterotetramers (a₂b₂) (Figure 1.7). This complementarity depends not only on the shape of the surface, but also extends to the weak interactions as mentioned earlier (Figure 1.2) that hold the complexes together. This complementary nature allows binding interactions between a protein and a small molecule or a protein with another macromolecule, and plays an important role in the function of proteins.¹⁷

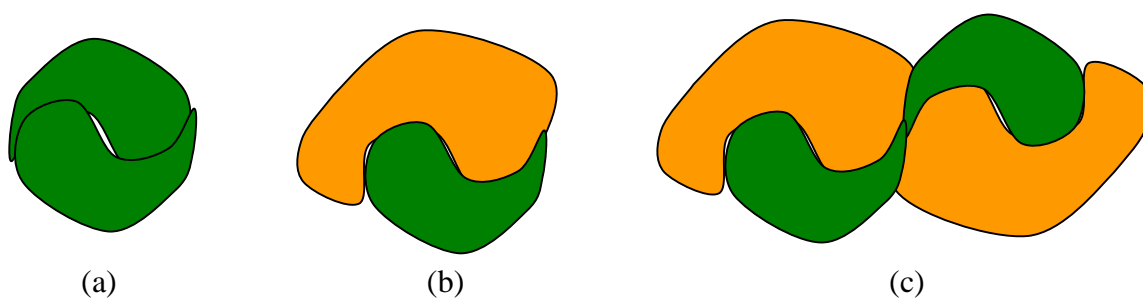


Figure 1.7 Molecular assemblies of folded proteins to form quaternary structures. (a) homodimer, a₂; (b) heterodimer, ab; and (c) heterotetramer, a₂b₂.

1.1.2 Relationship Between Polypeptide Structure and Function

The biological activity of a peptide or protein depends on its three-dimensional shape or native conformation. The functional diversity and versatility of proteins arise from the chemical diversity of the side chain of their constituent amino acids, the flexibility of the polypeptide chain, and the varying nature in which polypeptide chains with different amino acid sequences can fold. Although protein structure appears to be rigid and static from the X-ray crystallography pictures, in reality, proteins are flexible molecules.¹⁹ This flexibility is of particular importance, as binding of another molecule or ligand to the protein often

results in conformational changes that ultimately affect the function of the protein. For example, binding of calcium ions causes calpain (a cysteine protease discussed in detail in chapter 2) to change from an inactive to an active conformation, allowing proteolysis to occur.²⁰ Additionally, the function of many proteins involved in signalling, transport or catalysis, depends on the specificity of ligand binding, which arises from the complementing shape and charge distribution of donors and acceptors in the binding site of the protein surface. It is this complementary nature as well as conformational flexibility that allow a catalytic enzyme (or protease as addressed in this thesis) to bind specific substrates.²¹

Many structural components of cells and organisms, such as silk, collagen, elastin and keratin, are constructed purely from proteins. These structures are stabilized by protein-protein interactions that consist of numerous non-covalent interactions resulting from complementary interactions between protein surfaces on simple repeating secondary structures. Examples of such structures include collagen, which exists as a triple coiled helix (Figure 1.4), and silk, which consist of a stack of beta-sheets (Figure 1.8). In addition, protein stabilization can be accomplished through covalent cross-linking, which in collagen, is initiated by lysyl oxidase that converts lysine residues to peptidyl aldehydes capable of forming cross-linked chains.²²

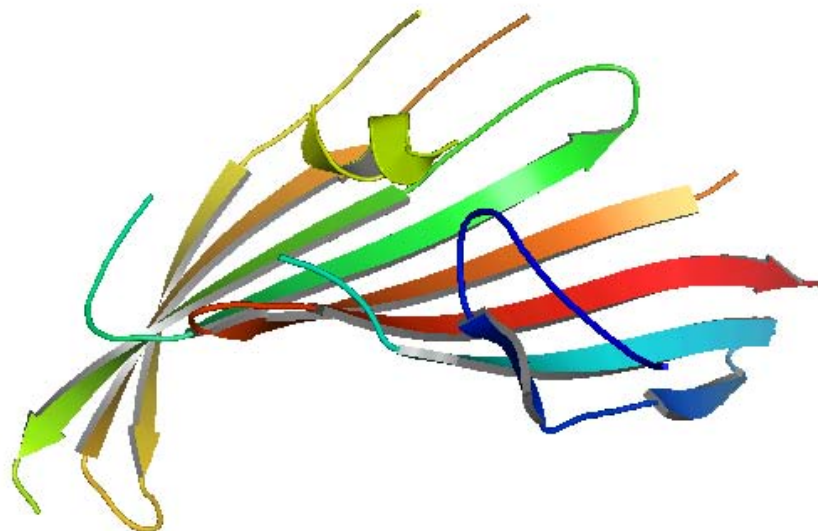


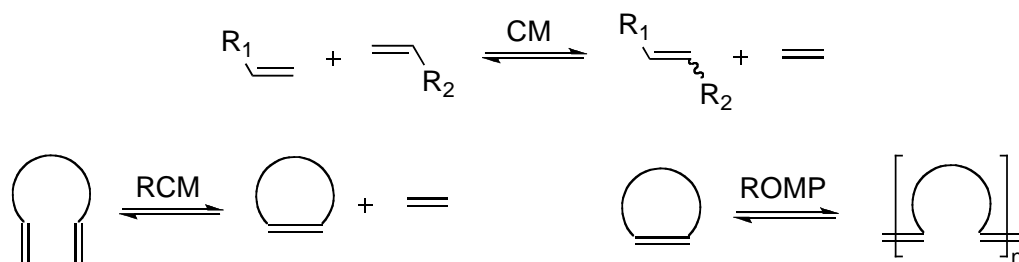
Figure 1.8 Schematic representations of silk [PDB:3UA0], a structural protein.

Peptide and protein structure can be disrupted by a variety of factors, such as elevated temperatures, denaturants and environmental conditions. These factors disrupt the weak interactions that stabilize the folded or native form of a protein, converting the structure to an unfolded or denatured state. This is usually characterized by the loss of biological activity, often leading to diseases.^{6,23}

Understanding peptide and protein structure and function is important in the development of therapeutics for the treatment of diseases. The realization that enzymes bind their substrates in an extended β -stranded conformation has led to the development of inhibitors that mimic the bioactive conformation.²⁴ Additionally, the ability to mimic the natural environment of structural proteins in wound healing, has led to the development of biocompatible materials, such as hydrogels, through the manipulation of natural peptide structure.²⁵⁻²⁷ These are all topics developed further in this thesis.

1.2 Conformational Manipulation by Olefin Metathesis

The chemical modification of peptides and proteins is a powerful method in manipulating peptide and protein conformation for the development of new therapeutics. Most strategies of peptide and protein chemical modification rely on the presence of nucleophilic residues of amino acids, such as lysine, cysteine, aspartic or glutamic acids.^{28,29} For example, crosslinking of proteins can be affected by oxidation of cystine residues to form disulfide bridges or formation of lactam bridges by reaction of lysine and aspartic acid.²⁹ An alternative method of chemical modification of peptides and proteins is olefin metathesis. Olefin metathesis is a useful metal-catalysed mediated reaction involving two olefin motifs to give rise to the formation of a new carbon-carbon bond (Scheme 1.1). Carbon-carbon bonds are non-reactive and not susceptible to enzyme degradation in comparison to amide bonds.



Scheme 1.1 Selected types of olefin metathesis: CM = cross metathesis, RCM = ring opening metathesis, ROMP = ring-opening metathesis polymerization.

Olefin metathesis is mediated by a metal catalysis such as the ruthenium-based catalysts, first developed by Grubbs,^{30,31} which combines high activity and excellent tolerance to many functional motifs. The Grubbs catalysts consist of a ruthenium atom surrounded by five ligands, and can be divided into two groups based on the nature of the ligands: (i) the first generation Grubbs catalysts, $L_2X_2Ru=CHR$ (where L is a phosphine ligand), and (ii) the second generation Grubbs catalysts, $(L)(L')X_2Ru=CHR$ (where L is a phosphine ligand and L' is a saturated N-heterocyclic carbene or NHC ligand) (see Figure 1.9). The second generation Grubbs catalysts are more reactive and air-stable than the first generation Grubbs catalysts.

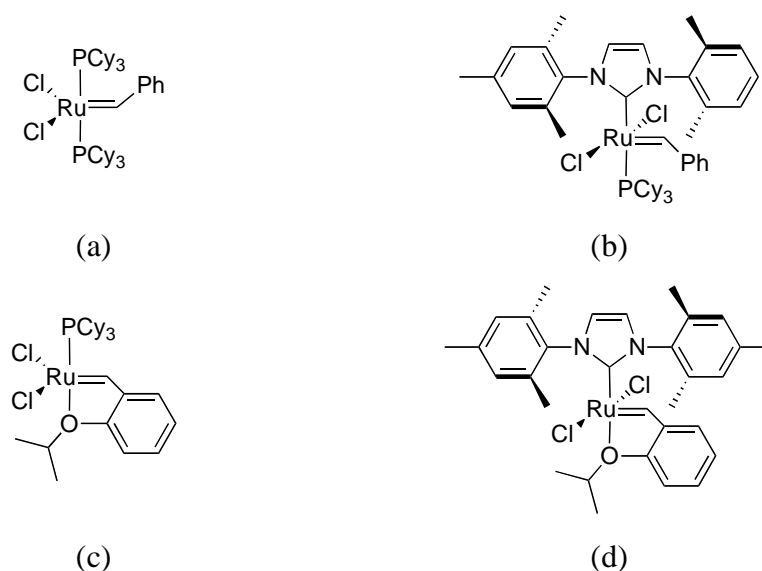


Figure 1.9 Well-defined ruthenium-based catalysts commonly used for olefin metathesis: (a) Grubbs 1st generation catalyst, (b) Grubbs 2nd generation catalyst, (c) Hoveyda-Grubbs 1st generation catalyst, and (d) Hoveyda-Grubbs 2nd generation catalyst.

The mechanism of metathesis, in which a new carbon-carbon bond is formed, proceeds through a series of [2 + 2] cycloadditions between an alkene and a metal carbene complex, followed by cycloreversion (outlined in Figure 1.10).³¹ The olefin then reacts with the carbene catalyst [M], forming the a metallacyclobutane intermediate. This intermediate undergoes cycloreversion to give either the original alkenes or a new alkene and an alkylidene with regeneration of the metal catalyst.

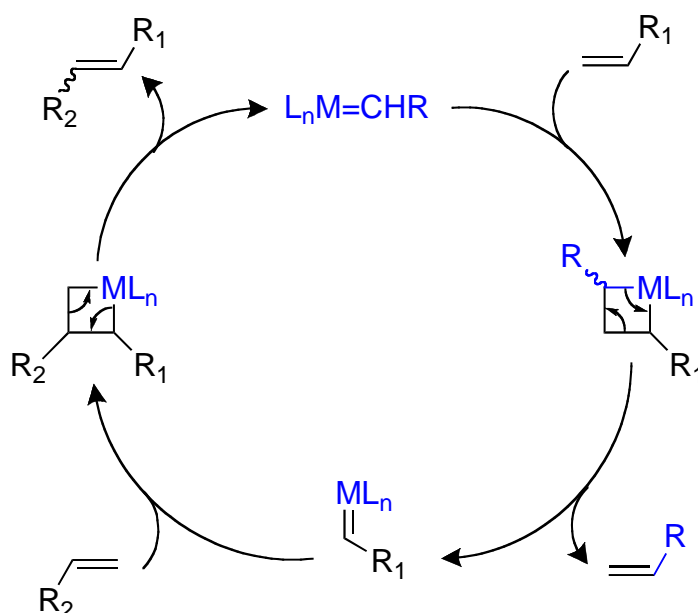


Figure 1.10 Mechanism of olefin metathesis. $L_nM=CHR$ is used to denote the carbene catalyst and L_n is the attached ligands.³¹

The extensive utility of olefin metathesis is due to the tolerance and selectivity of the ruthenium-based catalyst towards a multitude of functional groups during transformation. Olefin metathesis is useful in the modification of proteins and peptides as the resultant product of metathesis is the introduction of a non-labile carbon-carbon bond.³² This new carbon-carbon bond can lead to an increased stability of peptide secondary structure, which can improve metabolic stability and result in higher binding affinity towards biological targets. For example, ring-closing metathesis (RCM) transforms a diene into a cyclic alkene and has proven to be a potent method for creating macrocycles, which allows for constraining the flexible portions of a peptide chain (will be discussed in chapter 2). Similarly, ring-opening metathesis polymerization (ROMP) converts a cyclic olefin into an unsaturated polymer, which can be used as a tether for connecting two molecules; while cross metathesis (CM) provides a direct means of connecting two molecules. These

methods can be applied to the formation of peptide-based polymers (will be discussed in chapter 4).

1.2.1 Ring Closing Metathesis (RCM)

Ring-closing metathesis is a common form of metathesis that has been utilized in the synthesis of unnatural amino acids^{33,34} and in the design of conformationally constrained peptidomimetics.³⁵ RCM has been applied in the replacement of disulfide bridges, commonly found in natural peptides, and was used by Grubbs and coworkers³⁶ for the synthesis of cyclic peptide **1.1**, whereby the S-S bridge of cyclic peptide **1.2** had been replaced by a C=C (Figure 1.11a). The conformational analysis of resulting cyclic peptide **1.1** revealed the presence of intramolecular hydrogen bond analogous to that found in the corresponding disulfide-bridge cyclic peptide **1.2**.³⁶ Besides this, RCM has been applied for preparation of peptidomimetic inhibitor **1.3** based on the acyclic inhibitor **1.4** (Figure 1.11b).³⁷⁻³⁹ Tzantrizos and coworkers³⁷⁻³⁹ postulated that introducing a hydrocarbon bridge by linking the side-chains would introduce additional interactions in the binding pocket. The resulting cyclic inhibitor **1.3** was found to be more potent than the acyclic peptide **1.4**, and after structure-activity relationship studies, compound **1.5** was identified as an orally bioavailable clinical candidate for hepatitis C virus NS3 protease.⁴⁰ Both examples exemplify the effectiveness of RCM in the preparation of conformationally restricted peptides.

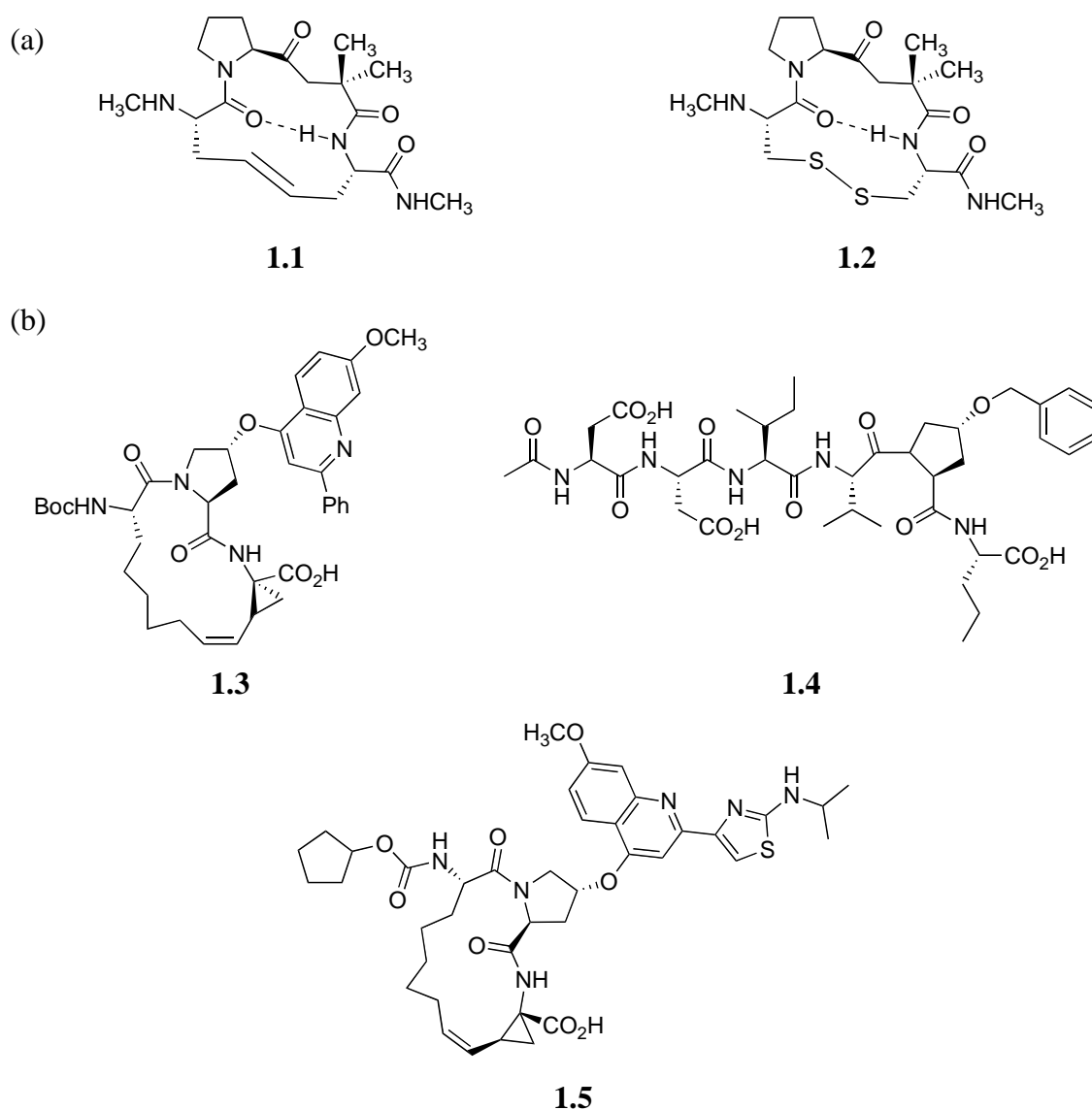


Figure 1.11 Compounds constrained by RCM: (a) disulfide bond mimic (b) β -strand mimics.

The mechanism of ring closing metathesis is similar to that of olefin metathesis (Figure 1.10). The forward reaction for ring closing metathesis is entropically driven by the production of volatile ethylene. The reactivity of ring-closing metathesis of olefins is influenced by the size of the rings formed.^{41,42} This is particularly apparent in the synthesis of large rings (macrocycles) as the efficiency of cyclization by RCM is governed by the extent of competing acyclic diene metathesis polymerization. Reduction of competing reactions is decreased by reacting olefins at low concentrations, elevated temperatures and increased catalyst loading thereby reducing the rate of oligomerization.⁴³ Ring closing metathesis in protein and peptide modification has provided access to β -turn analogues that are capable of mimicking the natural role of

β -turns in stabilizing short peptides,^{32,44} and has provided a means for the development of conformationally constrained β -stranded inhibitors.^{32,45,46} Work on using RCM to access conformationally constrained inhibitors for cysteine and serine proteases is presented in chapter 2.

1.2.2 Cross Metathesis (CM)

Cross metathesis, another variant of olefin metathesis, is a powerful and convenient synthetic technique for the synthesis of functionalized olefins from simple alkene precursors as shown in Scheme 1.1. The mechanism of cross metathesis is again as illustrated in Figure 1.11. However, cross metathesis has found comparatively limited use due to issues of a lack of product selectivity and stereoselectivity, coupled with a low catalyst activity. Nevertheless, Grubbs and co-workers⁴⁷ have established a general model for imparting selectivity in cross metathesis, by categorizing the olefins by their ability to undergo homodimerization. Additionally, the choice of olefin metathesis catalyst was found to be critical for product selectivity, regioselectivity and chemoselectivity. With an appropriate choice of Grubbs catalyst, cross metathesis has been successfully applied for the modification of biomolecules in aqueous conditions.⁴⁸ CM has been applied successfully by Davis and coworkers⁴⁹ to functionalize a model protein, in an aqueous environment, with carbohydrate and polyethylene glycol (PEG) moieties, while keeping the enzymatic activity intact. This exemplifies the usefulness of CM as a method for linking two biological molecules.

1.2.3 Ring Opening Polymerisation Metathesis (ROMP)

Ring opening polymerisation metathesis as depicted in Scheme 1.1 is widely used in polymer chemistry. The driving force of the reaction is the relief in the ring strain in cyclic olefins (such as norbornene). The mechanism of ROMP is similar to that illustrated in Figure 1.10. In ROMP, a metal carbene species is formed, which is followed by attack of the double bond in the ring structure, forming a highly strained metallacyclobutane intermediate. The ring then opens, resulting in a linear chain with a carbene attached. This carbene then reacts with the double bond of the following monomer, thus propagating the reaction.⁵⁰ The reactivity of ROMP is influenced by the substituents on the constrained,

cyclic olefins. For example, in the polymerization of a mixture of endo- and exo-2-norbornene derivatives, the exo-isomers are found to react faster than the endo- isomers, which is attributed to steric and electronic effects.⁵¹ Thus, the nature of the substituents on the cyclic olefin are considered when specific products are desired.⁵⁰ Currently, ROMP is one of the most powerful methods for the synthesis of novel materials with well-defined structures.⁵² Kiessling and coworkers⁵³⁻⁵⁵ used ROMP to synthesize bio-active polymers, including multivalent displays of carbohydrates and other bioactive ligands. Such polymers have recently been used to modulate immune responses *in vivo*.⁵⁵

1.3 Overview of Thesis

Understanding protein structure and function is central for the development of therapeutics for the treatment of diseases and novel biocompatible materials. To successfully develop novel inhibitors for a given protein and biocompatible materials, the structural arrangement, mode of substrate binding and arrangement, both before and after binding, are crucial in development of selective and potent inhibitors and useful biocompatible materials.

This thesis describes studies on the control of peptide structure and function through synthetic modifications, for the synthesis of novel enzyme inhibitors and biomaterials, primarily using olefin metathesis chemistry. Metathesis was chosen for the manipulation of peptide structure in order to induce a constraint in novel macrocyclic peptidomimetic inhibitors and to develop novel hydrogel matrices, which are of importance in the advancement of the pharmaceutical and medical industries.

Chapter two describes the controlled organization of secondary structure in peptides by ring closing metathesis for the design and synthesis of a new class of cyclic inhibitors constrained by the P₁ and P₃ residues or the P₂ and P₄ residues. These inhibitors are designed to be less peptidic in nature, with the incorporation of a pyrrole group in the peptide backbone. Additionally, the synthesis of the corresponding P₁-P₃ and P₁-P₄ acyclic protease inhibitors are also presented for comparison to the macrocyclic aldehydes derivatives. These acyclic inhibitors will provide an insight into the importance of the macrocycle on the potency of inhibition against cysteine and serine proteases.

Chapter three details the enzyme inhibition assays utilised to analyse the efficacy of cyclic and acyclic inhibitors prepared in chapter two. The assay protocols for *in vitro* testing against cysteine (calpain and cathepsin) and serine (α -chymotrypsin, human leukocyte elastase and trypsin) proteases are presented, followed by discussion of the potency of the inhibitors against each of the aforementioned proteases. The inhibitors selectivity between proteases of the same family (calpain vs. cathepsin and α -chymotrypsin vs. HLE) and between the cysteine and serine protease families are further discussed.

Chapter four discusses the controlled organization of the tertiary structure of naturally occurring proteins by aqueous metathesis for the synthesis of biocompatible hydrogels derived from gelatin. Optimisation of the hydrogel formation is investigated by: i) varying catalysts utilised and ii) varying quantities of starting gelatin and norbornene dicarboxylic acid. Additionally, mechanistic studies using MALDI are performed to provide an insight into the mode of hydrogel formation.

1.4 References for Chapter One

- [1] Alberts, B.; Johnson, A.; Lewis, J.; Raff, M.; Roberts, K.; Walter, P. *Molecular Biology of the Cell*; 4th ed. Garland Science: New York, **2002**; p. 1616.
- [2] Voet, D.; Voet, J. G. *Biochemistry*; 4th ed. Wiley: New York, **2010**; p. 1520.
- [3] Petsko, G. A.; Ringe, D. *Protein structure and function*; Lawrance, E.; Robertson, M., Eds. New Science Press Ltd., **2004**; p. 195.
- [4] Burley, S. K.; Petsko, G. A. *Adv. Protein Chem.* **1988**, *39*, 125–189.
- [5] Dunitz, J. D. *Chem. Biol.* **1995**, *2*, 709–712.
- [6] Jaenicke, R. *J. Biotechnol.* **2000**, *79*, 193–203.
- [7] Hol, W. G. *Prog. Biophys. Mol. Biol.* **1985**, *45*, 149–195.
- [8] Pauling, L.; Corey, R. B.; Branson, H. R. *Proc. Natl. Acad. Sci. U.S.A.* **1951**, *37*, 205–211.
- [9] Scott, J. E. *Trends Biochem. Sci.* **1987**, *12*, 318–321.
- [10] Loughlin, W. A.; Tyndall, J. D. A.; Glenn, M. P.; Fairlie, D. P. *Chem. Rev.* **2004**, *104*, 6085–6117.
- [11] Gellman, S. H. *Curr. Opin. Chem. Biol.* **1998**, *2*, 717–725.
- [12] Blanco, F.; Ramírez-Alvarado, M.; Serrano, L. *Curr. Opin. Struct. Biol.* **1998**, *8*, 107–111.
- [13] Schneider, J. P.; Kelly, J. W. *Chem. Rev.* **1995**, *95*, 2169–2187.
- [14] Walther, D.; Eisenhaber, F.; Argos, P. *J. Mol. Biol.* **1996**, *255*, 536–553.
- [15] Lesk, A. M.; Chothia, C. *Biophys. J.* **1980**, *32*, 35–47.
- [16] Rose, G. D.; Roy, S. *Proc. Natl. Acad. Sci. U.S.A.* **1980**, *77*, 4643–4647.
- [17] Jones, S.; Thornton, J. M. *Proc. Natl. Acad. Sci. U.S.A.* **1996**, *93*, 13–20.
- [18] Antson, A. A.; Dodson, E. J.; Dodson, G. G. *Curr. Opin. Struct. Biol.* **1996**, *6*, 142–150.
- [19] Karplus, M.; Petsko, G. A. *Nature* **1990**, *347*, 631–639.
- [20] Hanna, R. A.; Campbell, R. L.; Davies, P. L. *Nature* **2008**, *456*, 409–412.
- [21] Hammes, G. G. *Biochemistry* **2002**, *41*, 8221–8228.
- [22] Berisio, R.; Vitagliano, L.; Mazzarella, L.; Zagari, A. *Protein Pept. Lett.* **2002**, *9*, 107–116.
- [23] Ferreira, S. T.; De Felice, F. G. *FEBS Lett.* **2001**, *498*, 129–134.

- [24] Fairlie, D. P.; Tyndall, J. D. A.; Reid, R. C.; Wong, A. K.; Abbenante, G.; Scanlon, M. J.; March, D. R.; Bergman, D. A.; Chai, C. L. L.; Burkett, B. A. *J. Med. Chem.* **2000**, *43*, 1271–1281.
- [25] Hahn, M. S.; Teply, B. A.; Stevens, M. M.; Zeitels, S. M.; Langer, R. *Biomaterials* **2006**, *27*, 1104–1109.
- [26] Liao, E.; Yaszemski, M.; Krebsbach, P.; Hollister, S. *Tissue Eng.* **2007**, *13*, 537–550.
- [27] Willers, C.; Chen, J.; Wood, D.; Xu, J.; Zheng, M. H. *Tissue Eng.* **2005**, *11*, 1065–1076.
- [28] Hermanson, G. T. *Bioconjugate Techniques*; 2nd ed. Academic Press: San Diego, 2008.
- [29] Li, P.; Roller, P. P. *Curr. Top. Med. Chem.* **2002**, *2*, 325–341.
- [30] Trnka, T. M.; Grubbs, R. H. *Acc. Chem. Res.* **2001**, *34*, 18–29.
- [31] Dias, E. L.; Nguyen, S. T.; Grubbs, R. H. *J. Am. Chem. Soc.* **1997**, *119*, 3887–3897.
- [32] Brik, A. *Adv. Synth. Catal.* **2008**, *350*, 1661–1675.
- [33] Miller, S. J.; Grubbs, R. H. *J. Am. Chem. Soc.* **1995**, *117*, 5855–5856.
- [34] Miller, S. J.; Blackwell, H. E.; Grubbs, R. H. *J. Am. Chem. Soc.* **1996**, *118*, 9606–9614.
- [35] Ersmark, K.; Nervall, M.; Gutiérrez-de-Terán, H.; Hamelink, E.; Janka, L. K.; Clemente, J. C.; Dunn, B. M.; Gogoll, A.; Samuelsson, B.; Qvist, J.; Hallberg, A. *Bioorg. Med. Chem.* **2006**, *14*, 2197–2208.
- [36] Ravi, A.; Balaram, P. *Tetrahedron* **1984**, *40*, 2577–2583.
- [37] Poupart, M. A.; Cameron, D. R.; Chabot, C.; Ghire, E.; Goudreau, N.; Goulet, S.; Poirier, M.; Tsantrizos, Y. S. *J. Org. Chem.* **2001**, *66*, 4743–4751.
- [38] Tsantrizos, Y. S.; Bolger, G.; Bonneau, P.; Cameron, D. R.; Goudreau, N.; Kukulj, G.; LaPlante, S. R.; Llinàs-Brunet, M.; Nar, H.; Lamarre, D. *Angew. Chem. Int. Ed.* **2003**, *42*, 1356–1360.
- [39] Goudreau, N.; Brochu, C.; Cameron, D. R.; Duceppe, J.-S.; Faucher, A.-M.; Ferland, J.-M.; Grand-Maître, C.; Poirier, M.; Simoneau, B.; Tsantrizos, Y. S. *J. Org. Chem.* **2004**, *69*, 6185–6201.
- [40] Llinàs-Brunet, M.; Bailey, M. D.; Bolger, G.; Brochu, C.; Faucher, A.-M.; Ferland, J.-M.; Garneau, M.; Ghire, E.; Gorys, V.; Grand-Maître, C.; Halmos, T.; Lapeyre-Paquette, N.; Liard, F.; Poirier, M.; Rhéaume, M.; Tsantrizos, Y. S.; Lamarre, D. *J. Med. Chem.* **2004**, *47*, 1605–1608.

-
- [41] Fürstner, A. *Top. Catal.* **1997**, *4*, 285–299.
- [42] Ghosh, S.; Ghosh, S.; Sarkar, N. *J. Chem. Sci.* **2006**, *118*, 223–235.
- [43] Kotha, S.; Singh, K. *Eur. J. Org. Chem.* **2007**, 5909–5916.
- [44] Fink, B. E.; Kym, P. R.; Katzenellenbogen, J. A. *J. Am. Chem. Soc.* **1998**, *120*, 4334–4344.
- [45] Prabhakaran, E. N.; Rajesh, V.; Dubey, S.; Iqbal, J. *Tetrahedron Lett.* **2001**, *42*, 339–342.
- [46] Kazmaier, U.; Hebach, C.; Watzke, A.; Maier, S.; Mues, H.; Huch, V. *Org. Biomol. Chem.* **2005**, *3*, 136–145.
- [47] Chatterjee, A. K.; Toste, F. D.; Goldberg, S. D.; Grubbs, R. H. *Pure Appl. Chem.* **2003**, *75*, 421–425.
- [48] Kirshenbaum, K.; Arora, P. S. *Nat. Chem. Biol.* **2008**, *4*, 527–528.
- [49] Lin, Y. A.; Chalker, J. M.; Floyd, N.; Bernardes, G. J. L.; Davis, B. G. *J. Am. Chem. Soc.* **2008**, *130*, 9642–9643.
- [50] Grubbs, R. H.; Tumas, W. *Science* **1989**, *243*, 907–915.
- [51] Lapinte, V.; Brosse, J.-C.; Fontaine, L. *Macromol. Chem. Phys.* **2004**, *205*, 824–833.
- [52] Leitgeb, A.; Wappel, J.; Slugovc, C. *Polymer* **2010**, *51*, 2927–2946.
- [53] Mortell, K. H.; Gingras, M.; Kiessling, L. L. *J. Am. Chem. Soc.* **1994**, *116*, 12053–12054.
- [54] Lee, Y.; Sampson, N. S. *Curr. Opin. Struct. Biol.* **2006**, *16*, 544–550.
- [55] Puffer, E. B.; Pontrello, J. K.; Hollenbeck, J. J.; Kink, J. A.; Kiessling, L. L. *ACS Chem. Biol.* **2007**, *2*, 252–262.

CHAPTER TWO:
Design and Synthesis of
Protease Inhibitors

2.1 Introduction: Protease Conformation and Inhibitor Design

2.1.1 Overview and Classification of Proteases

Proteases are found universally in all organisms, accounting for approximately 2% of their genes.¹ They catalyse the hydrolysis of peptide bonds and as such are involved in numerous physiological processes through the controlled activation, synthesis and turnover of proteins. Consequently, proteases are important regulators of processes, such as cell maintenance, cell signalling, wound healing, cell differentiation and cell growth.² As proteases are involved in many physiological processes, their activity is tightly regulated, through a feedback mechanism, which usually involves the binding of either a substrate or signalling molecule to the protease.³⁻⁵ Many factors can affect the function of proteases, leading to undesired and unregulated proteolysis, which can result in abnormal development and diseases,⁶⁻⁸ such as Alzheimer's,⁹ cancer,¹⁰ stroke,¹¹ viral infections¹² and cataracts.^{13,14} The inhibition of proteases can slow the undesired processes that are characteristic of disease propagation or abnormal physiology.⁸ As a result, inhibitors of proteases have the potential to provide effective therapeutics for a wide range of diseases.^{7,8,15,16}

There are six known classes of proteases: serine, cysteine, aspartic acid, threonine, glutamic acid and metallo-proteases. These are primarily categorized by the make-up of the catalytic residue located in the active site, which usually determines the mechanism of peptide bond hydrolysis.^{17,18} Two distinct catalytic mechanisms for hydrolysis are observed, where; i) the key catalytic nucleophile is an intrinsic component of the active site (serine, cysteine and threonine proteases), and ii) an activated water molecule acts as a nucleophile (aspartic acid, glutamic acid and metallo-proteases).^{18,19}

2.1.2 Cysteine and Serine Proteases

All proteases bind their substrates in an active site groove or cleft. The nomenclature used to define the associated interactions is based on a notation developed by Schechter and Berger.²⁰ Here the amino acid side chains of the substrate are defined as P_n-P_n' and these

occupy corresponding enzyme subsites designated as S_n - S_n' . These interactions define the substrate into a β -strand like conformation that is critical to binding and inhibitor design as discussed in section 2.2.1. Substrate cleavage then occurs between P_1 and P_1' as shown in Figure 2.1.

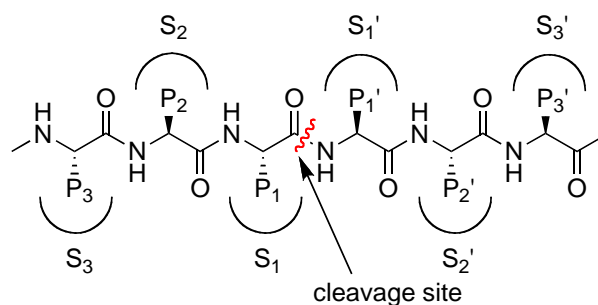
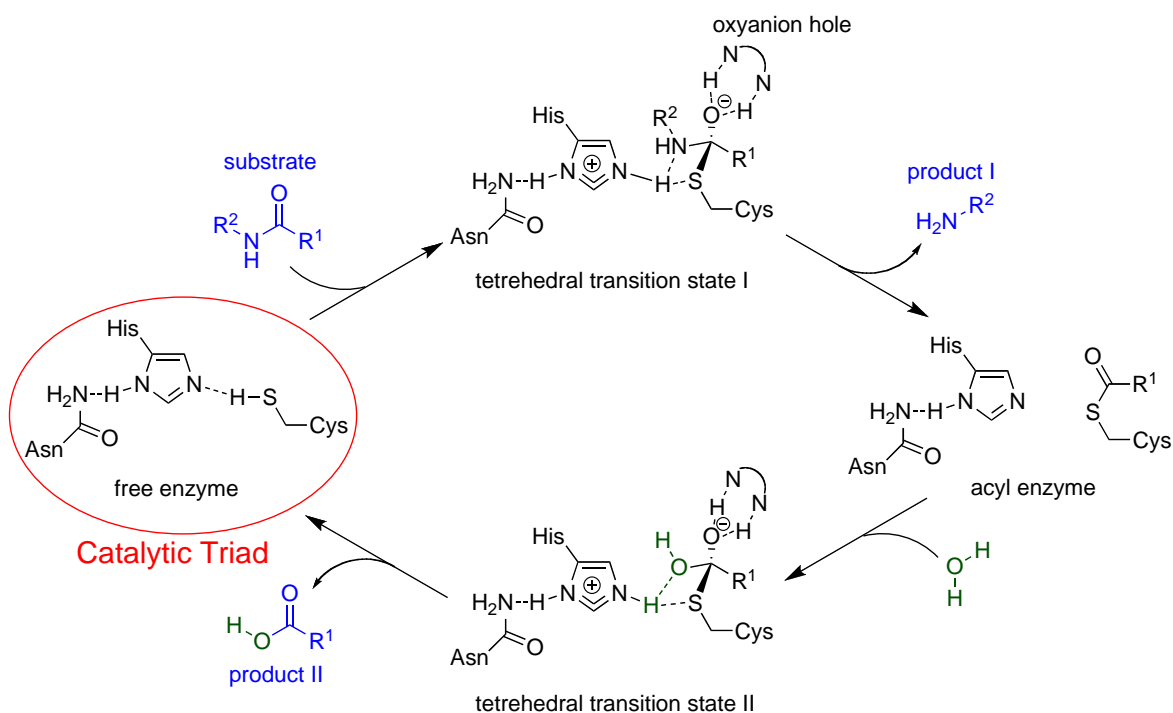


Figure 2.1 Schechter and Berger²⁰ representation showing the substrate residues (P) and protease binding sites (S). Prime and non-prime designations distinguish C- versus N-terminal sides respectively of the cleavage site.

Catalytic Mechanism

The active site of cysteine and serine proteases consists of i) a catalytic triad (Cys, His and Asn for cysteine proteases¹⁶ and His, Ser and Asp for serine proteases¹) that is responsible for the hydrolysis of the peptide bond (Figure 2.2) and ii) subsite binding pockets (designated S_1 - S_n and S_1' - S_n') that define the conformation of the bound substrate via hydrogen bonding, covalent and non-covalent interactions between these subsites and the amino acids of the substrate (Figure 2.1).

(a) Cysteine Protease



(b) Serine Protease

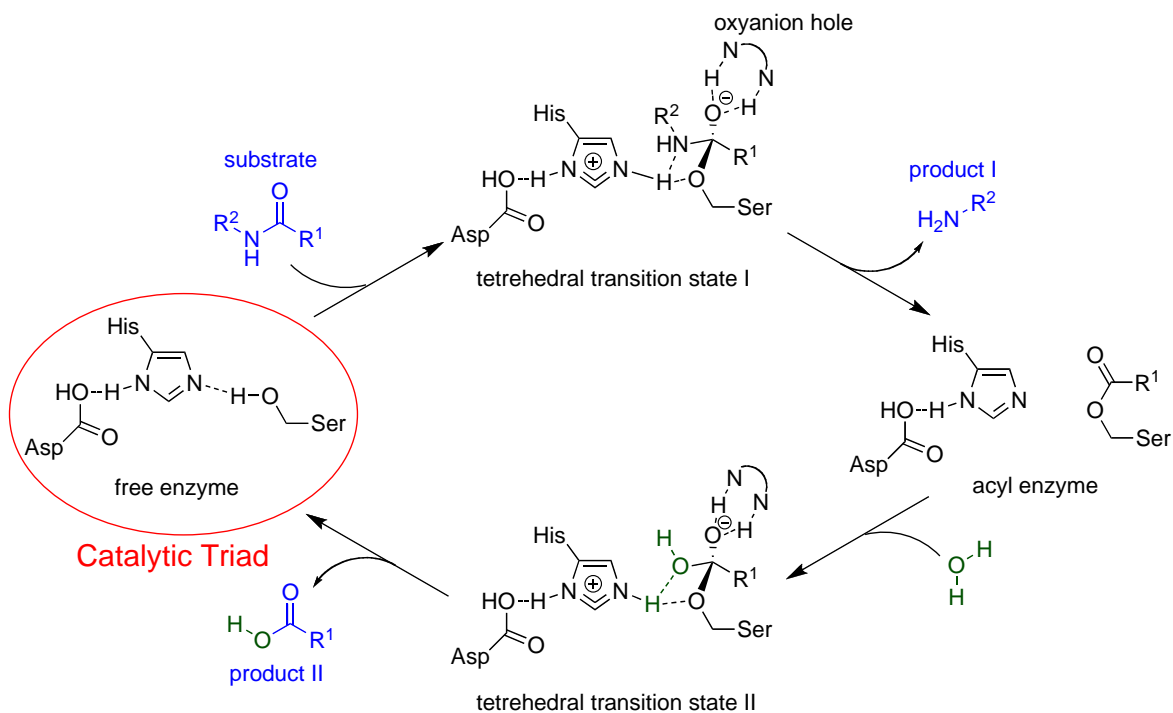


Figure 2.2 Mechanism of proteolysis of a) cysteine proteases and b) serine proteases (enzyme residues in black).

The Cys/Ser residues and His residues of the catalytic triad form a stable thiolate- (cysteine proteases) or hydroxy- (serine protease) imidazolium ion pair, which can hydrolyse the scissile bond of the substrate. The proteolysis of peptide bonds occurs in four stages, outlined in Figure 2.2. Initially, the substrate binds to the free enzyme, forming tetrahedral transition state I, which is stabilised by hydrogen bonding to Cys₂₅/Gln₁₉ (for cysteine protease (papain numbering system)) or Gly₁₉₃/Ser₁₉₅ (for serine protease (chymotrypsin numbering system)) that makes up the oxyanion hole. This is followed by acylation to give the acyl-enzyme intermediate with the release of product I (C-terminal substrate fragment). Hydrolysis then proceeds via a tetrahedral transition state II to regenerate the free enzyme and liberate product II (N-terminal substrate fragment).^{1,16}

Protease Selectivity

Protease selectivity is a key feature of inhibitors that is determined by the nature of amino acids within the catalytic active site.⁸ These amino acids define the groove or pocket in which substrates/inhibitors bind. It is the nature of these amino acids that confer selectivity within proteases in the same family.⁸

i) Calpains (Cysteine Protease)

Calpains are calcium-activated neutral cysteine proteases that are expressed ubiquitously in biological systems. They belong to the papain superfamily of cysteine proteases, and consist of at least 15 isoforms.²¹⁻²³ Two major isoforms have been identified; μ -calpain (calpain 1) and m-calpain (calpain 2), that differ in requirements of calcium concentration for activation (μ M and mM amounts respectively). Both are heterodimers, consisting of an 80 kDa subunit (domains I-IV) and a small 30 kDa subunit (domains V and VI) (see Figure 2.3). Domain II contains the active site, and is divided into two subdomains IIa and IIb. The active site Cys₁₀₅ resides in domain IIa, while His₂₆₂ and Asn₂₈₆, which complete the catalytic triad are located in domain IIb.²⁴ In the absence of calcium, the catalytic Cys₁₀₅ is 8.5 Å away from His₂₆₂, which is too far for the formation of the active catalytic triad. Upon binding of calcium, a conformational change occurs, reducing the distance between Cys₁₀₅ and His₂₆₂ to 3.7 Å, a distance at which proteolysis can occur (see Figure 2.4).^{25,26}

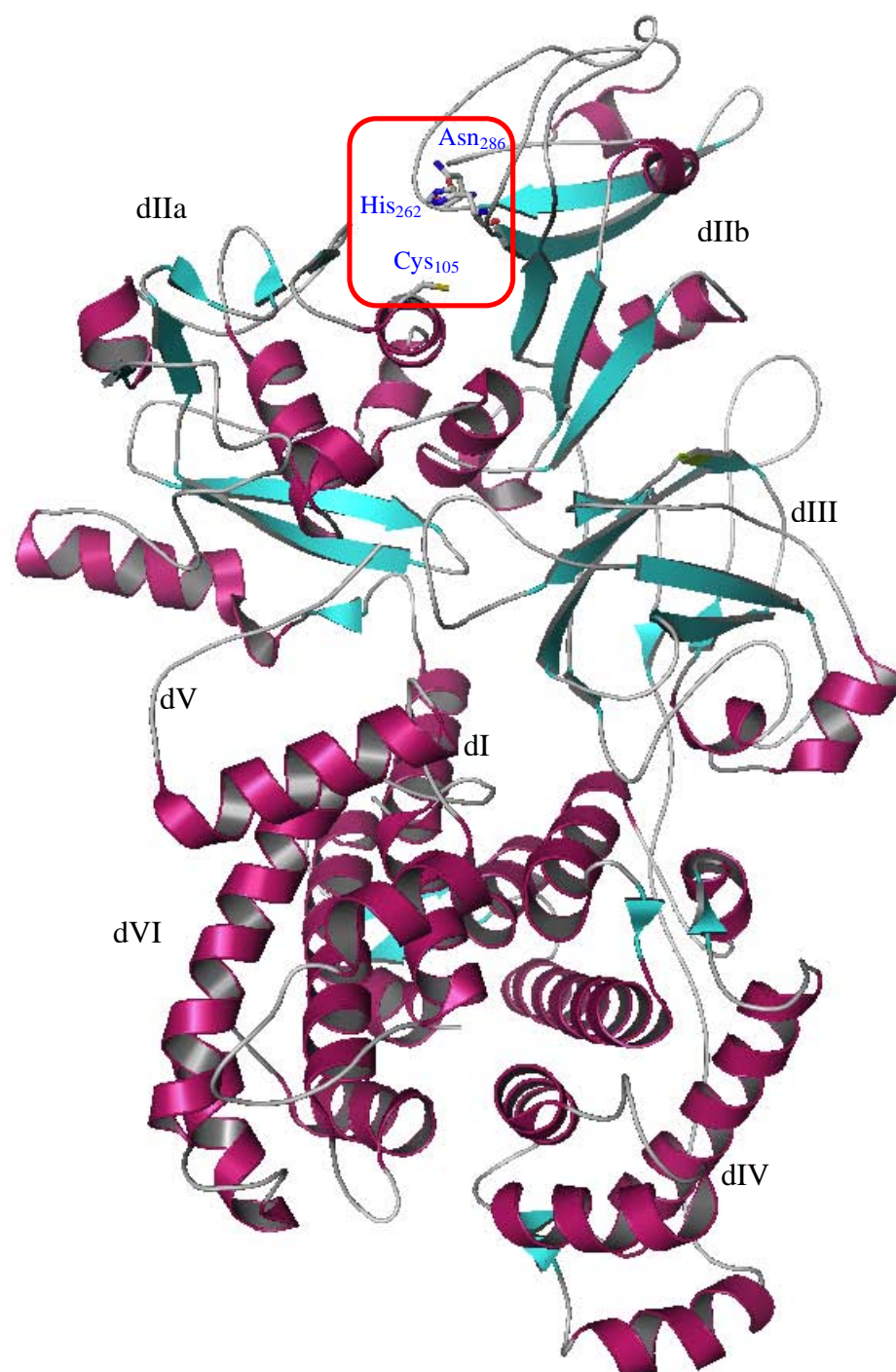


Figure 2.3 The structure of human m-calpain (PDB 1KFU).²⁴ Active site (red box) as ball and stick representation: Cys₁₀₅, His₂₆₂ and Asn₂₈₆.

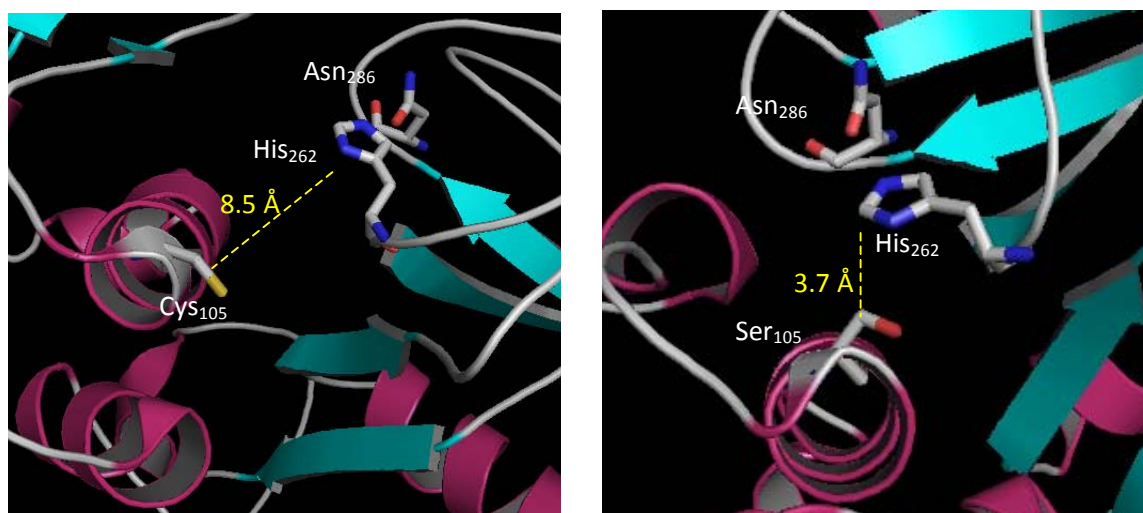


Figure 2.4 Arrangement of the active site of human m-calpain (PDB 1KFU)²⁴ without calcium bound²⁴ (left) and with calcium bound²⁷ (right).

Calpains have a limited and specific subsite specificity that is almost identical for both m- and μ -calpain. Several reviews^{21,28-31} on calpain inhibitors highlight that i) the P₁ position favours Leu over other amino acids and is the primary determinant of selectivity; ii) the P₂ position prefers Leu, Thr or Val but has little effect on specificity;² and iii) bulky aromatic groups such as Phe and Pro are favoured at P₃.³² Calpains are involved in many pathological diseases (described in the next section) and thus, they are ideal targets for inhibitor design. Knowledge on subsite specificity and mode of binding is critical for the design of potent and specific inhibitors. Calpains have generated much interest as these proteases have been implicated in the formation of cataracts, a disease which results in impaired vision and/or blindness.³³ For example, a topical treatment of CAT811, developed by our group, is at the forefront of cataracts treatment.³⁴

ii) Cathepsin (Cysteine Protease)

The cathepsins are a large family of cysteine proteases consisting of 11 isoforms (cathepsin B, C, F, H, K, L, O, S, V, W and X),³⁵ most of which are involved in protein degradation in lysosomes.³⁶ In particular, cathepsin L is a lysosomal cysteine protease that is synthesized as an inactive proenzyme containing an auto inhibitory 96-residue N-terminal propeptide. Removal of the propeptide from the active site produces mature cathepsin L of approximately 24kDa, which consists of two distinct left (L-) and right (R-) domains. The domains are separated by a 'V'-shaped active site cleft, whereby Cys₂₅ located in the L-domain and His₁₆₃ in the R-domain, form the catalytic active site of the enzyme (Figure

2.5).^{37,38} As per cathepsin L, cathepsin S is also a 24 kDa lysosomal cysteine protease, consisting of a single chain monomeric protein of 217 amino acids.³⁹ Unlike cathepsin L which is ubiquitously expressed, cathepsin S has a restricted tissue distribution.⁴⁰ It has two domains, which is separated by a long, narrow active site cleft where Cys₂₅, His₁₅₉ and Asn₁₇₅ are located. The structure of cathepsin S is highly similar to cathepsin L, displaying 57% sequence similarity.

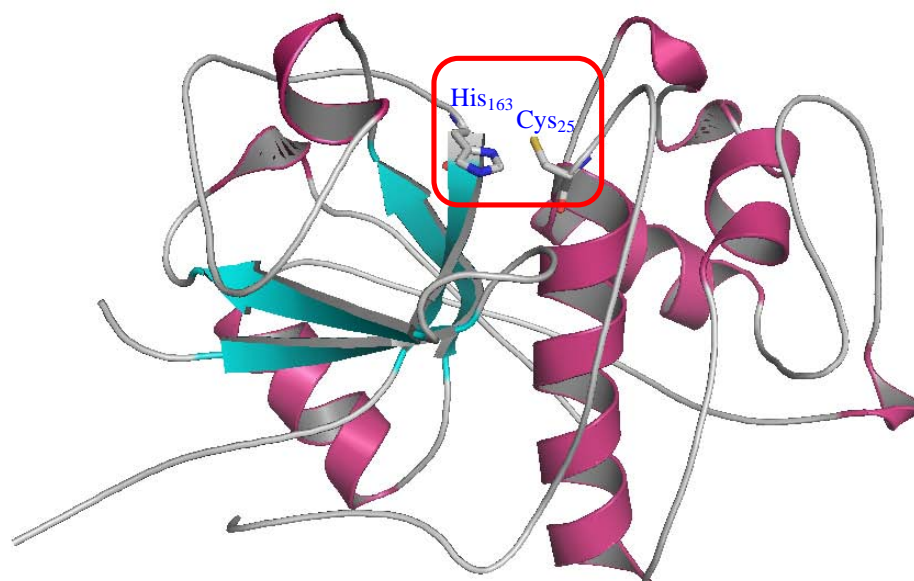


Figure 2.5 Mature cathepsin L (PDB 1ICF).⁴¹ Active site (red box) as ball and stick representation: Cys₂₅ and His₁₆₃.

Due to their structural similarity, cathepsins L and S have similar substrate specificity. In particular, both have broad substrate specificity, showing a preference for hydrophobic residues at the P₂ position, while a wide range of substituents can be accommodated at the P₁ position including Ala, Arg and Phe.^{37,39} The S₂-P₂ subsite is considered the primary determinant of specificity between cathepsin L and S, with cathepsin L preferring smaller hydrophobic groups, such as Leu and Val and cathepsin S preferring bulkier hydrophobic groups such as Phe.⁴² Portaro's study⁴³ of cathepsin L showed that bulky hydrophobic groups as well as positively charged residues (with the exception of Asp) are preferred at the P₃ position, due to the large S₃ pocket formed by the amino acids Asn₆₆, Glu₆₃ and Leu₆₉. While little structural information is known about the S₄ subsite of cathepsin L, preference for hydrophobic groups such as Phe and Leu at the P₄ position has been

shown.⁴³ In contrast, the S₃ pocket of cathepsin S is smaller than that of cathepsin L, and has a positively charged residue, Lys₆₄.⁴⁰

Cathepsins are viable drug targets due to their involvement in many diseases, such as osteoporosis, arthritis, immune-related diseases, atherosclerosis and cancer, as well as a variety of parasitic infections.^{36,44-48} Selective and potent inhibitors of cathepsin L and S are of great interest due to their involvement in tumor growth and invasion.⁴⁴⁻⁴⁶

iii) Chymotrypsin (Serine Protease)

Chymotrypsin, a member of the serine protease family,⁴⁹ contains 245 residues, arranged in two six-stranded beta barrels,⁵⁰ with the active site cleft located between the two barrels. The catalytic triad of chymotrypsin spans the active site cleft, with Ser₁₉₅ on one side and Asp₁₀₂ and His₅₇ on the other (Figure 2.6).

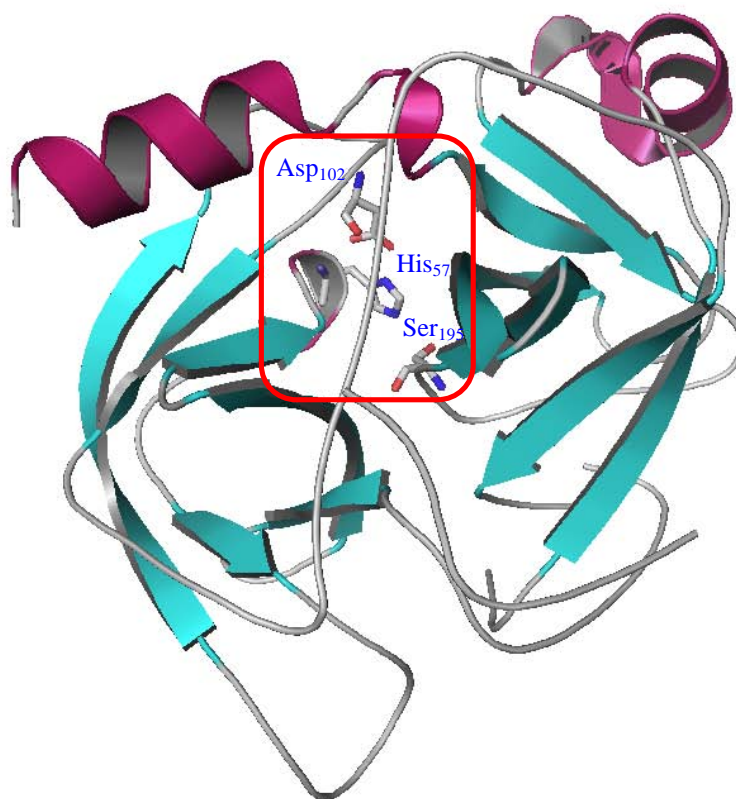


Figure 2.6 Structure of chymotrypsin (PDB 1AB9).⁵¹ Active site (red box) as ball and stick representation: Ser₁₉₅, Asp₁₀₂ and His₅₇.

Within the serine protease family, substrate binding is dominated by the S_1 - P_1 interaction. The S_1 subsite of α -chymotrypsin is characterised by a deep hydrophobic pocket and thus, large hydrophobic residues (Tyr, Trp, Phe, Leu, Met) are preferred at P_1 .⁵¹ In contrast, the S_2 - S_3 sites of chymotrypsin display little substrate discrimination, with the S_3 site being capable of accommodating both L- and D-amino acids.⁵² Apart from the S_1 - P_1 interaction, hydrogen bonding interactions between i) the carbonyl oxygen of Ser₂₁₄ and the NH of P_1 , ii) the NH of Trp₂₁₅ and the carbonyl of P_3 and iii) the carbonyl of Gly₂₁₆ and the NH of P_3 are critical for efficient substrate binding.⁵³ Chymotrypsin is one of the better studied proteases, and as such it is an ideal model for studying the versatility of an inhibitor design.

iv) Human Leukocyte Elastase (Serine Protease)

Human Leukocyte Elastase (HLE) is a hydrolytic enzyme contained within the azurophilic granules of a polymorphonuclear leukocyte. It is a glycoprotein, with a single peptide chain that forms two interacting antiparallel β -barrel cylindrical domains.^{54,55} The catalytic triad residues Ser₁₉₅, His₅₇ and Asp₁₀₂ of HLE are located in the crevice between the two domains (Figure 2.7).

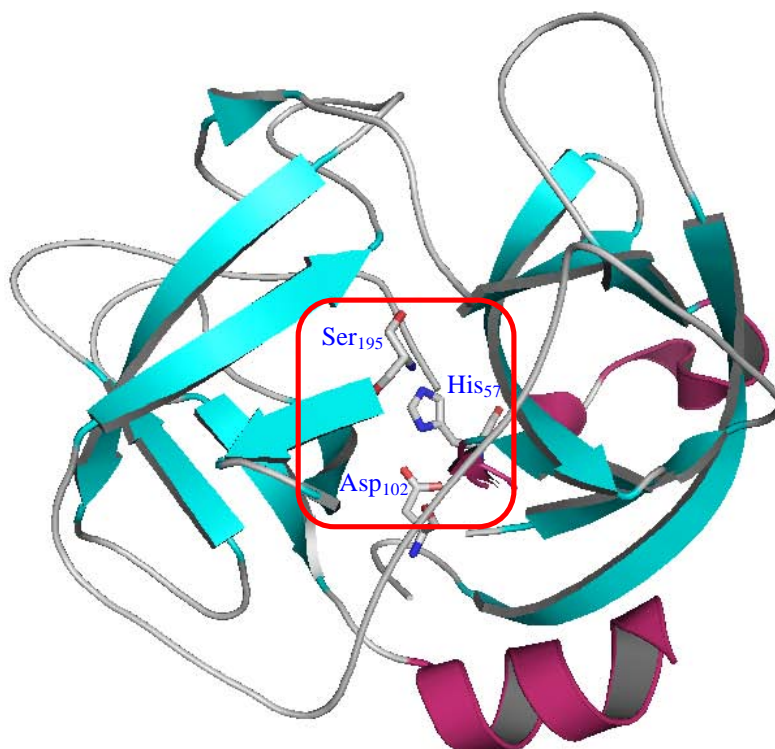


Figure 2.7 The structure of human leukocyte elastase (PDB 3Q76).⁵⁶ Active site (red box) as ball and stick representation: Ser₁₉₅, Asp₁₀₂ and His₅₇.

Studies on peptidic substrates and inhibitors against HLE⁵⁷⁻⁵⁹ have shown a clear preference for medium-sized alkyl chains at the P₁ position (e.g. Leu and Val) since the S₁ site is small due to the presence of Val₂₁₆ and Thr₂₂₆.⁶⁰ Interestingly, the nature of the P₁ substituent accommodated is dependent on substrate length, with specificity becoming broader with decreasing chain length.⁶¹ Likewise, the S₂ subsite of HLE prefers medium-sized hydrophobic side chains at P₂ and while the S₃ subsite is not important for selectivity, residues with elongated side chains do form favourable interactions with the hydrophobic surfaces of Phe₁₉₂ and Val₂₁₆.⁵⁵ Drug targets of human leukocyte elastase are of great interest due to their involvement in diseases such as chronic obstructive pulmonary diseases.^{62,63}

Physiological Implications of Cysteine and Serine Proteases.

As shown from the examples presented, cysteine and serine proteases have been implicated in numerous diseases and cellular processes and are thus, attractive targets for therapeutic drugs. The roles of the cysteine and serine proteases studied in this thesis are summarized in Table 2.1.

Table 2.1 Summary of cysteine and serine proteases and their implicated diseases.

Protease	Disease
Calpain ²¹ (cysteine)	<ul style="list-style-type: none"> • Cataracts • Muscular dystrophy • Platelet aggregation • Spinal cord injury • Thrombotic restenosis • Stroke • Brain trauma • Alzheimer • Cardiac ischaemia • Arthritis
Capathesin L/S (cysteine)	<ul style="list-style-type: none"> • Atherosclerosis⁶⁴ • Cancer^{44,65,66} • Cardiovascular Disease⁶⁷ • Rheumatoid arthritis^{68,69} • Multiple sclerosis⁶⁹
Chymotrypsin (serine)	<ul style="list-style-type: none"> • Parkinson's disease⁷⁰ • Alzheimer's disease^{71,72} • Cancer⁷³
Human Leukocyte Elastase ^{62,63} (serine)	<ul style="list-style-type: none"> • Adult respiratory distress syndrome • Pulmonary emphysema • Rheumatoid arthritis, • Cystic fibrosis • Chronic obstructive pulmonary disease

The development of non-invasive inhibitors of cysteine and serine proteases is highly desirable, as currently, there is a lack of such pharmaceutical treatments on the commercial market. As a result of their involvement in several diseases (Table 2.1), an increased understanding of these proteases will aid the treatment of diseases associated. Additionally, through specific inhibitor design, selective inhibition of proteases is a promising therapeutic strategy for combating diseases and improving the human lifestyle.

2.1.3 Current Design of Inhibitors of Cysteine and Serine Protease

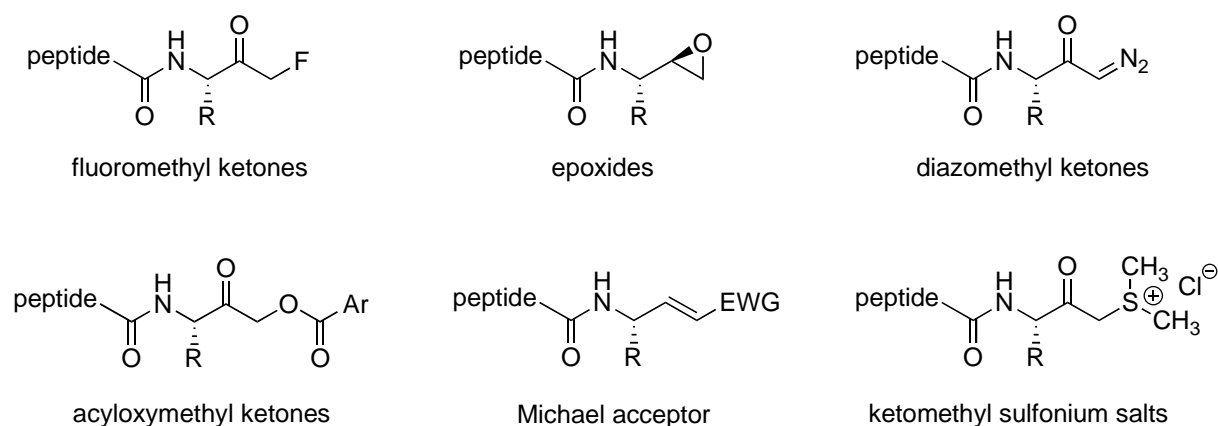
A vast number of inhibitors of serine and cysteine proteases exist, which are classified as either “active-site directed” or allosteric, depending on the mode of interaction with the enzyme.⁷⁴ “Active-site directed” protease inhibitors specifically bind to active site residues, most importantly P₁-P₃; and are further classified as either covalent/irreversible, covalent/reversible, non-covalent/irreversible or non-covalent/reversible inhibitors.¹⁶ Reversible inhibitors are removed from the active site by increasing concentrations of substrate and are characterised by non-covalent interactions (hydrogen bonding, ionic and van der Waals interaction) between the enzyme and inhibitor. However, some covalently bound inhibitors can result in reversible inhibition due to hydrolytically labile bonding. Examples of covalent reversible inhibitors include peptidyl aldehydes and nitriles as inhibitors of serine and cysteine protease. In contrast, irreversible inhibitors are commonly substrate-like and possess an electrophilic functional group capable of covalently binding to the enzyme, thereby rendering the enzyme inactive.¹⁶

Inhibitors of serine and cysteine proteases are often small peptide-based molecules consisting of 2-5 amino acids^{7,16,75} that are able to bind to specific regions of the enzyme. Reversible inhibitors are generally preferred over irreversible inhibitors in a therapeutic sense as the latter can covalently bind non-specifically to many nucleophiles en route to the intended target, resulting in toxic side effects.⁷ Additionally, for irreversible inhibitors to be effective, a high degree of selectivity is required to ensure that they do not deactivate other proteases with concomitant side effects. As a result, the design of inhibitors of serine and cysteine protease has been primarily directed towards the development of reversible inhibitors and in particular, those possessing an electrophilic isostere in order to achieve a greater affinity for the intended target.⁷

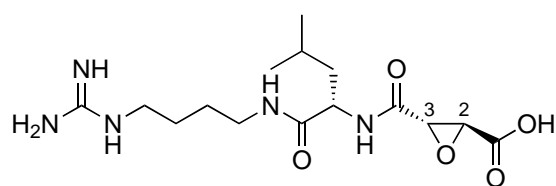
Cysteine Protease Inhibitors Features

Irreversible inhibitors of cysteine proteases typically contain electrophilic fluoromethyl ketones, epoxides, diazomethyl ketones, acyloxymethyl ketones, Michael acceptors or ketomethyl sulfonium salts (Figure 2.8a).^{16,76} For example, the epoxide-based inhibitor E-64 (**2.1**, Figure 2.8b), inhibits μ -calpain ($IC_{50} = 1.5 \mu M$), m-calpain ($IC_{50} = 1.1 \mu M$), papain ($IC_{50} = 0.29 \mu M$), cathepsin L ($IC_{50} = 0.11 \mu M$) and numerous cysteine protease, however shows no activity against serine proteases.^{6,77} The activity of E-64 is thought to be due to reaction of the thiol active site of cysteine with the C-2 carbon of the oxirane ring.^{78,79}

a) irreversible peptide inhibitors



b) selective irreversible inhibitor E-64



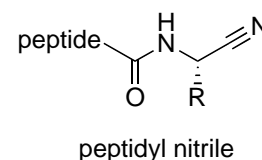
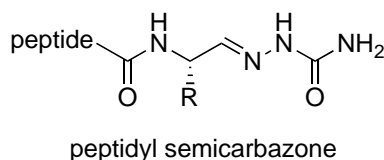
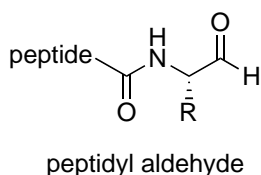
E-64 (**2.1**)

Figure 2.8 Irreversible peptide inhibitors of cysteine proteases.

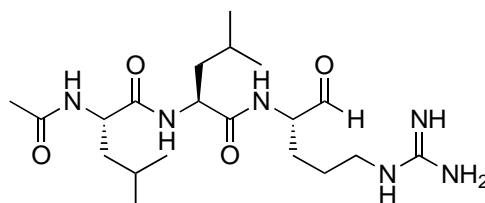
Reversible peptide inhibitors such as C-terminal aldehydes (Figure 2.9a) react with the active site cysteine to form reversible thioacetal transition-state analogues. For example, the classical peptidyl inhibitor, Leupeptin (**2.2**, Figure 2.9b), is a modest inhibitor of cathepsin B ($IC_{50} = 0.44 \mu M$), μ -calpain ($IC_{50} = 0.27 \mu M$) and m-calpain ($IC_{50} = 0.38 \mu M$), and has also been shown to inhibit serine proteases such as trypsin

($IC_{50} = 5.0 \mu M$).⁸⁰ Due to structural similarities within the cysteine proteases, peptidyl aldehydes such as leupeptin, show little selectivity between proteases within the cysteine protease family. Alternative groups, such as semicarbazones and peptidyl nitriles (Figure 2.9a), are reported to increase selectivity for one cysteine protease over another,⁷⁶ but often at the expense of potency.

a) reversible peptide inhibitors



b) selective reversible inhibitor Leupeptin (2.2)



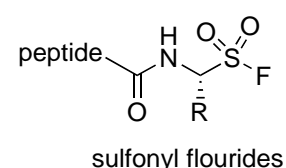
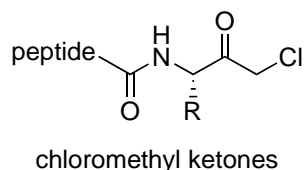
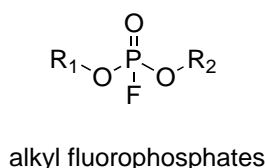
Leupeptin (2.2)

Figure 2.9 Reversible peptide inhibitors of cysteine proteases.

Serine Protease Inhibitors Features

Irreversible inhibitors of serine protease often possess a terminal electrophilic group such as an alkyl fluorophosphate, chloromethyl ketone, or sulfonyl fluoride (Figure 2.10a). Whilst, reversible inhibitors of serine protease usually possess an electrophilic functional group such as an aldehyde, boronic acid or activated ketone (Figure 2.10b) located at the C-terminus of the P_1 residue. These reversible-transition state analogues mimic the transition state of the amide bond hydrolysis when bound to the active site of the enzyme and thus, display a greater binding affinity than those that do not possess an electrophilic isostere.^{7,75}

a) irreversible peptide inhibitors



b) reversible peptide inhibitors

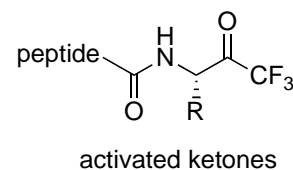
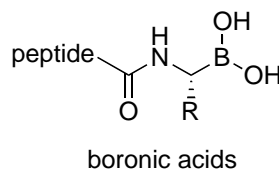
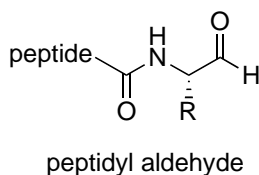


Figure 2.10 Current designs of (a) irreversible and (b) reversible peptide inhibitors of serine proteases.

Most of the protease inhibitors developed to date are relatively flexible structures that must pre-organize into a particular conformation prior to binding. More selective and potent protease inhibitors may be achieved through the development of conformationally restricted molecules that are fixed in the protease-binding conformation as discussed in the following section.⁸¹⁻⁸⁹

2.2 Improved Inhibitor Design for Cysteine and Serine Protease

2.2.1 Importance of β -Strand Conformation

Proteases (including serine, cysteine, aspartic and metallo-proteases) universally bind their substrates and inhibitors in an extended or β -strand conformation as depicted in Figure 2.11b.⁹⁰⁻⁹² This conformational requirement for recognition is defined by interactions between the P_n and S_n subsites as discussed in section 2.1.2. This important observation has led to inhibitors that are defined in a β -strand conformation by a component macrocycle. A classic β -strand is defined by torsion angles of ϕ , ψ and ω of 120° , 120° and 180° , respectively (Figure 2.11a), and is represented as an extended or “saw-tooth” arrangement of amino acids with the amide bonds being nearly co-planar. This results in

the amino acid side chains alternating above and below the plane of the peptide backbone (Figure 2.11b).⁹³ The presence of a β -strand then entropically favours binding to a protease as compared to a conformationally flexible analogue. These structures also offer advantages of increased stability to proteolytic cleavage.

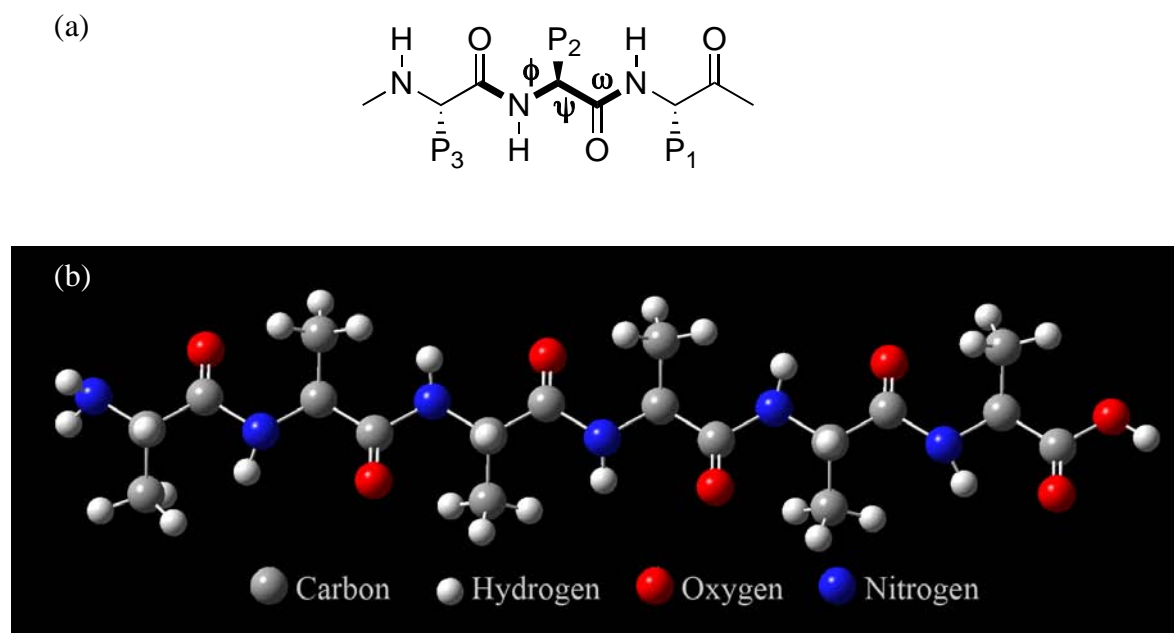


Figure 2.11 (a) Torsion angles, phi (ϕ), psi (ψ) and omega (ω); and (b) “saw-tooth” arrangement for amino acids for a peptide β -strand.

This chapter investigates the influence of constraining inhibitors into an extended β -strand conformation by linking the P_1 and P_3 or for the first time, the P_2 and P_4 residues, on binding affinity. The IC_{50} values of these inhibitors will be used to determine binding affinity; assuming that an increased binding affinity will be reflected in an increase in potency against the proteases tested (results presented in chapter 3). With few exceptions, existing macrocyclic inhibitors are constructed by linking the P_1 - P_3 residues, as illustrated by calpain inhibitor CAT811⁹⁴ (**2.3**, Figure 2.12) and serine protease inhibitor **2.4**⁸⁹ (Figure 2.13). These efforts have thus far been mainly focused on aspartic, serine and metallo proteases.⁸⁹ In addition, upon constraining both CAT811 **2.3** and inhibitor **2.4** maintain peptide-like structural features, and retain a β -strand conformation along an intact amino acid backbone. Thus far, there are no reported macrocyclic inhibitors that are constrained from the P_2 and P_4 residues. There is also a clear need to decrease the peptidic character of these inhibitors to increase biostability and drugability.

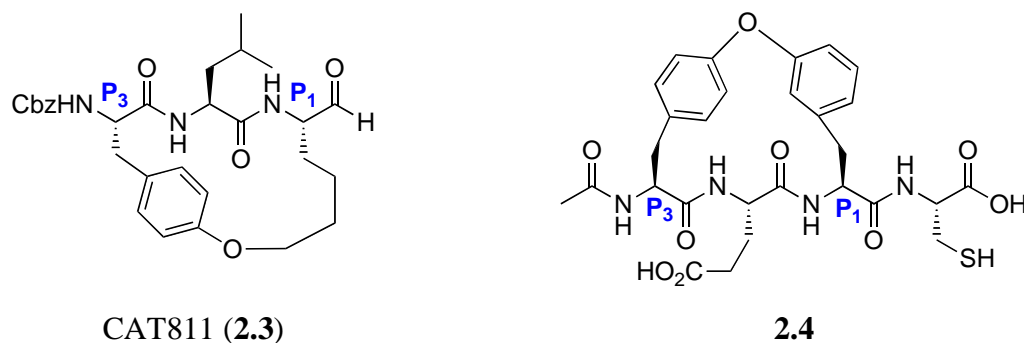


Figure 2.12 Macrocyclic inhibitors that mimic the extended β -strand conformation.

2.2.2 Importance of the Macrocycle for Conformational Constraint

Introduction of macrocyclic constraints to peptides can influence the orientation and thus, affect their ability to bind to a given protease.⁸⁹ These changes in structural orientation allow the molecule to pre-organize into a β -strand conformation that promotes the binding of the modified peptide to the active site. Several examples exist whereby the incorporation of a macrocycle into a peptide inhibitor amplifies the potency of the inhibitor. For example, Fairlie and co-workers⁸¹ compared the acyclic HIV-1 protease inhibitor **2.5** with its cyclic analogue **2.6** in competitive enzyme assays. The study showed the macrocyclic inhibitor to be more potent (75-fold) than the acyclic analogue.

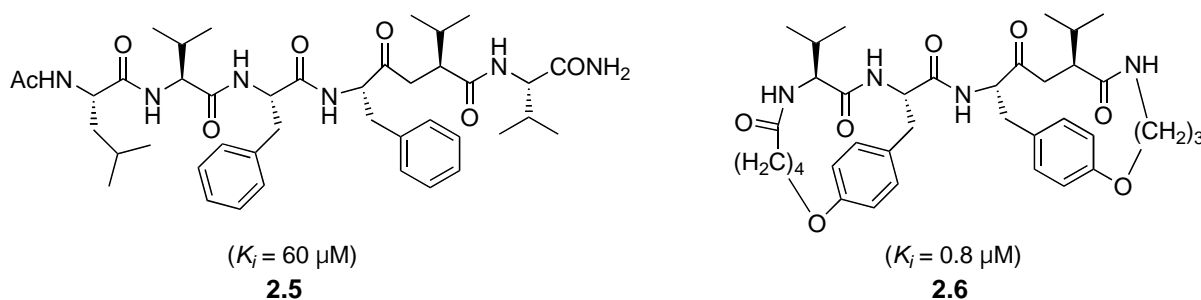


Figure 2.13 Acyclic versus macrocyclic inhibitors of HIV-1 protease.⁸¹

A similar increase in potency has been noted in our group. Macrocyclic aldehyde, CAT811 (**2.3**, Figure 2.14) was found to be approximately 4-fold more potent than its acyclic analogue, **2.7** (Figure 2.14).⁹⁴

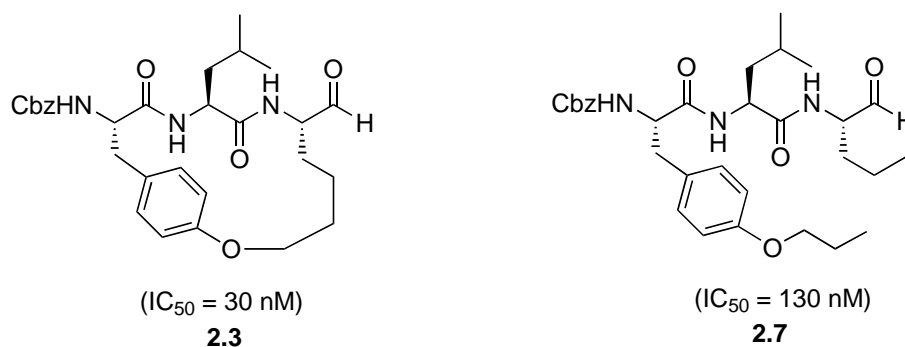


Figure 2.14 Acyclic versus macrocyclic inhibitors of m-calpain.⁹⁴

Cyclisation of peptides can be achieved by cyclisation through the N- and C- termini to form a new amide bond giving a macrocyclic system. Alternatively, the functional side groups of amino acids can be modified/utilised such that ring formation can be promoted.^{90,95} The latter will be further investigated within this study.

2.2.3 Methods for Introducing Conformation Restriction

A number of methods have been reported for introducing a conformational constraint. Constraining along the peptide backbone can be achieved through the introduction of a cyclic unit such as a lactam⁹⁶ or an aromatic pyrrole spacer,⁹⁷ which is known to promote a β -strand conformation. Additionally, an inhibitor can be conformationally constrained by macrocyclization such as ring-closing metathesis^{98,99} or Huisgen 1,3-dipolar cycloaddition as recently pioneered by us and others.^{96,100}

a) Ring-Closing Metathesis

Ring-closing metathesis is an efficient and mild method towards macrocyclization¹⁰¹ that has been widely utilised in conformationally constrained peptidomimetics (see chapter 1, section 1.2).^{97,102-107} This methodology was successfully applied to the synthesis of macrocyclic inhibitor of calpain, CAT811.⁹⁴

b) Huisgen 1,3-dipolar cycloaddition

An alternative method for macrocyclization is the Huisgen 1,3-dipolar cycloaddition.¹⁰⁸⁻¹¹¹ This form of cycloaddition has been found to be high yielding and is a highly modular reaction that is suitable for use in an aqueous environment.¹¹² Furthermore, alternating between catalysts, results in the generation of two isomeric linkers within the macrocycle

(Figure 2.15). It has been shown that the use of a copper (I) catalyst gives a 1,4-disubstituted triazole,¹¹²⁻¹¹⁴ whilst a ruthenium catalyst gives a 1,5-disubstituted triazole.¹¹⁵

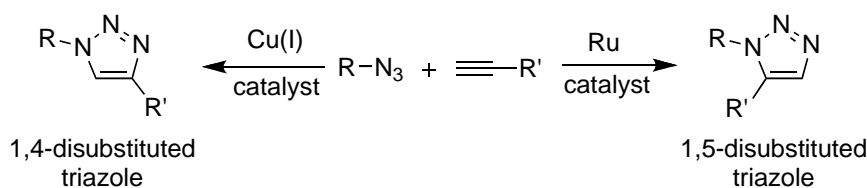


Figure 2.15 Isomeric linkers generated by Huisgen 1,3-dipolar cycloaddition.

The mechanism of copper-catalysed Huisgen 1,3-dipolar cycloaddition is outlined in Figure 2.16.¹¹⁶ Firstly, an alkyne (**a**) coordinates to a copper (I) catalyst [M] forming copper acetylide (**b**). The azide subsequently binds to the copper (**c**), resulting in the formation of a six-membered copper (III) metallacycle intermediate (**d**). Ring contraction proceeds, resulting in the formation of triazolyl-copper (**e**), followed by protonolysis to give the desired 1,4-triazole (**f**).

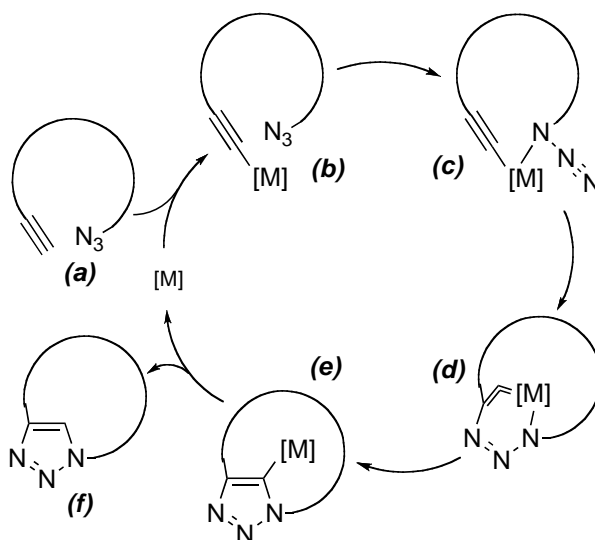


Figure 2.16 Mechanism of copper-catalysed Huisgen 1,3-dipolar cycloaddition. [M] is used to denote the copper catalyst and attached ligands.¹¹⁶

The Huisgen 1,3-dipolar cycloaddition has been successfully used in our group to furnish calpain inhibitors¹⁰⁰ (Figure 2.17) and provides a general means of constraining flexible peptides into the preferred β -strand geometry.

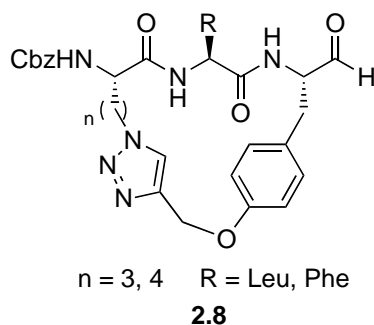


Figure 2.17 Constraining P₁ and P₃ residues by Huisgen 1,3-dipolar cycloaddition for the generation of macrocyclic β -stranded inhibitors.¹⁰⁰

2.3 Design and Synthesis of Macrocyclic Protease Inhibitors

Whilst cyclisation is an important tool for inducing preferred conformations of inhibitors, many of the current inhibitors are still highly peptidic in nature. We suggest that the introduction of a planar aromatic group, such as pyrrole, into the peptide backbone would reduce peptidic character while maintaining or even enhancing the β -strand geometry. Such structures should also have improved proteolytic stability.

This chapter describes the design and synthesis of a new class of macrocyclic protease inhibitor with a planar aromatic spacer in the peptide backbone that decreases the peptidic character while maintaining an appropriate geometry for protease binding. Two novel series of P₁-P₃ and P₂-P₄ cyclised protease inhibitors are presented (Figure 2.18). The pyrrole aromatic spacer in the backbone of the inhibitor retains the β -strand conformation while reducing the peptidic nature of the inhibitor. The macrocycle core is introduced by either ring closing metathesis or Huisgen 1,3-dipolar cycloaddition.

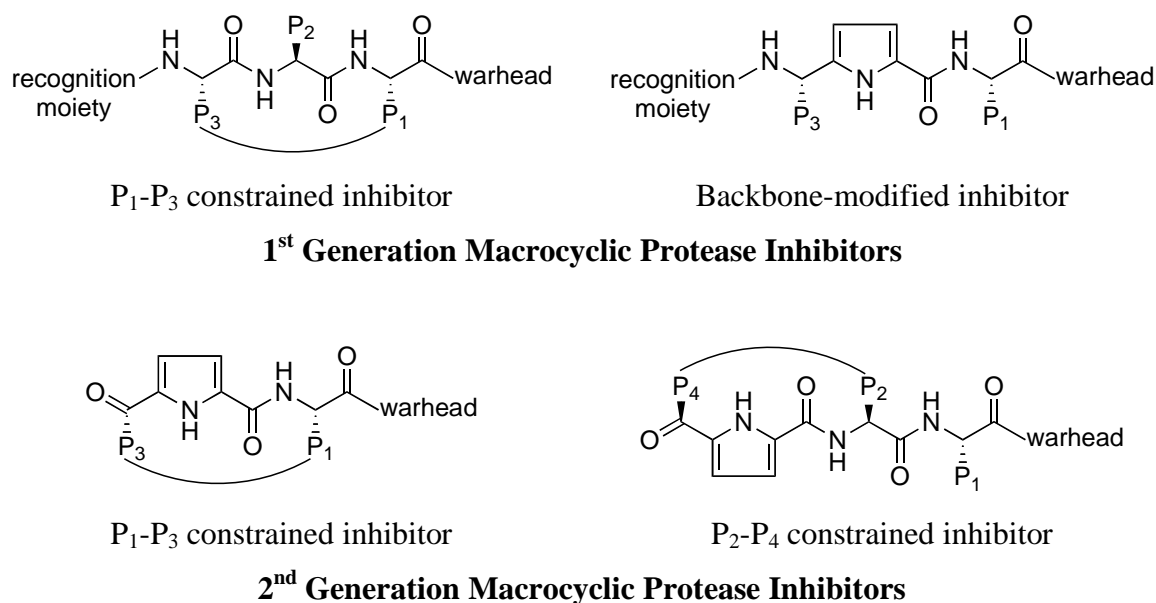
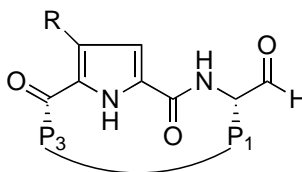
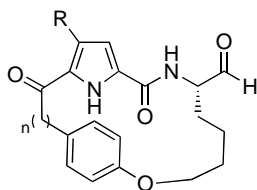
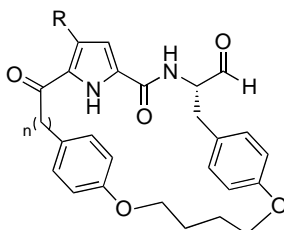


Figure 2.18 Scaffold of 1st generation inhibitors and 2nd generation macrocyclic protease inhibitors, which includes both cyclisation and introduction of a planar aromatic group.

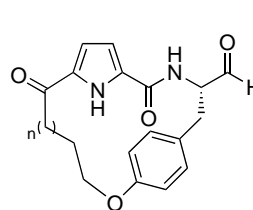
The target inhibitors (designated 2nd generation macrocycles) are outlined in Figure 2.19. An electrophilic aldehyde is incorporated at the C-terminus to allow reversible inhibition of the active sites of both serine and cysteine proteases. An aryl group was incorporated into the P₁ and/or P₃ position (Figure 2.19a); or the P₂ and/or P₄ position (Figure 2.19b) to further constrain the geometry of the inhibitor and to explore potential specificity effects based on binding preferences at this position. Additionally, varying the amino acid at P₁, P₂, and P₄ position should provide selectivity between protease families and classes (see section 2.1.2 for details on selectivity). For example, calpains^{21,28-31} are known to prefer Leu in the P₁ position, while chymotrypsin⁵¹ prefers Phe in the P₁ position. Using this knowledge, protease selectivity can be investigated by a simple change of the amino acid residue in the P₁ position to give the P₂-P₄ constrained macrocycles (Figure 2.19b).

a) P₁-P₃ Constrained 2nd Generation Protease InhibitorsR = H, CH₃P₃ = aryl, alkylP₁ = aryl, alkyl

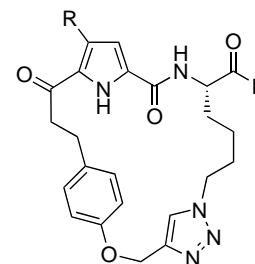
2.9 R = H, n = 1
 2.10 R = H, n = 2
 2.11 R = CH₃, n = 1
 2.12 R = CH₃, n = 2



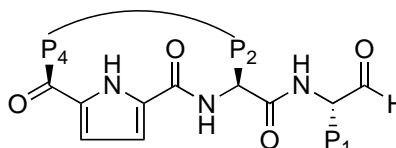
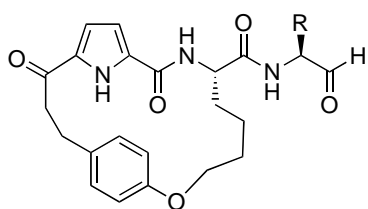
2.13 R = H, n = 1
 2.14 R = H, n = 2
 2.15 R = CH₃, n = 1
 2.16 R = CH₃, n = 2



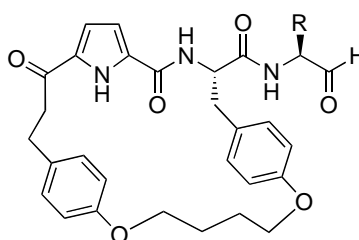
2.17 n = 1
 2.18 n = 2



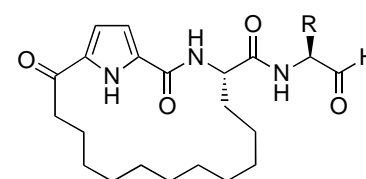
2.19 R = H
 2.20 R = CH₃

b) P₂-P₄ Constrained 2nd Generation Protease InhibitorsP₄ = aryl, alkylP₂ = aryl, alkylP₁ = Leu, Phe

2.21 R = Leu
 2.22 R = Phe



2.23 R = Leu
 2.24 R = Phe



2.25 R = Leu
 2.26 R = Phe

Figure 2.19 Target P₁-P₃ and P₂-P₄ constrained 2nd generation protease inhibitors.

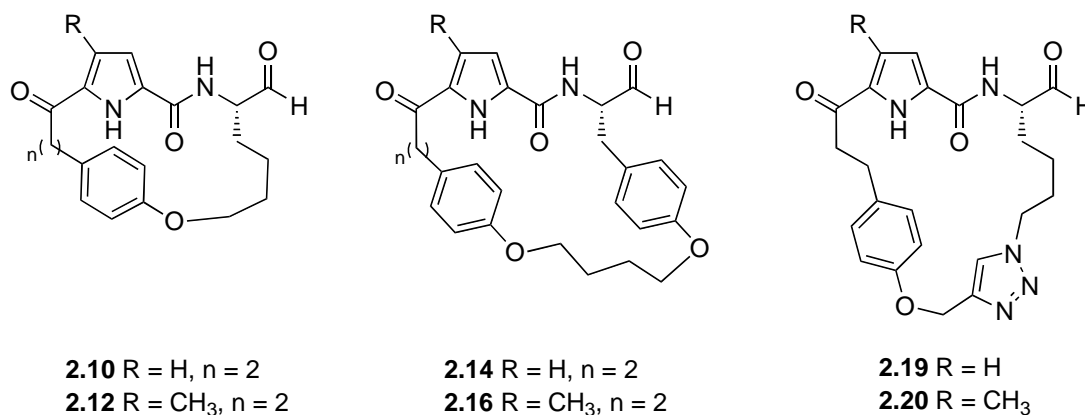
2.3.1 Molecular Modelling of Macrocyclic Protease Inhibitors

P₁-P₃ 2nd Generation Protease Inhibitors

The target macrocycles **2.10**, **2.12**, **2.14**, **2.16**, **2.19** and **2.20** (see Figure 2.19a) were subjected to preliminary molecular and docking studies against calpain, as conducted by a postdoctoral fellow in our group at the University of Canterbury (Dr. Steve McNabb). Molecular modelling was performed with Schrodinger Suite, 2005. The crystal structure of human mini calpain I (PDB 1ZCM)²⁵ was prepared using the protein preparation facility in Glide 4.0, by mutation *in silico* of Ser₁₁₅ to Cys₁₁₅ to re-establish the natural amino acid composition of calpain I (μ -calpain), followed by deprotonation of Cys₁₁₅ and protonation of His₂₇₂. The *in silico* ovine homology models were created by virtual mutation of the appropriate residues around the active site cleft. This structure was minimized using the OPLS2005 force field with a GB/SA water model. A docking grid was generated, and inhibitors were docked into the calpain model using GLIDE (Schrodinger)^{117,118} to establish the docking of the compounds.

Molecular and docking studies evaluate the position of this aldehyde carbonyl and its susceptibility for nucleophilic attack from the thiol cysteine, as required for reversible, covalent inhibition of calpain.⁹⁴ The target structures **2.10**, **2.12**, **2.14**, **2.16**, **2.19** and **2.20** were docked into ovine calpain I (μ -calpain) and ovine calpain II (m -calpain) 1st generation homology model, which exhibits a close homology to the human crystallin sequences.¹¹⁹ The results and parameters for the docking studies of macrocycles **2.10**, **2.12**, **2.14**, **2.16**, **2.19** and **2.20** are outlined in Table 2.2.

Table 2.2 Docking studies and parameters of macrocycles **2.10**, **2.12**, **2.14**, **2.16**, **2.19** and **2.20** against ovine calpain I/II.



Compound	Grid	Most Representative Pose	
		H-bonds ^{b,c}	WHD ^a (Å)
2.10	o-CAPN1	Gly ₂₀₈ (A), Gly ₂₀₈ (D), Gly ₂₇₁ (A), Ser ₂₅₁	3.96
	o-CAPN2	Gly ₁₉₈ (D), Gly ₂₆₁ (A)	4.33
2.12	o-CAPN1	Gly ₂₀₈ (A), Gly ₂₀₈ (D), Gly ₂₇₁ (A)	3.28
	o-CAPN2	Gly ₁₉₈ (A), Gly ₁₉₈ (D), Gly ₂₆₁ (A)	3.61
2.14	o-CAPN1	Gly ₂₀₈ (A), Gly ₂₀₈ (D), Gly ₂₇₁ (A), Ser ₂₅₁	3.77
	o-CAPN2	Gly ₁₉₈ (D), Gly ₂₆₁ (A), Ser ₂₄₁	3.59
2.16	o-CAPN1	Gly ₂₀₈ (D), Gly ₂₇₁ (A)	3.80
	o-CAPN2	Gly ₁₉₈ (A), Gly ₁₉₈ (D), Gly ₂₆₁ (A), Ser ₂₅₀	3.56
2.19	o-CAPN1	Gly ₂₀₈	3.48
	o-CAPN2	Gly ₁₉₈ (A), Gly ₁₉₈ (D), Gly ₂₆₁ (A), Ser ₂₄₁	3.92
2.20	o-CAPN1	Gly ₂₀₈ (D), Gly ₂₇₁ (A)	3.31
	o-CAPN2	Gly ₁₉₈ (A), Gly ₁₉₈ (D), Gly ₂₆₁ (A)	3.60

^a Warhead distance (WHD) is the distance between the carbonyl carbon of the aldehyde and the active site cysteine sulfur in Å

^b Hydrogen bonds from the carbonyl group of Gly₂₀₈, the NH group of Gly₂₀₈ and the carbonyl group of Gly₂₇₁ of the ovine I (o-CAPN1) homology model are labelled Gly₂₀₈(A), Gly₂₀₈(D) and Gly₂₇₁(A), respectively.

^c The analogous hydrogen bonds from the carbonyl group of Gly₁₉₈, the NH group of Gly₁₉₈ and the carbonyl group of Gly₂₆₁ of the ovine II (o-CAPN2) homology model are also labelled Gly₁₉₈(A), Gly₁₉₈(D) and Gly₂₆₁(A), respectively.

Representative poses of **2.10** and **2.14** (Figure 2.20) suggest that these compounds bind with ovine calpain II homology model with the required β -strand backbone conformation. In addition, the carbonyl aldehydes were orientated to allow nucleophilic attack of the thiol (Cys_{105}) of the enzyme active site, with a distance of 4.33 Å and 3.59 Å for macrocycles **2.10** and **2.14**, respectively. Macrocycles **2.10** and **2.14** adopted hydrogen bonds with Gly_{198} , Gly_{261} and Ser_{241} , suggesting that they bind tightly within the binding pocket. The well-defined interactions of macrocycles **2.10**, **2.12**, **2.14**, **2.16**, **2.19** and **2.20** with model ovine calpain I/II suggest that these compounds are promising targets as inhibitors of cysteine and serine proteases.

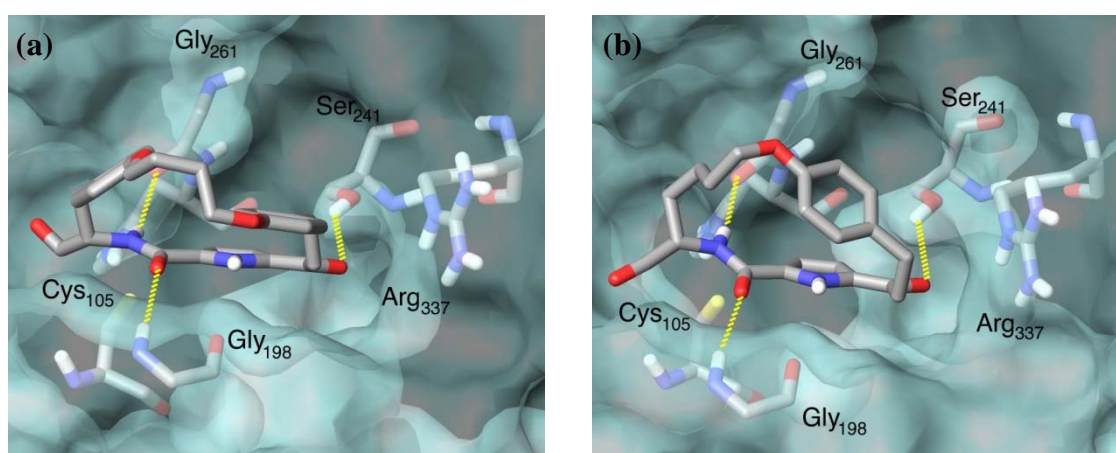
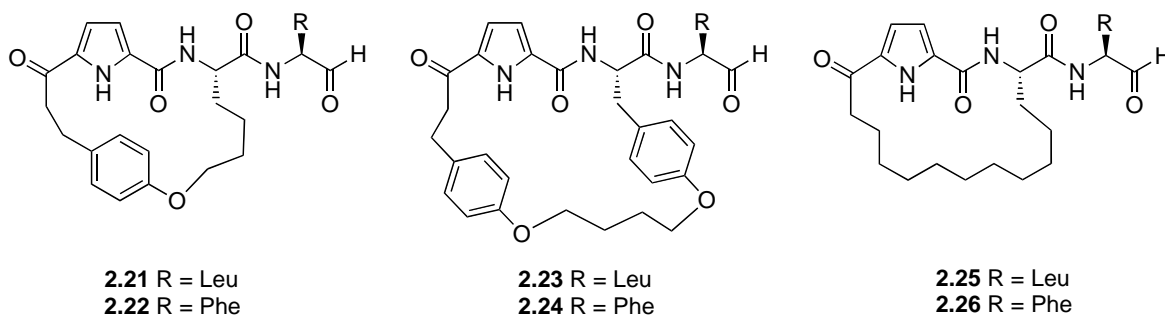


Figure 2.20 (a) Macrocycle **2.10** and (b) macrocycle **2.14** docked with ovine calpain II 1st generation homology model. Hydrogen bonding interactions with the corresponding amino acid are shown as yellow dashed lines.

P₂-P₄ 2nd Generation Protease Inhibitors

Molecular modelling and docking studies of the P₂-P₄ macrocycles **2.21**–**2.26** (see Figure 2.19b) with calpain were conducted in collaboration with Dr. Matt Sykes and Mr. Steven Nguyen (University of South Australia, Australia). Molecular modelling was conducted with OpenEye Scientific Software, 2010.¹²⁰ The crystal structure of rat mini calpain I (PDB 2G8E)¹²¹ was prepared using FRED Receptor, by removal of co-crystallized ligand, calcium ions and water molecules; followed by the addition of the following parameters: inner contour of 101 Å; outer contour of 1706 Å; custom constraint centred around sulphur of the active site cysteine; and a SMARTS constraint selecting for the aldehyde group. A docking grid was generated, and inhibitors were docked to the calpain model using FRED (version 2.2.5) to establish the docking of the compounds.

Table 2.3 Docking studies and parameters of macrocycles **2.21-2.26** against rat calpain I (rCAPN1)

Compound	Grid	Most Representative Pose	
		H-bonds ^b	WHD ^a (Å)
2.21	rCAPN1	Gly ₂₀₈ (A), Gly ₂₀₈ (D), Gly ₂₇₁ (A)	2.60
2.22	rCAPN1	Gly ₂₀₈ (A), Gly ₂₀₈ (D), Gly ₂₇₁ (A)	3.61
2.23	rCAPN1	Gly ₂₀₈ (A), Gly ₂₀₈ (D), Gly ₂₇₁ (A), Lys ₃₄₇ , Gly ₂₀₇	2.89
2.24	rCAPN1	Gly ₂₀₈ (D), Gly ₂₇₁ (A)	3.48
2.25	rCAPN1	Gly ₂₀₈ (A), Gly ₂₀₈ (D), Gly ₂₇₁ (A)	3.01
2.26	rCAPN1	Gly ₂₀₈ (A), Gly ₂₀₈ (D), Gly ₂₇₁ (A)	3.60

^a Warhead distance (WHD) is the distance between the carbonyl carbon of the aldehyde and the active site cysteine sulfur in Å

^b Hydrogen bonds from the carbonyl group of Gly₂₀₈, the NH group of Gly₂₀₈ and the carbonyl group of Gly₂₇₁ of the rCAPN1 homology model are labelled Gly₂₀₈(A), Gly₂₀₈(D) and Gly₂₇₁(A), respectively.

Representative poses of **2.23** and **2.25** (Figure 2.21) suggest that these compounds bind with rat calpain I homology model with the required β -strand backbone conformation. In addition, the carbonyl aldehydes were shown to be orientated to allow nucleophilic attack of the thiol (Cys₁₀₅) of the enzyme active site, with a distance of 2.89 Å and 3.01 Å for macrocycles **2.23** and **2.25**, respectively. Macrocycles **2.23** and **2.25** adopted hydrogen bonds with Gly₂₀₈ and Gly₂₇₁. The macrocycle **2.23** showed additional hydrogen bonds with Lys₃₄₇ and Gly₂₀₇, suggesting that it binds tightly within the binding pocket. The well-defined interactions of macrocycles **2.21-2.26** with model rat calpain I suggest that these compounds would be promising targets as inhibitors of cysteine and serine proteases.

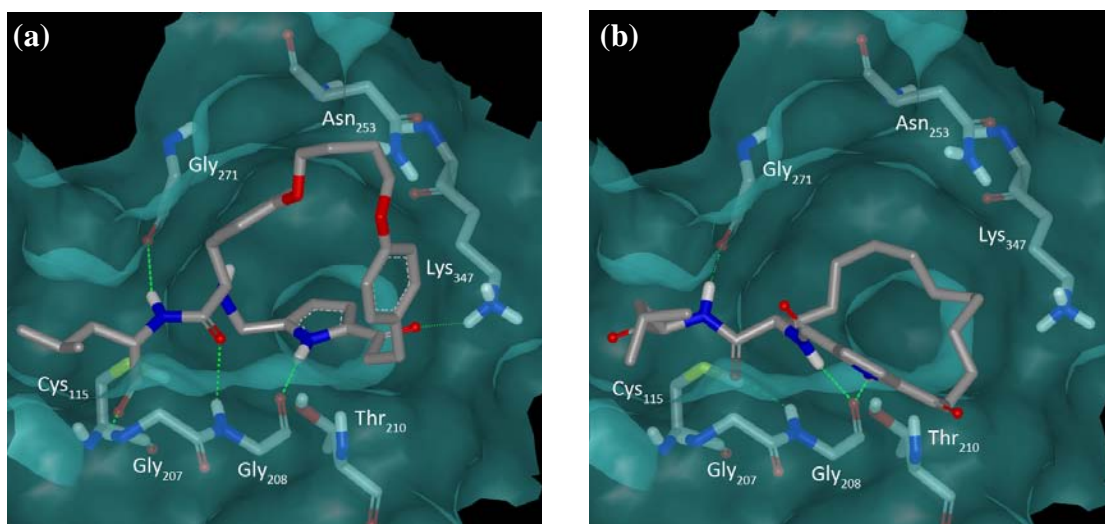


Figure 2.21 (a) Macrocycle **2.23** and (b) Macrocycle **2.25** docked with rat calpain I. Hydrogen bonding interactions with the corresponding amino acid are shown as green dashed lines.

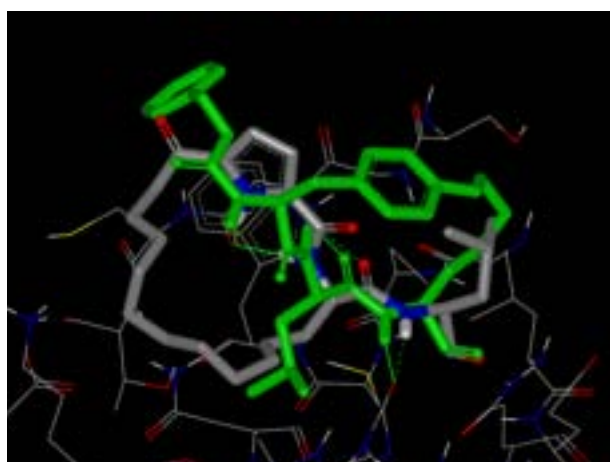


Figure 2.22 Overlay of CAT811 (1st generation P₁-P₃ macrocycle; green carbon) and macrocycle **2.25** (2nd generation P₂-P₄ macrocycle; grey carbon) showing alignment of peptide backbone.

A structural overlay of the P₂-P₄ macrocycle **2.25** with the 1st generation P₁-P₃ macrocyclic calpain inhibitor, CAT811 (Figure 2.22) shows good alignment of the peptide backbone and similar positioning of the aldehyde group. This suggests that the P₂-P₄ macrocycles are capable of adopting the β -strand conformation required for tight binding and has the potential to act as calpain inhibitors.

The subsequent sections highlight the synthesis of these P₁-P₃ and P₂-P₄ macrocyclic aldehydes using ring closing metathesis (RCM) or Huisgen 1,3-dipolar cycloaddition for the generation of potential proteases inhibitors.

2.3.2 Synthesis of 2nd Generation Macrocycles by Ring Closing Metathesis (RCM)

The target P₁-P₃ and P₂-P₄ 2nd generation macrocycles **2.9-2.18** and **2.21-2.26** were prepared from a common macrocyclic core **A**, which can be obtained from pyrroles **F** and acid chlorides **G**, as outlined in Figure 2.23. Friedel-Craft's acylation of pyrroles **F**, followed by hydrolysis and amidation of the resulting pyrroles **E** with amino acids **D** would give acyclic peptides **C**. The key macrocyclic core **A** can then be obtained by ring-closing metathesis of acyclic peptide **C**, followed by palladium-catalysed reduction of macrocycle **B**. Reduction of the C-terminal methyl ester would then give the required P₁-P₃ macrocyclic aldehydes. P₂-P₄ macrocycles can be obtained from hydrolysis of macrocyclic core **A**, followed by amidation with requisite amino alcohol and subsequent oxidation to the required aldehydes. Initially, the optimal reaction conditions for the synthesis of macrocyclic core **A** was investigated and is outlined below.

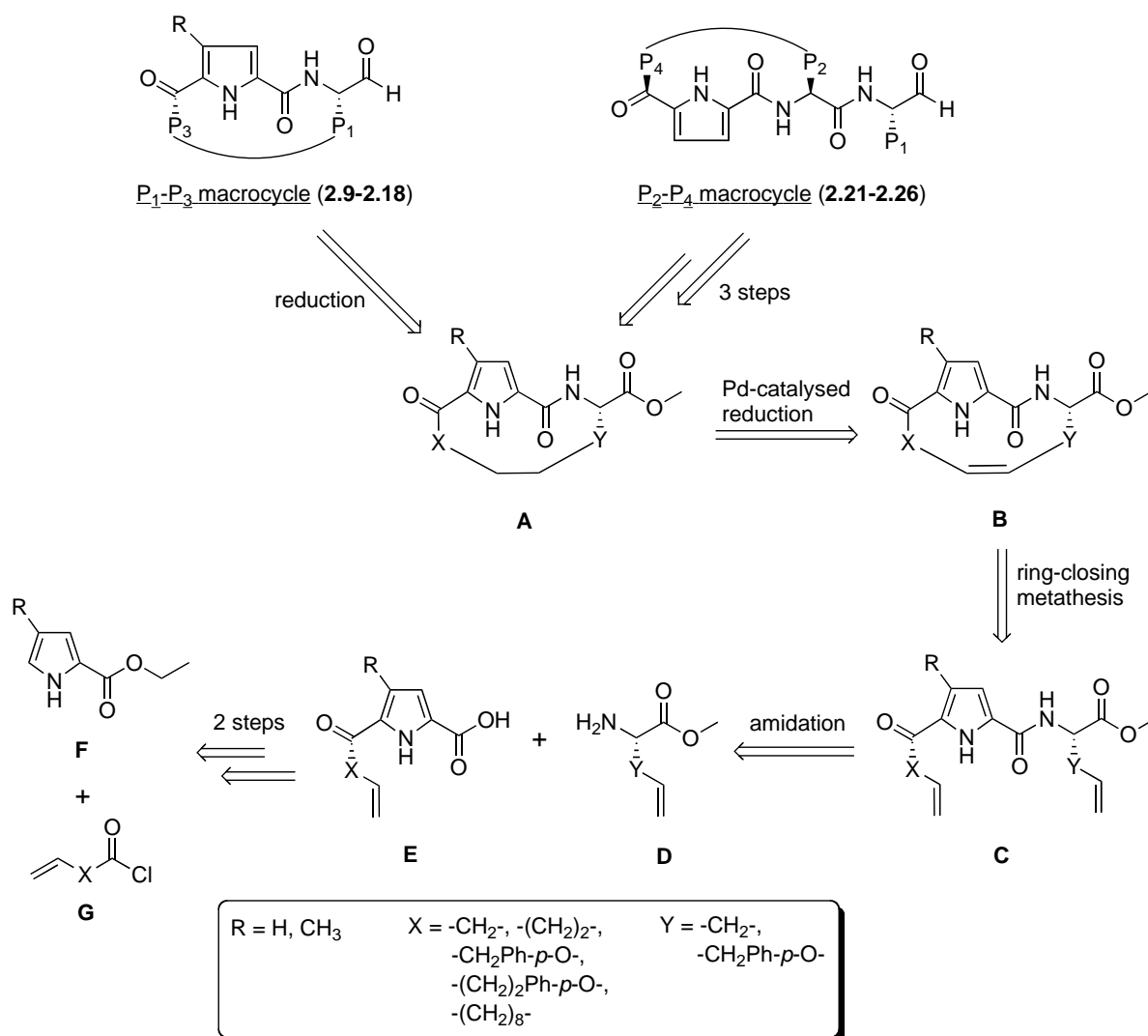
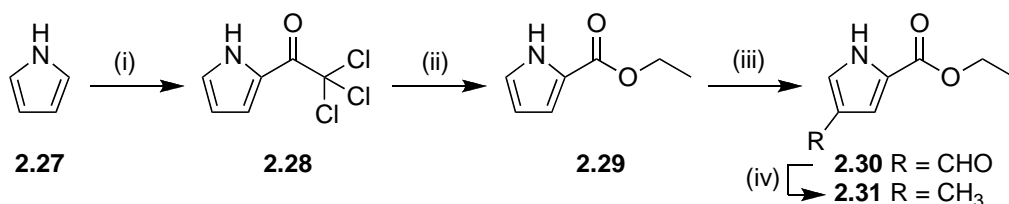


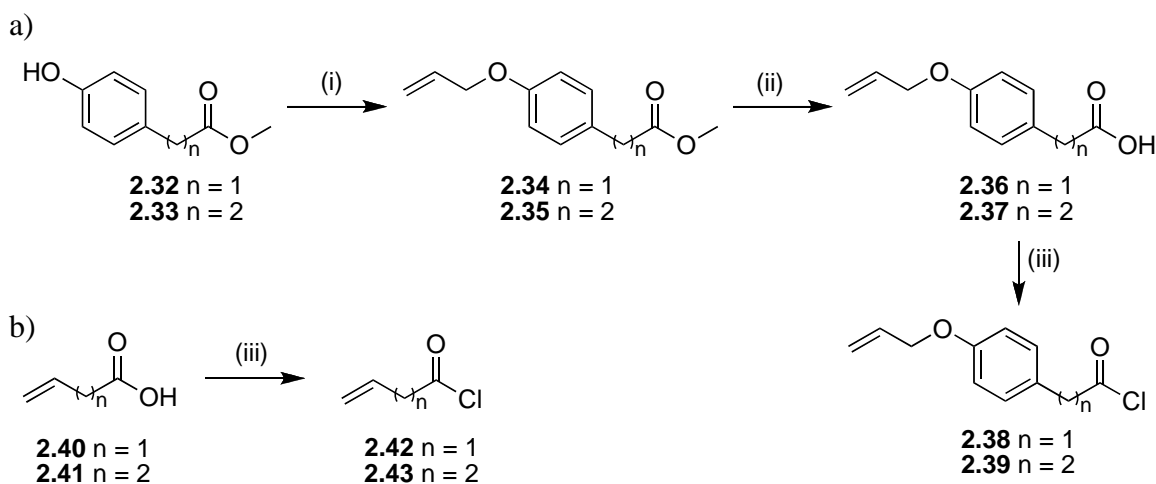
Figure 2.23 Retrosynthetic analysis of P_1 - P_3 and P_2 - P_4 macrocyclic aldehydes from macrocyclic core **A**

Pyrrole **2.27** was acylated at C_2 with trichloroacetyl chloride to give pyrrole **2.28** in good yield using a literature-based procedure.¹¹⁰ Nucleophilic substitution of trichloro pyrrole **2.28** with sodium ethoxide¹²² gave the required ethyl 1*H*-pyrrole-2-carboxylate **2.29**, which was subsequently reacted with 1,1-dichlorodimethyl ether in the presence of aluminium chloride¹²³ to give pyrrole **2.30**. Palladium/carbon reduction of pyrrole **2.30** gave the key 2,4-substituted pyrrole **2.31** in excellent yields (Scheme 2.1).



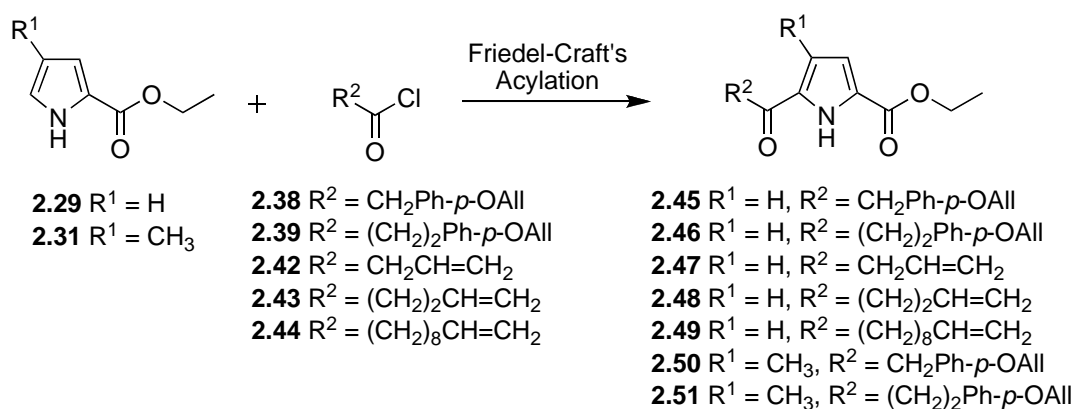
Scheme 2.1 Reagents and Conditions: i) $(\text{Cl})_3\text{CCOCl}$, Et_2O , rt, 3 h (84%); ii) NaOEt , EtOH , rt, 40 min, (91%); iii) MeOCHCl_2 , AlCl_3 , CH_2Cl_2 , CH_3NO_2 , $-20\text{ }^\circ\text{C}$, 18 h (44%); iv) H_2 , Pd/C , EtOH , rt, 9.5 h, (95%).

The other key starting materials, allyl derivatives **2.38**, **2.39**, **2.42** and **2.43** were prepared, to allow generation of 2,5- and 2,4,5-substituted pyrroles **2.45-2.51**, as shown in Scheme 2.3. *O*-Allylation¹²⁴ of commercially available methyl 4-hydroxyphenylacetate **2.32** and methyl 3-(4-hydroxyphenyl)propionate **2.33** gave esters **2.34** and **2.35**, respectively, in quantitative yields (Scheme 2.2). Subsequent saponification¹²⁵ of esters **2.34** and **2.35** gave carboxylic acids **2.36** and **2.37**, which were separately reacted with thionyl chloride^{126,127} to give acid chlorides **2.38** and **2.39** in excellent yields as shown in Scheme 2.2. These acid chlorides were used immediately without further purification. Commercially available 3-butenic acid **2.40** and 4-pentenoic acid **2.41** were similarly reacted with thionyl chloride^{126,127} to furnish acid chlorides **2.42** and **2.43** in quantitative yields (Scheme 2.2).

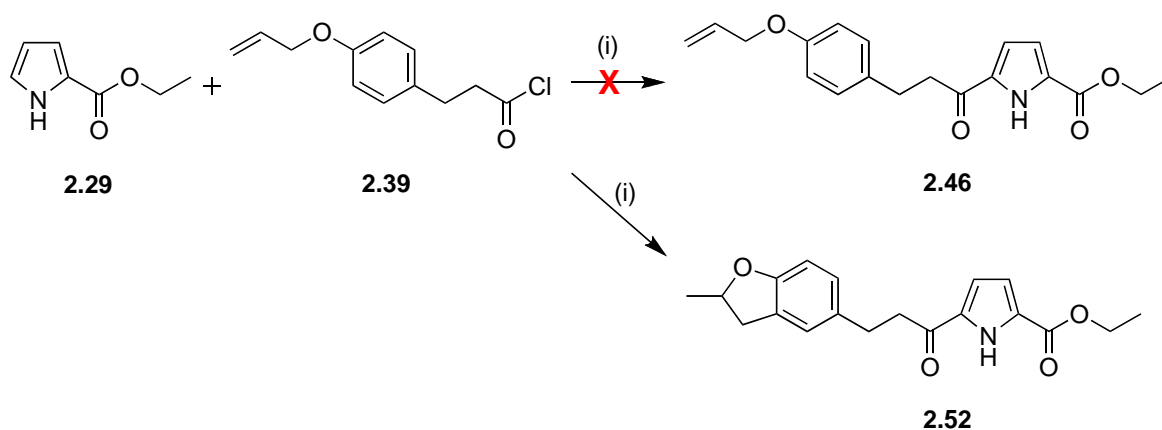


Scheme 2.2 Reagents and Conditions: i) Allyl Bromide, K_2CO_3 , TBAI, DMF , rt, 18 h, (100%); ii) $\text{LiOH}\cdot\text{H}_2\text{O}$, THF , H_2O , $40\text{ }^\circ\text{C}$, 3.5 h, (99-100%); iii) SOCl_2 , CH_2Cl_2 , $40\text{ }^\circ\text{C}$, 18 h, (100%).

With pyrroles **2.29/2.31** in hand, Friedel-Craft's acylation in the presence of acid chlorides **2.38/2.39/2.42/2.43/2.44** was attempted to give pyrroles **2.45-2.51** as shown in Scheme 2.3. Friedel-Crafts acylation of pyrroles with acid chlorides has been carried out in the presence of zinc chloride.¹²⁸ However, treatment of 2,5-substituted pyrrole **2.29** with allyl acid chloride **2.39**, in the presence of zinc chloride at 50 °C, failed to give the desired pyrrole **2.46**. Instead, pyrrole **2.52** was obtained as a result of a tandem Lewis acid catalysed Claisen rearrangement¹²⁹⁻¹³¹ of the tethered allyl phenyl ether as shown in Scheme 2.4. Several other Lewis acids have been shown to catalyse this Claisen hydroaryloxylation, such as aluminium chloride, boron trifluoride and zinc chloride,¹²⁹ and transition metal complexes, (e.g. copper (II) triflate, iridium (III) chloride/silver triflate,¹³¹ silver triflate, silver perchlorate¹³² and scandium (III) triflate).¹³⁰



Scheme 2.3 Friedel-Craft's acylation of pyrroles **2.29/2.31**.

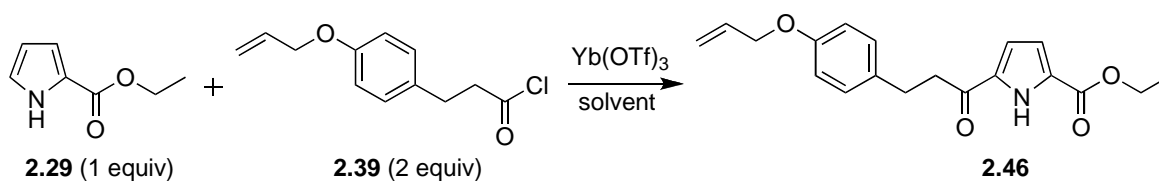


Scheme 2.4 Reagents and Conditions: i) ZnCl₂, 1,2-DCE, 50 °C (13%)

Ytterbium (III) triflate (Yb(OTf)₃), a transition metal complex, has also been shown to promote Friedel-Crafts acylation of pyrrole derivatives in nitromethane at room

temperature.¹¹⁹ Additionally, Yb(OTf)₃ has been shown to facilitate acylation without promoting the undesired Claisen hydroaryloxylation of the allyl phenyl ether motif.¹³³ As such, Friedel-Crafts acylation of pyrrole **2.29** was attempted in the presence of ytterbium (III) triflate (Yb(OTf)₃).

Reaction of pyrrole **2.29** and acid chloride **2.39**, in the presence of Yb(OTf)₃ catalyst (0.1 equiv) in nitromethane, gave the desired 2,5-substituted pyrrole **2.46** in moderate yield, see Table 2.4, entry 1. This yield is in accordance with known examples of Friedel-Crafts acylations of pyrroles.^{128,134} However, since pyrroles **2.45-2.51** are key intermediates in the synthesis of P₁-P₃ and P₂-P₄ 2nd generation macrocycles **2.9-2.18** and **2.21-2.26**, an optimisation of Friedel-Crafts acylation of pyrrole **2.46** was attempted as outlined in Table 2.4. Reaction of pyrrole **2.29** and acid chloride **2.39** with an increased Yb(OTf)₃ catalyst loading (0.5 and 1 equiv) resulted in an increased rate of consumption of the starting pyrrole, see Table 2.4, entries 2 and 3. However, a decrease in the isolated yields of the desired pyrrole **2.46** was observed due to the formation of a complex mixture of products that could not be efficiently separated. Treatment of pyrrole **2.29** and acid chloride **2.39** with 0.05 equivalents of Yb(OTf)₃ resulted in increased reaction times and did not improve yields of the desired product, Table 2.4, entry 4. The lower yield was consistent with the recovery of the starting pyrrole, while the increased reaction times allowed competing reactions to occur. Reaction of Yb(OTf)₃ (0.1 equiv) with pyrrole **2.29** and acid chloride **2.39** in either dichloromethane or 1,2-dichloroethane as a solvent instead of nitromethane, resulted in an increased reaction time and decreased yields of pyrrole **2.46**, Table 2.4, entries 5 and 6. Additionally, starting pyrrole **2.29** was recovered and a complex mixture of products that could not be efficiently separated was obtained, resulting in lower isolated yields.

Table 2.4 Optimisation of Friedel-Craft's acylation of pyrrole **2.29** and acid chloride **2.39**

Entry	Solvent	Equivalents Yb(OTf) ₃ ^a	Reaction time (h)	Yield of 2.46 (%)
1	Nitromethane	0.1	21	40^c
2	Nitromethane	0.5	2.5	11 ^d
3	Nitromethane	1	2.5	5 ^c
4	Nitromethane	0.05	140 ^b	23 ^c
5	Dichloromethane	0.1	140 ^b	26 ^d
6	1,2-Dichloroethane	0.1	140 ^b	11 ^c

^a Equivalents relative to **2.29**. ^b Starting material **2.29** recovered. ^c One-fold or ^d two-fold column chromatography (silica gel, EtOAc/petroleum ether 1 : 4) was utilised in purification of **2.46**.

With optimized conditions for the Friedel-Crafts acylation of 2,5-substituted pyrroles established, pyrroles **2.29** and **2.31** were allowed to separately react with acid chlorides **2.38**, **2.39**, and **2.42-2.44** under these conditions as shown Scheme 2.5. Pyrrole **2.29** was successfully acylated with acid chlorides **2.38**, **2.39** and **2.44** to give 2,5- substituted pyrrole **2.45**, **2.46** and **2.49** in low to moderate yields, see Table 2.5, entries 1, 2 and 5. However, synthesis of pyrrole **2.45** required 0.2 equivalents of Yb(OTf)₃ catalyst and an extended reaction time (93 h) to facilitate consumption of starting pyrrole **2.29**.

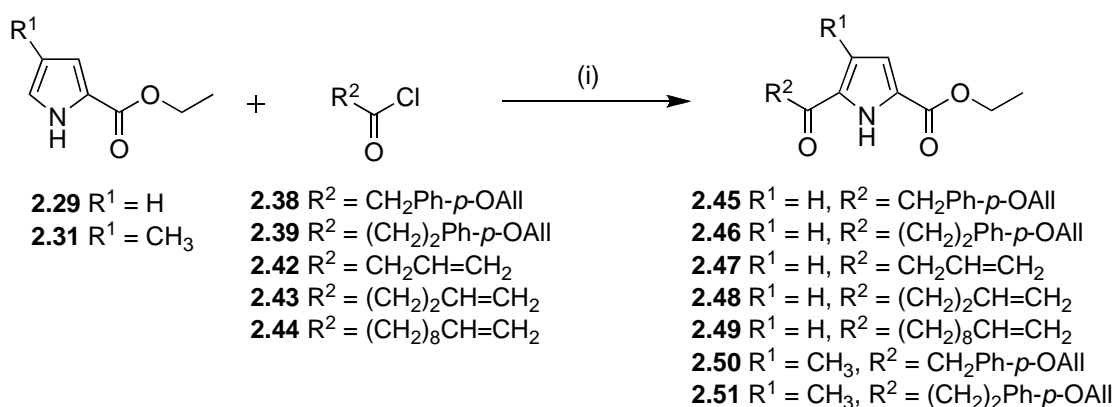
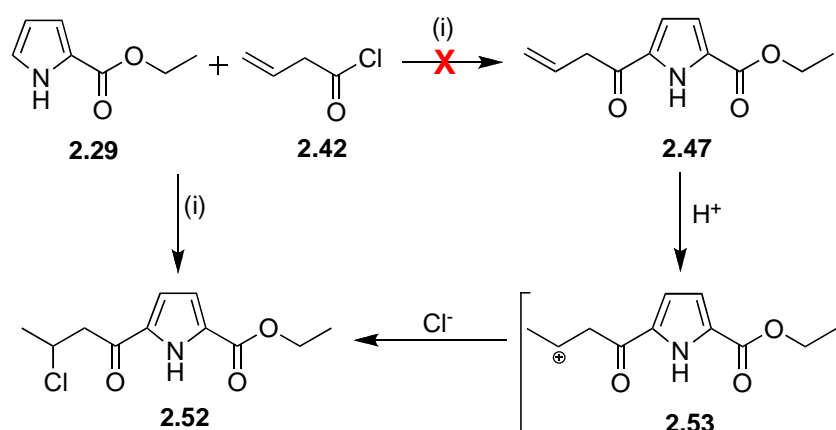
**Scheme 2.5** Reagents and Conditions: i) Yb(OTf)₃, CH₃NO₂, rt, 21 h, (0-53%).

Table 2.5 Friedel-Crafts acylation of pyrroles **2.29** and **2.31**.

Entry	Pyrrole	Acid Chloride	Product (Isolated yield %)
1	2.29	2.38	2.45 (17%)
2	2.29	2.39	2.46 (40%)
3	2.29	2.42	2.47 (0%)
4	2.29	2.43	2.48 (0%)
5	2.29	2.44	2.49 (53%)
6	2.31	2.38	2.50 (18%)
7	2.31	2.39	2.51 (33%)

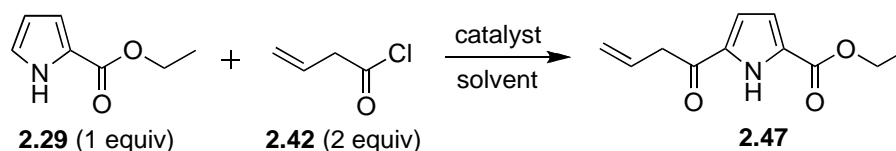
Interestingly, treatment of pyrrole **2.29** with acid chlorides **2.42** and **2.43** did not give the desired pyrrole **2.47** and **2.48**. Rather pyrrole **2.52** (Scheme 2.6) was obtained from reaction of pyrrole **2.29** with acid chloride **2.42** due to electrophilic addition of HCl to the allylic olefin, while reaction in the presence of acid chloride **2.43** gave starting pyrrole **2.29**, Table 2.5, entries 3 and 4. Formation of pyrrole **2.52** is a result of carbocation formation at the allylic olefin (**2.53**, Scheme 2.6) under acidic condition, facilitating addition of a chloride anion. To resolve this, basic aluminium oxide (Al_2O_3) was added, in order to quench any carbocation that might form.¹³⁵

**Scheme 2.6** Reagents and Conditions: i) $\text{Yb}(\text{OTf})_3$, CH_3NO_2 , rt, 21 h, (6%).

Addition of aluminium oxide (Al_2O_3) has been shown to suppress carbocation formation,¹³⁵ however reaction of pyrrole **2.29** with acid chloride **2.42** in the presence of Al_2O_3 proved to be unsuccessful, with only starting pyrrole **2.29** being recovered after reaction for 6 days, see Table 2.6, entry 1. Given this lack of success using $\text{Yb}(\text{OTf})_3$ in

nitromethane with basic Al_2O_3 as an additive, an alternative catalyst was investigated. The addition of aluminium chloride to pyrrole **2.29** failed to give the desired acylated pyrrole **2.47**, Table 2.6, entry 2. ^1H NMR analysis of the crude mixture suggested the loss of the pyrrole with characteristic pyrrolic proton resonances not observed between 6.25 - 6.95 ppm. The addition of basic additive Al_2O_3 to the reaction of pyrrole **2.29** and acid chloride **2.42** in the presence of AlCl_3 , did not catalyse acylation, with only starting pyrrole recovered after reaction for 7 days, Table 2.6, entry 3. As a result of difficulties in obtaining pyrroles **2.47** and **2.48**, the synthesis of $\text{P}_1\text{-P}_3$ macrocycles **2.17** and **2.18** was abandoned, and efforts were focused on the synthesis of the other $\text{P}_1\text{-P}_3$ and $\text{P}_2\text{-P}_4$ 2nd generation macrocycles **2.9-2.16** and **2.21-2.26**.

Table 2.6 Optimisation of Friedel-Craft's acylation of pyrrole **2.29**

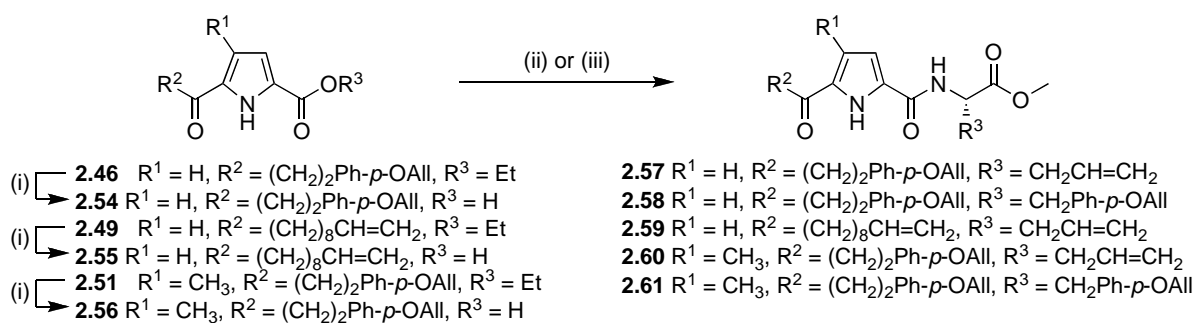


Entry	Solvent	Catalyst	Additive	Yield of 2.47 (%)
1	Nitromethane	$\text{Yb}(\text{OTf})_3$	Al_2O_3	0%
2	Dichloromethane	AlCl_3	-	0%
3	Dichloromethane	AlCl_3	Al_2O_3	0%

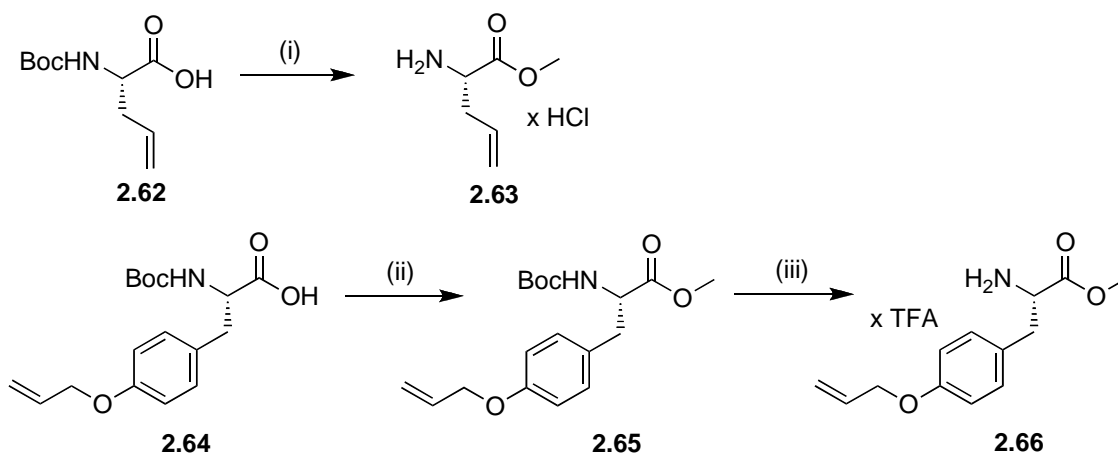
Pyrrole **2.29** was reacted with acid chlorides **2.38** and **2.39** in the presence of $\text{Yb}(\text{OTf})_3$ to give pyrroles **2.50** and **2.51** in low to moderate yields, see Table 2.5, entries 5 and 6. Purification of pyrroles **2.50** and **2.51** was difficult requiring multiple rounds of chromatography and extractions, which contributed to the low yields obtained. Subsequently, due to the low yields obtained, intermediates **2.50** and **2.51** were abandoned. Focus was thus directed at the synthesis of $\text{P}_1\text{-P}_3$ macrocycles **2.10**, **2.12**, **2.14**, **2.16** and $\text{P}_2\text{-P}_4$ macrocycles **2.21-2.26** from intermediate pyrroles **2.46**, **2.49** and **2.51**.

With key intermediates **2.46**, **2.49** and **2.51** in hand, esters **2.46**, **2.49** and **2.51** were hydrolysed to furnish carboxylic acids **2.54-2.56** in excellent yields (Scheme 2.7). The amino acids, **2.63** and **2.66**, required for subsequent amidation were prepared from readily available starting materials as shown in Scheme 2.8. Amino acid **2.63** was prepared in

quantitative yield from commercially available (*S*)-*N*-Boc-allylglycine, **2.62** (Scheme 2.8), on reaction with thionyl chloride in anhydrous methanol.^{136,137} Amino acid **2.66** was prepared by esterification of corresponding Boc-protected amino acid (Boc-*O*-allyl-*L*-tyrosine, **2.64**) (Scheme 2.8) with methyl iodide (MeI)¹³⁸ to give methyl ester **2.65**, and the Boc group was removed to give the free amino acid **2.66**.¹³⁹



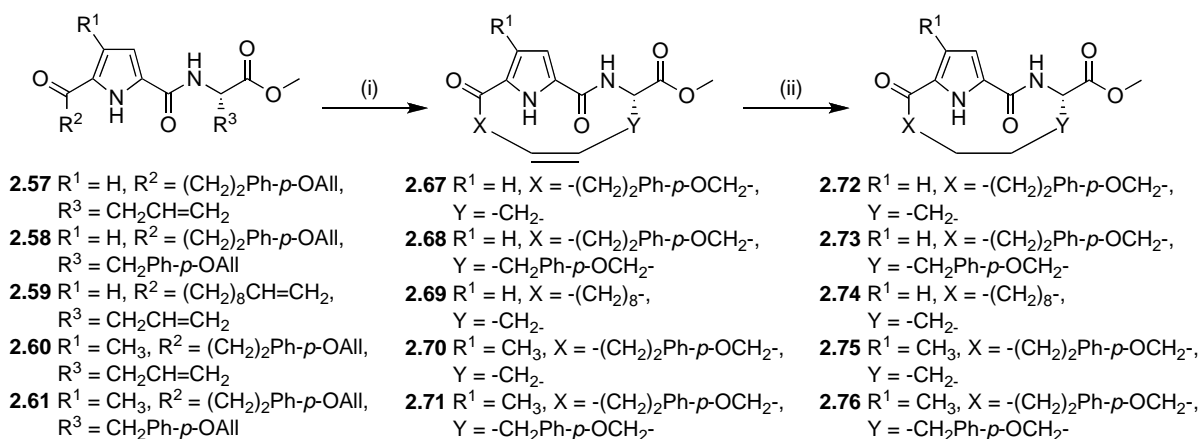
Scheme 2.7 Reagents and Conditions: (i) KOH, THF, H₂O, 40-50 °C, 18 h, (85-100%); ii) **2.63**, EDCI, HOBt, DIEA, anh. CH₂Cl₂, N₂, rt, 18 h, (33-94%); iii) **2.66**, HATU, HOBt, DIEA, anh. CH₂Cl₂, N₂, rt, 18 h, (48-94%).



Scheme 2.8 Reagents and Conditions: i) SOCl₂, anh. MeOH, 0 °C → rt, 16 h, (100%); ii) MeI, NaHCO₃, anh. DMF, rt, 50 h, (100%); iii) TFA, anh. CH₂Cl₂, 0 °C → rt, N₂, 5 h, (100%).

The carboxylic acids **2.54** and **2.56** were separately reacted with amino acid **2.63**, in the presence of 1-(3-dimethylaminopropyl)-3-ethylcarbodiimide hydrochloride (EDCI), 1-hydroxybenzotriazole (HOBt) and *N,N*-diisopropylethyl amine (DIEA) to give acyclic tripeptide **2.57** and **2.60** in excellent yields of 94% for both reactions. In comparison, amidation of carboxylic acid **2.54** with amino acid **2.66** furnished acyclic tripeptide **2.58** in

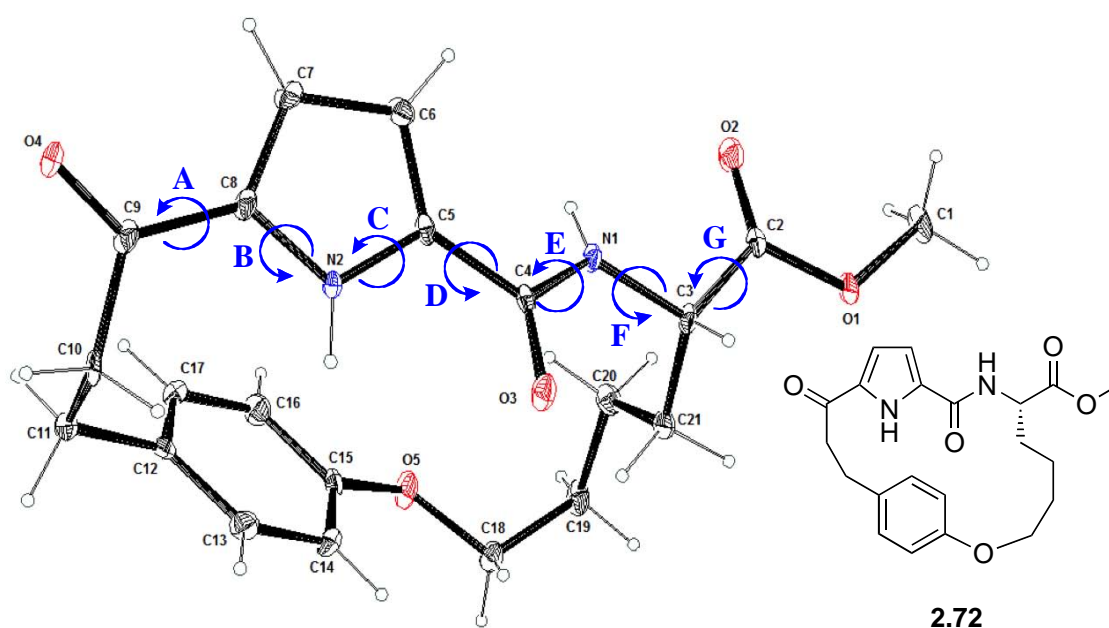
a reduced yield of 33%. However, the use of 2-(7-aza-1H-benzotriazole-1-yl)-1,1,3,3-tetramethyluronium hexafluorophosphate (HATU), in place of EDCI, in the coupling of carboxylic acid **2.54** with amino acid **2.66** gave peptide **2.58** in an improved yield of 94%. The amidation of carboxylic acid **2.55** with amino acid **2.63** gave acyclic peptide **2.59** in 48% yield, while the amidation of carboxylic acid **2.56** with amino acid **2.66** was also improved under these conditions, i.e. HATU/HOBt/DIEA, to give **2.61** in 83%.



Scheme 2.9 Reagents and Conditions: i) Grubbs 2nd Generation Catalyst, anh. CH₂Cl₂, 45 °C, 2 h, (15-71%); ii) H₂, Pd/C, EtOAc, rt, 18 h, (67-98%).

The dienes **2.57-2.61** were then cyclised by ring-closing metathesis (RCM) using 2nd generation Grubbs catalyst (20 mol%) in dichloromethane to give the key macrocyclic cores **2.67-2.71** in modest to good yield (15-71%), as a 1:1 mixture of *E/Z* isomers based on ¹H NMR spectrum. The *E/Z* isomer mixture was of no significance as the olefin was subsequently hydrogenated in the presence of hydrogen and palladium on carbon. Hydrogenation of macrocycle **2.67** in methanol gave a hemiketal, as evidenced by a singlet at 3.77 ppm in the ¹H NMR spectrum. This was supported in the ¹³C NMR spectrum with the absence of the ketone resonance at 191.9 ppm and two new resonances at 118.1 ppm from the carbon of the hemiketal and at 57.2 ppm from the methyl group. Substitution of methanol for ethyl acetate (EtOAc) or acetonitrile (ACN) in the hydrogenation reaction did, however, give the desired reduced macrocycle **2.55** in 67%. Similarly, hydrogenation of macrocyclic alkenes **2.67-2.71** in ethyl acetate gave the corresponding reduced macrocycles **2.72-2.76** in moderate yields.

A single X-ray crystallographic structure of macrocycle **2.72** was solved as depicted in Figure 2.24 in order to define the conformation of the component macrocycle. The crystal structure revealed that the macrocycle does not adopt a β -strand conformation, see dihedral angles depicted in Figure 2.23. Typically a β -strand has dihedral angles of $\phi = \psi = 120^\circ$ and $\omega = 180^\circ$.⁶⁴ However, constraining the P₁/P₂ and P₃/P₄ side chains in macrocycle **2.72** had resulted in an increase in the ψ dihedral angle at P₁/P₂ (C3 in Figure 2.24) to 171° , resulting in a slight bend in the C-terminus. This bend is of significance as this may result in the P₁ residue of the P₂-P₄ macrocycle not being in the optimal orientation for interaction with the protease active site.

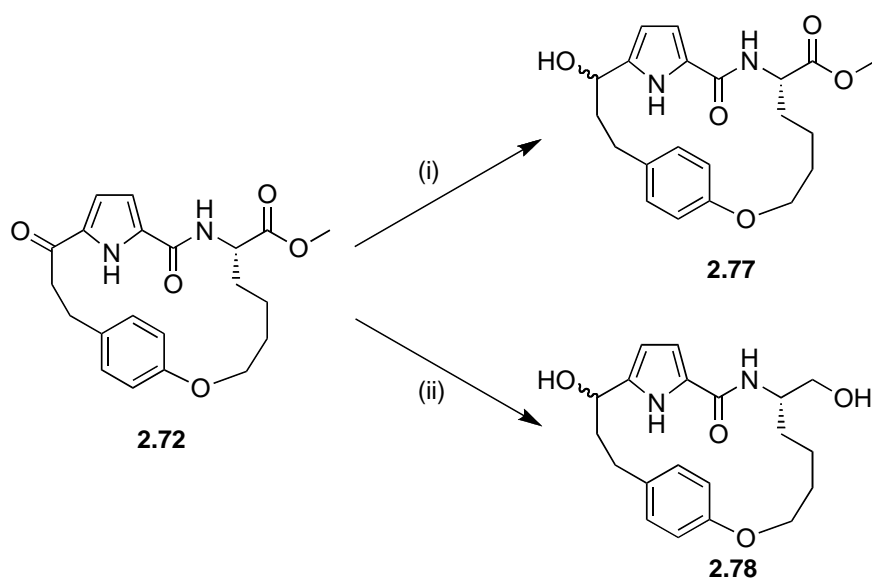


		Dihedral Angle
A	O4-C9-C8-N2	-168°
B	C9-C8-N2-C5	178°
C	C8-N2-C5-C4	-179°
D	N2-C5-C4-N1	151°
E	C5-C4-N1-C3 (ω)	-176°
F	C4-N1-C3-C2 (ϕ)	-123°
G	N1-C3-C2-O1 (ψ)	171°

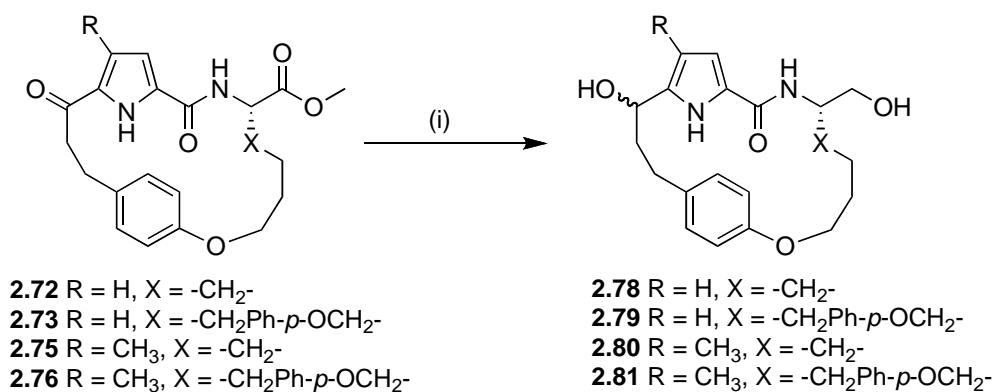
Figure 2.24 X-ray crystal structure and atom labeling of **2.72** (ORTEP). Displacement ellipsoids are shown at 50% probability label for non-H atoms. H atoms are depicted as small circles of arbitrary radii.

2.3.2.1 Preparation of P₁-P₃ Macrocyclic Protease Inhibitors

It was envisaged that P₁-P₃ macrocyclic aldehydes **2.10/2.12/2.14/2.16** would be obtained by selective reduction of the ester motif of macrocycles **2.72/2.73/2.75/2.76**, followed by oxidation of the resulting primary alcohols to the aldehyde. Reduction of macrocycle **2.72** was accomplished with lithium borohydride¹²⁸ from -78 °C to 0 °C, to give the macrocyclic alcohol **2.77**, whereby only the keto motif was reduced (Scheme 2.10). The macrocyclic alcohol **2.77** proved to be unstable and decomposed over 8h at room temperature. This proved problematic for the enzyme inhibition assay. Reaction of macrocyclic ester **2.72** with lithium borohydride at -78°C, followed by warming to room temperature, resulted in non-selective reduction of the both the ketone and ester groups to give the diol **2.78** (Scheme 2.10). However, it was postulated that the keto group could be regenerated during oxidation of the primary alcohol to the required aldehyde; hence macrocycles **2.72/2.73/2.75/2.76** were reduced to furnish macrocyclic diols **2.78-2.81** in good to excellent yields. Macrocyclic diols **2.78-2.81** were assayed against cysteine (calpain) and serine (α -chymotrypsin) proteases as discussed in detail in chapter 3 (section 3.3).

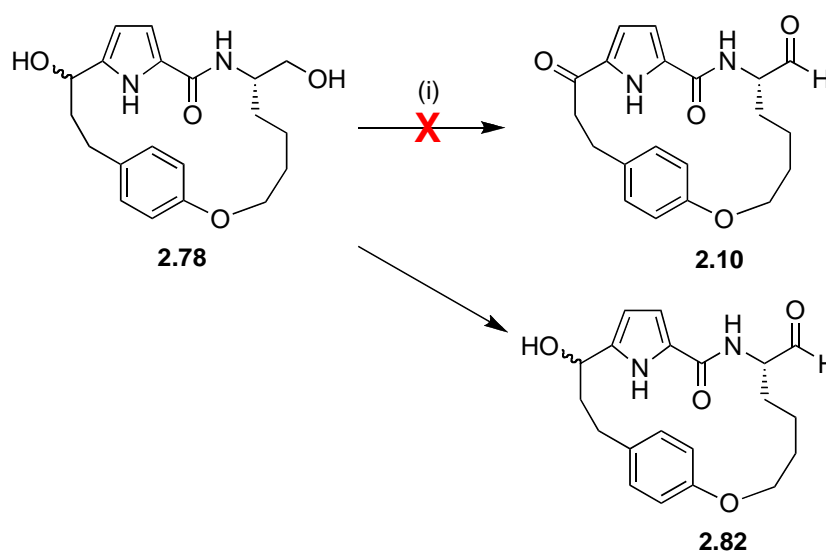


Scheme 2.10 Reagents and Conditions: i) LiBH₄, THF, -78 °C (3 h) → 0 °C (30 min), (50%); ii) LiBH₄, THF, -78 °C (1 h) → rt (1 h), (81%).



Scheme 2.11 Reagents and Conditions: i) LiBH₄, THF, -78 °C (1 h) → rt (1 h), (62-100%).

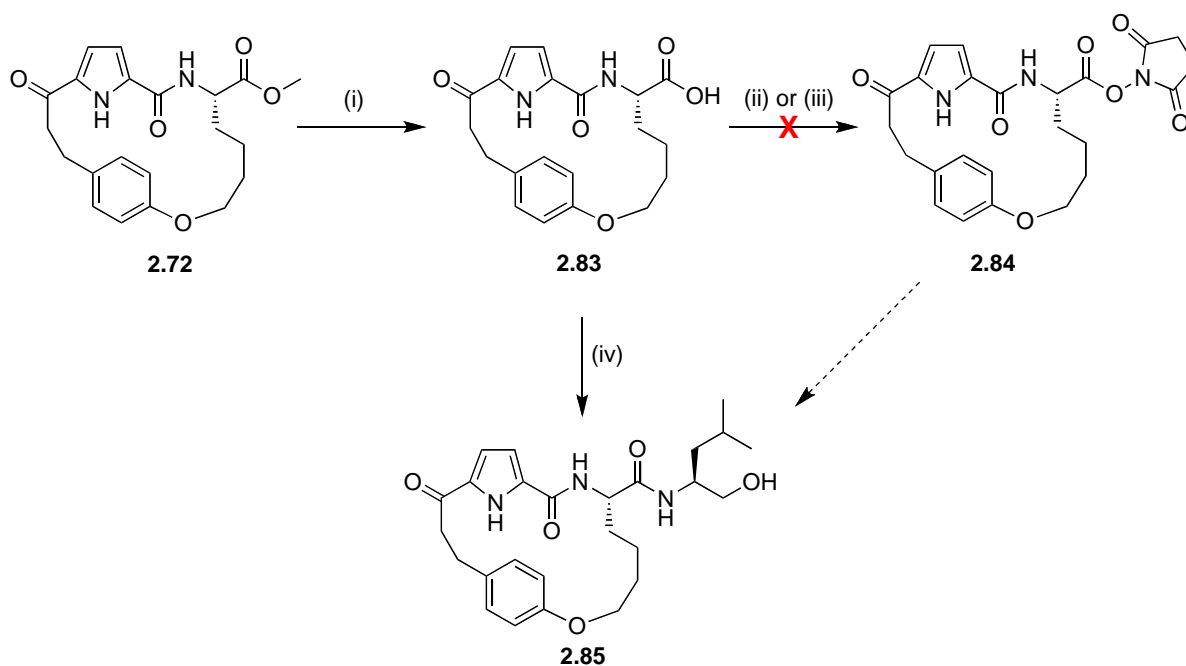
Oxidation of the alcohol groups of **2.78** was next attempted using sulfur trioxide-pyridine complex and dimethylsulfoxide in the presence of DIEA (Parikh-Doering Oxidation).¹⁴²⁻¹⁴⁵ These mild conditions are known to minimise potential epimerisation of the alpha-carbon adjacent to the aldehyde.¹⁴⁴ However, oxidation of the macrocyclic diol **2.78** under these conditions gave the macrocyclic aldehyde **2.82** (Scheme 2.12) as evidenced by the ¹H NMR spectrum. ¹H NMR analysis showed a resonance at 4.72 ppm due to the secondary alcohol and two aldehyde signals at 9.59 ppm and 9.61 ppm consistent with two diastereoisomers. The aldehyde **2.82** was also unstable and decomposed rapidly overnight (10 h). As a result, attention was focussed on the P₂-P₄ macrocyclic aldehydes.



Scheme 2.12 Reagents and Conditions: i) Isopropanol, DMSO, DIEA, SO₃Py, N₂, 0 °C → rt, 3 h.

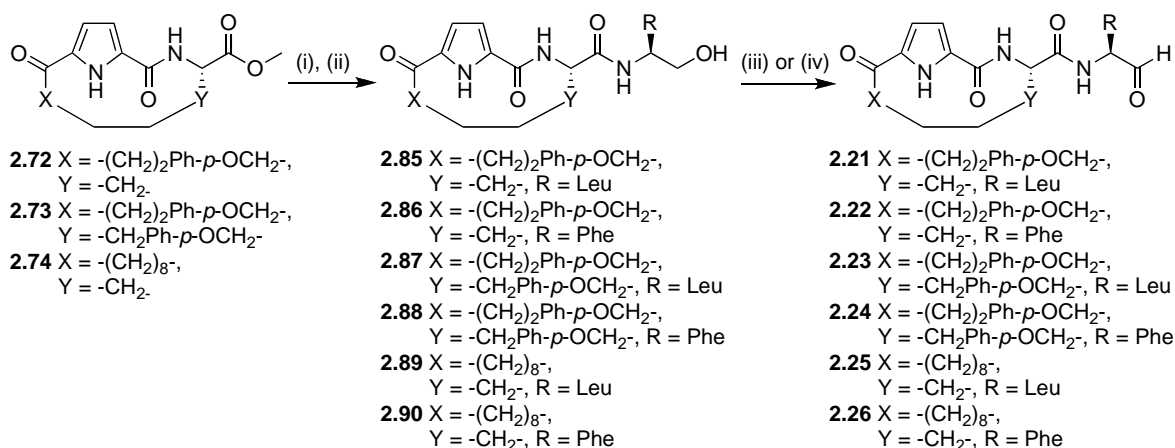
2.3.2.2 Preparation of P₂-P₄ Macrocyclic Protease Inhibitors

It was envisaged that P₂-P₄ macrocyclic aldehydes would be obtained by hydrolysis of ester motif of macrocycles **2.72-2.74**, followed by amidation of the resulting carboxylic acids with amino alcohols via a succinimide ester intermediate and oxidation of the primary alcohols to the aldehyde.¹⁴⁶ Hydrolysis of the macrocyclic ester **2.72**, with sodium hydroxide, gave the corresponding carboxylic acid **2.83** that was used without further purification. Subsequent reaction of carboxylic acid **2.83** with N-hydroxysuccinimide, in the presence of either EDCI or HATU only returned starting macrocycle **2.83**. As a result, amidation of carboxylic acid **2.83** with either (*L*)-leucinol or (*L*)-phenalaninol was attempted.



Scheme 2.14 Reagents and Conditions: i) 2M NaOH, THF, rt, 16 h (not isolated); ii) HOSu, EDCI, THF/CH₂Cl₂, rt, 18 h, (0%); iii) HOSu, HATU, THF/CH₂Cl₂, rt, 18 h, (0%); iv) (*L*)-Leucinol, HATU, HOBt, DIEA, anh. DMF, rt, 18 h, (83%).

Reaction of carboxylic acid **2.83** with (*L*)-leucinol, in the presence of HATU, gave the macrocyclic alcohol **2.85** in good yield. The macrocyclic esters **2.72-2.74** were similarly hydrolysed to their corresponding carboxylic acids and coupled with (*L*)-leucinol or (*L*)-phenalaninol, in the presence of HATU, to give the desired macrocyclic alcohols **2.85-2.90** in moderate to good yields (Scheme 2.21).



Scheme 2.15 Reagents and Conditions: i) 2M NaOH, THF, rt, 16 h (not isolated); ii) (*L*)-Leucinol or (*L*)-Phenalaninol, HATU, HOBT, DIEA, anh. DMF, N₂, rt, 18 h, (36-83%); iii) Isopropanol, DMSO, DIEA, SO₃Py, N₂, 0 °C → rt, 3 h, (0%); iv) Dess-Martin Periodinane, anh. CH₂Cl₂, N₂, rt, 1 h, (15-65%).

Oxidation of the alcohol **2.85** with Dess-Martin periodinane¹⁴⁷ gave the desired P₂-P₄ macrocyclic aldehyde **2.21** in a moderate yield of 37% after purification by high-pressure liquid chromatography (HPLC) as a single epimer. If epimerization had occurred, signals for both isomers, particularly the aldehyde hydrogen and the alpha-hydrogen of the P₁ residue, would have been evident in the ¹H and ¹³C NMR. The P₁ residue, which is directly connected to the aldehyde, is more susceptible to epimerization than the P₂ residue that is part of the macrocycle. These signals were clearly defined as single resonances in the ¹H and ¹³C NMR spectra of aldehyde **2.21** confirming the formation of a single epimer (Figure 2.25). The macrocyclic alcohols **2.86-2.90** were similarly oxidised with Dess-Martin periodinane to give the desired P₂-P₄ macrocyclic aldehydes **2.22-2.26** in low to moderate yields. Analysis of the ¹H NMR spectra of aldehydes **2.22-2.26** again showed the formation of a single epimer. Interestingly, attempted oxidation of the macrocyclic alcohols with sulfur trioxide-pyridine complex and dimethylsulfoxide (Parikh-Doering conditions) in this case failed to give the desired aldehydes. With requisite macrocyclic alcohols **2.85-2.90** and aldehydes **2.21-2.26** in hand, inhibition studies against cysteine (calpain and cathepsin) and serine (α-chymotrypsin and HLE) proteases were conducted and are discussed in detail in chapter 3 (section 3.4).

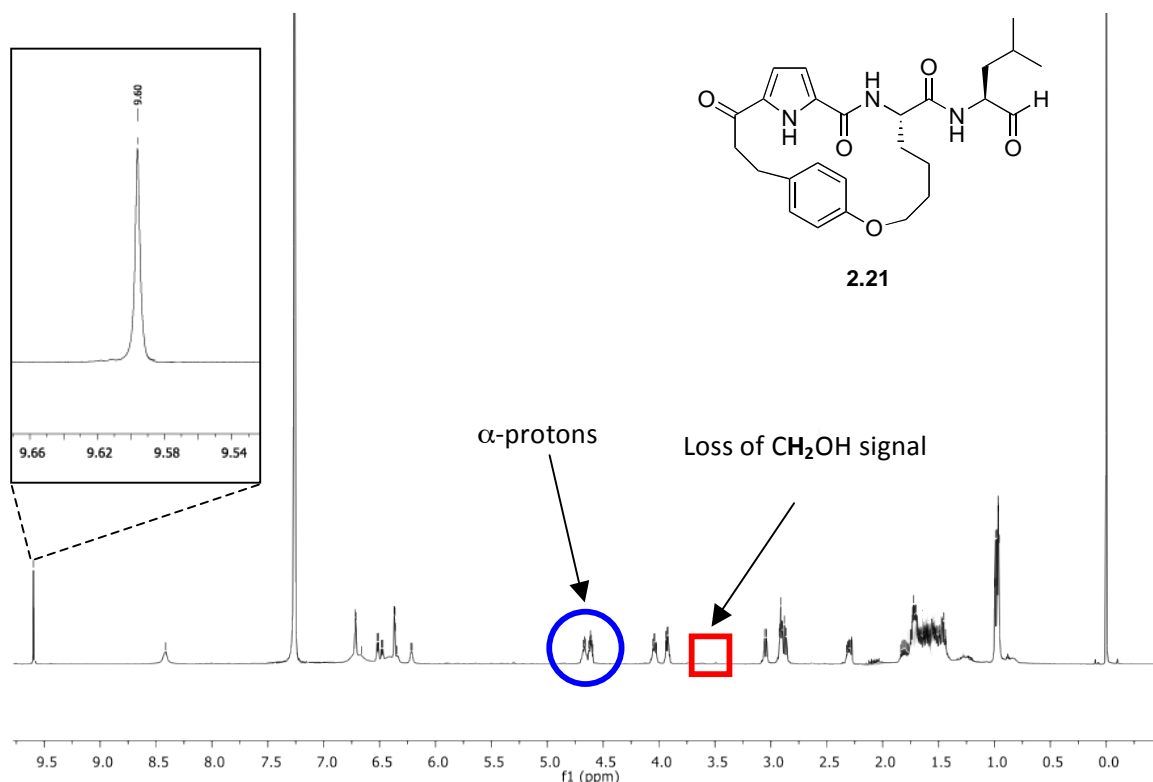


Figure 2.25 ¹H NMR spectrum of aldehyde **2.21** showing the single resonances for the CHO peak (enlarged inset) and the α-protons (circled in blue); and the loss of CH₂OH signal (red square box).

2.3.3 Synthesis of 2nd Generation P₁-P₃ Macrocycles by Huisgen 1,3-Dipolar Cycloaddition

The macrocyclic core of P₁-P₃ 2nd generation macrocycles **2.19** and **2.20** (Figure 2.26) would be obtained using a Huisgen cycloaddition as the key step. Initial Friedel-Craft's acylation of pyrroles **2.29** and **2.31** with acid chloride **2.98**, followed by subsequent hydrolysis would give intermediate pyrroles **2.96** and **2.97** as shown in Figure 2.25. The key macrocyclic esters **2.91** and **2.92** would be obtained by separate amidation of pyrroles **2.96** and **2.97** with amino acid **2.95**, followed by Huisgen 1,3-dipolar cycloaddition of acyclic peptides **2.93** and **2.94**. Subsequent reduction of the C-terminal methyl ester substituent to an aldehyde would then give potential protease inhibitors with the macrocycle linking P₁ to P₃ as discussed in section 2.3. The key intermediates **2.96** and **2.97** would be obtained in a similar manner to the preparation of intermediates **2.45-2.51** as discussed in section 2.3.2.

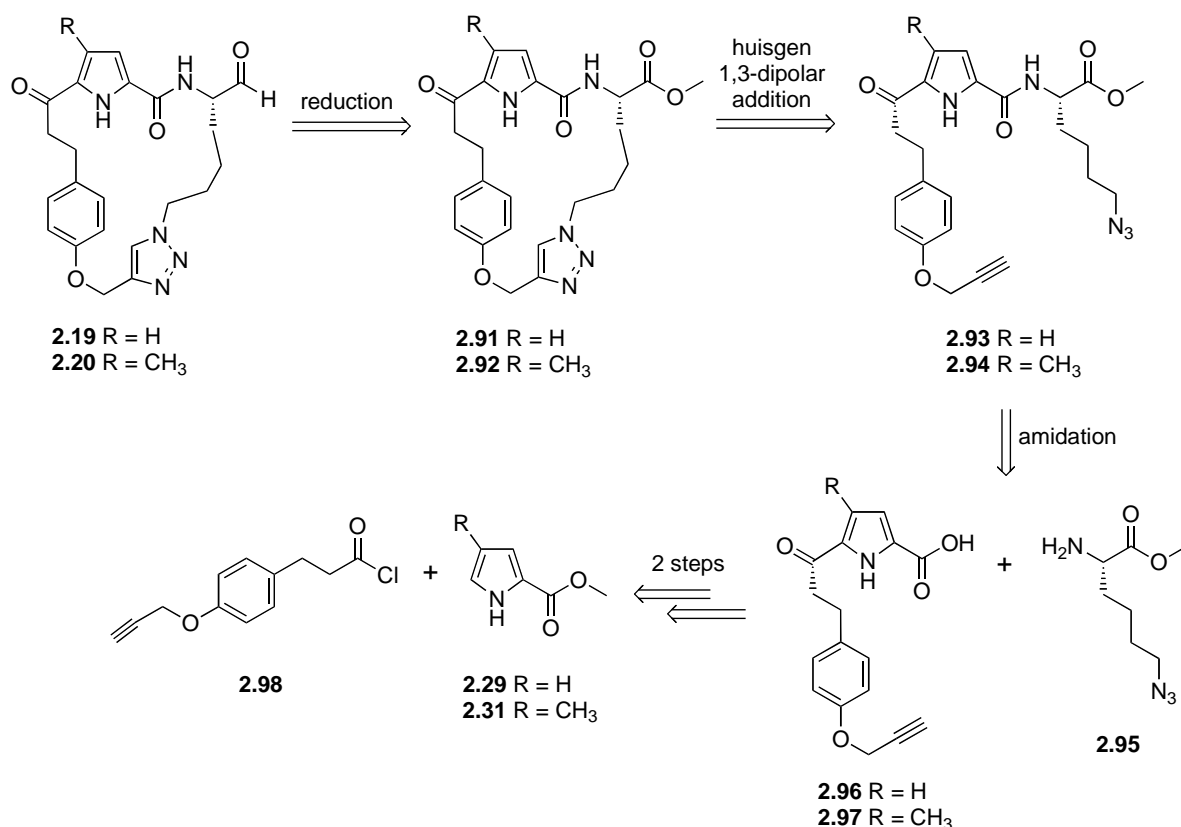
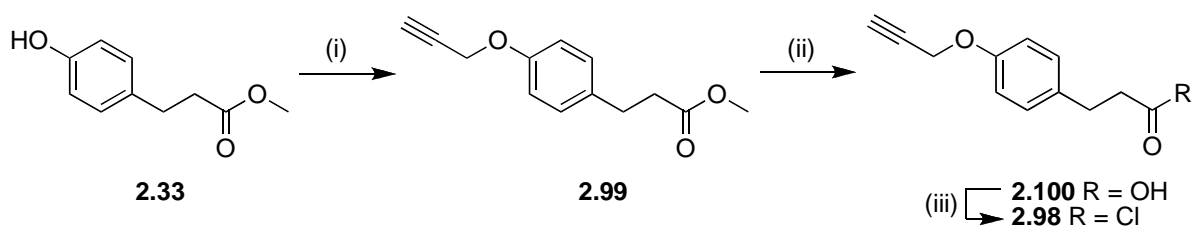


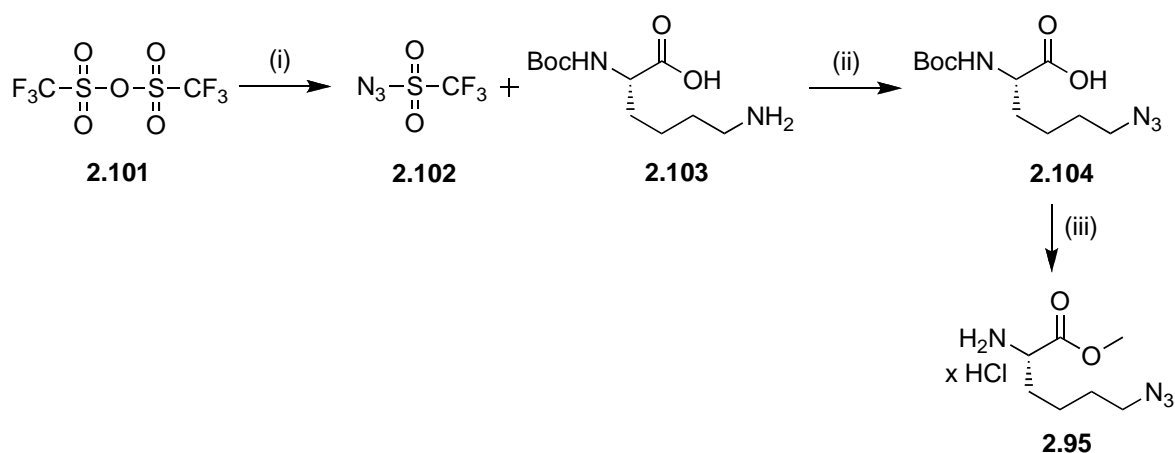
Figure 2.26 Retrosynthetic analysis of P₁-P₃ macrocyclic aldehydes by Huisgen 1,3-dipolar addition.

O-Allylation^{148,149} of commercially available methyl 3-(4-hydroxyphenyl)propionate **2.33** with propargyl bromide gave **2.99** in excellent yield (Scheme 2.16). Subsequent saponification of the methyl ester of **2.99** gave carboxylic acid **2.100**, which was reacted with thionyl chloride to give the acid chloride **2.98** in excellent yield. Acid chloride **2.98** was used without purification for the generation of 2,5- and 2,4,5-substituted pyrroles, **2.96** and **2.97**, as shown in Figure 2.26.



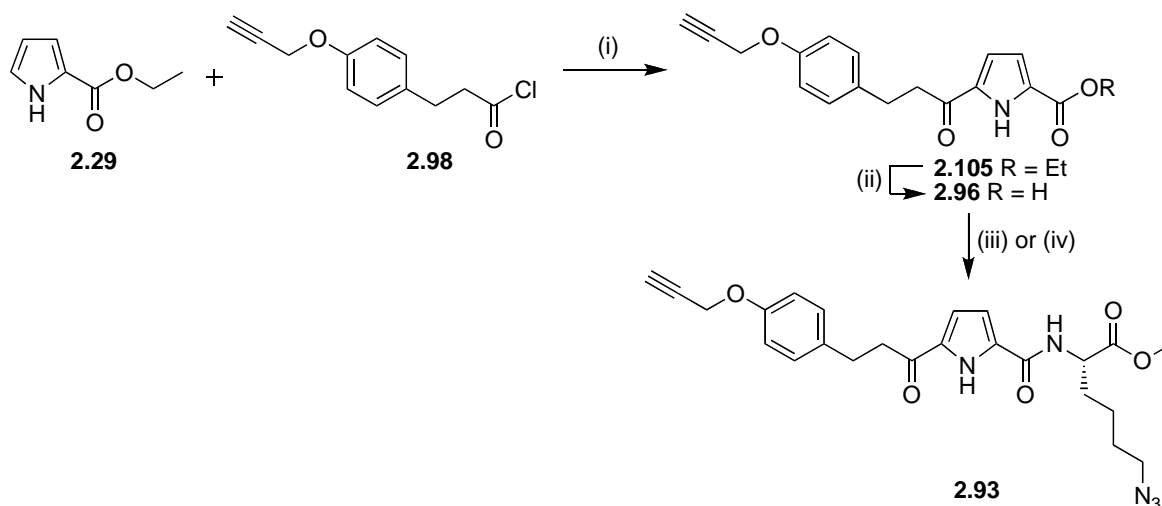
Scheme 2.16 Reagents and Conditions: (i) Propargyl Bromide, K₂CO₃, TBAI, DMF, rt, 18 h, (99%); (ii) LiOH·H₂O, THF, H₂O, 40 °C, 3.5 h, (98%); (iii) SOCl₂, CH₂Cl₂, 40 °C, 18 h, (100%).

The amino acid azide **2.95**, required for amidation of pyrrole **2.96/2.97**, was prepared by reaction of commercially available *N* α -Boc-*L*-lysine **2.103** with triflic azide **2.102** as shown in Scheme 2.17. Triflic azide **2.102** was freshly prepared from reaction of triflic anhydride **2.101** with sodium azide.¹⁵⁰ Simultaneous removal of the Boc protecting group and esterification of *N* α -Boc-azido-*L*-lysine **2.104** was achieved by treatment with thionyl chloride in anhydrous methanol to give azide amino acid **2.95** in 72% yield.



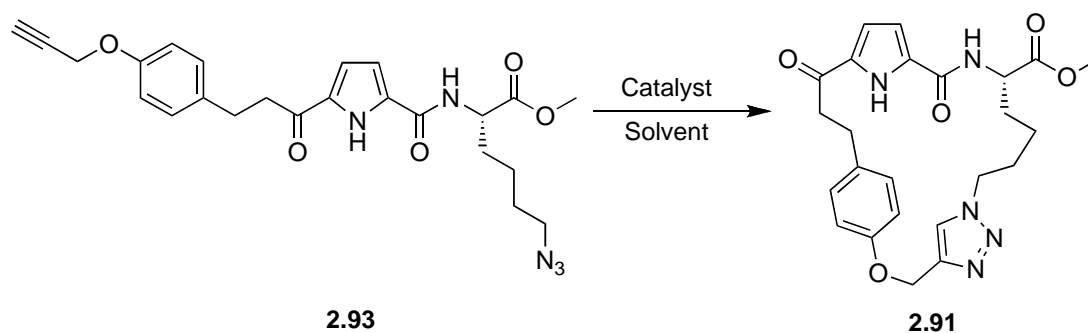
Scheme 2.17 Reagents and Conditions: (i) NaN_3 , anh. CH_3CN , 0°C , 2 h (not isolated); (ii) Et_3N , $\text{CuSO}_4 \cdot 5\text{H}_2\text{O}$, $\text{CH}_3\text{CN}/\text{H}_2\text{O}$, 0°C (3 h) \rightarrow rt (16 h) (48%); (iii) SOCl_2 , anh. MeOH, 0°C (1 h) \rightarrow rt (16 h) (72%).

The pyrrole **2.29** was reacted with acid chloride **2.98**, under Friedel-Craft's acylation conditions in the presence of $\text{Yb}(\text{OTf})_3$, to give ester **2.105** in an isolated yield of 24%, with starting pyrrole **2.29** being isolated as a major by-product. Increasing the equivalents of $\text{Yb}(\text{OTf})_3$ (0.2 equiv) or the reaction time did not improve yields. The thus obtained pyrrole ester **2.105** was hydrolysed on treatment with potassium hydroxide to give the corresponding carboxylic acid **2.96**, which was amidated with amino acid **2.95** using the previously established EDCI/HOBt/DIEA conditions to give the acetylene azide **2.93** in a 33% yield. Amidation of carboxylic acid **2.96** with amino acid **2.95** was also attempted in the presence of HATU, however in this case, a diminished yield of the desired acetylene azide **2.93** was obtained (Scheme 2.18).



Scheme 2.18 *Reagents and Conditions:* i) $\text{Yb}(\text{OTf})_3$, CH_3NO_2 , rt, 21 h, (24%); ii) KOH , THF , H_2O , 40–50 °C, 18 h, (94%); iii) **2.95**, EDCI , HOBt , DIEA , anh. CH_2Cl_2 , N_2 , rt, 18 h, (33%); iv) **2.95**, HATU , HOBt , DIEA , anh. CH_2Cl_2 , N_2 , rt, 18 h, (14%).

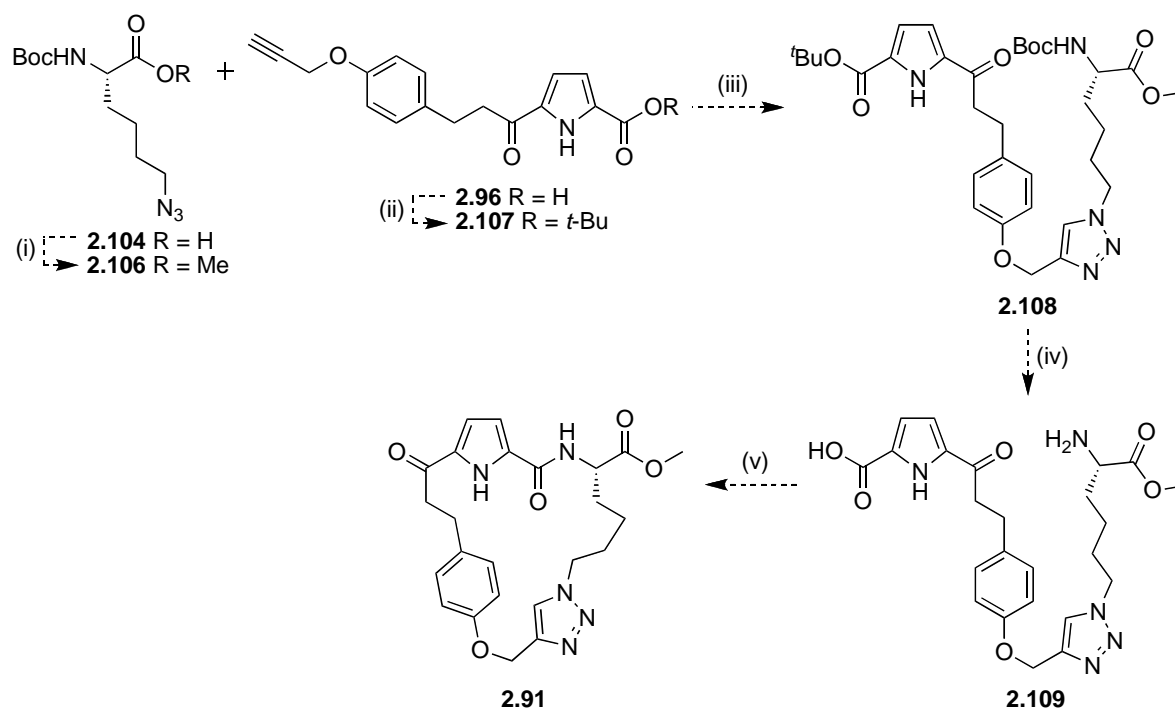
Intramolecular Huisgen 1,3-dipolar cyclisation of acetylene azide **2.93** was attempted as shown in Table 2.7. Reaction with copper sulphate ($\text{CuSO}_4 \cdot 5\text{H}_2\text{O}$) in the presence of sodium ascorbate (NaAsc) (Table 2.7, entry 1) failed to give the desired macrocycle **2.91** with only starting material being recovered after 20 h reaction. Reaction of **2.93** with copper wire (Table 2.7, entry 2), or copper nanopowder (Table 2.7, entry 3) in the presence of triethylamine hydrochloride salt similarly gave only returned starting material. The use of more forcing reaction conditions, by refluxing **2.93** in the presence of copper bromide (CuBr) and 1,8-diazabicyclo[5.4.0]undec-7-ene (DBU) in toluene, did however give the desired macrocycle **2.91** in moderate yields (Table 2.7, entry 4).

Table 2.7 Intramolecular Huisgen 1,3-dipolar cycloaddition reaction of acetylene azide **2.102**.

Entry	Catalyst	Solvent	Temp. (°C)	Time (h)	Yield of 2.91 (%)
1	CuSO ₄ ·5H ₂ O (1 equiv) + NaAsc (1 equiv)	1 : 1 THF/H ₂ O	rt	20	0 ^a
2	Cu Wire	10 : 1 CH ₃ CN/H ₂ O	35	20	0 ^a
3	Cu Nanopowder (0.2 equiv) + Et ₃ N·HCl (0.2 equiv)	2 : 1 <i>t</i> -BuOH/H ₂ O	rt	48	0 ^a
4	CuBr (1 equiv) + DBU (1 equiv)	Toluene	110	2.5	26 ^b

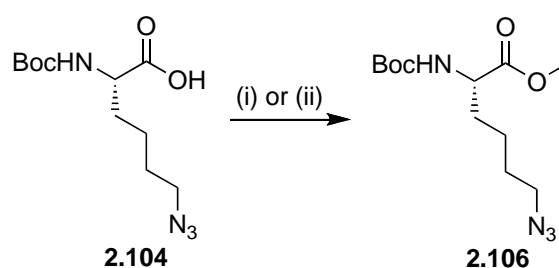
^a Starting material recovered (Entry 1: 58%, Entry 2: 75%, Entry 4: 62%). ^b Reaction purified by preparative TLC.

An alternative synthetic route to macrocycle **2.91** was investigated as shown in Scheme 2.19 in an attempt to improve yields. This sequence involved first forming the triazole linker to give compound **2.108** using Huisgen 1,3-dipolar cycloaddition, followed by amidation induced cyclization to give the desired macrocycle **2.91**. Protection of the carboxy-terminal of amino acid **2.104** and pyrrole **2.96** was conducted prior to Huisgen 1,3-dipolar cycloaddition reaction (Scheme 2.19). The use of *t*-butyl and boc protecting group allowed simultaneous removal of these groups prior to peptide cyclisation.



Scheme 2.19 *Reagents and Conditions:* (i) NaHCO_3 , TBAI, MeI, anh. DMF, N_2 , rt; (ii) $(\text{COCl})_2$, DMF, anh. CH_2Cl_2 , rt; then KO^tBu , anh. *t*-BuOH, 40°C ; (iii) $\text{CuSO}_4 \cdot 5\text{H}_2\text{O}$, NaAsc, 2 : 1 *t*-BuOH/ H_2O , rt; (iii) HATU, HOBT, DIEA, anh. CH_2Cl_2 , N_2 , rt.

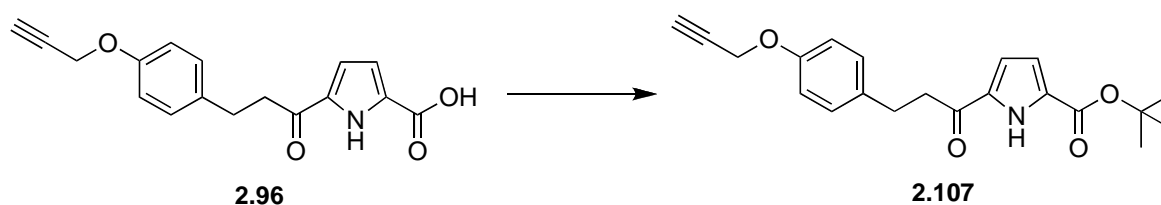
Protection of amino acid **2.104** was achieved by methylation of the terminal carboxylic acid, in the presence of methyl iodide and potassium carbonate to give amino acid **2.106** in 40% yield. The use of potassium carbonate instead of sodium bicarbonate gave an improved yield of 80%.



Scheme 2.20 *Reagents and Conditions:* (i) K_2CO_3 , TBAI, MeI, anh. DMF, N_2 , rt, 90 h, (40%); (ii) NaHCO_3 , TBAI, MeI, anh. DMF, N_2 , rt, 90 h, (80%).

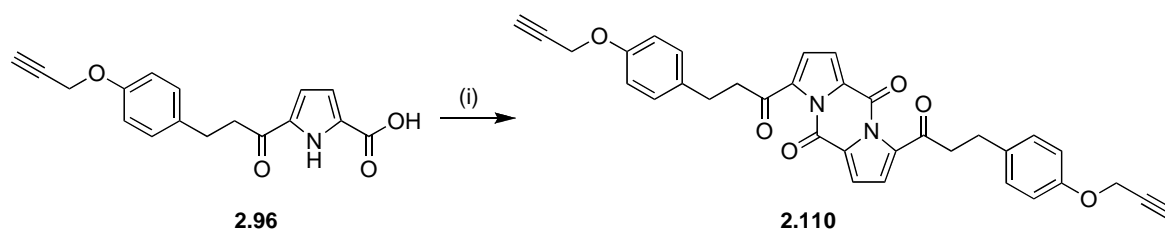
A series of reaction conditions for the protection of carboxylic acid **2.96** with *t*-butyl was investigated, as shown in Table 2.8. Reaction of amino acid **2.96** with oxalyl chloride, followed by the addition of *t*-butanol gave a complex mixture of by-products from which the protected amino acid **2.107** was isolated in a very low yield of 5%, (Table 2.8, entry 1). Alternatively, reaction of amino acid **2.96** with phosphoryl chloride (Table 2.8, entry 2), followed by the addition of *t*-butanol, gave only returned starting carboxylic acid **2.96**. Steglich esterification,¹⁵¹ a mild and convenient reaction for the formation of *t*-butyl esters was next attempted (Table 2.8, entry 3). Reaction of **2.96** under these conditions (4-DMAP, EDCl, *t*-BuOH) gave the *bis*-pyrrole **2.110** in a high yield of 84% (Table 2.8, entry 3; Scheme 2.21). The pyrrole ester **2.107** was finally obtained in high yield by initial conversion of carboxylic acid **2.96** to its corresponding acid chloride using thionyl chloride, followed by esterification with potassium *t*-butoxide (Table 2.8, entry 4).

Table 2.8 Esterification of carboxylic acid **2.96**



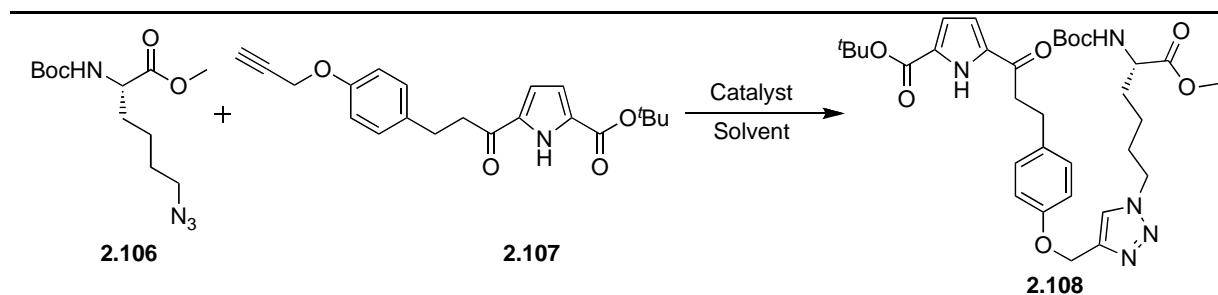
Entry	Reaction Conditions	Yield of 2.107 (%)
1	(i) (COCl) ₂ , anh. DMF, anh. CH ₂ Cl ₂ , rt, 1 h; (ii) <i>t</i> -BuOH, KO ^t Bu, 40 °C, 2 h	5
2	(i) POCl ₃ , 40 °C 18 h; (ii) <i>t</i> -BuOH, KO ^t Bu, 40 °C, 2 h	0 ^a
3	(i) DMAP, anh. <i>t</i> -BuOH, anh. CH ₂ Cl ₂ , EDCl, 0 °C (2 h) → rt (16 h)	0 ^b
4	(i) SOCl ₂ , rt 18 h; (ii) <i>t</i> -BuOH, KO ^t Bu, 40 °C, 3 h	83

^a Starting material recovered (70%). ^b Dimer product obtained (see Scheme 2.21)



Scheme 2.21 Reagents and Conditions: i) 4-DMAP, anh. *t*-BuOH, anh. CH₂Cl₂, EDCI, 0 °C (2 h) → rt (16 h) (84%)

Table 2.9 Formation of triazole **2.108** by Intermolecular Huisgen 1,3-dipolar cycloaddition.



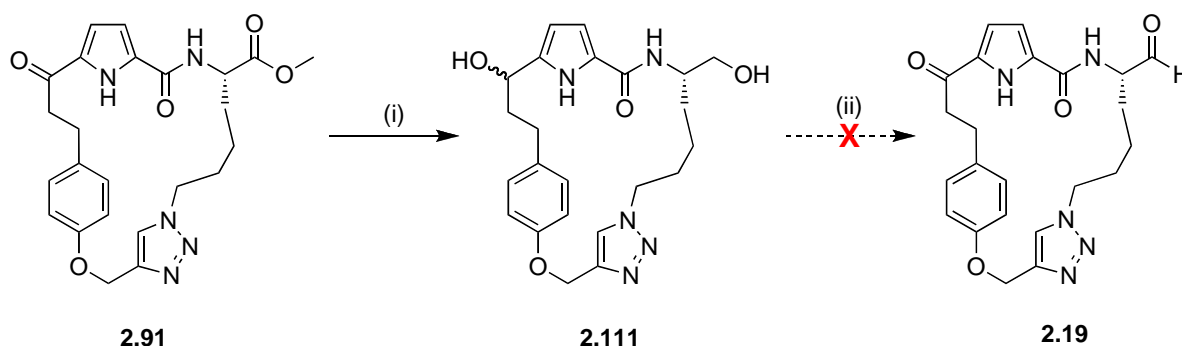
Entry	Catalyst	Solvent	Temp. (°C)	Time (h)	Yield of 2.108 (%)
1	CuSO ₄ ·5H ₂ O (0.01 equiv) + NaAsc (0.1 equiv)	2 : 1 <i>t</i> -BuOH/H ₂ O	rt	450	0 ^a
2	Cu Nanopowder (0.1 equiv)	2 : 1 <i>t</i> -BuOH/H ₂ O	rt	450	0 ^a
3	Cu Nanopowder (0.2 equiv) + Et ₃ N·HCl (0.2 equiv)	2 : 1 <i>t</i> -BuOH/H ₂ O (10 mM)	rt	144	0 ^a
4	Cu Nanopowder (0.2 equiv) + Et ₃ N·HCl (0.2 equiv)	2 : 1 <i>t</i> -BuOH/H ₂ O (33 mM)	rt	144	0 ^b

^aNo product formation by NMR and IR. ^bDesired product observed by NMR, Ratio of **2.108** : **2.107** = 2 : 1.

With amino acid **2.106** and pyrrole ester **2.107** in hand, intermolecular Huisgen 1,3-dipolar cycloaddition was attempted in the presence of copper sulphate (CuSO₄·5H₂O) and sodium ascorbate (NaAsc) (Table 2.9, entry 1). However, the desired triazole **2.108** was not obtained after 18 days with starting materials **2.106** and **2.107** being the major products. Reaction with copper nanopowder (Table 2.9, entry 2), or 10 mM copper nanopowder/triethyl amine salt solution (Table 2.9, entry 3) again failed to give the triazole

2.108 with starting amino acid **2.106** and pyrrole ester **2.107** being recovered after 18 and 6 days, respectively. Increasing the concentration of copper nanopowder/triethyl amine salt from 10 mM to 33 mM and reaction for 6 days led to some success (Table 2.9, entry 4). However, an ^1H NMR spectrum of the crude mixture showed that the starting pyrrole was not entirely consumed, with the desired triazole **2.108** and starting ester **2.107** being obtained in a ratio of 2 : 1. Due to difficulties in separation of the desired compound and starting material, the earlier route to macrocycle **2.91** was adopted.

The desired P₁-P₃ macrocyclic aldehyde **2.19** would be obtained by selective reduction of the ester of **2.91**, followed by oxidation of the resulting primary alcohol **2.111** (Scheme 2.22). Reduction of the ester of macrocycle **2.91** was attempted (LiBH_4), however only the reduced keto derivative, macrocycle **2.111**, was obtained in a low yield of 10%. As a result, the synthesis of P₁-P₃ macrocyclic aldehyde **2.19** and **2.20** by Huisgen 1,3-dipolar cycloaddition was abandoned.

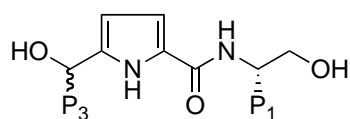


Scheme 2.22 Reagents and Conditions: i) LiBH_4 , THF, $-78\text{ }^\circ\text{C}$ (1 h) \rightarrow rt (1 h) (10%); ii) Isopropanol, DMSO, DIEA, SO_3Py , N_2 , $0\text{ }^\circ\text{C}$ \rightarrow rt, 3 h.

2.4 Design and Synthesis of Acyclic Protease Inhibitors

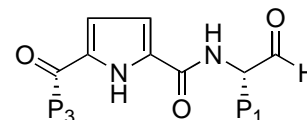
This section describes the design and synthesis of acyclic analogues of the P₁-P₃ and P₂-P₄ 2nd generation macrocyclic inhibitors (macrocycles **2.21-2.26** and **2.78-2.79**), which were prepared for comparative inhibition assay. The acyclic analogues **2.112-2.113** (Figure 2.27a) and **2.116-2.121** (Figure 2.27b) contain the same substituent at the P₂, P₃ and P₄ compared to the macrocyclic derivatives **2.78-2.79** and **2.21-2.26** (section 2.3.2), respectively. The shorter acyclic P₁-P₃ aldehyde analogues **2.114-2.115** (Figure 2.27a), containing one amino acid less, allow for comparisons with the P₁-P₄ analogues and can be

prepared by substituting the P₁ position with leucinol and phenylalaninol, which can be subsequently oxidized to obtain the required aldehyde motif. The only constraint within the acyclic derivatives is a pyrrole motif in the peptide backbone.



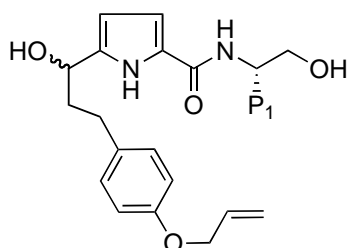
P₃ = aryl

P₁ = aryl, alkyl



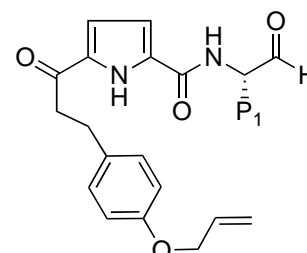
P₃ = aryl

P₁ = Leu, Phe



2.112 P₁ = CH₂CH=CH₂

2.113 P₁ = CH₂Ph-*p*-OCH₂CH=CH₂



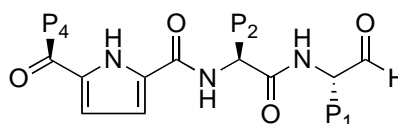
2.114 P₁ = Leu

2.115 P₁ = Phe

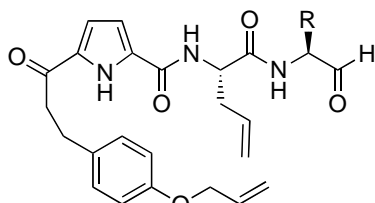
a) Acyclic Analogue of P₁-P₃ Constrained 2nd Generation Protease Inhibitors

P₄ = aryl, alkyl

P₂ = aryl, alkyl

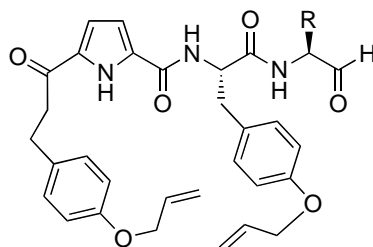


P₁ = Leu, Phe



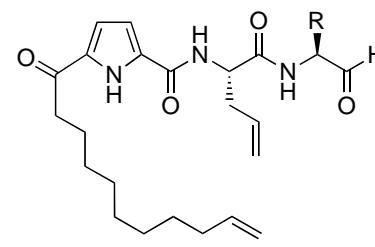
2.116 R = Leu

2.117 R = Phe



2.118 R = Leu

2.119 R = Phe



2.120 R = Leu

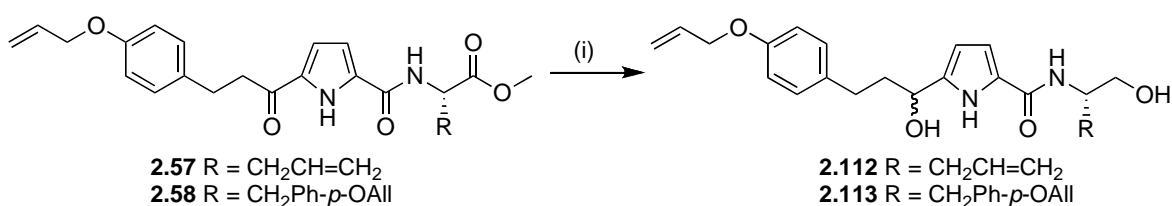
2.121 R = Phe

b) P₁-P₄ Acyclic Analogue of P₂-P₄ Constrained 2nd Generation Protease Inhibitors

Figure 2.27 Target structures for the acyclic P₁-P₃ and P₁-P₄ 2nd generation protease inhibitors.

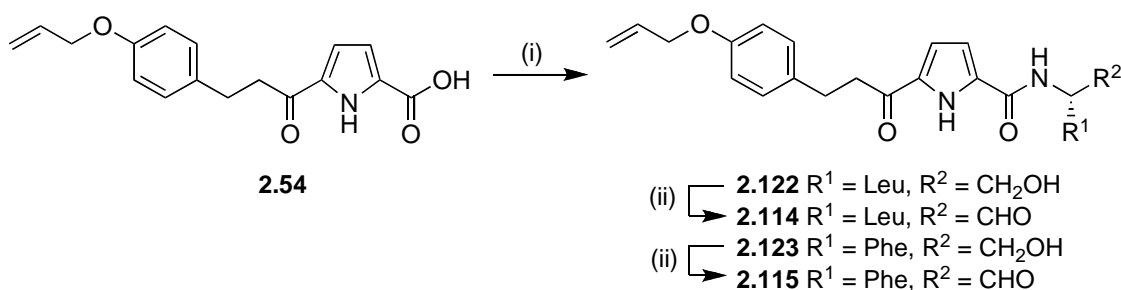
2.4.1 Synthesis of P₁-P₃ Acyclic Protease Inhibitors

The P₁-P₃ acyclic diols **2.112-2.113** and aldehydes **2.114-2.115** were prepared as shown in Scheme 2.23 and 2.24 in order to elucidate the importance of the P₁-P₃ 2nd generation macrocyclic core (macrocycles **2.78** and **2.79**, section 2.3.2.1). Acyclic esters **2.57** and **2.58** were successfully reduced to their corresponding diols **2.112** and **2.113** using lithium borohydride in high yields of 78%.



Scheme 2.23 Reagents and Conditions: i) LiBH₄, THF, -78 °C (1 h) → rt (1 h), (78%).

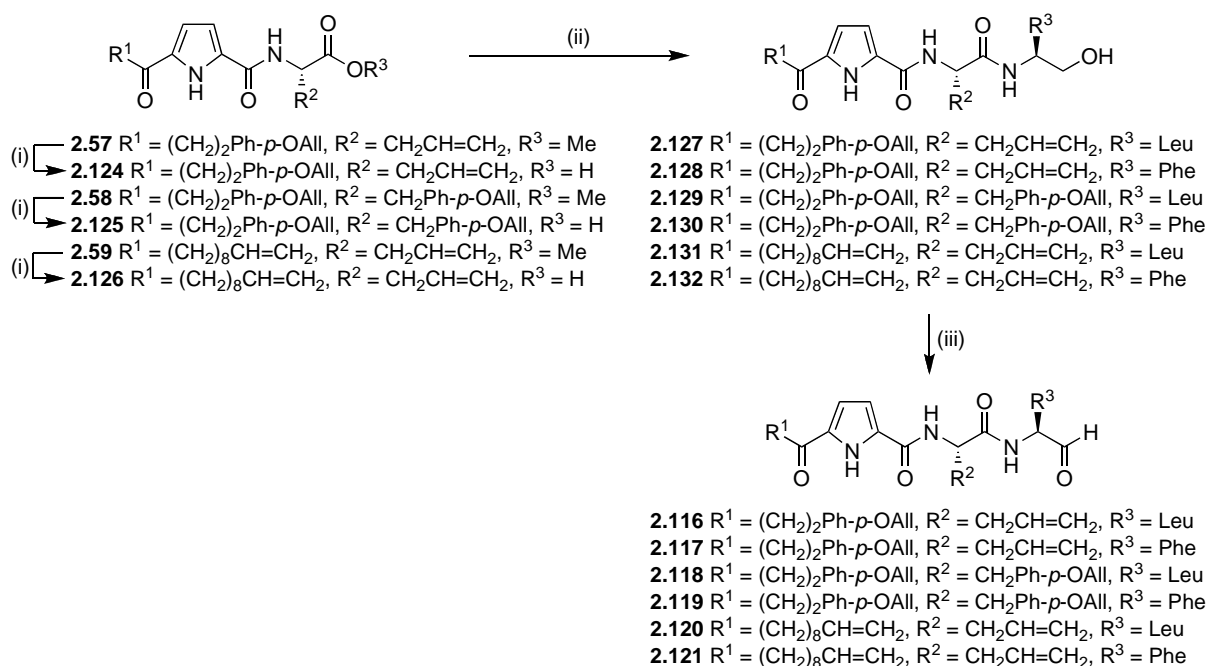
Amidation of carboxylic acid **2.54** with (*L*)-leucinol or (*L*)-phenalaninol in the presence of HATU (described in section 2.3.2.2) gave the peptidyl alcohols **2.122** and **2.123** in yields of 62% and 82%, respectively. Oxidation of the alcohol groups of **2.122** and **2.123** was achieved in the presence of Dess-Martin periodinane to give aldehydes **2.114** and **2.115** in 33% and 39% yields respectively. ¹H NMR spectra of aldehydes **2.114** and **2.115** showed a single resonance at 9.66 and 9.70 ppm, respectively, consistent with a single aldehyde. With requisite acyclic alcohols **2.112-2.113** and aldehydes **2.114-2.115** in hand, inhibition studies against serine (α -chymotrypsin and HLE) and cysteine (calpain and cathepsin) proteases were conducted and will be discussed in detail in chapter 3.



Scheme 2.24 Reagents and Conditions: i) (*L*)-Leucinol or (*L*)-Phenalaninol, HATU, HOBT, DIEA, anh. DMF, N₂, rt, 18 h, (62-82%); ii) Dess-Martin Periodinane, anh. CH₂Cl₂, N₂, rt, 1 h, (33-39%).

2.4.2 Synthesis of P₁-P₄ Acyclic Protease Inhibitors

The P₁-P₄ acyclic aldehydes **2.116-2.121** were prepared as shown in Scheme 2.25 in order to elucidate the influence of the P₂-P₄ 2nd generation macrocyclic core found in macrocycles **2.21-2.26** (section 2.3.2.2). Acyclic esters **2.57-2.59** were hydrolysed to their corresponding carboxylic acids **2.124-2.126**, which were used without further purification. Subsequent amidation of carboxylic acids **2.124-2.126** with (*L*)-leucinol or (*L*)-phenylalaninol in the presence of HATU gave alcohols **2.127-2.132** in moderate to high yields. Alcohols **2.127-2.132** were then oxidised in the presence of Dess-Martin periodinane to give the required P₁-P₄ acyclic aldehydes **2.116-2.121** in moderate yields. ¹H NMR spectra of aldehydes **2.116-2.121** again showed a single aldehyde resonance at 9.35-9.64 ppm.



Scheme 2.25 Reagents and Conditions i) 2M NaOH, THF, rt, 16 h (not isolated); ii) (*L*)-Leucinol or (*L*)-Phenalaninol, HATU, HOBT, DIEA, anh. DMF, N₂, rt, 18 h, (57-92%); iii) Dess-Martin Periodinane, anh. CH₂Cl₂, N₂, rt, 1 h, (21-53%).

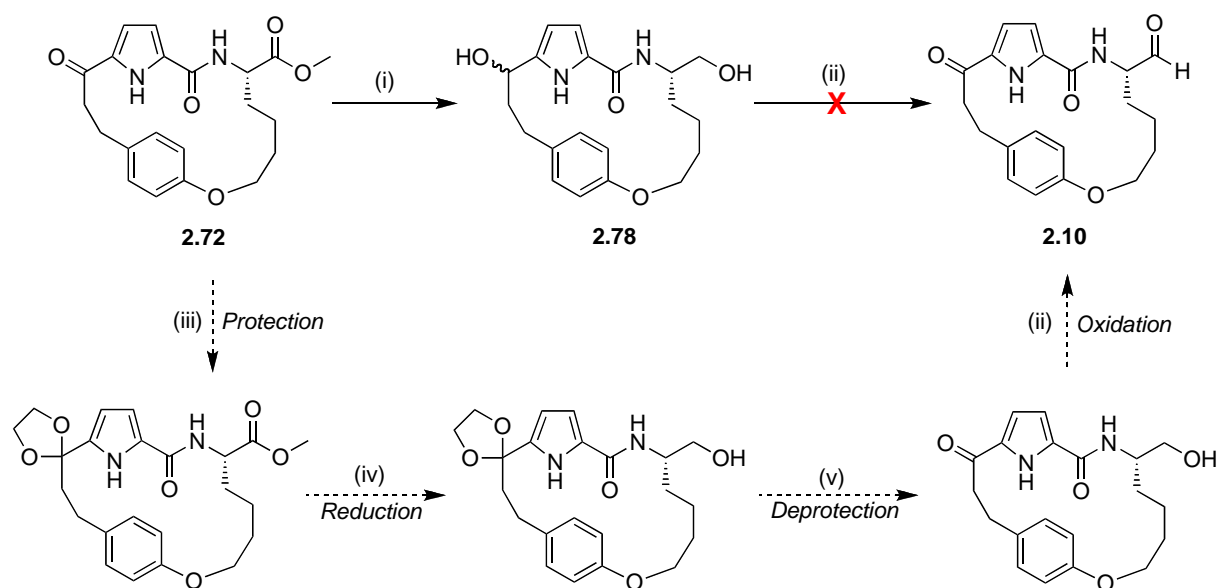
With requisite acyclic alcohols **2.127-2.132** and aldehydes **2.116-2.121** in hand, inhibition studies against serine (α -chymotrypsin and HLE) and cysteine (calpain and cathepsin) proteases were conducted and will be discussed in detail in chapter 3.

2.5 Conclusions and Future Work

In summary a new class of P₁-P₃ and P₂-P₄ cyclised protease inhibitors were designed and synthesised. All inhibitors contained a planar pyrrole aromatic spacer to retain the preferred β -strand conformation, while reducing the peptidic nature of the inhibitor. The cyclised core was introduced through either ring closing metathesis or Huisgen 1,3-dipolar cycloaddition.

2,5- and 2,4,5-substituted pyrroles **2.45-2.51** were prepared in moderate yields via Friedel-Crafts acylation of pyrroles **2.29** and **2.31** to give the required precursors for ring closing metathesis. The P₁-P₃ and P₂-P₄ 2nd generation macrocyclic protease inhibitors **2.78-2.81**, **2.85-2.90** and **2.21-2.26** were synthesised via ring closing metathesis in moderate yields to provide a range of potential inhibitors for assay against cysteine and serine proteases. The P₁-P₃ and P₁-P₄ acyclic protease inhibitors **2.112-2.121** were designed and synthesised to provide an insight into the importance of a macrocycle towards the potency of inhibition against serine and cysteine proteases.

Future investigations into alternative methods for the synthesis of the P₁-P₃ 2nd generation macrocyclic aldehydes **2.10** (Section 2.3.2.1) should be conducted. The proposed selective reduction of the ester motif of the macrocyclic precursor **2.72** proved to be difficult using LiBH₄ as a reagent. Since the keto group was more susceptible to reduction, as an alternative route it may prove advantageous to protect the keto group as an acetal prior to reduction of the ester group.¹⁵² Acid deprotection of the acetal group would unmask the keto group allowing for the oxidation of the primary alcohol to yield the desired aldehyde **2.10** (Scheme 2.26).



Scheme 2.26 Reagents and Conditions i) LiBH_4 , THF, -78°C (1 h) \rightarrow rt (1 h), (62-100%); ii) Isopropanol, DMSO, DIEA, SO_3Py , N_2 , 0°C \rightarrow rt, 3 h; iii) $\text{HOCH}_2\text{CH}_2\text{OH}$, TsOH, benzene; iv) LiAlH_4 , THF; v) 1M HCl, THF

Additional investigations into $\text{P}_2\text{-P}_4$ series of potential macrocyclic inhibitors would involve the investigation of different P_1 residues (R_1) to incorporate selectivity for alternative protease families. For example, having positively charged residues such as Lys or Arg would provide compounds with potential selectivity towards trypsin-like threonine protease such as proteasomes,⁷ which has been implicated in cancer. Furthermore, optimisation of the macrocycle ring-size (n) and incorporation of additional recognition motifs by extension at the N-terminus (A) (Figure 2.28) would provide an opportunity to establish the optimal potency and selectivity for a specific protease family. Incorporation of alternative reversible warheads (R_2), such as nitrile groups (CN) is of high interest, as this group is known to interact selectively with cysteine proteases (in particular cathepsins).¹⁵³⁻¹⁵⁴

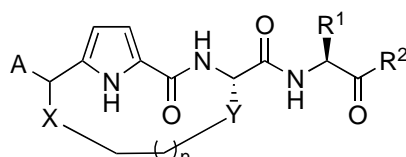


Figure 2.28 Formula of possible future compounds to be investigated.

2.6 References for Chapter Two

- [1] Hedstrom, L. *Chem. Rev.* **2002**, *102*, 4501–4524.
- [2] Goll, D. E.; Thompson, V. F.; Li, H.; Wei, W.; Cong, J. *Physiol. Rev.* **2003**, *83*, 731–801.
- [3] Solomon, M.; Belenghi, B.; Delledonne, M.; Menachem, E.; Levine, A. *Plant Cell* **1999**, *11*, 431–444.
- [4] Thornberry, N. A.; Lazebnik, Y. *Science* **1998**, *281*, 1312–1316.
- [5] Flaumenhaft, R.; Rifkin, D. B. *Curr. Opin. Cell Biol.* **1991**, *3*, 817–823.
- [6] Powers, J. C.; Asgian, J. L.; Ekici, O. D.; James, K. E. *Chem. Rev.* **2002**, *102*, 4639–4750.
- [7] Abbenante, G.; Fairlie, D. P. *Med. Chem.* **2005**, *1*, 71–104.
- [8] Leung, D.; Abbenante, G.; Fairlie, D. P. *J. Med. Chem.* **2000**, *43*, 305–341.
- [9] Potter, H.; Nelson, R. B.; Das, S.; Siman, R.; Kayyali, U. S.; Dressler, D. *Ann. N. Y. Acad. Sci.* **1992**, *674*, 161–173.
- [10] Koblinski, J. E.; Ahram, M.; Sloane, B. F. *Clin. Chim. Acta* **2000**, *291*, 113–135.
- [11] Lo, E. H.; Dalkara, T.; Moskowitz, M. A. *Nat. Rev. Neurosci.* **2003**, *4*, 399–415.
- [12] Houghton, M.; Weiner, A.; Han, J.; Kuo, G.; Choo, Q. L. *Hepatology* **1991**, *14*, 381–388.
- [13] Wride, M. A. *Ex. Rev. Op.* **2007**, *2*, 833–844.
- [14] Zhan, H.; Yamamoto, Y.; Shumiya, S.; Kunimatsu, M.; Nishi, K.; Ohkubo, I.; Kani, K. *Histochem. J.* **2001**, *33*, 511–521.
- [15] Senokuchi, K.; Nakai, H.; Nakayama, Y.; Odagaki, Y.; Sakaki, K.; Kato, M.; Maruyama, T.; Miyazaki, T.; Ito, H.; Kamiyasu, K.; Kim, S.; Kawamura, M.; Hamanaka, N. *J. Med. Chem.* **1995**, *38*, 2521–2523.
- [16] Otto, H.-H.; Schirmeister, T. *Chem. Rev.* **1997**, *97*, 133–171.
- [17] Vicik, R.; Busemann, M.; Baumann, K.; Schirmeister, T. *Curr. Top. Med. Chem.* **2006**, *6*, 331–353.
- [18] Mykles, D. L. *Method Cell Biol.* **2001**, *66*, 247–287.
- [19] Demuth, H. U. *J. Enzym. Inhib.* **1990**, *3*, 249–278.
- [20] Schechter, I.; Berger, A. *Biochem. Biophys. Res. Commun.*, **1967**, *27*, 157–62.
- [21] Pietsch, M.; Chua, K. C. H.; Abell, A. D. *Curr. Top. Med. Chem.* **2010**, *10*, 270–293.

- [22] Bondareva, L. A.; Nemova, N. N. *Russ. J. Bioorg. Chem.* **2008**, *34*, 266-273.
- [23] Dear, T. N.; Boehm, T. *Gene*, **2001**, *274*, 245-252.
- [24] Strobl, S.; Fernandez-Catalan, C.; Braun, M.; Huber, R.; Masumoto, H.; Nakagawa, K.; Irie, A.; Sorimachi, H.; Bourenkow, G.; Bartunik, H.; Suzuki, K.; Bode, W. *Proc. Natl. Acad. Sci. U.S.A.* **2000**, *97*, 588-592.
- [25] Moldoveanu, T.; Campbell, R. L.; Cuerrier, D.; Davies, P. L. *J. Mol. Biol.* **2004**, *343*, 1313-1326.
- [26] Moldoveanu, T.; Hosfield, C. M.; Lim, D.; Elce, J. S.; Jia, Z.; Davies, P. L. *Cell* **2002**, *108*, 649-660.
- [27] Hanna, R. A.; Campbell, R. L.; Davies, P. L. *Nature* **2008**, *456*, 409-412.
- [28] Donkor, I.O. *Current Medicinal Chemistry* **2000**, *7*, 1171-1188.
- [29] Perrin, B.J.; Huttenlocher, A. *International Journal of Biochemistry & Cell Biology* **2002**, *34*, 722-725.
- [30] Iqbal, M.; Messina, P.A.; Freed, B.; Das, M.; Chetterjee, S.; Tripathy, R.; Tao, M.; Josef, K.A.; Dembofsky, B. *Bioorganic & Medicinal Chemistry Letters* **1997**, *7*, 539-544.
- [31] Huang, Y.; Wang, K.K.W. *Trends in Molecular Medicine* **2001**, *7*, 355-362.
- [32] Cuerrier, D, Moldoveanu, T, Davies, P. L. *J. Biol. Chem.* **2005**, *280*, 40632-40641.
- [33] The Fred Hollows Foundation. <http://www.hollows.org.au/> (Access Date: 24 April 2012)
- [34] Calpain Therapeutics. <http://calpaintherapeutics.com/> (Access Date: 25 April 2012)
- [35] Rossi, A.; Deveraux, Q.; Turk, B.; Sali, A. *Biol. Chem.* **2004**, *385*, 363-372.
- [36] Turk, V.; Turk, B.; Turk, D. *EMBO J.* **2001**, *20*, 4629-4633.
- [37] Kirschke, H.; Langer, J.; Wiederanders, B.; Ansorge, S.; Bohley, P. *Eur. J. Biochem.* **1977**, *74*, 293-301.
- [38] Chowdhury, S. F.; Joseph, L.; Kumar, S.; Tulsidas, S. R.; Bhat, S.; Ziomek, E.; Ménard, R.; Sivaraman, J.; Purisima, E. O. *J. Med. Chem.* **2008**, *51*, 1361-1368.
- [39] Mcgrath, M. E.; Palmer, J. T.; Brömme, D.; Somoza, J. R. *Protein Sci.* **1998**, *7*, 1294-1302.
- [40] Leroy, V.; Thurairatnam, S. *Expert Opin. Ther. Patents* **2004**, *14*, 301-311.
- [41] Guncar, G.; Pungercic, G.; Klemencic, I.; Turk, V.; Turk, D. *EMBO J.* **1999**, *18*, 793-803.

- [42] Irie, O.; Ehara, T.; Iwasaki, A.; Yokokawa, F.; Sakaki, J.; Hirao, H.; Kanazawa, T.; Teno, N.; Horiuchi, M.; Umemura, I.; Gunji, H.; Masuya, K.; Hitomi, Y.; Iwasaki, G.; Nonomura, K.; Tanabe, K.; Fukaya, H.; Kosaka, T.; Snell, C. R.; Hallett, A. *Bioorg. Med. Chem. Lett.* **2008**, *18*, 3959–3962.
- [43] Portaro, F.C.V.; Santos, A.B.F.; Cezari, M.H.S.; Juliano, M.A.; Juliano, L.; Carmona, E. *Biochem. J.* **2000**, *347*, 123-129.
- [44] Gocheva, V.; Zeng, W.; Ke, D.; Klimstra, D.; Reinheckel, T.; Peters, C.; Hanahan, D.; Joyce, J. A. *Genes Dev.* **2006**, *20*, 543–556.
- [45] Turk, V.; Kos, J.; Turk, B. *Cancer Cell* **2004**, *5*, 409–410.
- [46] Joyce, J. A.; Baruch, A.; Chehade, K.; Meyer-Morse, N.; Giraudo, E.; Tsai, F.-Y.; Greenbaum, D. C.; Hager, J. H.; Bogoy, M.; Hanahan, D. *Cancer Cell* **2004**, *5*, 443–453.
- [47] Lecaille, F.; Kaleta, J.; Brömme, D. *Chem. Rev.* **2002**, *102*, 4459–4488.
- [48] Sajid, M.; McKerrow, J. H. *Mol. Biochem. Parasitol.* **2002**, *120*, 1–21.
- [49] Barrett, A.J.; Rawlings, N.D. *Arch. Biochem. Biophys.* **1995**, *318*, 247-250.
- [50] Blow, D.M. In *The Enzymes*; 3rd ed.; Boyer, P.D.; Academic Press: Boca Raton, 1971; Vol 3.
- [51] Czapinska, H.; Otlewski, *Eur. J. Biochem.* **1999**, *260*, 571-595.
- [52] Schellenberger, V.; Braune, K.; Hofmann H.-J.; Jakubke, H.-D. *Eur. J. Biochem.* **1991**, *199*, 623-636.
- [53] Perona, J.J.; Craik, C.S. *J. Biol. Chem.* **1997**, *272*, 29987-29990.
- [54] Sinha, S.; Watorek, W.; Karr, S.; Giles, J.; Bode, W.; Travis, J. *Proc. Natl. Acad. Sci. U.S.A.* **1987**, *84*, 2228–2232.
- [55] Bode, W.; Meyer, E.; Powers, J. C. *Biochemistry* **1989**, *28*, 1951–1963.
- [56] Hansen, G.; Gielen-Haertwig, H.; Reinemer, P.; Schomburg, D.; Harrenga, A.; Niefind, K. *J. Mol. Biol.* **2011**, *409*, 681–691.
- [57] Powers, J.C.; Gupton, B.F.; Harley, A.D.; Nishino, N.; Whitley, R.J. *Biochim. Biophys. Acta* **1977**, *485*, 156-166.
- [58] Nakajima, K.; Powers, J.C.; Ashe, B.; Zimmerman, M. *J. Biol. Chem.* **1979**, *254*, 4027-4032.
- [59] McRae, B.; Nakajima, K.; Travis, J. Powers J.C. *Biochemistry* **1980**, *19*, 3973-3978.
- [60] Shotton, D. M.; Watson, H. C. *Nature* **1969**, *25*, 811-816.

- [61] Stein, R.L.; Strimpler A.M.; Hori H.; Powers J.C. *Biochemistry* **1987**, *26*, 1301-1305.
- [62] Ohbayashi H. *Expert Opin. Ther. Patents* **2002**, *12*, 65-84.
- [63] Hansen, G.; Gielen-Haertwig, H.; Reinemer, P.; Schomburg, D.; Harrenga, A.; Niefind, K. *J. Mol. Biol.* **2011**, *409*, 681–691.
- [64] Sukhova, G. K.; Zhang, Y.; Pan, J.-H.; Wada, Y.; Yamamoto, T.; Naito, M.; Kodama, T.; Tsimikas, S.; Witztum, J. L.; Lu, M. L.; Sakara, Y.; Chin, M. T.; Libby, P.; Shi, G.-P. *J. Clin. Invest.* **2003**, *111*, 897–906.
- [65] Skrzypczak, M.; Springwald, A.; Lattrich, C.; Häring, J.; Schüler, S.; Ortmann, O.; Treeck, O. *Cancer Invest.* **2012**, *30*, 398–403.
- [66] Chang, W. S. W.; Wu, H. R.; Yeh, C. T.; Wu, C. W.; Chang, J. Y. *J Cancer Mol* **2007**, *3*, 5–14.
- [67] Lutgens, S. P. M.; Cleutjens, K. B. J. M.; Daemen, M. J. A. P.; Heeneman, S. *The FASEB Journal* **2007**, *21*, 3029–3041.
- [68] Yasuda, Y.; Kaleta, J.; Brömme, D. *Adv. Drug Deliv. Rev.* **2005**, *57*, 973–993.
- [69] Leung-Toung, R.; Zhao, Y.; Li, W.; Tam, T. F.; Karimian, K.; Spino, M. *Curr. Med. Chem.* **2006**, *13*, 547–581.
- [70] McNaught, K. S.; Jenner, P. *Neurosci. Lett.* **2001**, *297*, 191–194.
- [71] Keller, J. N.; Hanni, K. B.; Markesbery, W. R. *J. Neurochem.* **2000**, *75*, 436–439.
- [72] Pallarès, I.; Vendrell, J.; Avilés, F. X.; Ventura, S. *J. Mol. Biol.* **2004**, *342*, 321–331.
- [73] Kennedy, A. R. *Pharmacol. Ther.* **1998**, *78*, 167–209.; Hempel, D.; Wojtukiewicz, M. Z.; Kozłowski, L.; Romatowski, J.; Ostrowska, H. *Tumour Biol.* **2011**, *32*, 753–759.
- [74] Pratt, R. *BioMed. Chem. Lett.* **1992**, *2*, 1327-1326.
- [75] Sanderson, P. E. *Med. Res. Rev.* **1999**, *19*, 179–197.
- [76] Rasnick, D. *Prespect. Drug. Discov. Des.* **1996**, *6*, 47-63.
- [77] Donkor, I. O. *Curr. Med. Chem.* **2000**, *7*, 1171-1188.
- [78] Matsumoto, K.; Mizoue, K.; Kitamura, K.; Tse, W.-C.; Huber, C. P.; Ishida, T. *Biopolymers* **1999**, *51*, 99-107
- [79] Yabe, Y.; Guillaume, D.; Rich, D. H. *J. Am. Chem. Soc.* **1988**, *110*, 4043-4044.
- [80] Leung-Toung, R.; Li, W.; Tam, T. F.; Karimian, K. *Curr. Med. Chem.* **2002**, *9*, 979-1002.

- [81] Fairlie, D. P.; Tyndall, J. D. A.; Reid, R. C.; Wong, A. K.; Abbenante, G.; Scanlon, M. J.; March, D. R.; Bergman, D. A.; Chai, C. L. L.; Burkett, B. A. *J. Med. Chem.* **2000**, *43*, 1271–1281.
- [82] Glenn, M. P.; Pattenden, L. K.; Reid, R. C.; Tyssen, D. P.; Tyndall, J. D. A.; Birch, C. J.; Fairlie, D. P. *J. Med. Chem.* **2002**, *45*, 371–381.
- [83] Reid, R. C.; Pattenden, L. K.; Tyndall, J. D. A.; Martin, J. L.; Walsh, T.; Fairlie, D. P. *J. Med. Chem.* **2004**, *47*, 1641–1651.
- [84] Morgan, B.A.I Gainor, J.A. *Annu. Rep. Med. Chem.* **1989**, *24*, 243.
- [85] Ripka, A. S.; Rich, D. H. *Curr. Opin. Chem. Biol.* **1998**, *2*, 441–452.
- [86] Adessi, C.; Soto, C. *Curr. Med. Chem.* **2002**, *9*, 963–978.
- [87] Lipinski, C. A.; Lombardo, F.; Dominy, B. W.; Feeney, P. J. *Adv. Drug Deliv. Rev.* **2001**, *46*, 3–26.
- [88] Park, S.-J.; Lee, K.-I. *Bull. Korean Chem. Soc.* **2005**, *26*, 327–330.
- [89] Tyndall, J. D.; Fairlie, D. P. *Curr. Med. Chem.* **2001**, *8*, 893–907.
- [90] Li, P.; Roller, P.P. *Current Topics in Medicinal Chemistry* **2002**, *2*, 325–341.
- [91] Tyndall, J. D. A.; Nall, T.; Fairlie, D. P. *Chem. Rev.* **2005**, *105*, 973–999.
- [92] Madala, P. K.; Tyndall, J. D. A.; Nall, T.; Fairlie, D. P. *Chem. Rev.* **2010**, *110*, PR1–PR31.
- [93] Loughlin, W.A.; Tyndall, J.D.A.; Glenn M.O.; Fairlie, D.P. *Chem. Rev.* **2004**, *104*, 6085–6117.
- [94] Abell, A. D.; Jones, M. A.; Coxon, J. M.; Morton, J. D.; Aitken, S. G.; McNabb, S. B.; Lee, H. Y.-Y.; Mehrtens, J. M.; Alexander, N. A.; Stuart, B. G.; Neffe, A. T.; Bickerstaffe, R. *Angew. Chem. Int. Ed.* **2009**, *48*, 1455–1458.
- [95] Giannis, A.; Kolter, T. *Angew. Chem. Int. Ed.* **1993**, *32*, 1244–1267.
- [96] White, C. J.; Yudin, A. K. *Nat. Chem.* **2011**, *3*, 509–524.
- [97] Abell, A. D. *Lett. Pept. Sci.* **2002**, *8*, 267–272.
- [98] Abell, A. D.; Alexander, N. A.; Aitken, S. G.; Chen, H.; Coxon, J. M.; Jones, M. A.; McNabb, S. B.; Muscroft-Taylor, A. *J. Org. Chem.* **2009**, *74*, 4354–4356.
- [99] Brik, A. *Adv. Synth. Catal.* **2008**, *350*, 1661–1675.
- [100] Pehere, A. D.; Abell, A. D. *Org. Lett.* **2012**, *14*, 1330–1333.
- [101] Gradillas, A.; Perez-Castells, J. *Angewandte Chemie International Edition* **2006**, *45*, 6086–6101.

- [102] Ersmark, K.; Nervall, M.; Gutierrez-de-Teran, H.; Hamelink, E.; Janka, L. K.; Clemente, J. C.; Dunn, B. M.; Gogoll, A.; Samuelsson, B.; Aqvist, J.; Hallberg, A. *Bioorg. Med. Chem.* **2006**, *14*, 2197-2208.
- [103] Miller, S. J.; Blackwell, H. E.; Grubbs, R. H. *J. Am. Chem. Soc.* **1996**, *118*, 9606-9614.
- [104] Gardiner, J.; Abell, A. D. *Tetrahedron Lett.* **2003**, *44*, 4227-4230.
- [105] Humphries, M. E.; Murphy, J.; Phillips, A. J.; Abell, A. D. *J. Org. Chem.* **2003**, *68*, 2432-2436.
- [106] Gardiner, J.; Anderson, K. H.; Downard, A.; Abell, A. D. *J. Org. Chem.* **2004**, *69*, 3375-3382.
- [107] Aitken, S. G.; Abell, A. D. *Aust. J. Chem.* **2005**, *58*, 3-13.
- [108] Whiting, M.; Muldoon, J.; Lin, Y.-C.; Silverman, S. M.; Lindstrom, W.; Olson, A. J.; Kolb, H. C.; Finn, M. G.; Sharpless, K. B.; Elder, J. H.; Fokin, V. V. *Angew. Chem. Int. Ed.* **2006**, *45*, 1435-1439.
- [109] Whiting, M.; Muldoon, J.; Lin, Y.-C.; Silverman, S. M.; Lindstrom, W.; Olson, A. J.; Kolb, H. C.; Finn, M. G.; Sharpless, K. B.; Elder, J. H.; Fokin, V. V. *Angew. Chem.* **2006**, *118*, 1463-1467.
- [110] Moorhouse, A. D.; Moses, J. E. *ChemMedChem.* **2008**, *3*, 715-523.
- [111] Bock, V. D.; Speijer, D.; Hiemstra, H.; van Maarseveen, J. H. *Org. Biomol. Chem.* **2007**, *5*, 971-975.
- [112] Evans, R. *Aust. J. Chem.* **2007**, *60*, 384-395.
- [113] Rostovtsev, V. V.; Green, L. G.; Fokin, V. V.; Sharpless, K. B. *Angew. Chem.* **2002**, *114*, 2708-2711.
- [114] Rostovtsev, V. V.; Green, L. G.; Fokin, V. V.; Sharpless, K. B. *Angew. Chem. Int. Ed.* **2002**, *41*, 2596-2599.
- [115] Imperio, D.; Pirali, T.; Galli, U.; Pagliai, F.; Cafici, L.; Canonico, P. L.; Sorba, G.; Genazzani, A. A.; Tron, G. C. *Bioorg. Med. Chem.* **2007**, *15*, 6748-6757.
- [116] Himo, F.; Lovell, T.; Hilgraf, R.; Rostovtsev, V. V.; Noodleman, L.; Sharpless, K. B.; Fokin, V. V. *J. Am. Chem. Soc.*, **2005**, *127*, 210-216.
- [117] Glide, version 4.0, Schrödinger, LLC, New York, NY, 2005.
- [118] Friesner, R. A.; Banks, J. L.; Murphy R. B.; Halgren, T. A.; Klicic, J. J.; Mainz, D. T.; Repasky, M. P.; Knoll, E. H.; Shelly, M.; Perry, J. K.; Shaw, D. E.; Francis, P.; Shenkin, P. S. *J. Med. Chem.* **2004**, *47*, 1739-1749.
- [119] Komoto, I.; Matsuo, J.-i.; Kobayahi, S. *Topics Catal.* **2002**, *19*, 43-47.

- [120] OEChem, version 1.7.4, OpenEye Scientific Software, Inc., Santa Fe, NM, USA, www.eyesopen.com, **2010**.
- [121] Cuerrier, D.; Moldoveanu, T.; Inoue, J.; Davies, P. L.; Campbell, R. L. *Biochemistry* **2006**, *45*, 7446-7452.
- [122] Bailey, D. M.; Johnson, R. E.; Albertson, N. F. *Org. Synth.* **1971**, *51*, 100-102.
- [123] Garrido, D. O. A.; Buldain, G.; Ojea, M. I.; Frydman, B. *J. Org. Chem.* **1988**, *53*, 403-407.
- [124] Bayardon, J.; Sinou, D. *Tetrahedron Asymmetry* **2006**, *16*, 2965-2972.
- [125] Yang, D.; Wang, H.-L.; Sung, Z.-N.; Chung, N.-W.; Shen, J.-G. *J. Am. Chem. Soc.* **2006**, *128*, 6004-6005.
- [126] Lafitte, V. G. H.; Aliev, A. E.; Hailes, H. C.; Bala, K.; Golding, P. *J. Org. Chem.* **2005**, *70*, 2701-2707.
- [127] Ohkata, K.; Tamura, Y.; Shetuni, B. B.; Takagi, R.; Miyanaga, W.; Kojima, S.; Paquette, L. A. *J. Am. Chem. Soc.* **2004**, *126*, 16783-16792.
- [128] Martyn, D. C.; Vernall, A. J.; Clark, B. M.; Abell, A. D. *Org. Biomol. Chem.* **2003**, *1*, 2103-2110.
- [129] Lutz, R. P. *Chem. Rev.* **1984**, *84*, 205-247.
- [130] Zulfiqar, F.; Kitazume, T. *Green Chem.* **2000**, *2*, 296-297.
- [131] Grant, V. H.; Liu, B. *Tetrahedron Lett.* **2005**, *46*, 1237-1239.
- [132] Ito, Y.; Kato, R.; Hamashima, K.; Kataoka, Y.; Oe, Y.; Ohta, T.; Furukawa, I. *J. Organomet. Chem.* **2007**, *692*, 691-697.
- [133] Sharma, G. V. M.; Ilangovan, A.; Mahalingam, A. K. *J. Org. Chem.* **1998**, *63*, 9103-9104.
- [134] Schmuck, C.; Geiger, L. *J. Am. Chem. Soc.* **2004**, *126*, 8898-8899.
- [135] Si, Y.-G.; Chen, J.; Li, F.; Li, J.-H.; Qin, Y.-J.; Jiang, B. *Adv. Synth. Catal.* **2006**, *348*, 898-904.
- [136] Goudreau, N.; Brochu, C.; Cameron, D. R.; Duceppe, J. S.; Faucher, A.-F.; Ferland, J.-M.; Crand-Maitre, C.; Poirier, M.; Simoneau, B.; Tsantrizos, Y. S. *J. Org. Chem.* **2004**, *69*, 6185-6201.
- [137] Kaul, R.; Suprenant, S.; Lubell, W. D. *J. Org. Chem.* **2005**, *70*, 3838-3844.
- [138] Gu, W.; Liu, S.; Silverman, R. B. *Org. Lett.* **2002**, *4*, 4171-4174.
- [139] Abell, A. D.; Brown, K. M.; Coxon, J. M.; Jones, M. A.; Miyamoto, S.; Neffe, A. T.; Nikkel, J. M.; Stuart, B. G. *Peptides* **2005**, *26*, 251-258.

- [140] Abell, A. D.; Martyn, D. C.; May, B. C. H.; Nabbs, B. K. *Tetrahedron Lett.* **2002**, *43*, 3673-3675.
- [141] Tian, Z.-Q.; Brown, B. B.; Mack, D. P.; Hutton, C. A.; Bartlett, P. A. *J. Org. Chem.* **1997**, *62*, 514-522.
- [142] Jones, M. A.; Morton, J. D.; Coxon, J. M.; McNabb, S. B.; Lee, H. Y.-Y.; Aitken, S. G.; Mehrtens, J. M.; Robertson, L. J. G.; Neffe, A. T.; Miyamoto, S.; Bickerstaffe, R.; Gately, K.; Wood, J. M.; Abell, A. D. *Bioorg. Med. Chem.* **2008**, *16*, 6911-6923.
- [143] Abell, A. D.; Jones, M. A.; Neffe, A. T.; Aitken, S. G.; Cain, T. P.; Payne, R. J.; McNabb, S. B.; Coxon, J. M.; Stuart, B. G.; Pearson, D.; Lee, H. Y.-Y.; Morton, J. D. *J. Med. Chem.* **2007**, *50*, 2916-2920.
- [144] Parikh, J. R.; Doering, W. V. E. *J. Am. Chem. Soc.* **1967**, *89*, 5505-5507.
- [145] Hamada, Y.; Shioiri, T. *Chem. Pharm. Bull.* **1982**, *30*, 1921-1924.
- [146] Fukiage, C.; Azuma, M.; Nakamura, Y.; Tamada, Y.; Nakamura, M.; Shearer, T. R. *Biochim. Biophys. Acta* **1997**, *1361*, 304-312.
- [147] Dess, D. B.; Martin, J. C. *J. Am. Chem. Soc.* **1991**, *113*, 7277-7287.
- [148] Mullen, D. G.; Desai, A. M.; Waddell, J. N.; Cheng, X.; Kelly, C. V.; McNerny, D. Q.; Majoros, I. J.; Baker, J. R. Jr.; Sander, L. M.; Orr, B. G.; Holl, M. M. B. *Bioconjugate Chem.* **2008**, *19*, 1748-1752.
- [149] Mullen, D. G.; McNerny, D. Q.; Desai, A. M.; Cheng, X.; DiMaggio, S.C.; Kotlyar, A.; Zhong, Y.; Kelly, C. V.; Thomas, T. P.; Majoros, I. J.; Orr, B. G.; Baker, J. R. Jr.; Holl, M. M. B. *Bioconjugate Chem.* **2011**, *22*, 679-689.
- [150] Yan, R. B.; Yang, F.; Wu, Y. F.; Zhang, L. H.; Ye, X. S. *Tetrahedron Lett.* **2005**, *46*, 8993-8995.
- [151] Neises, B.; Steglich, W. *Angew. Chem. Int. Ed.* **1978**, *17*, 522-524.
- [152] Greene, T.W.; Wuts, P.G.M. *Protective Groups in Organic Synthesis* (2nd Ed.) **1991**, Wiley & Sons.
- [153] Dufour, E.; Storer, A. C.; Menard, R. *Biochemistry* **1995**, *34*, 9136-9143.
- [154] Frizler, M.; Stirnberg, M.; Sisay, M. T.; Gütschow, M. *Curr. Top. Med. Chem.* **2010**, *10*, 294-322.

CHAPTER THREE:
Enzyme Assays and Results

3.1 Introduction: Protease Inhibition Assays

The biological activities of the macrocyclic and acyclic peptidic inhibitors reported in this thesis were determined by measuring the inhibition constants (IC_{50} and K_i) using established *in vitro* assays as discussed below. The IC_{50} indicates the concentration of inhibitor required to decrease the activity of the target protease by 50%, while K_i is the inhibition constant that defines the binding affinity of the inhibitor. The IC_{50} is a relative value, the magnitude of which is dependent on the concentration of substrate used in the assay. It is related to K_i through the Cheng-Prusoff equation (1),¹ where the K_i value is a constant for a given compound against a specific protease. However, as the substrate concentration approaches 0, the IC_{50} value approximates to the K_i value.²

$$IC_{50} = K_i \left(1 + \frac{[S]}{K_m} \right) \quad (1)$$

Protease assays are classified into two groups on the basis of the sampling method used: (i) continuous assays; and (ii) discontinuous assays. Continuous assays allow real-time monitoring of enzyme activity, while discontinuous assays require aliquots of the samples to be removed at different time points.³ An example of a continuous assay is a spectrophotometric assay, whereby enzyme activity is monitored through spectrophotometric methods, such as absorption spectrophotometry or fluorescence spectrophotometry. Spectrophotometric assays are easy to handle and allow intervention in ongoing reactions (e.g. by additions) at any time during the reaction and were used in the work described in this chapter.

3.2 Assay Protocols for Cysteine and Serine Proteases

3.2.1 Calpain Inhibition Assay: BODIPY-Casein Fluorescence

The *in vitro* assay of calpain was carried out using an established fluorescence assay protocol.⁵ Casein labelled with the fluorophore, 4,4-difluoro-5,7-dimethyl-4-bora-3a,4a-diaza-s-indacene-3-propionic acid (BODIPY) was used as the substrate in this assay. In the

absence of calpain, fluorescence is not observed due to auto-quenching of adjacent intramolecular interactions of fluorophores. Enzyme catalysed proteolysis of the substrate results in an increase in fluorescence observed (see Figure 3.1). Therefore, the inhibitory activity of an inhibitor can be measured by calculating the change in fluorescence over a known period of time.

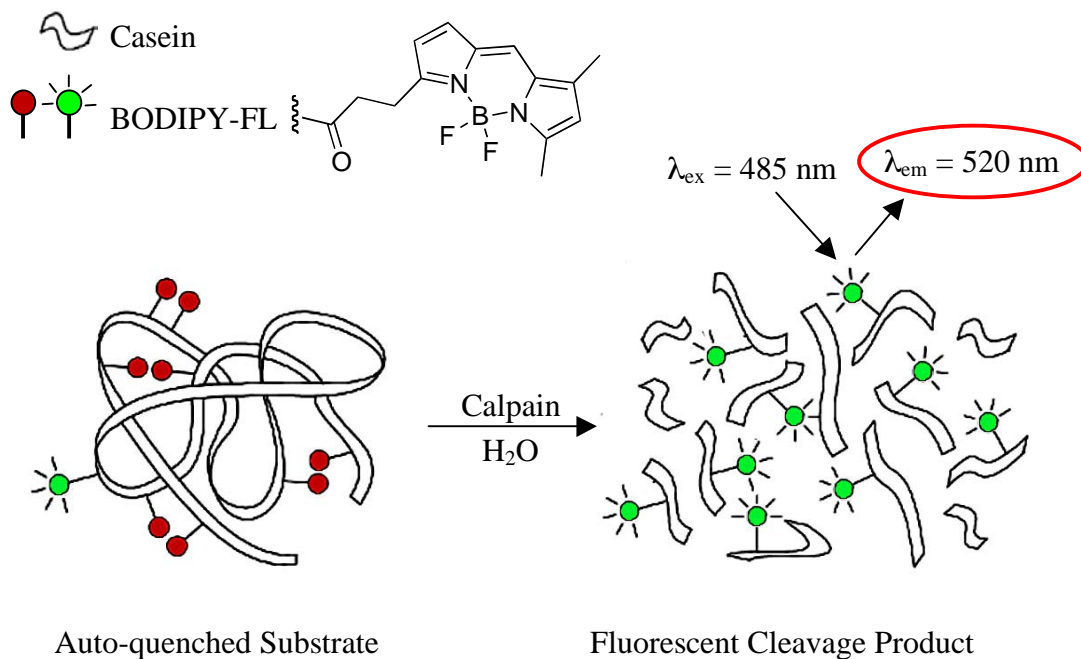


Figure 3.1 Schematic representation of the fluorescence calpain assay.

μ -Calpain (calpain 1) and m-calpain (calpain 2), isolated from sheep lung and purified by ion-exchange chromatography, were separately diluted to give a linear response over the course of the assay.* The substrate solution (0.0005% BODIPY-FL casein* in 10 mM MOPS buffer, pH 7.5 containing 10 mM CaCl₂, 0.1 mM NaN₃ and 0.1% mercaptoethanol) was prepared freshly on the day.

The inhibition assays were performed in 96-well black *Whatman* plates using three controls: (i) a calcium blank (negative control) to demonstrate that the substrate does not undergo self-decomposition; (ii) an EDTA blank (negative control) to demonstrate that calpain activity requires calcium ions for activation; and (iii) an enzyme activity blank (positive control) to show that the enzyme is active under the assay conditions. The calcium blank contained 50 μ L of ultrapure water and 50 μ L of enzyme buffer (20 mM MOPS, pH 7.5 containing 2 mM EGTA, 2 mM EDTA, 0.035% v/v 2-mercaptoethanol,

*Calpains and BODIPY-FL labelled casein were provided courtesy of Lincoln University, New Zealand

220-270 mM NaCl), and the EDTA blank contained 50 μL of 50 mM EDTA/NaOH, pH 7.5 solution and 50 μL of the enzyme in enzyme buffer (20 mM MOPS, pH 7.5 containing 2 mM EGTA, 2 mM EDTA, 0.035% v/v 2-mercaptoethanol, 220-270 mM NaCl). The enzyme activity blank contained 50 μL of 4% DMSO in ultrapure water* and 50 μL of enzyme solution. For enzyme inhibition assays, 4% DMSO in ultrapure water was replaced with 50 μL of inhibitor solution in 4% DMSO in ultrapure water (see Figure 3.2 for a schematic of enzyme inhibition assay layout). The reaction was initiated by the addition of 100 μL of substrate solution at 37 $^{\circ}\text{C}$ and the hydrolysis was monitored for 10 min in a BMG Fluostar with an excitation of 485 nm and emission of 520 nm. The percentage inhibition was determined as 100 times the activity of the inhibitor present divided by the activity of the enzyme activity control. Assays were performed in duplicate, with serial dilutions of inhibitor (7 dilutions per assay) from a range of 50 μM to 10 nM. For an example of raw data and IC_{50} calculation see appendix A2.

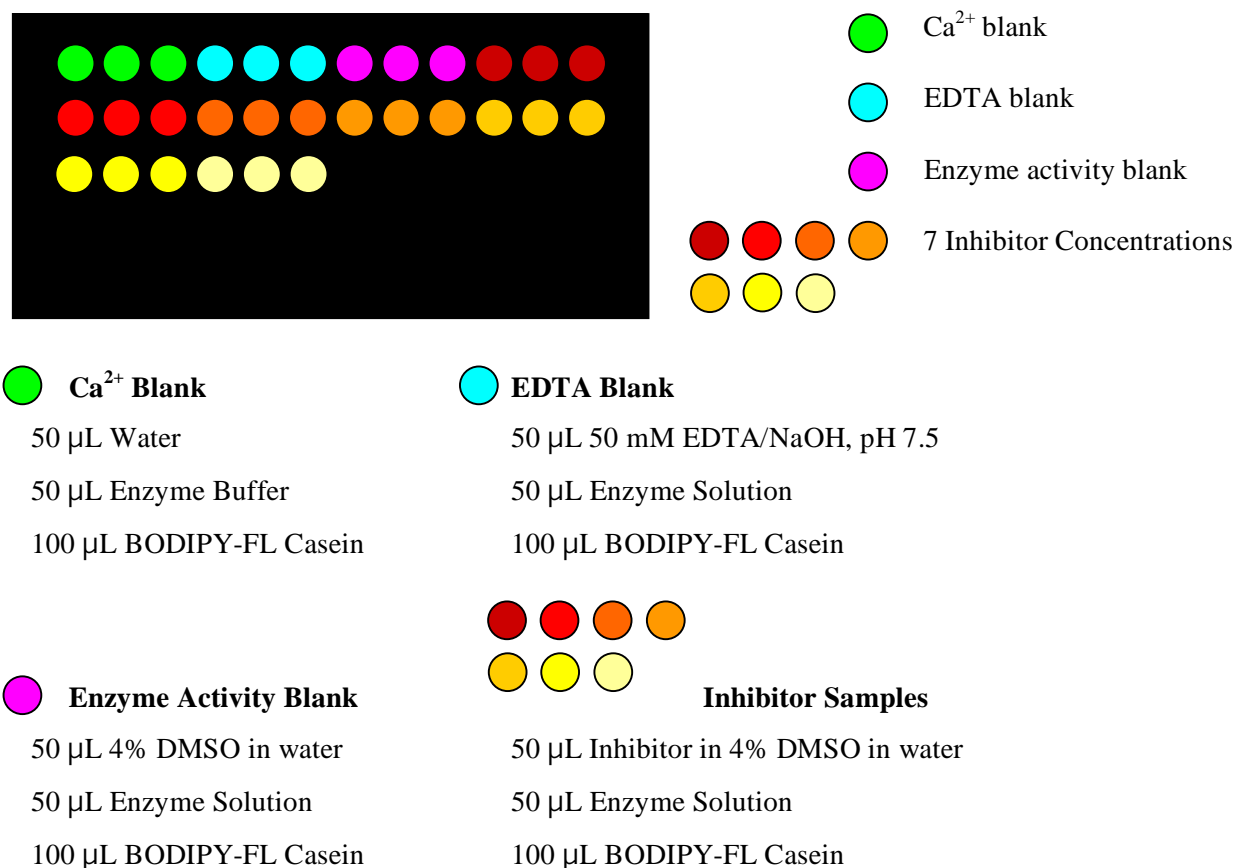


Figure 3.2 Schematic representation of a typical calpain inhibition assay.

Validation of the BOPIPY-casein Assay Protocol

The assay protocol and analysis was validated with the known inhibitors SJA6017 and CAT811 (see Table 3.1). The aldehydes displayed a curved line (Figure 3.3) associated with a slow binding behaviour when assayed against calpain (section 3.3.1.1). Initial attempts to fit the data points with an equation for slow binding inhibition⁸ was unsuccessful due to an insufficient amount of data points per curve. As a result, a linear regression was completed over data points from $t = 390\text{-}570$ s, corresponding to the steady state rate of slow binding inhibition, which gave a good correlation with linear behaviour. As such, the slopes from the data points between 390-570 s were used for IC_{50} calculations for all calpain inhibition assays (see Figure 3.4).

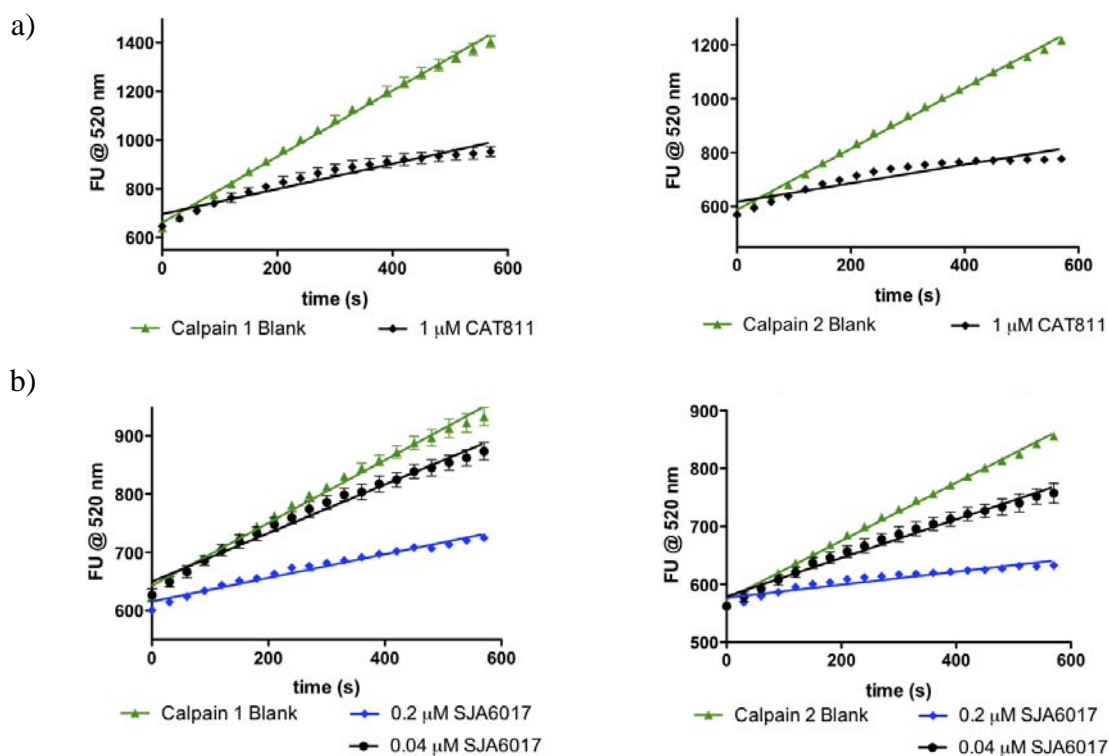


Figure 3.3 Interaction of aldehydes (a) CAT811 and (b) SJA6017 with calpain 1 and 2.

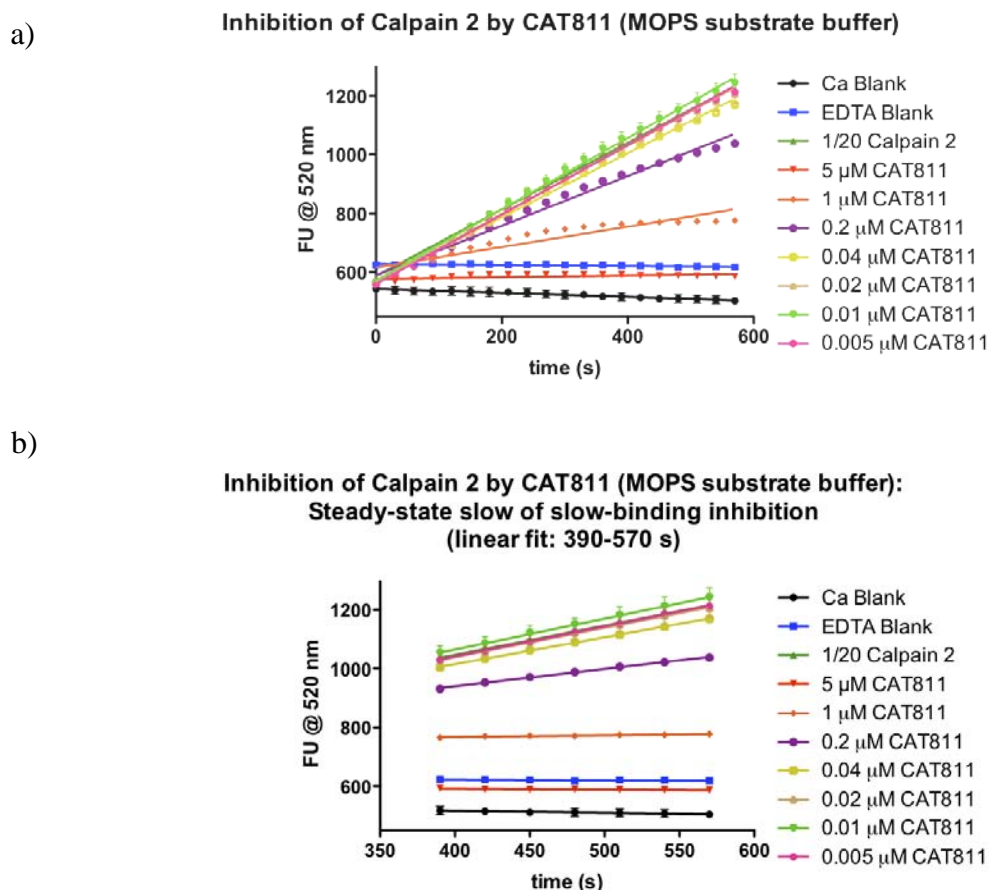
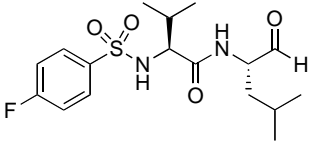
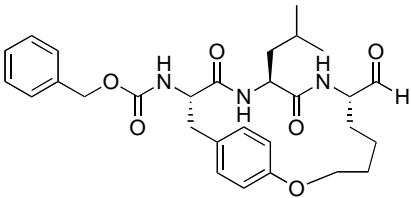


Figure 3.4 Example of graph used for the IC_{50} calculation for a typical calpain inhibition assay.

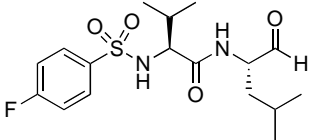
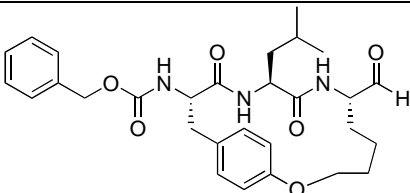
Inhibition assays of inhibitor SJA6017 with BODIPY-casein gave an average 56 nM inhibition against m-calpain ($IC_{50} = 78 \text{ nM}$)⁹, while an IC_{50} of 84 nM for μ -calpain ($IC_{50} = 8 \text{ nM}$)⁹ was obtained. The variation in IC_{50} values of SJA6017 obtained utilising the BODIPY-casein fluorescence assay compared to literature values is attributed to the difference in implemented assay protocol (Coomassie Blue vs. BODIPY-casein assay), which can easily influence the IC_{50} values. The limitations of the Coomassie Blue colorimetric assay¹⁰ utilized by Inoue⁹ is that it can only detect 5-10 mg of calpain, and thus, is less sensitive and reliable compared to the BODIPY-casein assay used, which is capable of detecting 50-100 ng of calpain.⁵

Table 3.1 IC₅₀ values for aldehydes SJA6017 and CAT811 against μ -calpain (calpain 1) and m-calpain (calpain 2).

CMPD	IC ₅₀ (nM)			
	μ -calpain		m-calpain	
	(Calpain 1)		(Calpain 2)	
	Reported	Obtained	Reported	Obtained
	8 ^[9]	84	73 ^[9]	56
	134 ^[7]		80 ^[7]	
	220 ^[11]	336	30 ^[11]	209

Interestingly, the IC₅₀ values for SJA6017 were found to be lower (i.e. more potent) than values obtained by at Lincoln University⁷ using the same BODIPY-casein assay protocol. In contrast, the IC₅₀ values for CAT811 were found to be higher (i.e. less potent) than the values determined at Lincoln University¹¹ (see Table 3.1), using the same assay protocol. The inhibition assays were repeated for SJA6017 and CAT811 using TRIS-HCl buffer in place of MOPS buffer (see Table 3.2) to investigate the effect of a different buffer solution on the assay protocol. The inhibition assays of SJA6017 and CAT811 in MOPS buffer were found to give lower IC₅₀ values in comparison to the IC₅₀ values obtained in TRIS buffer. This phenomenon is most likely a result of interactions of the aldehyde inhibitors with the TRIS-NH₂ group, which does not occur in the presence of MOPS.

Table 3.2 IC₅₀ values for aldehydes SJA6017 and CAT811 in MOPS and TRIS buffer for calpain 1 and calpain 2.

CMPD	IC ₅₀ (nM)			
	μ-calpain (Calpain 1)		m-calpain (Calpain 2)	
	MOPS	TRIS	MOPS	TRIS
		82	108	54
	336	424	209	329

The discrepancies between the obtained IC₅₀ values for SJA6017 and CAT811 and reported literature values^{7,9,11} is most likely due to differences in data analysis. To confirm this, one set of raw data for SJA6017 against m-calpain, performed at Lincoln University by Mehrtens,⁷ was re-analysed using both the standard methodology (0-570s) and the slow binding inhibition methodology (360-570s) (see Figure 3.5).

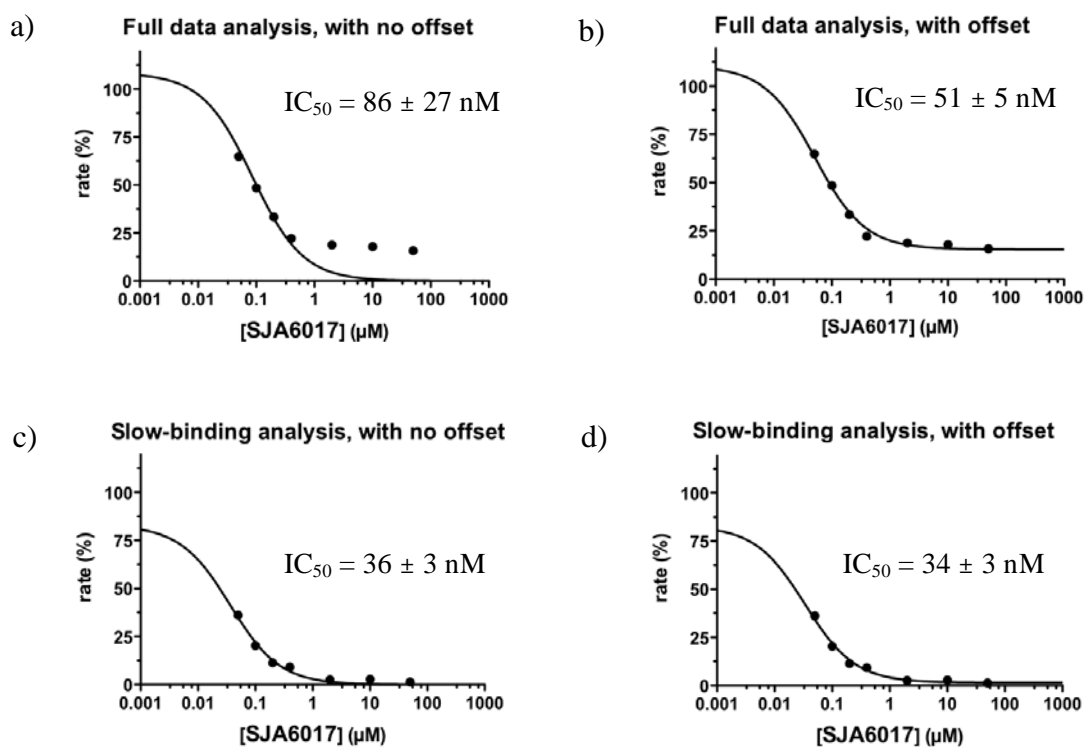


Figure 3.5 IC₅₀ analysis of SJA6017 using data obtained from Mehrtens's thesis.⁷

Analysis of the raw data for SJA6017 using the standard methodology (0-570 s) produced an IC_{50} value of 86 nM against m-calpain, which compares well to that reported by Mehrtens (80 nM) (Figure 3.5, graph (a)). However, it can be seen from graph (a) (Figure 3.5) that the IC_{50} curve does not fit the data points nicely, as the plot did not plateau at 0% enzyme activity even at high inhibitor concentrations. Thus, an offset was applied to the equation in analysis such that the obtained curve fits the raw data, resulting in a decrease in IC_{50} value to 51 nM (Figure 3.5, graph (b)). Applying the methodology for slow binding analysis (analysis from 390-570s) gave IC_{50} values for SJA6017 of 36 nM and 34 nM, when analysed with and without an offset (Figure 3.5, graphs (c) and (d)). Hence, slow binding inhibition methodology proved to be a more reliable analysis technique for aldehyde inhibitors. Additionally, the concentration range investigated by Mehrtens⁷ was not optimal, as seen in Figure 3.5, with the lowest concentration being 50 nM, which does not span all ranges of the sigmoidal curve. The discrepancies between the IC_{50} values obtained experimentally for SJA6017 compared to those obtained by Mehrtens⁷ using the same calpain assay methodology is most likely due to the use of a non-optimal concentration range and the data analysis methodology. Hence the obtained IC_{50} values of SJA6017 and CAT811 obtained in Adelaide, utilising the above method of analysis, is considered accurate and valid.

3.2.2 α -Chymotrypsin Assay

The *in vitro* α -chymotrypsin assay was carried out using a spectrophotometric assay protocol established in Adelaide by Peddie and Pietsch.¹² The assay protocol uses 4-nitroanilide, Suc-Ala-Ala-Pro-Phe-pNA (Suc-AAPF-pNA) as a substrate, of which the hydrolysis gives p-nitroaniline that absorbs at 405 nm (see Figure 3.6). The inhibitory activity of an inhibitor is then measured by calculating the change in absorption over a known period of time.

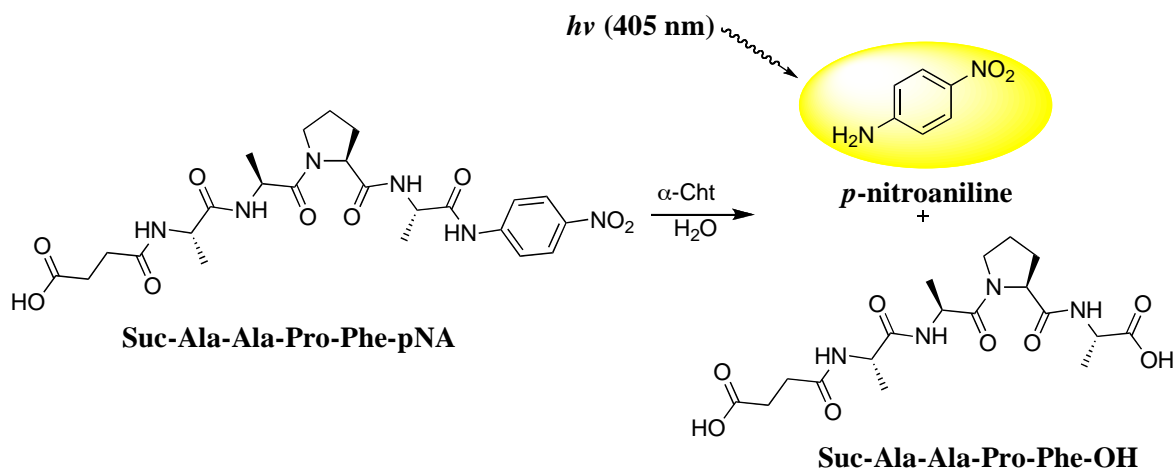


Figure 3.6 Schematic representation of the absorption α -chymotrypsin assay.

The activity of bovine α -chymotrypsin was assayed spectrophotometrically using a UV-Vis spectrophotometer equipped with a thermostated multicell holder, using 1 cm path length cuvettes (1 mL). TRIS-HCl (77 mM) was used as the buffer with 20 mM CaCl_2 added at a pH of 7.8, which is optimum for α -chymotrypsin activity.¹³ The enzyme solution (21.9 mg/mL) in 1 mM HCl, substrate solutions (20 mM Suc-Ala-Ala-Pro-Phe-pNA) in DMSO and inhibitor solutions in DMSO were prepared freshly daily for each assay.

Three controls were used: (i) a non-enzymatic hydrolysis of substrate blank (negative control) to ensure that the substrate is not degraded over time; (ii) a substrate degradation by inhibitor blank (negative control) to ensure that the substrate is not degraded by the inhibitor in the absence of the enzyme; and (iii) an enzyme activity blank (positive control). The enzyme inhibition assays were performed in the presence of 6% v/v DMSO in a volume of 1 mL, containing 0.011 $\mu\text{g/mL}$ enzyme, different concentrations of substrate (Suc-Ala-Ala-Pro-Phe-pNA) and inhibitor solutions. Each cuvette contained 890 μL of assay buffer (77 mM TRIS-HCl with 20 mM CaCl_2 , pH 7.8), 10 μL of substrate solution (1-10 mM Suc-Ala-Ala-Pro-Phe-pNA in DMSO), inhibitor stock, and DMSO were added to give a total volume of 950 μL . The enzymatic reaction was initiated by addition of 50 μL of enzyme solution. The enzyme activity blank was determined by addition of DMSO instead of the inhibitor solution. The non-enzymatic hydrolysis blank was initiated by addition of DMSO and 1 mM HCl instead of inhibitor and enzyme solution, respectively; and the substrate degradation blank was initiated by addition of

1mM HCl instead of the enzyme solution. The progress of the reaction was monitored for 6 min in a Varian Cary 5000 UV-VIS-NIR spectrophotometer at 405 nm. The rate of enzyme-catalyzed hydrolysis of 100 μ M substrate was determined without inhibitor in each experiment and was set to 100%. The K_i values of all inhibitors were determined graphically according to the method of Dixon¹⁴ using the average of percentage rates in three separate experiments at two different substrate concentration (see appendix A3 for an example of raw data and K_i calculation).

3.2.3 Cathepsin L, Cathepsin S, Human Leukocyte Elastase and Bovine Trypsin Assays

The *in vitro* assays for cathepsin L, cathepsin S, human leukocyte elastase and bovine trypsin were performed by Prof. Dr. Michael Gütschow at the University of Bonn, Germany using established assay protocols.¹⁵⁻¹⁷ These assays use a 4-nitroanilide-based substrate as per the α -chymotrypsin assay described above. The inhibition assays were conducted at five different inhibitor concentrations and the subsequent enzymatic cleavage of the substrate yielding *p*-nitroaniline absorbance (UV-Vis 405 nm) was monitored over 10 min. The IC_{50} values were obtained from the linear steady-state turnover of the substrate as detailed in the experimental section of chapter 5.

3.3 Inhibitor Structure-Activity Relationship

The cyclic and acyclic inhibitors reported in chapter 2 and summarised in Figure 3.8 were assayed against enzymes from the cysteine protease family (calpain, cathepsin S and cathepsin L) and the serine protease family (α -chymotrypsin, trypsin and human leukocyte elastase). The following discussion addresses the structure-activity relationship of these inhibitors with regards to proteases within the same class and across another family of proteases.

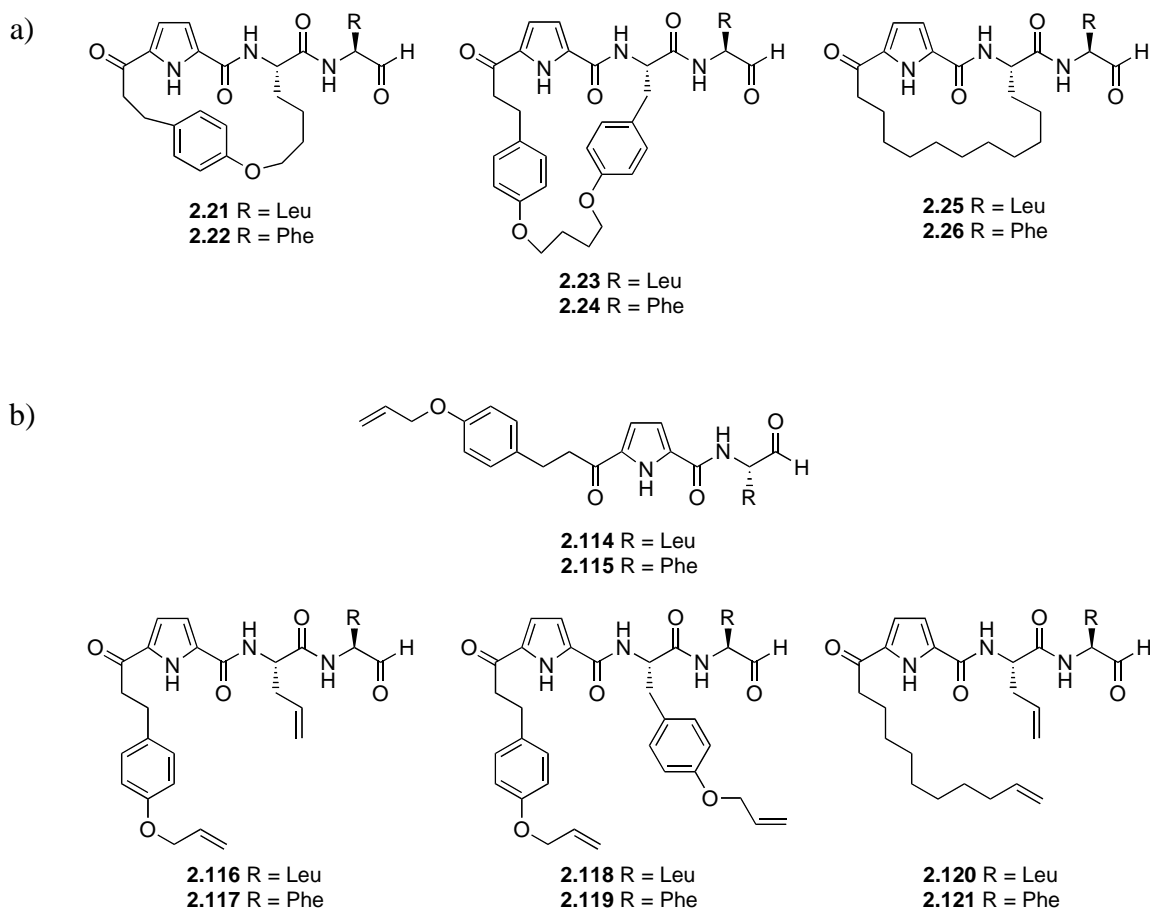


Figure 3.8 Structures of (a) macrocyclic and (b) acyclic 2nd generation protease inhibitor.

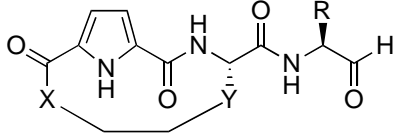
3.3.1 Structure-Activity of Peptidyl Macrocyclic Alcohols and Aldehydes Against Cysteine Proteases

3.3.1.1 Calpain

Inhibitors of calpains are of significant interest as therapeutics for the potential treatment of cataracts (see chapter 2, section 2.1.2). Ovine calpain was used in the assays as ovine lens crystallin proteins show high homology with those from human.^{18,19} Inhibitors were assayed against m-calpain (CAPN2), the predominant calpain in ovine lens. The most potent inhibitors of m-calpain were also assayed against μ -calpain (CAPN1) to determine selectivity between the two calpain isoforms. The results of these assays are shown in Table 3.3

Table 3.3 IC₅₀ values of (a) macrocyclic aldehydes and (b) acyclic aldehydes against μ -calpain and m-calpain.

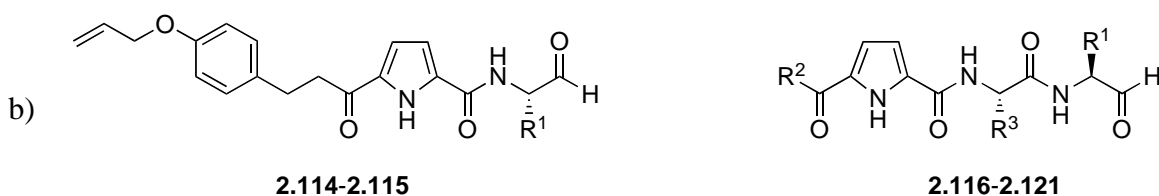
a)



CMPD	R	X	Y	Cysteine Protease	
				(IC ₅₀ (μM)) [#]	
				m-calpain (CAPN2)	μ -calpain (CAPN1)
2.21	Leu	-(CH ₂) ₂ Ph- <i>p</i> -OCH ₂ -	-CH ₂ -	0.249	0.324
2.22	Phe	-(CH ₂) ₂ Ph- <i>p</i> -OCH ₂ -	-CH ₂ -	0.153	n.d.
2.23	Leu	-(CH ₂) ₂ Ph- <i>p</i> -OCH ₂ -	-CH ₂ Ph- <i>p</i> -OCH ₂ -	0.203	n.d.
2.24	Phe	-(CH ₂) ₂ Ph- <i>p</i> -OCH ₂ -	-CH ₂ Ph- <i>p</i> -OCH ₂ -	0.246	n.d.
2.25	Leu	-(CH ₂) ₈ -	-CH ₂ -	0.066	0.042
2.26	Phe	-(CH ₂) ₈ -	-CH ₂ -	0.156	n.d.

n.d = Not determined, due to insufficient supply CAPN1.

[#] Standard deviation are found in the raw data, Appendix A5



CMPD	R ¹	R ²	R ³	Cysteine Protease	
				(IC ₅₀ (μM)) [#]	
				m-calpain (CAPN2)	μ -calpain (CAPN1)
2.114	Leu	–	–	3.11	n.d.
2.115	Phe	–	–	8.9	n.d.
2.116	Leu	-(CH ₂) ₂ Ph- <i>p</i> -OAll	-CH ₂ CH=CH ₂	0.067	n.d.
2.117	Phe	-(CH ₂) ₂ Ph- <i>p</i> -OAll	-CH ₂ CH=CH ₂	0.823	n.d.
2.118	Leu	-(CH ₂) ₂ Ph- <i>p</i> -OAll	-CH ₂ Ph- <i>p</i> -OAll	7.76	n.d.
2.119	Phe	-(CH ₂) ₂ Ph- <i>p</i> -OAll	-CH ₂ Ph- <i>p</i> -OAll	1.3	n.d.
2.120	Leu	-(CH ₂) ₈ CH=CH ₂	-CH ₂ CH=CH ₂	0.040	0.055
2.121	Phe	-(CH ₂) ₈ CH=CH ₂	-CH ₂ CH=CH ₂	0.072	n.d.

n.d = Not determined, due to insufficient CAPN1.

[#] Standard deviation are found in the raw data, Appendix A5

The derivatives containing a C-terminal primary alcohol (**2.78-2.81**, **2.85-2.90**, **2.112-2.113**, **2.122-2.123**, **2.127-2.134**) were all inactive against against m-calpain (CAPN2) (see Appendix A4). This supports an earlier observation that an aldehyde group, or other reactive warhead, is required for potent inhibition of calpain.¹¹ In support, the macrocyclic aldehydes **2.21-2.26** and the corresponding acyclic derivatives **2.114-2.121** were all active against m-calpain with IC₅₀ values as shown in Table 3.3.

The most potent 18-membered macrocyclic inhibitor, aldehyde **2.25** (IC₅₀ = 0.066 μM), contains an unsubstituted aliphatic ring with a Leu at the P₁ position. This macrocyclic inhibitor (**2.25**) is more potent than the lead structure CAT811 (IC₅₀ = 0.209 μM)[#], which has a smaller and conformationally more rigid 17-membered ring system. The aryl group within the macrocycle of CAT811 further constrains the geometry of the backbone into a β-strand, which is known to favour binding to a protease (see chapter 2, section 2.2.1). The structure overlay of **2.25** and CAT811, docked into μ-calpain (Figure 3.9), shows good alignment of the peptide backbone from P₁-P₃ residues, indicating that **2.25** adopts a β-strand conformation, similar to that of CAT811. Hence, it appears that an increase in flexibility of the backbone as in **2.25** increases inhibitor binding. The effect of ring size on inhibitor potency has been noted previously.¹¹ The structural overlay of **2.25** bound to μ-calpain clearly illustrates that this new class of inhibitor positions the ring constraint for interaction with the S₂ and S₄ binding sites of the active site, rather than S₁ and S₃ for CAT811. Thus the macrocycle of **2.25** uniquely links the P₂ and P₄ residues, leaving the P₁ position free for introducing any number of groups to provide further interactions with the protease active site.

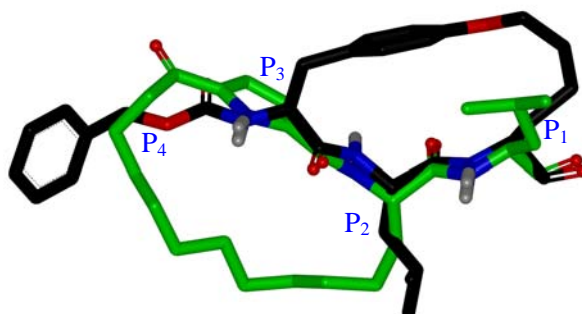


Figure 3.9 Superimposition of aldehyde **2.25** (green carbon atoms) and CAT811 (black carbon atoms) docked into μ-calpain.

[#] 2-fold less potent than the lead structure, CAT811 based on literature (IC₅₀ = 0.030 μM¹¹) | 99

The analogous macrocyclic aldehyde (**2.26**) with a Phe in place of Leu at P₁ was found to be 2-fold less potent (**2.26**: IC₅₀ = 0.156 μM) than **2.25**. This suggests that Leu is favoured over Phe in the S₁ pocket for m-calpain, an observation previously noted in literature.^{20,21} Interestingly, incorporation of an aryl group into the ring system, as in **2.21** and **2.22**, resulted in a 2-fold decrease in potency (**2.21**: IC₅₀ = 0.249 μM; **2.22**: IC₅₀ = 0.153 μM) as compared to the macrocyclic analogues **2.25** and **2.26**. A structure overlay of macrocycles **2.21** and **2.25**, docked into μ-calpain (Figure 3.10a) reveals that both ring systems adopt a β-strand conformation. However, with an aryl group (**2.21**) in the 18-membered ring, the pyrrole group in the peptide backbone changes orientation that results in a decrease in the number of hydrogen bonding interactions within the enzyme active site. This somewhat justifies the decrease in inhibitor potency observed for macrocycle **2.21** compared to **2.25** (Figure 3.10c).

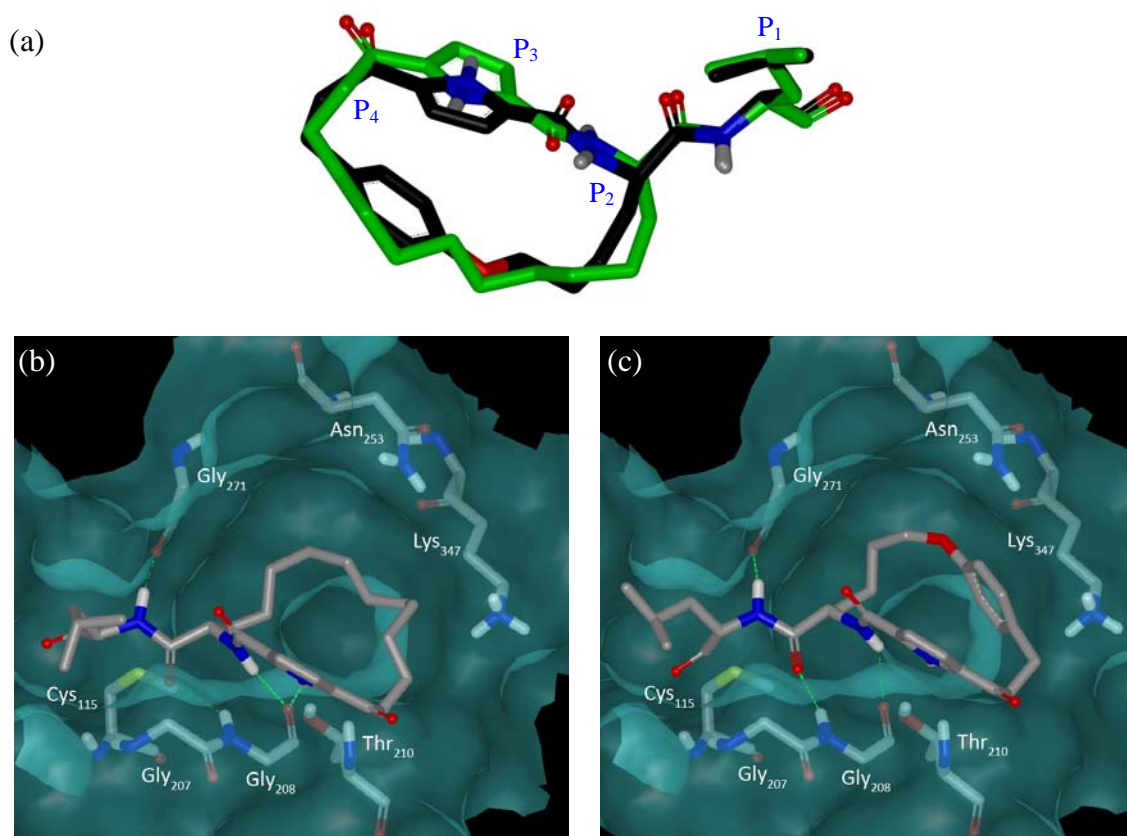


Figure 3.10 (a) Superimposition of aldehyde **2.25** (green carbon atoms) with aldehyde **2.21** (black carbon atoms); (b) Aldehyde **2.25** and (c) aldehyde **2.21** docked into μ-calpain (Hydrogen bonding interactions indicated by green dotted lines)

The introduction of an additional aryl group, to give a 24-membered ring size, also decreased potency (**2.23**: $IC_{50} = 0.203 \mu\text{M}$; **2.24**: $IC_{50} = 0.246 \mu\text{M}$). A structural overlay of aldehydes **2.25** and **2.23** docked into μ -calpain, reveals that the larger ring size of **2.23** results in a slight bend in the peptide backbone, with a deviation from the desired β -strand conformation from P_1 - P_3 (Figure 3.11a). The structural overlay also suggests that the ring system of macrocycle **2.23** may be too bulky for tight fitting into the active site of calpain (Figure 3.11b). This contrasts with results obtained for chymotrypsin as discussed later.

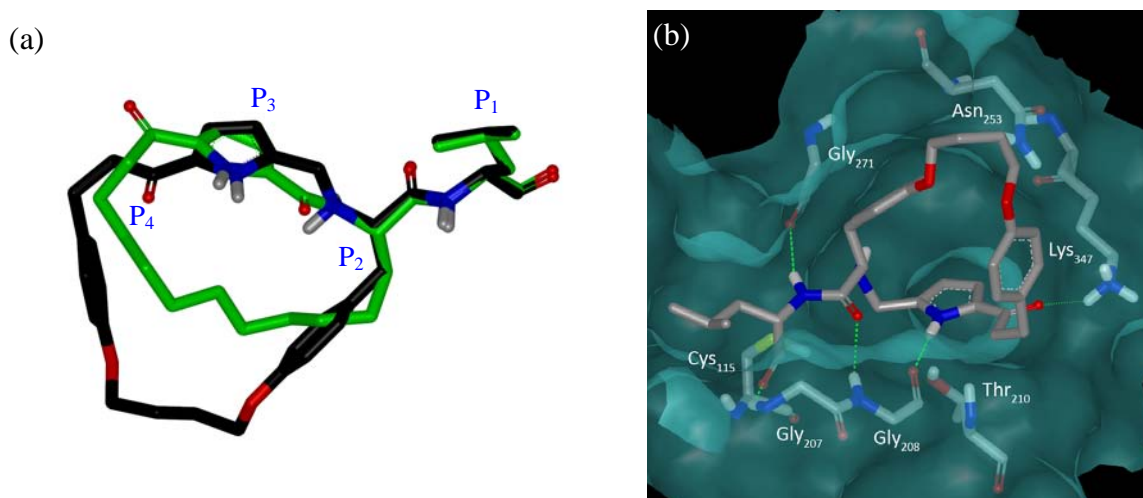


Figure 3.11 (a) Superimposition of aldehyde **2.25** (green carbon atoms) with aldehyde **2.23** (black carbon atoms); (b) Aldehyde **2.23** docked into μ -calpain (Hydrogen bonding interactions indicated by green dotted line)

The most potent acyclic inhibitor of m -calpain was the acyclic aldehyde **2.120** ($IC_{50} = 0.040 \mu\text{M}$), the direct analogue of the most potent 18-membered macrocycle **2.25**. Again, a Leu residue was found to be favoured over a Phe residue at P_1 , with a 2-fold decrease in potency observed for the P_1 -Phe analogue **2.121** ($IC_{50} = 0.072 \mu\text{M}$). This trend was also evident on comparing acyclic aldehydes **2.114** (P_1 -Leu; $IC_{50} = 3.11 \mu\text{M}$) with **2.115** (P_1 -Phe; $IC_{50} = 8.9 \mu\text{M}$) and **2.116** (P_1 -Leu; $IC_{50} = 0.067 \mu\text{M}$) with **2.117** (P_1 -Phe; $IC_{50} = 0.823 \mu\text{M}$); all of which showed a decrease in potency with substitution of Leu to Phe at P_1 . The exception to this is the acyclic aldehyde **2.118** (P_1 -Leu; $IC_{50} = 7.76 \mu\text{M}$), which was less potent than **2.119** (P_1 -Phe; $IC_{50} = 1.3 \mu\text{M}$), however it should be noted that neither are particularly potent inhibitors. The aldehydes **2.118** and **2.119** were docked into μ -calpain in order to gain some insight into this observation, with the results shown in Figure 3.12. The results reveal that the orientation of aldehydes **2.118** and **2.119** when

bound to m-calpain were not optimum, with the P₂ residues fitting into the S₁ site instead of required S₂ site, thus supporting the high IC₅₀ value obtained.

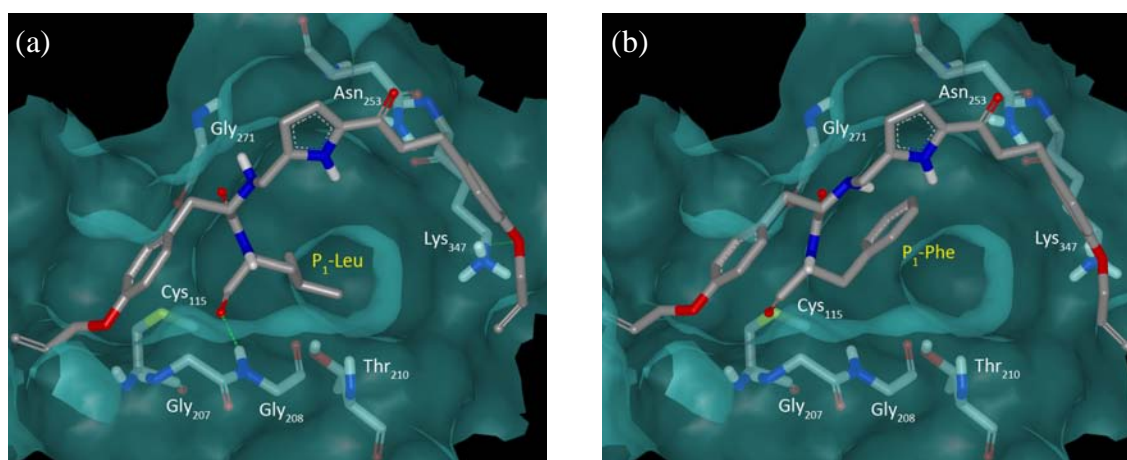


Figure 3.12 (a) Aldehyde **2.118** and (b) aldehyde **2.119** docked into μ -calpain.

Furthermore, the shorter acyclic aldehydes **2.114-2.115**, containing one amino acid less, were less potent than the C-terminal extended acyclic aldehydes (**2.116-2.121**), suggesting that the extended inhibitors **2.114-2.115** better align within the subsites of calpain, due to increased interactions within the enzyme binding pocket (Table 3.3b). The incorporation of long aliphatic side chains at the P₄ position as in **2.120**, presumably enhances interaction with the enzyme pocket, perhaps through hydrophobic interactions with the hydrophobic S₄ pocket, as shown in Figure 3.13.

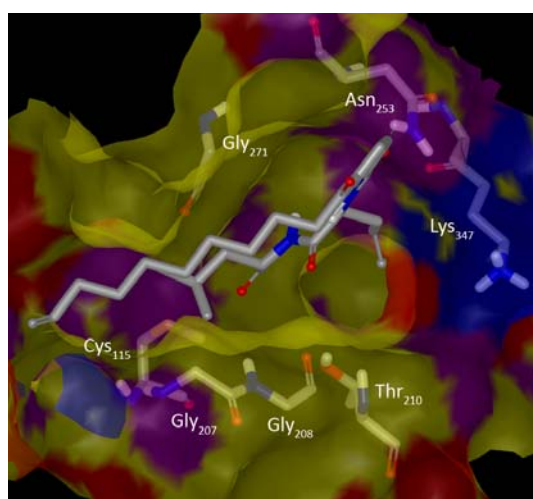


Figure 3.13 Aldehyde **2.120** docked into μ -calpain, showing the electrostatic potential of the enzyme binding pocket (Yellow: most hydrophobic; Purple: slightly hydrophobic; Red: electronegative; Blue: electropositive)

A comparison of the IC_{50} values of acyclic aldehydes **2.116-2.121** with macrocyclic aldehydes **2.21-2.26** reveals several distinct trends. Firstly, the aliphatic 18-membered macrocyclic aldehydes **2.25** and **2.26** and their corresponding acyclic analogues **2.120** and **2.121** are similarly potent against m-calpain, suggesting that there is no gain in constraining the backbone into a macrocycle in this case, however biostability may be enhanced. A structural overlay of aldehydes **2.25** and **2.120** docked with μ -calpain (Figure 3.14), shows good alignment of the peptide backbones and that linking P_2 and P_4 with a ring (as in **2.25**) appears to have little influence on the overall β -strand backbone, supporting the potency data obtained against calpain.

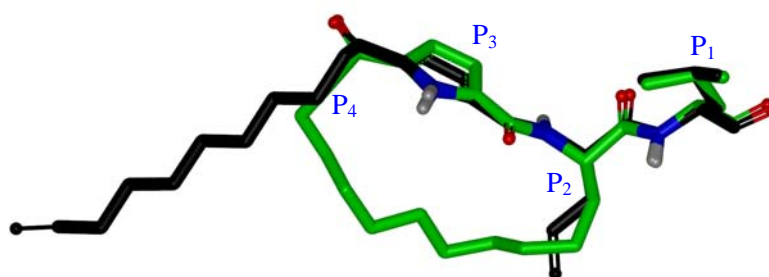


Figure 3.14 Superimposition of aldehyde **2.25** (green carbon atoms) and acyclic aldehyde **2.120** (black carbon atoms) docked into μ -calpain.

In contrast, the more conformationally constrained 18-membered macrocyclic aldehydes **2.21** and **2.22**, with an aryl group in the ring, are approximately 3-fold less potent against m-calpain than their corresponding acyclic analogues **2.116** and **2.117**. A structural overlay of aldehydes **2.21** and **2.116** docked in μ -calpain (Figure 3.15), suggests that both aldehydes adopt the desired β -strand conformation for active site binding. However, the X-ray structure of intermediate **2.72**, a precursor of aldehyde **2.21** (as discussed in chapter 2, section 2.3.2), showed an increase in the ψ dihedral angle at P_1 and P_2 (from 120° to 171°) suggesting a decreased in the propensity of **2.21** to adopt a β -strand. For acyclic aldehyde **2.116**, the aryl group appears to be misaligned with the pyrrole of the backbone, which may enable it to adopt a better fit within the enzyme pocket, thus allowing for increased interactions with the residues in the S_3 pocket.

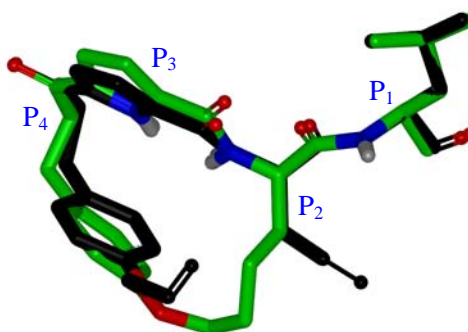


Figure 3.15 Superimposition of aldehyde **2.21** (green carbon atoms) and acyclic aldehyde **2.116** (black carbon atoms) docked into μ -calpain.

The 24-membered macrocycles **2.23** and **2.24** were 5-fold more potent than their corresponding acyclic analogues **2.118** and **2.119**. An overlay of aldehydes **2.23** and **2.118** docked in μ -calpain, suggests that linking the P₂ and P₄ residues with a ring encourages the formation of a β -stand conformation as is required for binding (Figure 3.16).

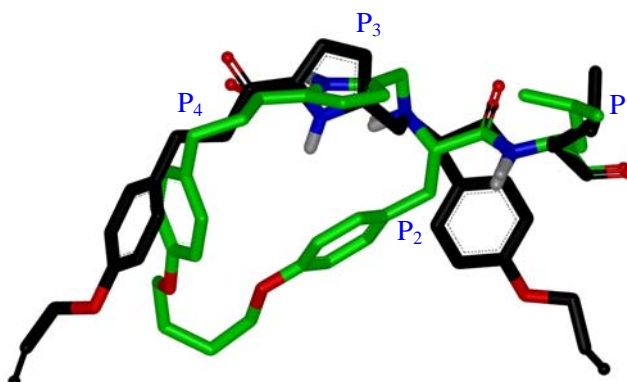


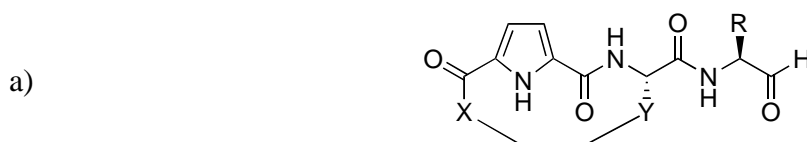
Figure 3.16 Superimposition of aldehyde **2.23** (green carbon atoms) and acyclic aldehyde **2.118** (black carbon atoms) docked into μ -calpain.

The most potent inhibitors of m-calpain, macrocyclic aldehydes **2.21** and **2.25** and acyclic aldehyde **2.120**, were also tested against μ -calpain as shown in Table 3.3. The data reveals similar potency towards both calpains. This is unsurprising as m-calpain and μ -calpain have a high degree of structural similarity.²³ The ability of macrocycle **2.25** to slow calpain induced opacification of human lenses is currently being evaluated in the UK.

3.3.1.2 Cathepsin L and Cathepsin S

The inhibitors **2.21-2.26** and **2.114-2.121** described in chapter 2 were also tested against cathepsin L and cathepsin S (outlined in section 3.2.3) as an alternative cysteine protease from the papain superfamily. The cathepsins are viable drug targets due to their involvement in many diseases, such as osteoporosis, arthritis, immune-related diseases, atherosclerosis and cancer (see chapter 2, section 2.1.2). The results of these studies are shown in Table 3.4.

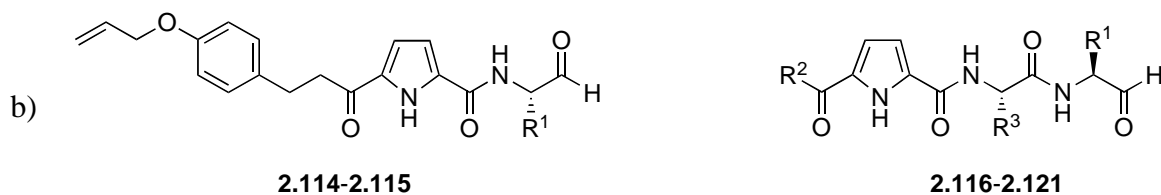
Table 3.4 IC₅₀ values of (a) macrocyclic aldehydes and (b) acyclic aldehydes against Cathepsin L (CatL) and Cathepsin S (CatS).



CMPD	R	X	Y	Cysteine Protease (IC ₅₀ (μM)) [#]	
				CatL	CatS
2.21	Leu	-(CH ₂) ₂ Ph- <i>p</i> -OCH ₂ -	-CH ₂ -	0.0047	0.0217
2.22	Phe	-(CH ₂) ₂ Ph- <i>p</i> -OCH ₂ -	-CH ₂ -	n.d.	n.d.
2.23	Leu	-(CH ₂) ₂ Ph- <i>p</i> -OCH ₂ -	-CH ₂ Ph- <i>p</i> -OCH ₂ -	0.0207	0.0014
2.24	Phe	-(CH ₂) ₂ Ph- <i>p</i> -OCH ₂ -	-CH ₂ Ph- <i>p</i> -OCH ₂ -	0.206	0.0066
2.25	Leu	-(CH ₂) ₈ -	-CH ₂ -	0.003	0.0017
2.26	Phe	-(CH ₂) ₈ -	-CH ₂ -	0.0115	0.0017

n.d. = not determined due to insufficient sample.

[#] Standard deviation are found in the raw data, Appendix A5



CMPD	R ¹	R ²	R ³	Cysteine Protease (IC ₅₀ (μM)) [#]	
				CatL	CatS
2.114	Leu	–	–	>50	5.6
2.115	Phe	–	–	>50	14
2.116	Leu	-(CH ₂) ₂ Ph- <i>p</i> -OAll	-CH ₂ CH=CH ₂	0.0931	0.0019
2.117	Phe	-(CH ₂) ₂ Ph- <i>p</i> -OAll	-CH ₂ CH=CH ₂	1.72	0.0563
2.118	Leu	-(CH ₂) ₂ Ph- <i>p</i> -OAll	-CH ₂ Ph- <i>p</i> -OAll	0.0115	0.0014
2.119	Phe	-(CH ₂) ₂ Ph- <i>p</i> -OAll	-CH ₂ Ph- <i>p</i> -OAll	0.366	0.0214
2.120	Leu	-(CH ₂) ₈ CH=CH ₂	-CH ₂ CH=CH ₂	0.921	0.0105
2.121	Phe	-(CH ₂) ₈ CH=CH ₂	-CH ₂ CH=CH ₂	1.39	0.176

[#] Standard deviation are found in the raw data, Appendix A5

The macrocyclic aldehydes **2.21-2.26** and corresponding acyclic derivatives **2.114-2.121** were all active against cathepsin L and cathepsin S with the IC₅₀ values shown in Table 3.4. Again inhibitors with a Leu at the P₁ (**2.21/2.23/2.25/2.114/2.116/2.118/2.120**) were more potent against both cathepsin L and cathepsin S compared to the analogous inhibitors with Phe at P₁ (**2.22/2.24/2.26/2.115/2.117/2.119/2.121**). For example, P₁-Leu 24-membered macrocyclic aldehyde **2.23** (IC₅₀ = 0.0207 μM) was 10-fold more potent against cathepsin L than its corresponding P₁-Phe analogue (aldehyde **2.24**). This observation is consistent with literature which suggests that small hydrophobic groups such as Leu is favoured in the S₁ pocket for cathepsin L.²⁴ The most potent macrocyclic inhibitor, aldehyde **2.25**, contains an unsubstituted aliphatic 18-membered ring system with a Leu at the P₁ position and is particularly potent against both cathepsins (IC₅₀ = 0.003 μM (CatL); IC₅₀ = 0.0017 μM (CatS)). An increase in ring size (from 18-membered to 24-membered) and the introduction of two aryl groups into the macrocycle (aldehydes **2.23** and **2.24**) resulted in a decrease in potency against cathepsin L (**2.23**: IC₅₀ = 0.0207 μM; **2.24**: IC₅₀ = 0.206 μM). This decrease in potency is consistent with reports that cathepsin L prefers to bind small hydrophobic groups at the S₂ site.²⁴ In contrast, inhibitors containing a 24-membered ring system (**2.23** and **2.24**) displayed high potencies (in the low

nanomolar range) against cathepsin S (**2.23**: $IC_{50} = 0.0014 \mu\text{M}$ and **2.24**: $IC_{50} = 0.0066 \mu\text{M}$). This suggests that the binding pocket of cathepsin S is able to facilitate binding interactions of the larger 24-membered macrocycles.

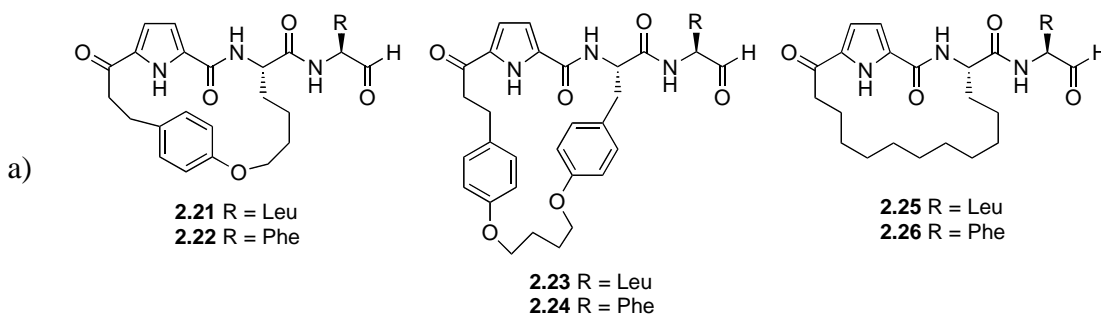
The macrocyclic aldehyde **2.25**, which lacks aryl groups within its macrocyclic core, displays little selectivity between the two isoforms (CatL and CatS), corroborating the need for bulky aromatic groups at either P_2 or P_4 to impart selectivity. Incorporating an aryl group at the P_4 site in the macrocyclic core as in **2.21**, results in some selectivity for cathepsin L over cathepsin S. In contrast, the presence of aryl groups at both P_2 and P_4 (see **2.23** & **2.24**) reverses selectivity to favour cathepsin S over cathepsin L. This observation is consistent with literature that suggests that for cathepsin L and S, selectivity is determined primarily by the S_2 - P_2 interaction.²⁴ It is known that cathepsin L prefers small hydrophobic groups in the S_2 pocket, while cathepsin S prefers bulkier hydrophobic groups.

A comparison of the IC_{50} values obtained for acyclic aldehydes (**2.114-2.121**) with those of the macrocyclic aldehydes (**2.21-2.26**) reveals some significant trends. Firstly, inhibitors in both series with Leu at P_1 (**2.21/2.23/2.25/2.114/2.116/2.118/2.120**) were more potent against cathepsin L and cathepsin S compared to those with Phe at P_1 (**2.22/2.24/2.26/2.115/2.117/2.119/2.121**). Acyclic aldehydes, with aryl groups at both P_2 and P_4 (**2.118-2.119**) have enhanced selectivity (10-fold) for cathepsin S compared to cathepsin L. Importantly, the macrocycles **2.21-2.26** are significantly more potent than the acyclic derivatives (**2.114-2.121**) against both cathepsins. We suggest, as outlined in chapter 2, section 2.2.1, that this is likely due to the macrocycle stabilizing a β -strand conformation to the backbone as is required for binding to proteases, specifically cathepsin L and cathepsin S in this case.²⁵ It is also important to note that the introduction of a pyrrole into the backbone, as a replacement for the P_3 amino acid, decreases the peptidic character of the inhibitor, which offers significant advantage as a potential therapeutic or lead structure.

3.3.1.3 Inhibitor Selectivity Within Cysteine Protease Family

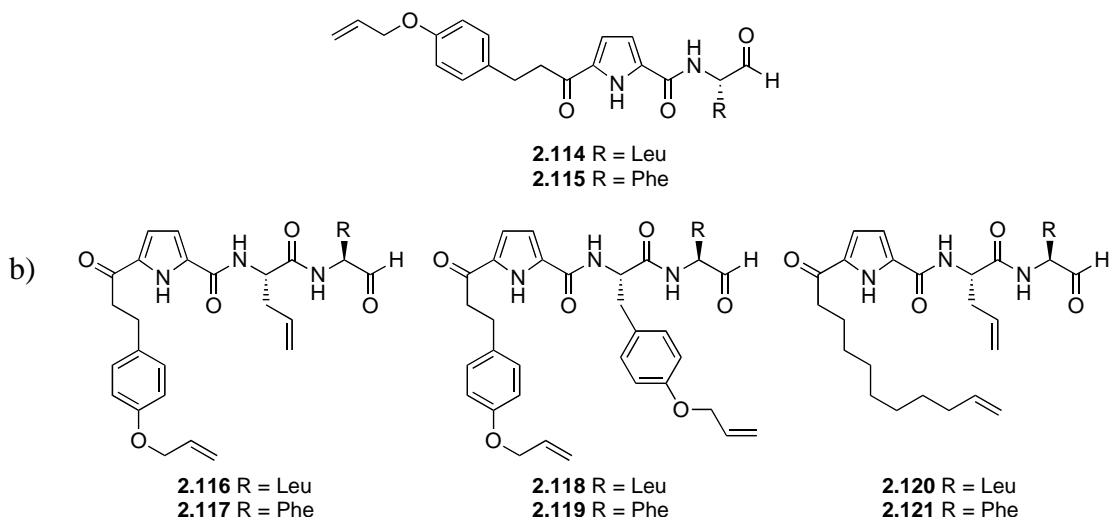
The selective inhibition of one protease within the same family is a difficult and challenging task. All the proteases discussed to date (i.e calpain and cathepsin) are cysteine proteases and as such have the same mechanism of substrate hydrolysis involving a common catalytic triad. Hence, the development of selective inhibitors of these enzymes requires exploitation of the different selectivity between the P_n (inhibitor) and S_n (enzyme) site. Data on the potencies of aldehydes **2.21-2.26** and **2.114-2.121** against these two classes of cysteine protease are summarised in Table 3.5.

Table 3.5 Potency of (a) macrocyclic and (b) acyclic aldehydes against cysteine proteases, calpain and cathepsin.



CMPD	Cysteine Protease: IC ₅₀ (μM) [#]		
	m-capain (CAPN2)	CatL	CatS
2.21	0.249	0.0047	0.0217
2.22	0.153	n.d. ¹	n.d. ¹
2.23	0.203	0.0207	0.0014
2.24	0.246	0.206	0.0066
2.25	0.066	0.003	0.0017
2.26	0.156	0.0115	0.0017

[#] Standard deviation are found in the raw data, Appendix A5



CMPD	Cysteine Protease: IC ₅₀ (μM) [#]		
	m-capain (CAPN2)	CatL	CatS
2.114	3.11	>50	5.6
2.115	8.9	>50	14
2.116	0.067	0.0931	0.0019
2.117	0.823	1.72	0.0563
2.118	7.76	0.0115	0.0014
2.119	1.3	0.366	0.0214
2.120	0.040	0.921	0.0105
2.121	0.072	1.39	0.176

¹ n.d. = not determined due to insufficient sample.

[#] Standard deviation are found in the raw data, Appendix A5

All of the macrocyclic (**2.21-2.26**) and acyclic (**2.114-2.121**) aldehydes tested were active against the cysteine proteases tested. The aldehyde inhibitors with a Leu at P₁ (see **2.23/2.25/2.114/2.116/2.118/2.120**) were all more potent against calpain and cathepsin L/S than those with a Phe at P₁ (**2.24/2.26/2.115/2.119/2.121**).

The macrocyclic aldehydes (**2.21-2.26**) were the most potent inhibitors of cathepsin L/S, with the 18-membered macrocycle **2.25** exhibiting the greatest potency (CatL IC₅₀ = 0.003 μM; CatS IC₅₀ = 0.0017 μM). Macrocyclic aldehyde **2.25** was also the most potent inhibitor of calpain (IC₅₀ = 0.066 μM). The lack of selectivity observed for macrocyclic inhibitor **2.25** presumably reflects a common mode of binding to all the proteases.²⁶

Selectivity for cathepsin S was achieved with acyclic aldehydes **2.118** and **2.119** showing a 10-fold and 60-fold selectivity over cathepsin L and calpain, respectively. This can be attributed to the presence of the aryl groups at the P₂ and P₄ site, which is consistent with cathepsin S's preference for bulky hydrophobic groups binding in the S₂ pocket.²⁴ By comparison, both cathepsin L and calpain are known to prefer smaller aliphatic groups at this position.^{24,27}

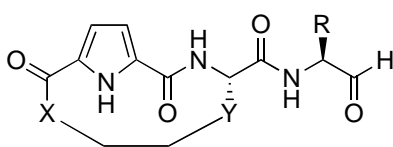
3.3.2 Structure-Activity of Peptidyl Macrocyclic Alcohols and Aldehydes Against Serine Proteases

3.3.2.1 α -Chymotrypsin

The inhibitors **2.21-2.26** and **2.114-2.121** described in chapter 2 were also tested against a serine protease (α -chymotrypsin) with the results shown in Table 3.6. α -Chymotrypsin is one of the better studied proteases, and as such it is an ideal model for studying the versatility of an inhibitor design. The *in vitro* α -chymotrypsin assay was conducted using the spectrophotometric assay outlined in section 3.2.2.

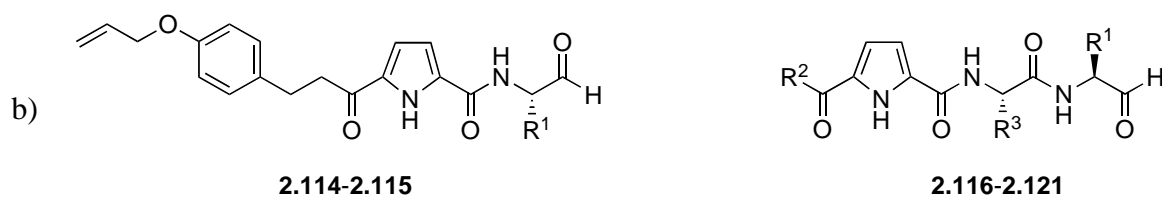
Table 3.6 IC₅₀ values of (a) macrocyclic aldehydes and (b) acyclic aldehydes against bovine α -chymotrypsin.

a)



CMPD	R	X	Y	K_i (μM) [#]
				bCT
2.21	Leu	-(CH ₂) ₂ Ph- <i>p</i> -OCH ₂ -	-CH ₂ -	>50
2.22	Phe	-(CH ₂) ₂ Ph- <i>p</i> -OCH ₂ -	-CH ₂ -	0.431
2.23	Leu	-(CH ₂) ₂ Ph- <i>p</i> -OCH ₂ -	-CH ₂ Ph- <i>p</i> -OCH ₂ -	1.917
2.24	Phe	-(CH ₂) ₂ Ph- <i>p</i> -OCH ₂ -	-CH ₂ Ph- <i>p</i> -OCH ₂ -	0.033
2.25	Leu	-(CH ₂) ₈ -	-CH ₂ -	>50
2.26	Phe	-(CH ₂) ₈ -	-CH ₂ -	2.525

[#] Standard deviation are found in the raw data, Appendix A5



CMPD	R ¹	R ²	R ³	<i>K_i</i> (μM) [#]
				bCT
2.114	Leu	–	–	>50
2.115	Phe	–	–	>50
2.116	Leu	-(CH ₂) ₂ Ph- <i>p</i> -OAll	-CH ₂ CH=CH ₂	0.939
2.117	Phe	-(CH ₂) ₂ Ph- <i>p</i> -OAll	-CH ₂ CH=CH ₂	0.056
2.118	Leu	-(CH ₂) ₂ Ph- <i>p</i> -OAll	-CH ₂ Ph- <i>p</i> -OAll	>50
2.119	Phe	-(CH ₂) ₂ Ph- <i>p</i> -OAll	-CH ₂ Ph- <i>p</i> -OAll	0.688
2.120	Leu	-(CH ₂) ₈ CH=CH ₂	-CH ₂ CH=CH ₂	>50
2.121	Phe	-(CH ₂) ₈ CH=CH ₂	-CH ₂ CH=CH ₂	2.474

[#] Standard deviation are found in the raw data, Appendix A5

All the derivatives with a C-terminal primary alcohol (**2.78-2.81**, **2.85-2.90**, **2.112-2.113**, **2.122-2.123**, **2.127-2.134**) were inactive against α-chymotrypsin (see Appendix A4). This is not surprising given that a C-terminal aldehyde (or other electrophilic group) is generally required for potent inhibition of α-chymotrypsin.²⁸ In support, macrocyclic aldehydes **2.21-2.26** and the corresponding acyclic aldehydes **2.114-2.121** were all active against α-chymotrypsin, with IC₅₀ values as shown in Table 3.6.

The macrocyclic aldehydes (**2.22**, **2.24** and **2.26**) with a benzyl group (Phe) at P₁ were the most potent of the aldehydes tested against α-chymotrypsin, with IC₅₀ values of 0.431, 0.033 and 2.525 μM, respectively. The P₁-Leu variants (**2.21**, **2.23** and **2.25**) were all significantly less potent, presumably since an aromatic Phe residue is favoured over Leu at P₁ (see section 2.1.2 for a discussion).²⁹ Incorporation of an aryl group into the macrocycle, as in **2.22**, **2.24** and **2.26**, results in an increase in potency against α-chymotrypsin by up to 100-fold (**2.26**: IC₅₀ = 2.525 μM, no aryl group; **2.22**: IC₅₀ = 0.431 μM, one aryl group; **2.24**: IC₅₀ = 0.033 μM, two aryl groups). Again this is consistent with the known preference of α-chymotrypsin for hydrophobic groups that can interact with the appropriate binding domain.²⁹

The acyclic aldehydes with a Phe at P₁ (**2.117**, **2.119** and **2.121**) were also observed to be more potent than those derivatives with Leu at P₁ (**2.116**, **2.118** and **2.120**). In addition, aldehyde **2.119** is 20-fold less potent than its macrocyclic analogue (**2.24**, IC₅₀ = 0.033 μM, see Table 3.6), presumably due to its enhanced conformational flexibility. A comparison of the IC₅₀ values obtained for the potent acyclic aldehydes **2.117** (aryl group at P₄), **2.119** (aryl group at P₂ and P₄) and **2.121** (no aryl group) suggests that an aromatic group is preferred at P₄, but not at P₂. In particular, acyclic inhibitor **2.117** (IC₅₀ = 0.056 μM) with an aryl group at P₄, is 12-fold more potent than acyclic inhibitor **2.119** (IC₅₀ = 0.688 μM), which contains an aryl group at both the P₂ and P₄ positions. The shorter acyclic aldehydes **2.114** and **2.115**, containing one amino acid less, were all inactive against α-chymotrypsin, suggesting a preference for extended peptidic inhibitors that provide an opportunity for increased interactions within the enzyme binding pocket of α-chymotrypsin.

The introduction of a macrocycle that links P₂ and P₄ as in aldehydes **2.23** (IC₅₀ = 1.917 μM) and **2.24** (IC₅₀ = 0.033 μM) enhances potency by at least 20-fold in comparison to their corresponding acyclic aldehydes **2.118** (IC₅₀ > 50 μM) and **2.119** (IC₅₀ = 0.688 μM). Such a cyclisation presumably decreases the conformational flexibility of the side chains while stabilising the preferred β-stranded backbone conformation.

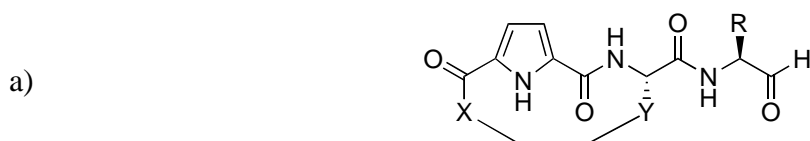
Interestingly, the smaller macrocycles (18-membered compared to 24-membered ring system) that link P₂ and P₄ are less favoured. The 18-membered macrocycles **2.21** (IC₅₀ > 50 μM) and **2.22** (IC₅₀ = 0.431 μM), containing an aryl group in the ring system, showed a decrease in potency in comparison to the acyclic derivatives **2.116** (IC₅₀ = 0.939 μM) and **2.117** (IC₅₀ = 0.056 μM). The 18-membered aliphatic macrocyclic aldehydes **2.25** (IC₅₀ > 50 μM) and **2.26** (IC₅₀ = 2.525 μM), are similarly potent to the corresponding acyclic analogues **2.120** (IC₅₀ > 50 μM) and **2.121** (IC₅₀ = 2.474 μM). We suggest that the introduction of an 18-membered aliphatic macrocycle as in **2.25** and **2.26** stabilises the β-strand conformation required for tight binding. By contrast, the introduction of an 18-membered macrocycle containing a single aryl group in the ring system as in **2.21** and **2.22**, leads to a decrease in the β-stranded nature. This was supported by the X-ray structure of intermediate **2.72**, a precursor of aldehyde **2.21** (as discussed in chapter 2, section 2.3.2), which showed an increase in the ψ dihedral angle at P₁ and P₂ (from 120° to 171°). This

increase in dihedral angle corresponds to a decrease the β -stranded nature, which results in the decreased probability of enzyme-inhibitor binding.

3.3.2.2 Human Leukocyte Elastase (HLE)

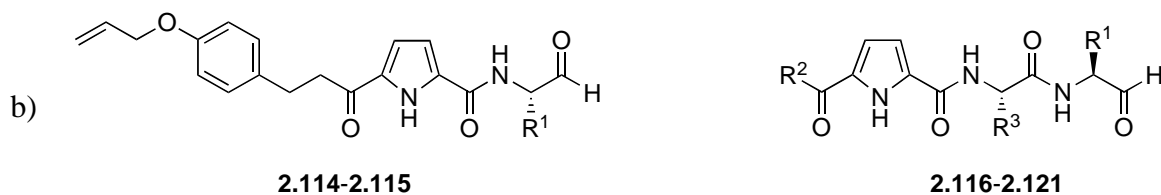
The inhibitors **2.21-2.26** and **2.114-2.121** described in chapter 2 were also tested against a second serine protease, Human Leukocyte Elastase (HLE) to further explore selectivity. The results of these studies are shown in Table 3.7. Inhibitors of human leukocyte elastase (HLE) are of significant interest for the potential treatment of chronic obstructive pulmonary diseases (see chapter 2, section 2.1.2). The *in vitro* assays for HLE were performed by Prof. Dr. Michael Gütschow at the University of Bonn, Germany using established assay protocols (outlined in section 3.2.3).^{15,17}

Table 3.7 IC₅₀ values of (a) macrocyclic aldehydes and (b) acyclic aldehydes against human leukocyte elastase (HLE).



CMPD	R	X	Y	IC ₅₀ (μM) [#]
				HLE
2.21	Leu	-(CH ₂) ₂ Ph- <i>p</i> -OCH ₂ -	-CH ₂ -	>50
2.22	Phe	-(CH ₂) ₂ Ph- <i>p</i> -OCH ₂ -	-CH ₂ -	>50
2.23	Leu	-(CH ₂) ₂ Ph- <i>p</i> -OCH ₂ -	-CH ₂ Ph- <i>p</i> -OCH ₂ -	1.820
2.24	Phe	-(CH ₂) ₂ Ph- <i>p</i> -OCH ₂ -	-CH ₂ Ph- <i>p</i> -OCH ₂ -	1.720
2.25	Leu	-(CH ₂) ₈ -	-CH ₂ -	>50
2.26	Phe	-(CH ₂) ₈ -	-CH ₂ -	>50

[#] Standard deviation are found in the raw data, Appendix A5



CMPD	R ¹	R ²	R ³	IC ₅₀ (μM) [#]
				HLE
2.114	Leu	–	–	>50
2.115	Phe	–	–	>50
2.116	Leu	-(CH ₂) ₂ Ph- <i>p</i> -OAll	-CH ₂ CH=CH ₂	0.859
2.117	Phe	-(CH ₂) ₂ Ph- <i>p</i> -OAll	-CH ₂ CH=CH ₂	1.46
2.118	Leu	-(CH ₂) ₂ Ph- <i>p</i> -OAll	-CH ₂ Ph- <i>p</i> -OAll	0.465
2.119	Phe	-(CH ₂) ₂ Ph- <i>p</i> -OAll	-CH ₂ Ph- <i>p</i> -OAll	0.524
2.120	Leu	-(CH ₂) ₈ CH=CH ₂	-CH ₂ CH=CH ₂	0.148
2.121	Phe	-(CH ₂) ₈ CH=CH ₂	-CH ₂ CH=CH ₂	0.52

[#] Standard deviation are found in the raw data, Appendix A5

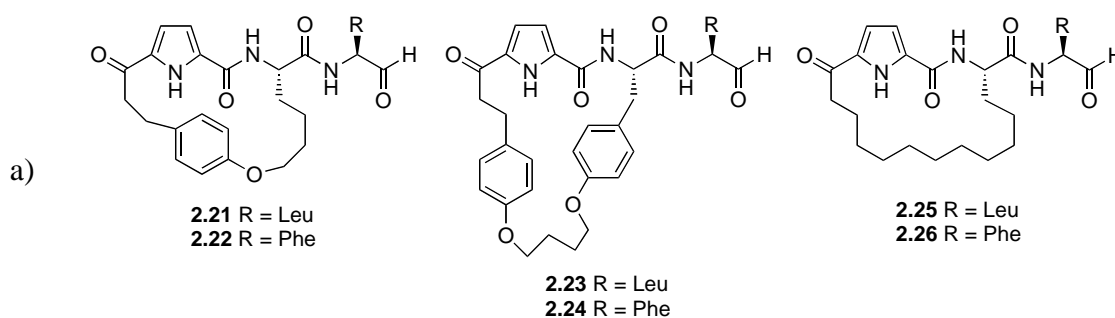
The 18-membered macrocyclic aldehydes **2.21**, **2.22**, **2.25** and **2.26** were inactive against HLE at a concentration of 50 μM, while the larger 24-membered macrocyclic aldehydes **2.23** and **2.24** were weakly active against HLE, with an IC₅₀ value of 1.82 μM and 1.72 μM respectively (Table 3.7a). This difference may reflect the presence of a hydrophobic aryl group at the P₂ position in the ring system of **2.23** and **2.24**. This is consistent with HLE's preference towards hydrophobic groups in the S₂ pocket.³⁰ As previously discussed (section 3.3.2.1), the 24-membered ring system may also better stabilize the β-strand conformation required for inhibitor binding.

The acyclic aldehydes **2.116-2.121** inhibited HLE with IC₅₀ values in the range of 0.15 – 1.5 μM (Table 3.7b). Aldehydes with Leu at P₁ (**2.116/2.118/2.120**) were more potent than the Phe variants (**2.117/2.119/2.121**), consistent with HLE's preference for medium-sized alkyl chains at the P₁ position.³¹ In addition, an aryl group (**2.118/2.119**) or a long aliphatic side chain (**2.120/2.121**) at P₂ further enhances potency, consistent with the preference that HLE has for larger side chain groups at this position.³⁰ The shorter acyclic aldehydes **2.114** and **2.115** containing one amino acid less, were all inactive against HLE, suggesting a preference for extended peptidic inhibitors that provide an opportunity for increased interactions within the enzyme binding pocket of HLE.

3.3.2.3 Inhibitor Selectivity Within the Serine Protease Family

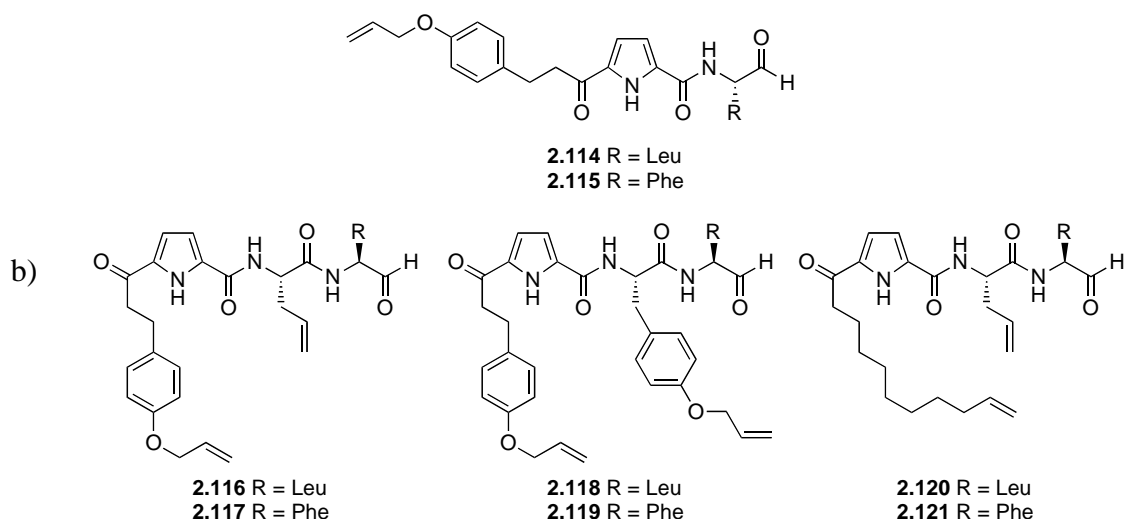
As discussed in section 3.3.1.3, selective inhibition of one enzyme within the same protease family is a challenging task. The IC_{50} of the inhibitors **2.21-2.26** and **2.114-2.121** between bovine α -chymotrypsin, human leukocyte elastase (HLE) and trypsin, all of which are serine proteases, are summarised in Table 3.8.

Table 3.8 IC_{50} values of (a) macrocyclic aldehydes and (b) acyclic aldehydes against bovine α -chymotrypsin (bCT), human leukocyte elastase (HLE) and trypsin.



CMPD	Serine Protease [#]		
	bCT (K_i (μ M))	HLE (IC_{50} (μ M))	Trypsin (IC_{50} (μ M))
2.21	>50	>50	n.i.
2.22	0.431	>50	n.i.
2.23	1.917	1.820	n.i.
2.24	0.033	1.720	n.i.
2.25	>50	>50	n.i.
2.26	2.525	>50	n.i.

[#] Standard deviation are found in the raw data, Appendix A5



CMPD	Serine Protease [#]		
	bCT (K_i (μ M))	HLE (IC_{50} (μ M))	Trypsin (IC_{50} (μ M))
2.114	>50	>50	n.i.
2.115	>50	>50	n.i.
2.116	0.939	0.859	n.i.
2.117	0.056	1.46	n.i.
2.118	>50	0.465	n.i.
2.119	0.688	0.524	n.i.
2.120	>50	0.148	n.i.
2.121	2.474	0.52	n.i.

n.i = no inhibition.

[#] Standard deviation are found in the raw data, Appendix A5

The macrocyclic (**2.21-2.26**) and acyclic (**2.114-2.121**) aldehydes tested displayed some selectivity for the serine proteases used in the study, with the key features highlighted below. The macrocyclic aldehydes (**2.21-2.26**) were generally more potent towards α -chymotrypsin compared to HLE, though no such trend is apparent for acyclic inhibitors **2.114-2.121**, see Table 3.8. Inhibitors with a Phe at P₁ (**2.23/2.25/2.114/2.116/2.118/2.120**) were slightly more potent against α -chymotrypsin compared to those with a Leu at P₁ (**2.24/2.26/2.115/2.119/2.121**). However, HLE showed no such preference toward the P₁ substituent. The macrocyclic inhibitor **2.24**, containing two aryl groups in the ring system, was the most potent inhibitor of both HLE and α -chymotrypsin. By comparison, the macrocyclic inhibitor containing one aryl group at P₄ in the ring system (**2.22**) or an aliphatic ring system (**2.26**) displayed weak or no inhibition of α -chymotrypsin and HLE,

respectively. This is consistent with α -chymotrypsin and HLE's preference for bulky hydrophobic groups binding at the S_2 positions^{30,32} (as discussed in sections 3.3.2.1 and 3.3.2.2).

The acyclic aldehydes (**2.114-2.121**) were more potent against HLE than the macrocyclic aldehydes (**2.21-2.26**), with inhibitors containing aryl or long aliphatic groups at P_2 being preferred. In contrast, the incorporation of a single aryl group at the P_4 position (**2.117**) was more potent against α -chymotrypsin. However, a significant decrease in potency is apparent on introduction of an additional aryl group at P_2 (**2.119**), which is presumably due to its enhanced conformational flexibility (see section 3.3.2.1).

None of the macrocyclic (**2.21-2.26**) and acyclic (**2.114-2.121**) aldehydes were active against trypsin at a concentration of 50 μM . This is not surprising given that the specificity of trypsin is determined by the S_1 site, which is known to favour basic residues such as Lys and Arg, due to the presence of a negatively charged Asp in the S_1 pocket.³²

3.3.3 Summary: Structure-Activity Relationship for Cysteine and Serine Protease Inhibition

A comparison of the efficacies of the aldehyde inhibitors (**2.21-2.26** and **2.114-2.121**) against the proteases discussed above provides an opportunity to elucidate structural preferences of the cysteine/serine protease families. The similar mode of action of cysteine and serine proteases (see chapter 2, section 2.1.2 for further discussion) creates many challenges with regards to designing inhibitor selectivity. The results and trends for the macrocyclic and acyclic aldehyde series are summarised in Table 3.9

Table 3.9 Trends observed for macrocyclic and acyclic aldehydes against cysteine proteases and serine proteases.

	Cysteine Proteases			Serine Proteases	
	Calpain	CatL	CatS	bCT	HLE
P ₁ specificity	Leu	Leu	Leu	Phe	No pref.
P ₂ specificity	Aliphatic	Aliphatic	Aromatic	Aromatic	No pref.
P ₄ specificity	Aliphatic	No pref.	No pref.	Aromatic	No pref.
Cyclisation	Favoured	Favoured	Favoured	Favoured	Disfavoured
Ring Size	18-mem	18-mem	No pref.	24-mem	24-mem

It was considered that the introduction of different substituents at P₁ within the macrocyclic aldehyde series (**2.21-2.26**) might influence selectivity between the cysteine proteases and α -chymotrypsin (serine protease). Here, the S₁ subsite for α -chymotrypsin is characterised by a deep hydrophobic pocket and thus, large hydrophobic residues are preferred at P₁.²⁹ Interestingly, no preference for substituents at P₁ (Leu or Phe) was observed for HLE (serine protease), with the ring size (18-membered vs. 24-membered) being the primary determinant for activity of the macrocyclic aldehydes.

The macrocycle of aldehydes **2.21-2.26** improves potency towards all proteases except HLE as compared to the analogous acyclic aldehydes **2.114-2.121**. As discussed earlier (see section 2.2.1) an appropriate ring pre-organizes the peptidic backbone into a β -strand conformation required for inhibitor binding to the active site. The larger 24-membered macrocyclic aldehydes (**2.23/2.24**) were found to be more potent inhibitors of α -chymotrypsin and HLE (serine proteases) compared to calpain and cathepsin L (cysteine proteases), presumably since these proteases have a deep and/or large binding pocket to accommodate the larger macrocycle. In contrast, calpain and cathepsin L (cysteine proteases) were found to prefer smaller 18-membered macrocycles, while interestingly, cathepsin S did not display any preference towards the size of the macrocycle, with the main influence of cathepsin S selectivity being the residue at the P₄ position (Phe).

The introduction of aryl groups into the ring system as in **2.21**, **2.22**, **2.25** and **2.26** did not improve selectivity towards any particular family (c.f. CatS and bCT in Table 3.9). However, for the cysteine proteases studied, calpain appears to prefer aliphatic groups

between the linked P₂ and P₄ site, while cathepsins L and S are able to accommodate both aliphatic and aryl groups at the P₄ site. By contrast, serine proteases (HLE and α -chymotrypsin) appear to favour aryl groups at both the P₂ and P₄ site, which is consistent with their known preference for bulkier hydrophobic groups such as phenyl.^{29,30}

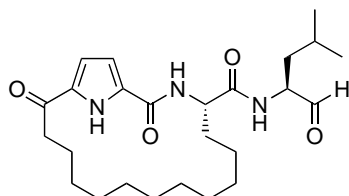
3.4 Conclusions

In summary, a new class of macrocyclic protease inhibitors linked through the P₂ and P₄ residues, were tested against a series of serine and cysteine proteases. All the inhibitors were active towards the cysteine (calpain and cathepsin) and serine proteases (α -chymotrypsin and HLE). Inhibitors with Leu at P₁ (**2.21/2.23/2.25/2.114/2.116/2.118/2.120**) were found to be more potent against cysteine proteases, calpain and cathepsins, while inhibitors with Phe at P₁ (**2.22/2.24/2.26/2.115/2.119/2.121**) were more potent against the serine protease α -chymotrypsin. Inhibitors with a Leu at P₁ and small aliphatic groups (e.g. allyl glycine) at P₂ (**2.21/2.25/2.116**) were potent inhibitors of calpain and cathepsin L, while the introduction of an aromatic group at P₂ (**2.23/2.118**) gave potent inhibitors of cathepsin S. In contrast, inhibitors with a Phe at P₁ and aromatic groups in the P₂ and/or P₄ position (**2.24/2.119**) were selective and potent inhibitors of the serine proteases, α -chymotrypsin and HLE.

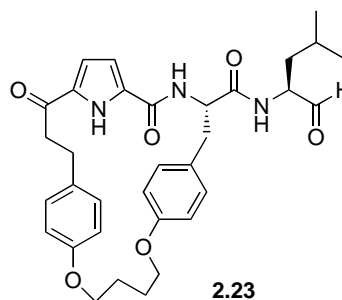
Introduction of a macrocyclic ring that uniquely links P₂ and P₄ results in improved potency against all proteases except for HLE. Linking these residues, rather than the P₁ and P₃ residues as in previous studies, means that the P₁ position is free for introducing any number of groups. Molecular docking studies on the macrocyclic aldehydes (**2.21-2.26**) docked into μ -calpain suggest that the ring system pre-organizes the backbone of the inhibitor into the preferred β -strand conformation. The component pyrrole replaces the amino acid residue at P₃ to effectively decrease the peptide character of the inhibitor, while also promoting the requisite β -stranded conformation. The size of the macrocycle was found to influence selectivity, with the 18-membered ring leading to potent inhibitors of calpain and cathepsin L (both cysteine proteases), while the larger 24-membered ring favours the inhibition of serine proteases (α -chymotrypsin and HLE). The cysteine protease, cathepsin S, does not display a preference for ring size, with both the 18- and 24-membered

macrocycle being equally potent inhibitors. Selectivity of inhibition for cathepsin S over calpain and cathepsin L is essentially determined by the residue at the P₂ position.

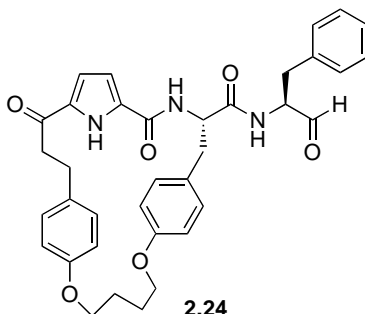
The macrocyclic aldehyde with an 18-membered ring and aliphatic alkyl group linking P₂ and P₄ (**2.25**) is the most versatile cysteine protease inhibitor, displaying potent inhibition of calpain, cathepsin L, cathepsin S. By comparison, the larger macrocyclic aldehyde **2.23**, with two component aryl groups, is the most potent inhibitor of cathepsin S (IC₅₀ = 0.0014 μM) with significant selectivity over calpain, cathepsin L, α-chymotrypsin and HLE. The most potent serine protease inhibitor (IC₅₀ of 0.033 μM against α-chymotrypsin) proved to be the analogue **2.24**, which is the direct analogue of **2.23** differing only by having a Phe instead of a Leu at P₁. This macrocycle is also a potent inhibitor of cathepsin S with an IC₅₀ of 0.0066 μM.

**2.25**

m-Calpain: IC₅₀ = 0.066 μM
 Cathepsin L: IC₅₀ = 0.003 μM
 Cathepsin S: IC₅₀ = 0.0017 μM

**2.23**

Cathepsin S: IC₅₀ = 0.0014 μM
 Selectivity 31-fold

**2.24**

α-Chymotrypsin: IC₅₀ = 0.033 μM
 Cathepsin S: IC₅₀ = 0.0066 μM

These 2nd generation macrocyclic inhibitors uniquely links the P₂ and P₄ residues, leaving the P₁ position free to allow for the introduction any number of groups to tailor for selectivity. Additionally, the ability to introduce any number of ring systems adds to the versatility of these inhibitors. Thus, this new class of macrocyclic protease inhibitor is ideally suited to targeting other proteases, particularly other classes cysteine proteases and proteases with chymotrypsin-like activities (e.g. proteasome).

3.5 References for Chapter Three

- [1] Cheng, Y.; Prusoff, W. H. *Biochem. Pharmacol.* **1973**, *22*, 3099–3108.
- [2] Burlingham, B. T.; Widlanski, T. S. *J. Chem. Educ.* **2003**, *80*, 214–218.
- [3] Passonneau, J. V.; Lowry, O. H. *Enzymatic Analysis: A Practical Guide*; The Humana Press Inc.: Totowa NJ, **1993**, pp. 85–110.
- [4] Bisswanger, H. *Enzyme Kinetics: Principles and Methods*; 2nd ed; Wiley-VCH: Weinheim, **2008**, Chapter 3, pp. 228-257.
- [5] Thompson, V. F.; Saldaña, S.; Cong, J.; Goll, D. E. *Anal. Biochem.* **2000**, *279*, 170–178.
- [6] Jones, L. J.; Upson, R. H.; Haugland, R. P.; Panchuk-Voloshina, N.; Zhou, M.; Haugland, R. P. *Anal. Biochem.* **1997**, *251*, 144–152.
- [7] Mehrtens, J. M. The design, synthesis and biological assay of cysteine protease specific inhibitors., University of Canterbury: Caterbury NZ, **2007**, Chapter 5, pp. 120–134.
- [8] Morrison, J. F. *Trends Biochem. Sci.* **1982**, *7*, 102-105.
- [9] Inoue, J.; Nakamura, M.; Cui, Y.-S.; Sakai, Y.; Sakai, O.; Hill, J. R.; Wang, K. K. W.; Yuen, P. W. *J. Med. Chem.* **2003**, *46*, 868–871.
- [10] Buroker-Kilgore, M.; Wang, K. K. W. *Anal. Biochem.* **1993**, *208*, 387-392.
- [11] Abell, A. D.; Jones, M. A.; Coxon, J. M.; Morton, J. D.; Aitken, S. G.; McNabb, S. B.; Lee, H. Y.-Y.; Mehrtens, J. M.; Alexander, N. A.; Stuart, B. G.; Neffe, A. T.; Bickerstaffe, R. *Angew. Chem. Int. Ed.* **2009**, *48*, 1455–1458.
- [12] Peddie, V.; Pietsch, M.; Bromfield, K. M.; Pike, R. N.; Duggan, P. J.; Abell, A. D. *Synthesis* **2010**, *11*, 1845-1859.
- [13] Liljeblad, A.; Kanerva, L. T. *Tetrahedron* **2006**, *62*, 5831–5854.
- [14] Dixon, M. *Biochem. J.* **1953**, *55*, 170.
- [15] Frizler, M.; Stirnberg, M.; Sisay, M. T.; Gütschow, M. *Curr. Top. Med. Chem.* **2010**, *10*, 294–322.
- [16] Gütschow, M.; Pietsch, M.; Themann, A.; Fahrig, J.; Schulze, B. *J. Enz. Inhib. Med. Chem.* **2005**, *20*, 341-347.
- [17] Sisay, M. T.; Hautmann, S.; Mehner, C.; König, G. M.; Bajorath, J.; Gütschow, M. *ChemMedChem* **2009**, *4*, 1425-1429.

- [18] Jones, M. A.; Morton, J. D.; Coxon, J. M.; McNabb, S. B.; Lee, H. Y.-Y.; Aitken, S. G.; Mehrtens, J. M.; Robertson, L. J. G.; Neffe, A. T.; Miyamoto, S.; Bickerstaffe, R.; Gately, K.; Wood, J. M.; Abell, A. D. *Bioorg. Med. Chem.* **2008**, *16*, 6911–6923.
- [19] Robertson, L. J. G.; Morton, J. D.; Yamaguchi, M.; Bickerstaffe, R.; Shearer, T. R.; Azuma, M. *Invest. Ophth. Vis. Sci.* **2005**, *46*, 4634–4640.
- [20] Pietsch, M.; Chua, K. C. H.; Abell, A. D. *Curr. Top. Med. Chem.* **2010**, *10*, 270–293.
- [21] Donkor, I. O. *Expert Opin. Ther. Patents* **2011**, *21*, 601–636.
- [22] Robertson, L. J. G.; Morton, J. D.; Yamaguchi, M.; Bickerstaffe, R.; Shearer, T. R.; Azuma, M. *Invest. Ophth. Vis. Sci.* **2005**, *46*, 4634–4640.
- [23] Jones, M. A.; Morton, J. D.; Coxon, J. M.; McNabb, S. B.; Lee, H. Y.-Y.; Aitken, S. G.; Mehrtens, J. M.; Robertson, L. J. G.; Neffe, A. T.; Miyamoto, S.; Bickerstaffe, R.; Gately, K.; Wood, J. M.; Abell, A. D. *Bioorg. Med. Chem.* **2008**, *16*, 6911–6923.
- [24] Irie, O.; Ehara, T.; Iwasaki, A.; Yokokawa, F.; Sakaki, J.; Hirao, H.; Kanazawa, T.; Teno, N.; Horiuchi, M.; Umemura, I.; Gunji, H.; Masuya, K.; Hitomi, Y.; Iwasaki, G.; Nonomura, K.; Tanabe, K.; Fukaya, H.; Kosaka, T.; Snell, C. R.; Hallett, A. *Bioorg. Med. Chem. Lett.* **2008**, *18*, 3959–3962.
- [25] Tyndall, J. D.; Fairlie, D. P. *Curr. Med. Chem.* **2001**, *8*, 893–907.
- [26] Berti, P.; Storer, A. *J. Mol. Biol.* **1995**, *246*, 273–283.
- [27] Cuerrier, D.; Moldoveanu, T.; Davies, P. L. *J. Biol. Chem.* **2005**, *280*, 40632–40641.
- [28] Sanderson, P. E. *Med. Res. Rev.* **1999**, *19*, 179–197.
- [29] Czapinska, H.; Otlewski, *Eur. J. Biochem.* **1999**, *260*, 571–595.
- [30] Bode, W.; Meyer, E.; Powers, J. C. *Biochemistry* **1989**, *28*, 1951–1963.
- [31] Shotton, D. M.; Watson, H. C. *Nature* **1969**, *25*, 811–816.
- [32] Hedstrom, L. *Chem. Rev.* **2002**, *102*, 4501–4524.

CHAPTER FOUR:
New Gelatin-Based Materials by
ROMP

4.1 Introduction

As previously stated, the focus of this thesis is to control peptide structure and function through synthetic modification. Chapter 2 and 3 discussed in detail the controlled organization of secondary structure in peptides via ring closing metathesis (RCM) to afford novel inhibitors of cysteine and serine protease. In this chapter, the controlled organization of the tertiary structure of naturally occurring peptides is investigated for the formation of biocompatible hydrogels derived from gelatin. Methacrylate-functionalized gelatin is crosslinked with norbornene dicarboxylic acid by aqueous metathesis to afford hydrogels with varying degrees of crosslinking by varying the ratio of gelatin and norbornene dicarboxylic acid. The varying degrees of crosslinking may provide differing physical properties, which can potentially tailor this class of polymer hydrogels for specific applications in regenerative medicine.

4.1.1 Ruthenium-Catalyzed Aqueous Olefin Metathesis

Olefin metathesis, as catalyzed by transition metal-based carbene complexes, is one of the most useful reactions for carbon-carbon bond formation.¹⁻⁵ Variations of this carbon-carbon bond formation, particularly ring-opening metathesis polymerization (ROMP), have been successfully used in the synthesis of polymer-based macromolecules and hydrogels.^{6,7} Ruthenium-based complexes (Figure 4.1) are particularly useful due to their increased stability in various media and tolerance to a variety of functional groups (see chapter 1 for an in depth discussion of ROMP).

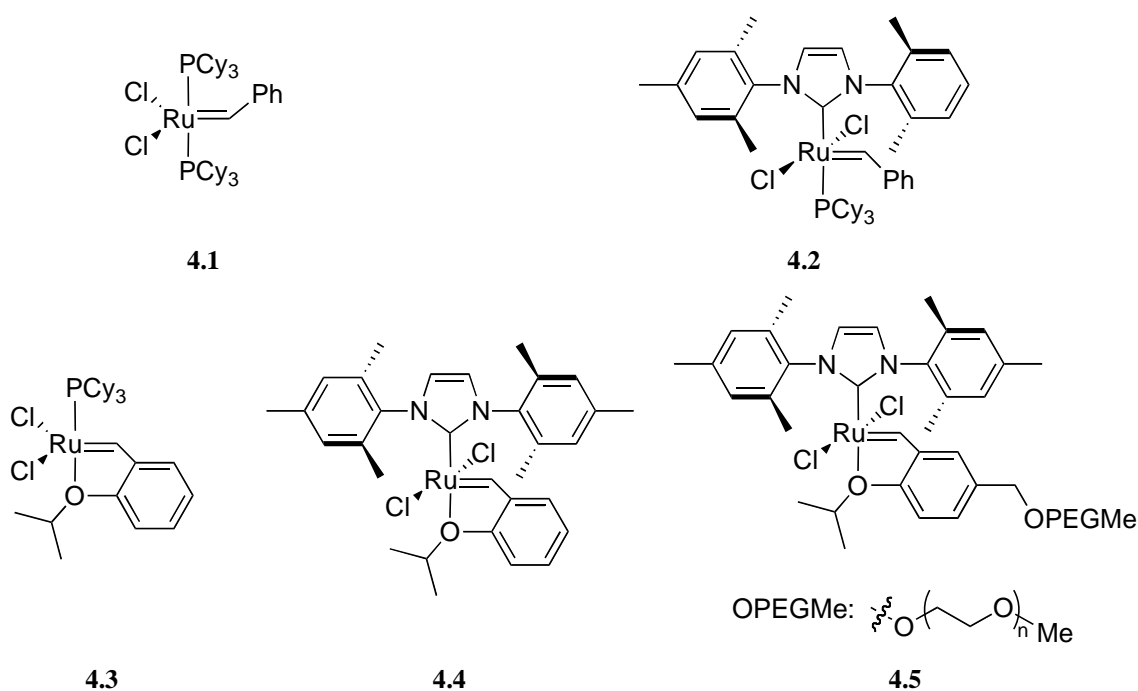


Figure 4.1 Well-defined ruthenium catalyst for olefin metathesis: **4.1** Grubbs 1st Generation (GI), **4.2** Grubbs 2nd Generation (GII), **4.3** Hoveyda-Grubbs 1st Generation (HGI), **4.4** Hoveyda-Grubbs 2nd Generation (HGII) and **4.5** water-soluble Hoveyda-Grubbs 2nd Generation (HG2-S) catalysts.

Chemical transformations in industry often require the use of organic solvents as a reaction media. However, there is a need for a move to water-based chemistry for environmental benefits, though this often results in both insolubility of most organometallic catalyst in water media, coupled with a decrease of reaction rate and efficiency. As a result, reactions in aqueous media require harsh reaction conditions such as elevated temperatures and increased catalyst loading, which can be detrimental for temperature sensitive reagents and can ultimately affect the overall properties of the synthesized materials. Several methods of improving solubility of organometallic catalyst in water currently exists, such as the use of surfactants that can form micelles⁸⁻¹⁰ or the development of water soluble catalysts.¹¹

4.1.2 Hydrogels in Biomedical Applications

The advancement of medical technology has vastly improved the lifestyle and living conditions in the twentieth and twenty-first centuries. However, this advancement and improvement in lifestyle is coupled with an increase in an average lifespan of the population, leading to increases in patients suffering from degenerative diseases and

injuries. Conventional treatments requiring surgery and organ transplant are invaluable, however many issues can arise from such invasive methods, including tissue damage, organ incompatibility and internal or external scarring. These potential problems have led to the development of regenerative medicines to combat these diseases and injuries.¹²

Regenerative medicine¹³ is an interdisciplinary field of research focused on the repair, replacement or regeneration of damaged cells or tissues in order to restore impaired function. It involves the use of various therapeutic strategies, such as the use of biomaterials, cell therapy, or a combination of both, allowing regeneration of damaged tissues by supporting endogenous regeneration.

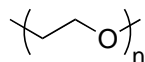
The use of biomaterials as a form of regenerative medicine has generated significant interest in the ability to tailor materials for specific functions, such as for drug delivery systems or tissue healing. In particular, biomaterials can be used as extracellular matrixes for tissue regeneration due to their capacity to interact with cells, tissues and biological systems, when implanted into the body.¹⁴ For a biomaterial to be useful in tissue repair several requirements need to be achieved; i) the material must be biocompatible and when implanted it should act as a temporary substitute of the extracellular matrix, enabling the growth of new tissue by cell proliferation; and ii) the material should degrade over time as the formation of new tissue progresses. Additionally, the properties of these biomaterials, such as the mechanical and thermal properties, water uptake, swelling and degradation, need to be tailored to the biomedical application.¹⁵⁻¹⁷ A focus of biomaterial research is directed at the generation of a series of polymer-based materials that are non-toxic, degradable and histo-compatible and this has led to a series of polyglycols, polysaccharides and peptidic based polymers.¹⁸

Current designs of materials for use in biomedical and regenerative medicine integrate principles from molecular and cell biology to mimic certain aspects of the natural extracellular matrix (ECM).¹⁹ Hydrogels show innate structural and compositional similarities to the extracellular matrix (ECM). They exhibit complex structural networks that promote survival and cellular proliferation and hence these polymer-based materials have received extensive attention in the field of regenerative therapy.²⁰

Hydrogels are three-dimensional crosslinked polymer networks formed from hydrophilic homopolymers, copolymers or macromers, and are insoluble polymer matrices that can retain large volumes of water, causing the network to swell in aqueous medium. They are thought to encourage accelerated tissue formation, as they offer an environment that resembles the highly hydrated state of natural tissues.²⁰ The network structure of hydrogels can be quantitatively described by several molecular parameters including the extent of swelling and content of water retained, which is dependent on the hydrophilicity of the polymer chains; and the crosslinking density, which directly affects the mechanical properties of the material.²⁰ The crosslinking of hydrogels allows control over the gels' final chemistry, macroscopic and degradation properties. These crosslinks can be formed by ionic interactions, physical interactions, chemical and hydrogen bonding. Simple changes in processing conditions (e.g. macromer concentration) can lead to a range of gel properties,^{21,22} whereas mixing different macromers in solution prior to polymerization can lead to networks that contain both synthetic and natural components.²³

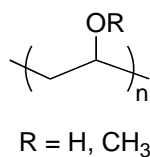
Synthetic hydrogels are commonly derived from single units and blends of polymers such as poly(ethylene glycol) **4.6**,²⁴⁻²⁷ poly(vinyl alcohol) **4.7**,^{25,28,29} and polyacrylates such as poly(2-hydroxyethyl methacrylate) **4.8**³⁰ (Figure 4.2). Synthetic gels exhibit several advantages over naturally occurring gels due to (i) the ease of large-scale production; (ii) high tunability; and (iii) consistent and reproducible properties between syntheses. However, these gels risk contamination during formation and are thus often subjected to several purification processes in order to remove hazardous contaminants. In contrast, hydrogel formation derived from biological sources (Figure 4.2) such as agarose **4.9**,³¹ alginate **4.10**,^{32,33} chitosan **4.11**,^{34,35} hyaluronic acid **4.12**,^{19,34,35} fibrin^{36,37} and collagen³⁸⁻⁴⁰ are widely thought to have an edge over synthetic biomaterials where biocompatibility is concerned. These natural gels offer better chemical and morphological cues to cells and offer environmental advantages, as they are capable of biomimicry of tissues and ECM. However, natural polymer-hydrogels often exhibit several issues that include (i) variability in batch-to-batch formulation; (ii) weak mechanical properties compared to their synthetic counterparts; and (iii) unpredictable stability and degradation behavior.

a) Synthetic polymers



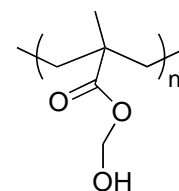
Poly(ethylene glycol)

4.6



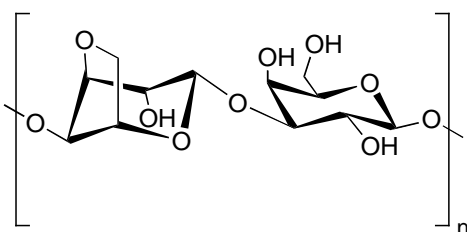
Poly(vinyl alcohol)*

4.7

Poly(2-hydroxyethyl
methacrylate)

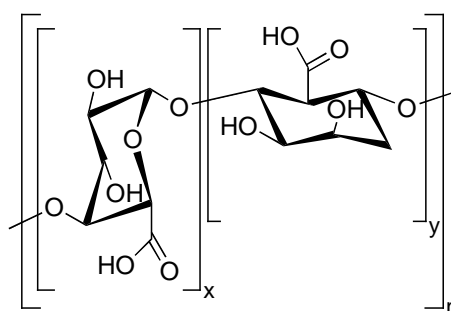
4.8

b) Natural polymers



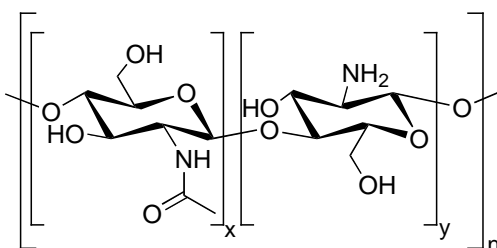
Agarose

4.9



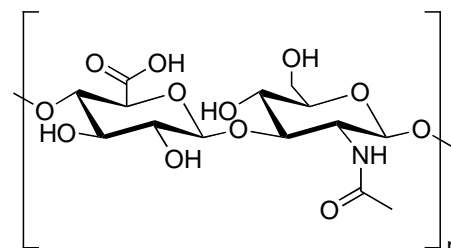
Alginate

4.10



Chitosan

4.11



Hyaluronic acid

4.12

Figure 4.2 (a) Synthetic and (b) natural building blocks used for the formation of hydrogels. *Poly(vinyl alcohol) exists as a mixture of acetylated and non-acetylated monomers.

4.1.3 The Extracellular Matrix

Cells reside in a dynamic framework composed of biopolymers called the extracellular matrix (ECM). The ECM (Figure 4.3) is composed of water and extracellular macromolecules, primarily consisting of polysaccharides (e.g. proteoglycans, hyaluronic acid), and fibrous proteins (e.g. collagen, elastin, fibronectin, laminin and vitronectin) that make up the matrix and have structural and adhesive functions.

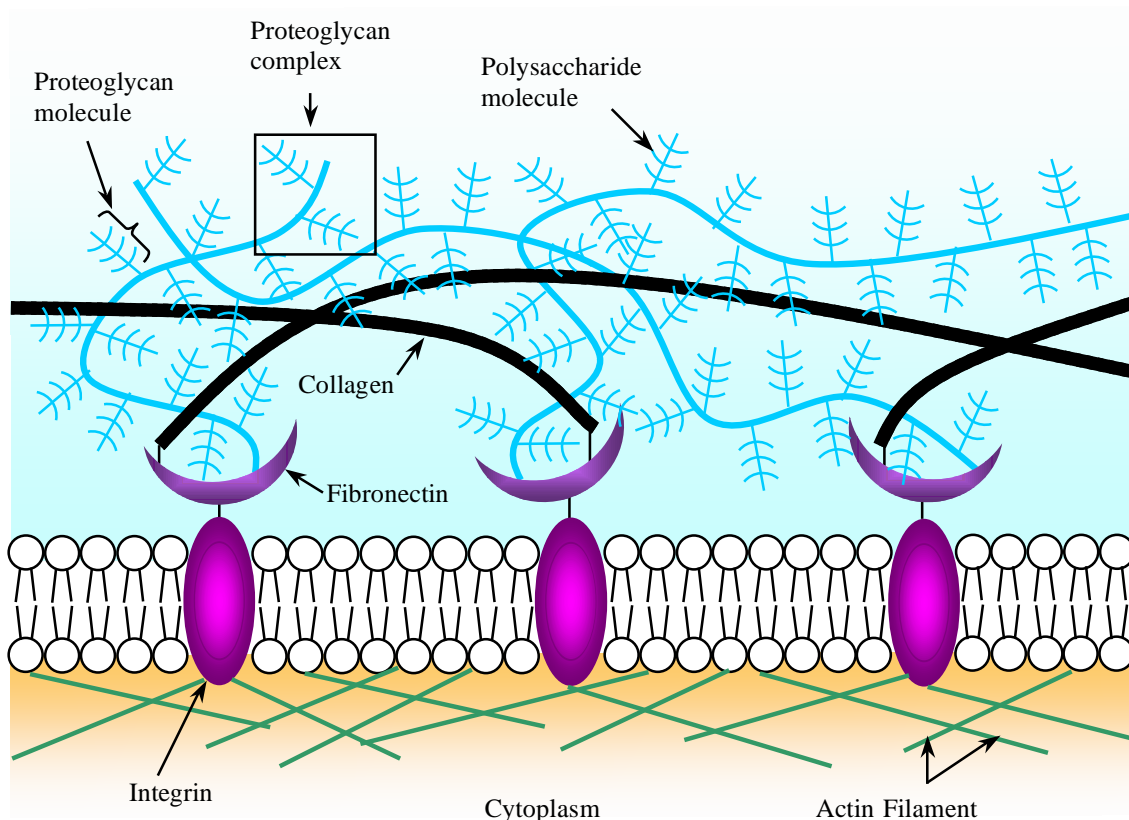


Figure 4.3 Overview of the composition and macromolecular organization of the extra cellular matrix.

Proteoglycans⁴¹ are proteins that are heavily substituted with glycosaminoglycans (GAGs). GAGs are linear polysaccharides made from repeating disaccharide units of an acylated amino sugars alternating with uronic acid. Examples of GAG chains include hyaluronan (HA), heparan sulfate (HS), chondroitin sulfate (CS), dermatan sulfate (DS) and keratan sulfate (KS). As GAGs possess a negatively charged sulfate or carboxylate group, they tend to repel each other and anions while attracting cations, facilitating the interaction with water molecules and giving hydration characteristics and resilience to compressional forces.⁴² In connective tissue, proteoglycans form a gel-like structure, which resists compressive forces on the matrix and allows rapid diffusion of nutrients, metabolites and hormones between the blood and the tissue cells. Additionally, fibrous proteins present in the ECM such as collagen fibrils provide durability and tensile strength for the surrounding tissue, while the rubber-like elastin fibers provide resilience.⁴³ Together with the entrapped interstitial fluid, ECM exhibits a gel-like consistency.

The structural organization of these protein components in the ECM is dictated by (i) mutual cell control; (ii) the variability of protein component concentrations; and (iii) their organization within the ECM; which gives rise to a diversity of matrix forms, each adapted to the functional requirements of the particular tissue.⁴⁴ In addition to structural support, the ECM is capable of storing and sequestering growth factors, cytokines and developmental control factors for organ and tissue development/repair. As a result, polymers that are able to store this biologically relevant information can serve as scaffolds that mimic this biophysical environment of cells and can be used to imitate the environment necessary for tissue-specific evolution and maturation of cells.

Collagen

Collagen is the most abundant structural protein in animals and is the main component of connective tissue. Collagen is predominantly synthesized by the fibroblasts and undergoes self-organized helicalization during its biosynthesis.⁴⁵ Currently, there are 28 known types of collagen, with types I-IV being the most abundant. Types I-III exhibit similar structural features, appearing as long thin fibrils, while type IV forms a two-dimensional net-like structure.^{45,46} These fibrous proteins have a unique structural motif, comprising of three polypeptide chains (α -chains) that are arranged in left-handed helical conformation, which coil around one another to form a right-handed superhelix structure (Figure 4.4). The α -chains contain a highly repetitive triad sequence of (Xaa-Yaa-Gly)_n, with Xaa predominantly proline (Pro) and Yaa being mostly hydroxyproline (Hyp), giving rise to a left handed helical conformation (polyproline II-type helix) that is more elongated than typical α -helices due to a lower amount of hydrogen bonding interactions.⁴⁵

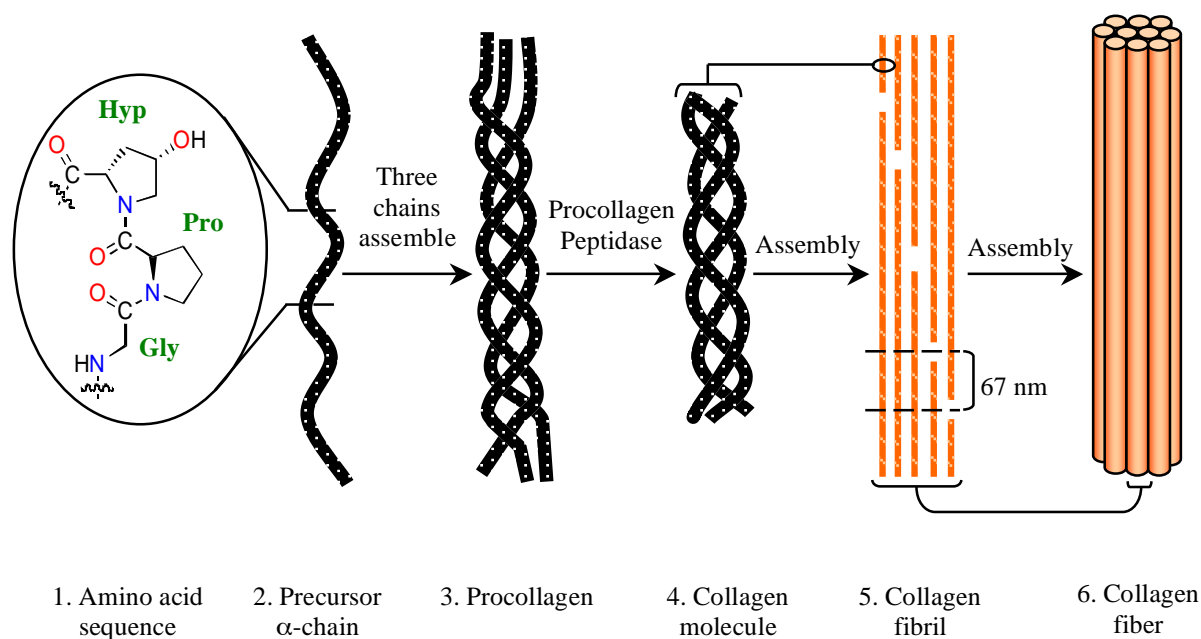


Figure 4.4 Collagen hierarchy from the micromolecular to macromolecular level.

The self-assembly of collagen into fibers takes place over multiple steps from the expression of procollagen, enzymatic modifications, to their assembly into collagen fibrils and finally, into collagen fibers (Figure 4.4).⁴⁷ The triple helical formation and stabilization relies on weak, cooperative forces and is dependent on the amino acid sequence. For example, hydrogen bonds between the peptide backbone NH of glycine with the peptide carbonyl group in an adjacent polypeptide is important for stabilizing the triple helix. In addition, hydroxyproline, hydroxylysine, lysine, aspartic acid and glutamic acid tend to stabilize the triple helix, while aromatic amino acids destabilize the helix.^{48,49} As a result, exchanges, deletions and mutations of single amino acids can be deleterious to triple helical formation, which is evident by failed assembly of the collagen chains in diseases.^{50,51}

Once secreted into the extracellular space, these collagen molecules assemble into higher-ordered structures (Figure 4.4), which is governed by the type of collagen. For example, Type I collagen, found within the human body, are known to form fibrils with a diameter of 50-200 nm. The tensile strength of individual collagen fibrils depends on; i) the diameter of the fibril; and ii) the extent of crosslinking between collagen strands in the triple helix.⁵² These fibrils then form organized parallel bundles of fibrils to give a single

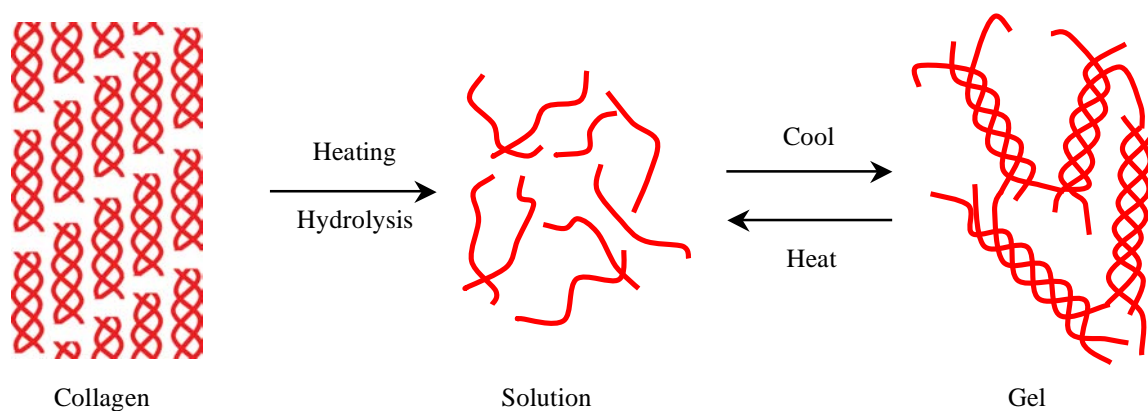
collagen fiber (Figure 4.4) that is commonly observed in tendons, where the fiber connects muscle tissue to bones. Furthermore, the assembly of collagen molecules is an entropy-driven process, due to the loss of water molecules from the protein surface, resulting in favourable fibril and fiber formation.⁴⁶

Collagen gels can be formed *in situ* and can be easily manipulated as a natural delivery device for cells and growth factors.⁵³ Additionally, they have also been used to make hydrogels for vocal cord regeneration,³⁸ spinal cord conduit repair⁵⁴ and cartilage defects.^{39,40,55} However, collagen materials show significant shrinkage in physiological environments⁵⁶⁻⁵⁸ and suffer from drawbacks such as heterogeneity, instability (e.g. loss of structural integrity) and potential immunogenicity.⁵⁹ Collagen immunogenicity has been found to be reduced by; i) enzymatic treatment (e.g. by pepsin), leading to partial degradation; or ii) by physical and chemical crosslinking. Given the fibrous bundle structure of collagen, the hierarchical level at which crosslinks are introduced is a key parameter when studying the chemical and mechanical properties of collagen. Crosslinking techniques⁶⁰⁻⁶² that have been attempted in order to maintain mechanical integrity of collagen post synthesis, have only led to slight variation of macroscopic mechanical properties. Methods directed to collagen interfibril crosslinking⁶³⁻⁶⁵ have been partially successful, but procedures that can easily tune the final properties of collagen materials are still lacking.

Gelatin

A commonly used alternative in biomaterial synthesis is gelatin. Gelatin is produced by thermal denaturation or physical and chemical degradation of collagen, involving the breakdown of the aforementioned triple-helices of collagen to form random coils (Figure 4.5). Gelatin exists as a heterogeneous mixture of single and multi-stranded polypeptides, with an average molecular weight ranging from 40-90 kDa.⁶⁶ and readily dissolves in water at temperatures above 35 °C (helix-to-coil transition temperature, T_c), to form solutions with low viscosity. In addition, the flexible random coils of gelatin consisting of approximately 100-200 amino acid residues, are capable of forming a thermally reversibly network that resembles the triple helix of collagen, in aqueous media.⁶⁷

Figure 4.5 Denaturation process of collagen to obtain gelatin and the thermal solution-gel transformation of gelatin.



At temperatures above T_c , dissolution of gelatin occurs as the cooperative interactions between gelatin chains are disrupted, leading to the increased formation of random single coils. Cooling the gelatin solution to temperatures below T_c results in the reformation of the physical networks, leading to gel formation. This solution-gel transformation is due to a conformational disorder-order transition of gelatin chains, which form thermoreversible networks by associating helices in regions commonly referred to as junction zones, that are stabilized by hydrogen bonds.^{68,69} Subsequent drying of the gels lead to the formation of physically crosslinked films through the junction zones. Due to the varying crosslinked network observed between samples, the physical properties of gelatin-gels often vary between samples depending on factors such as amino acid composition, the molecular weight, the concentration, the environment of formation (e.g. pH, temperature) and the presence of additives.⁶⁸⁻⁷⁰ Furthermore, gelatin is highly hygroscopic⁷¹ and can easily undergo structural changes during (re)wetting or storage, which can affect its overall helical content, thermal transitions and mechanical properties.^{72,73}

Currently gelatin is widely used in the medical industry as pharmaceuticals (drug delivery),⁷⁴ wound dressings⁷⁵ and adhesives in clinics.⁷⁶ It exhibits low level of immunogenicity,^{59,76} cytotoxicity,⁷⁷ and is biodegradable with excellent biocompatibility, plasticity and adhesiveness. The commercial advantage of gelatin over collagen is its; i) low cost; ii) ease of handling; and iii) wide range of processing techniques can be applied to form sponges and hydrogels.

The use of gelatin in regenerative medicine necessitates that it can be fabricated, in a consistent manner, to give stable scaffolds while being able to control the mechanical and chemical properties of synthetic gelatin films.⁷⁸ The varying hydrogel properties often observed between synthesis can be decreased by chemical and physical crosslinking methods, thus resulting in an increase in stability of the gel in aqueous media.⁷⁴ Typically, gelatin is known to contain a high quantity of glycine (25%), proline (18%) and hydroxyproline (14%), which exhibits a similar to the composition to collagen.⁷⁴ Its reactivity arises from the presence of functional amino acids, such as aspartic acid (6%) and lysine (4%). The lysine residues are thought to play an important role in the natural crosslinking of gelatin.⁷⁴ As previously mentioned, the helical content, degree of crosslinking and source of gelatin are known to influence the physical properties of the resultant gelatin-gel. Furthermore, the mode of crosslinking imparts differing mechanical properties on the gel.⁷⁸

A common synthetic route utilized in mimicking this natural crosslinking behavior is the physical crosslinking of either methacrylate or phenolic functionalized gelatin.⁷⁹ Such physical methods include the use of microwave irradiation, dehydrothermal treatment (DHT), ultraviolet and gamma irradiation treatment. The advantage of physical crosslinking is that they do not contain by-products that can cause potential cytotoxicity of the gel, whereas their main drawback arises from the difficulty to obtain consistent degrees of crosslinking.

Due to the presence of a large number of reactive functional groups in gelatin, it can also readily undergo chemical crosslinking. Commonly used examples of crosslinking agents include:

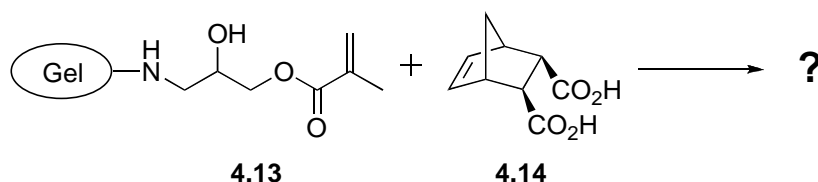
- Aldehydes (formaldehyde, glutaraldehyde, glyceraldehyde).^{78,80,81}
- Poly(ethylene glycol) diacrylate.⁸²
- Genipin.⁸³⁻⁸⁵
- Carbodiimides.⁸⁶⁻⁸⁸
- Diisocyanates.^{89,90}

The limitations in the use of chemical crosslinking agents are the potential entrapment of unreacted crosslinking reagents within the scaffold. This can lead to the release of the

trapped reagent during *in vivo* biodegradation that can be potentially toxic, and can affect the integrity of additional substances incorporated within the gel (e.g. growth factors or cytokines).⁸¹ As a result, there is an increased interest in the use of natural crosslinking agents with low toxicity, such as the used of enzymes for crosslinking^{92,93} or the used of naturally derived crosslinking agents (e.g. genipin).

4.1.4 Objectives

In this study, gelatin type A is functionalized with glycidyl methacrylate at the amino functions as shown in Scheme 4.1. This then allows chemical crosslinking via olefin metathesis to give novel biocompatible gelatin-gels. As gelatin is water soluble, olefin metathesis reactions will be performed in aqueous media, with the use of either ruthenium-based Grubbs catalyst (Figure 4.1, compound **4.1** and **4.2**) in emulsions,^{94,95} or newly developed aqueous-soluble Hoveyda-Grubbs catalyst (Figure 4.1, compound **4.5**).^{96,97} The development of novel gelatin hybrid materials and the chemistry of these materials is discussed in detail, with focus on the aqueous metathesis of methacrylate-functionalized gelatin (gel-GMA, **4.13**) and norbornene dicarboxylic acid (NBE-OH, **4.14**) (Scheme 4.1).



Scheme 4.1

The objectives of this chapter are:

1. To develop a series of novel biocompatible peptide-based hydrogels from the chemical crosslinking of gelatin and norbornene dicarboxylic acid with defined tertiary structure.
2. To determine the ideal reaction conditions for aqueous metathesis in generation novel of gelatin biomaterials.
3. To investigate the physical properties of hybrid materials by varying substituent ratios during aqueous metathesis.
4. To investigate the mechanism of novel gelatin-NBE hybrid material formation.

Through development of novel peptide-based hydrogels using environmentally friendly, aqueous based reactions, we aim to develop hydrogels that are cost effective, biofriendly and exhibit tunable tailored physical and chemical properties with potential use in the medical industry as tools for regenerative medicine.

4.2 Synthesis and Characterization of Gelatin Hybrid Materials

4.2.1 Investigation of Ideal Reaction Conditions for Aqueous Metathesis.

Commercially available type A gelatin was allowed to react with glycidyl methacrylate (GMA) in phosphate buffer pH 9.6 to obtain GMA-functionalized gelatin (gel-GMA). Type A gelatin was used in this study as it has been previously utilized in hydrogel formulations^{89,98-100} and in clinically approved products, such as Gelfoam.¹⁰¹ The reaction was performed in a basic buffer system to ensure that free amino groups could react with GMA. The degree of substitution of gelatin by GMA was quantified using trinitrobenzene sulfonate (TNBS) colorimetric assay¹⁰² and ranged from 57-69% substitution (see chapter 5, section 5.4 for procedural details). The ¹H NMR spectra of the resulting gel-GMA (a) and unfunctionalised gelatin (b) are shown in Figure 4.6. The spectrum of gel-GMA shows characteristic peaks at δ 5.83 and 6.25, corresponding to the geminal methylene protons of the introduced methacrylate groups.

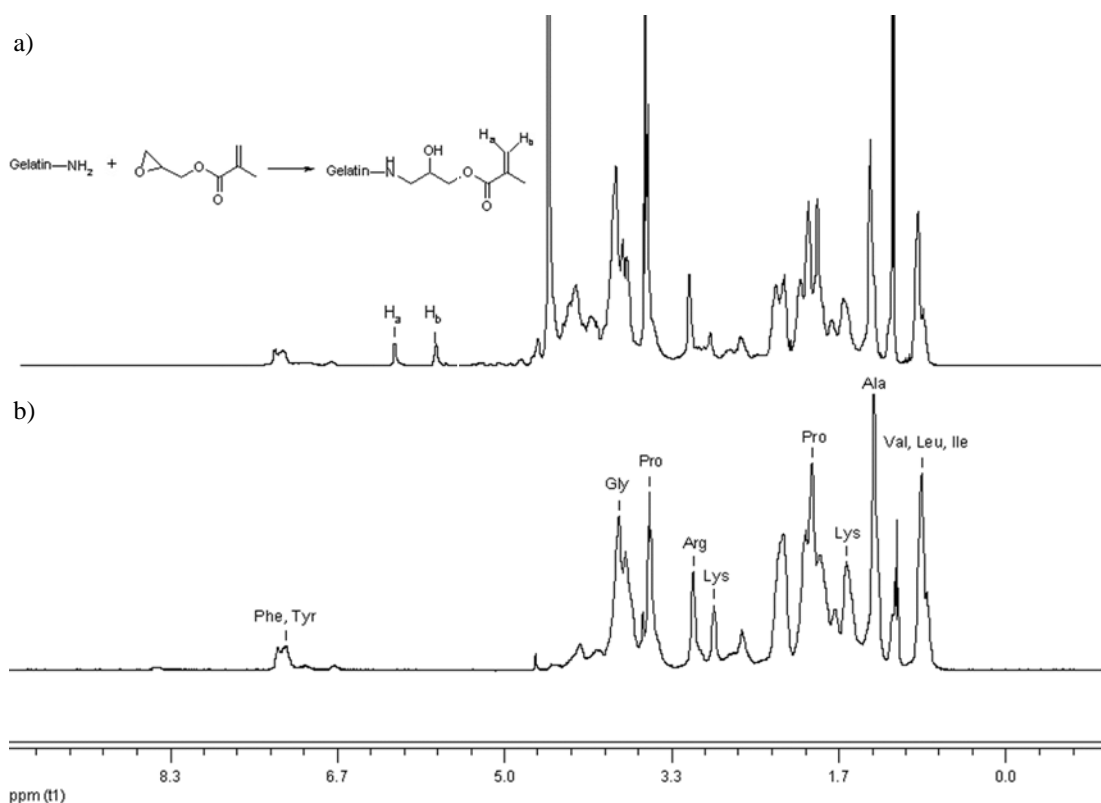


Figure 4.6 ¹H NMR spectra of gel-GMA (a) and unfunctionalized gelatin (b).

Gel-GMA was then allowed to react with norbornene dicarboxylic acid (NBE-OH) in aqueous phosphate buffer, pH 7.4 while varying; i) the catalysts utilized and ii) the ratio of catalyst loading to the combined ratio of gel-GMA/NBE-OH monomers, Table 4.1. The catalysts chosen for investigation were Grubb's 1st generation (GI) and 2nd generation (GII) catalyst (Figure 4.1, compound **4.1** and **4.2**), and a water-soluble derivative of Hoveyda-Grubbs (HG2-S) catalyst (Figure 4.1, compound **4.5**). Due to the air-sensitive nature of GI and GII catalysts, all metathesis reactions were performed under an inert atmosphere and reactions were deemed complete once gelation was observed. Furthermore, since GI and GII catalysts are insoluble in aqueous medium, reactions using these catalysts were subjected to emulsification in toluene/hexadecane^{94,95} before addition to the aqueous solution, Table 4.1, entries 1-3. Metathesis reactions of gel-GMA/NBE-OH were conducted at temperatures above helix-to-coil transition temperatures (35 °C),^{66,67} as disaggregation of the gelatin chains occurs and crosslinking at this temperature would allow stabilization of gelatin in the random coil state.

Table 4.1 Investigation of the reaction conditions for aqueous metathesis using various catalyst and differing ratios of monomers to catalyst.

Entry	Gel-GMA (equiv)	NBE-OH (equiv)	Catalyst ^a	Catalyst (mol%)	Atmosphere	[Mon ^b] : [Cat]	Gelation
1	1	1	GI	5	N ₂	20 : 1	Y
2	1	1	GI	1	N ₂	100 : 1	Y
3	1	1	GII	1	N ₂	100 : 1	Y
4	1	1	HG2-S	2	N ₂	50 : 1	N
5	1	1	HG2-S	5	N ₂	20 : 1	Y
6	1	1	HG2-S	5	Air	20 : 1	N

^a GI: Grubbs' 1st generation catalyst; GII: Grubbs' 2nd generation catalyst; HG2-S: Water soluble derivative of Hoveyda-Grubbs 2nd generation catalyst. ^b Combined monomer ratio of Gel-GMA and NBE-OH

Metathesis of gel-GMA and NBE-OH was successfully accomplished utilizing Grubbs' 1st (GI) and 2nd (GII) generation catalysts and a water soluble derivative of Hoveyda-Grubbs' 2nd generation (HG2-S) catalyst, as can be seen in entries 1, 2, and 3 of Table 4.1. In particular, reaction of gel-GMA and NBE-OH with 5 mol% GI resulted in a rapid increase in viscosity followed by gel formation within 30 sec to 1 min, Table 4.1, entry 1. A repeat of this reaction using reduced GI catalyst loading (1 mol%) resulted in the formation of an opaque, sticky polymer within 3 to 5 min, Table 4.1, entry 2. Similarly, an opaque, sticky polymer was obtained within 3 to 5 min using GII-catalyzed aqueous metathesis, with a 1 mol% loading, Table 4.1, entry 3. The similar time frames required for gel formation using both GI and GII catalysts indicates that these catalysts have similar reactivity in catalyzing the metathesis of gel-GMA and NBE-OH.

In contrast, emulsification was not required for reactions involving water-soluble derivative of Hoveyda-Grubbs 2nd generation catalyst (HG2-S), Table 4.1, entries 4-6. The HG2-S catalyst is capable of dissolving in phosphate buffer due to the presence of the water-soluble polyethylene glycol (PEG) side chains.^{96,97} Upon addition of 1 mol% HG2-S to the monomer solution, viscosity did not increase after 1 h. Addition of a further 1 mol% HG2-S resulted in no change and gelation was not observed after 16 h, Table 4.1, entry 4. However, increasing the catalyst loading to 5 mol% of HG2-S, gave rise to a clear transparent gel formed after 16 h, Table 4.1, entry 5. The combination of higher catalyst loading and a longer reaction time for gelation indicates that the rate of HG2-S-catalyzed

metathesis is much slower than that of GI- or GII-catalyzed metathesis. This reaction was repeated with 5 mol% of HG2-S in the presence of air (Table 4.1, entry 6), as the catalyst is stable to air^{96,97} and being able to conduct the reaction under atmospheric conditions is an industrial advantage. Interestingly, the viscosity (as determined visually) of the solution remained unchanged after 16 h, indicating that crosslinking had not occurred. To date, studies have shown that metathesis reactions involving HG2-S catalyst are rapid reactions that are completed within a short time frame and/or with the presence of an organic solvent.^{96,97} In contrast, the metathesis reaction for gel-GMA and NBE-OH required a longer reaction time due to the lower reactivity of HG2-S in a pure aqueous media. This suggests that the water-soluble HG2-S is not stable when exposed to atmospheric conditions for a long period of time and the presence of a pure aqueous solution may have accelerated the decomposition of the catalyst.

Polymer gels, when formed, were dried in a 37 °C oven before subjecting samples to crosslinking analysis, Table 4.1, Entries 1-3 and 5. When a reaction did not result in an increase in viscosity, an aliquot of the solution was transferred to a petri dish and dried in a 37 °C oven in order to obtain a film for crosslinking analysis, Table 4.1, Entries 4 and 6. The crosslinking analysis involved heating the samples at 50 °C and testing for dissolution in water. Crosslinking was deemed successful if no dissolution occurred after 5 h. Crosslinking analysis of the synthetic samples (Table 4.1, entries 1-6) revealed that the gels isolated for entries 1-3 and 5 (Table 4.1) were the result of GI, GII and HG2-S catalyzed crosslinking of gel-GMA and NBE-OH. Additionally, crosslinking analysis revealed that attempts of crosslinking gel-GMA and NBE-OH at both low concentrations of HG2-S and high concentrations of HG2-S under an atmospheric atmosphere (Table 4.1, Entries 4 and 6) did not occur.

Polymer gels obtained through crosslinking of gel-GMA/NBE-OH (Table 4.1, Entries 2, 3 and 5) were characterized by thermal gravimetric analysis (TGA) and temperature modulated differential scanning calorimetry (TMDSC). TGA analysis of the dried polymer gels showed a mass loss (2-5% at 120-140 °C) for all samples (Figure 4.6), corresponding to the loss of water in the polymer gel material. All samples showed thermal stability up to ~ 300 °C. These synthetic polymer gels show similar percentage mass loss (2-5%) and thermal stability (~ 300 °C) to pure gelatin and gel-GMA. (Figure 4.6).

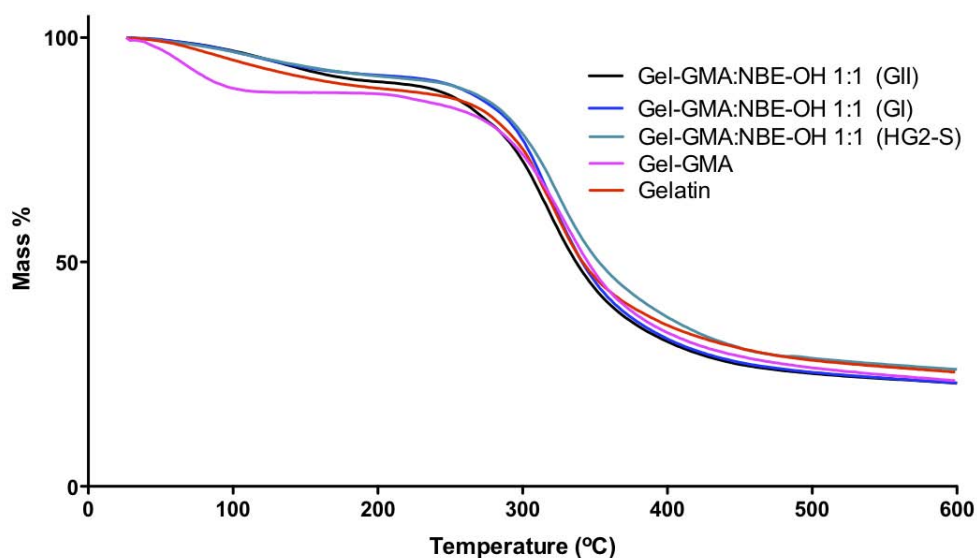
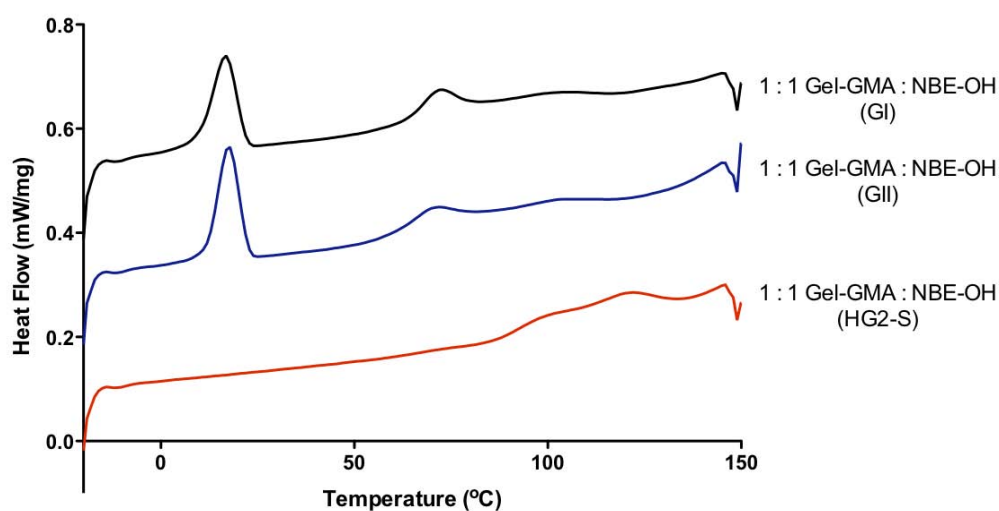


Figure 4.6 TGA data for polymer gels synthesized using GI, GII and HG2-S catalysts and comparison with pure gelatin and gel-GMA.



Entry	Gel-GMA (equiv)	NBE-OH (equiv)	Catalyst	T_m (°C)
1	1	1	GI	69
2	1	1	GII	72
3	1	1	HG2-S	100

^a GI: Grubbs' 1st generation catalyst; GII: Grubbs' 2nd generation catalyst; HG2-S: Water soluble derivative of Hoveyda-Grubbs 2nd generation catalyst.

Figure 4.7 Summary of TMDSC data for polymer gels synthesized using GI, GII and HG2-S catalysts.

TMDSC data of the dried samples displayed an endothermic signal corresponding to the crystalline melting temperature (T_m) of the polymer gels (Figure 4.7). The polymer gels formed via GI- and GII-catalyzed crosslinking exhibited similar T_m values of 69 °C and 72 °C respectively (Figure 4.7, Entries 1 and 2). Additionally, the TMDSC of these polymer gels also displayed a T_m due to hexadecane at 18 °C (lit. m.p.: 18 °C¹⁰³), which suggested entrapment of hexadecane in the polymer gel matrix as a result of using of toluene/hexadecane in the emulsion process. In contrast, the polymer gel obtained from HG2-S mediated crosslinking showed a single T_m of 100 °C (Figure 4.7, entry 3), which is significantly higher than that observed in the gel-samples catalyzed by GI and GII catalysts.

The differences in T_m suggests differing degrees of crosslinking possibly due to the increased reaction time required for the less reactive HG2-S catalyst (16 h) in comparison to the more reactive GI or GII catalyst (3-5 min). The implications of this variance in crosslinking as mentioned previously (section 4.1.3., under Gelatin) would lead to differences in physical properties of the polymer gel formed. For polymer gels with the high level of crosslinking, a more rigid/brittle gel would be observed while a low level of crosslinking could give a more flexible and pliable gel. Being able to tailor these properties of the polymer gel would be a great advantage in regenerative medicine and the results presented show the potential array of polymer gels that can be formed.

In summary, the rate of polymer gel formation was shown to be influenced by choice of catalyst utilized in the aqueous metathesis reaction. The use of GI and GII in an emulsion system rapidly furnished polymer gels within 3-5 min, at a loading of 1 mol%, Table 4.1, Entries 2 and 3. In contrast, aqueous metathesis reaction of gel-GMA and NBE-OH catalyzed by HG2-S (Table 4.1, entry 5) required a prolonged reaction time for polymer gel formation. Furthermore, HG2-S catalyst is not available commercially and requires the need to be synthesized.⁹⁷ While both GI and GII catalysts are commercially available and rapidly furnished polymer gels, GI catalyst is inexpensive, thus making GI catalyst more economically viable. As a result, GI catalyst was chosen for further investigation of aqueous metathesis reactions of gel-GMA and NBE-OH due to modest price and ease to obtain commercially.

4.2.2 Validation of Crosslinking Between Gel-GMA and NBE-OH.

With conditions for polymer gel formation established, gel-GMA and NBE-OH crosslinking was validated by performing a series of control experiments to confirm that polymer gel formation proceeded only in the presence of a catalyst and when both required monomers were present, Table 4.2. In order to establish that polymer gel formation was the result of crosslinking between gel-GMA and NBE-OH, reactions were performed by omitting either gel-GMA (Table 4.2, entry 1) or NBE-OH (Table 4.2, entry 2). Furthermore, to establish that polymer gel formation was due to catalytic metathesis reaction, a model reaction for gel-GMA and NBE-OH, in the absence of catalyst, was performed (Table 4.2, entry 3).

Table 4.2 Control reactions for the validation of crosslinking reaction.

Entry	Gel-GMA (equiv)	NBE-OH (equiv)	Catalyst ^a	Catalyst Eq. (mol%)	[Mon] : [Cat]
1	2	0	GI	0.01 (1 mol%)	100 : 1
2	0	2	GI	0.01 (1 mol%)	100 : 1
3	1	1	-	-	-

^a GI: Grubbs' 1st generation catalyst

These model reactions confirmed our earlier observation that gel formation results from the crosslinking of gel-GMA and NBE-OH. Reactions of both gel-GMA in the absence of NBE-OH (Table 4.2, entry 1) and NBE-OH in the absence of gel-GMA (Table 4.2, entry 2) resulted in no change in viscosity of the solution. This indicated that both monomers were required for polymer gel formation. Similarly, gelation was not observed in the reaction of gel-GMA/NBE-OH in the absence of catalyst (Table 4.2, entry 3), confirming the involvement of the catalyst in the formation of polymer gels.

As an increase in viscosity was not observed in all the model reactions, control reactions containing gel-GMA (Table 4.2, Entries 1 and 3) were aliquoted into petri dishes and dried in a 37 °C to obtain films for crosslinking analysis. The clear films obtained were found to dissolve in water when heated to 50 °C, indicating that self-crosslinking of gel-GMA (Table 4.2, entry 1) and crosslinking of gel-GMA/NBE-OH in the absence of catalyst

(Table 4.2, entry 3) had not taken place. This confirmed that cross-metathesis of gel-GMA did not occur and that polymer gel formation of gel-GMA/NBE-OH requires the presence of a catalyst.

The reaction of NBE-OH alone in the presence of catalyst (Table 4.2, entry 2) was analyzed by NMR and IR spectroscopic techniques to determine if self-polymerization of NBE-OH had occurred. The ^1H NMR spectrum of the NBE-OH reaction (Table 4.2, entry 3) indicated the presence of unreacted NBE-OH, with a characteristic signal from the proton on the constrained bicyclic system of NBE-OH at δ 6.1 ppm. In addition, the ^1H NMR spectrum revealed a lack of resonances in the region of δ 5-6 ppm, which is indicative of *cis/trans* alkenes that would be observed upon ring-opening of the bicyclic ring system. This confirmed that self-polymerization of NBE-OH in the presence of catalyst had not occurred and that polymer gel formation of gel-GMA/NBE-OH requires the presence of both monomers in the presence of a catalyst. These control experiments confirmed that the polymer gel samples previously isolated (Table 4.1) were a result of catalytic metathesis of gel-GMA/NBE-OH as in the absence of either monomers and/or catalyst, polymer gel formation does not occur.

4.2.3. Effect of NBE-OH Concentration on Polymer Gel Characteristics

With the successful formation of polymer gels containing gel-GMA/NBE-OH, our attention was directed towards the synthesis of polymer gels with differing mechanical properties, that could potentially be tailored for use in regenerative medicine. In particular, varying mechanical properties can be achieved by altering the concentration of NBE-OH with respect to gel-GMA. Varying the amounts of NBE-OH could possibly result in; i) grafting of NBE-OH chains on gel-GMA via cross metathesis, followed by ring opening metathesis polymerization (CM-ROMP); ii) varying amounts of crosslinking between gel-GMA and NBE-OH due to ring opening cross metathesis (ROCM); or iii) a mixture of both mechanisms, all of which could potentially affect the mechanical properties of the polymer gels.

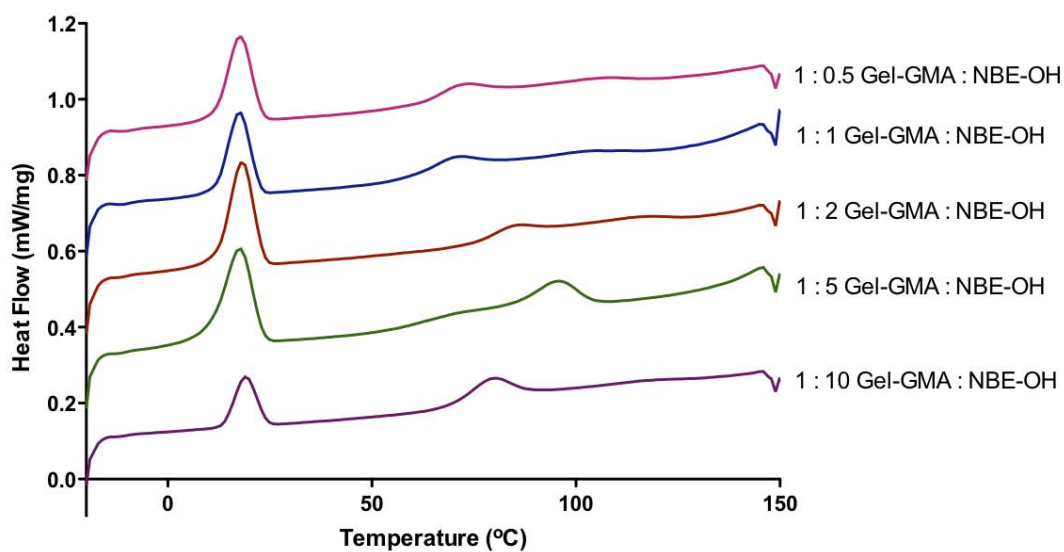
Table 4.3 Varying ratios of NBE-OH for the metathesis reaction.

Entry	Gel-GMA (equiv)	NBE-OH (equiv)	Catalyst ^a	Catalyst Eq. (mol%)	[Mon] : [Cat]
1	1	0.5	GI	0.01 (1 mol%)	100 : 1
2	1	1	GI	0.01 (1 mol%)	100 : 1
3	1	2	GI	0.01 (1 mol%)	100 : 1
4	1	5	GI	0.01 (1 mol%)	100 : 1
5	1	10	GI	0.01 (1 mol%)	100 : 1

^a GI: Grubbs' 1st generation catalyst.

The synthesis of novel gel-GMA/NBE-OH polymer gel was carried out by varying the amount of NBE-OH with respect to gel-GMA, Table 4.3. For all samples, gelation occurred within minutes, with differing textural properties of polymer gels (before drying) depending on the amounts of NBE-OH to gel-GMA being observed. Upon increasing the amount of NBE-OH with respect to gel-GMA, the texture changed from a rubber/latex like gel to a smaller solid/clumpy gel. A high amount of NBE-OH, typically above 5 equivalents (Table 4.3, Entries 4 and 5), resulted in an instantaneous increase in the viscosity of the solution upon the addition of GI catalyst, followed by a rapid formation of a clumpy gel within minutes. These textural differences observed with varying NBE-OH concentration suggest the possibility of either; i) an increase in cross-metathesis; or ii) ring-opening metathesis polymerization; resulting in an extended norbornene chain (i.e. grafting). In order to determine the mode of formation of these polymer gels mechanistic studies were conducted and are discussed in detail, in section 4.6.4.

Thermogravimetric analysis (TGA) of the dried polymer gels showed a mass loss (2-5% at 120-140 °C), corresponding to the loss of polymer gel bound water and thermal stability up to ~ 300 °C was observed for all samples. In addition, TMDSC analysis of the polymer gels showed an endothermic signal corresponding to the crystalline melting temperature (T_m) of the polymer gels in the range of 64-85 °C (Figure 4.8) and also a T_m around 17-19 °C (lit. m.p.: 18 °C¹⁰³) due to the use of hexadecane in the emulsion process. No significant change in T_m was observed upon increasing the ratio of NBE-OH.



Entry	Gel-GMA (equiv)	NBE-OH (equiv)	Catalyst ^a	T _m (°C)
1	1	0.5	GI	71
2	1	1	GI	69
3	1	2	GI	85
4	1	5	GI	64
5	1	10	GI	81

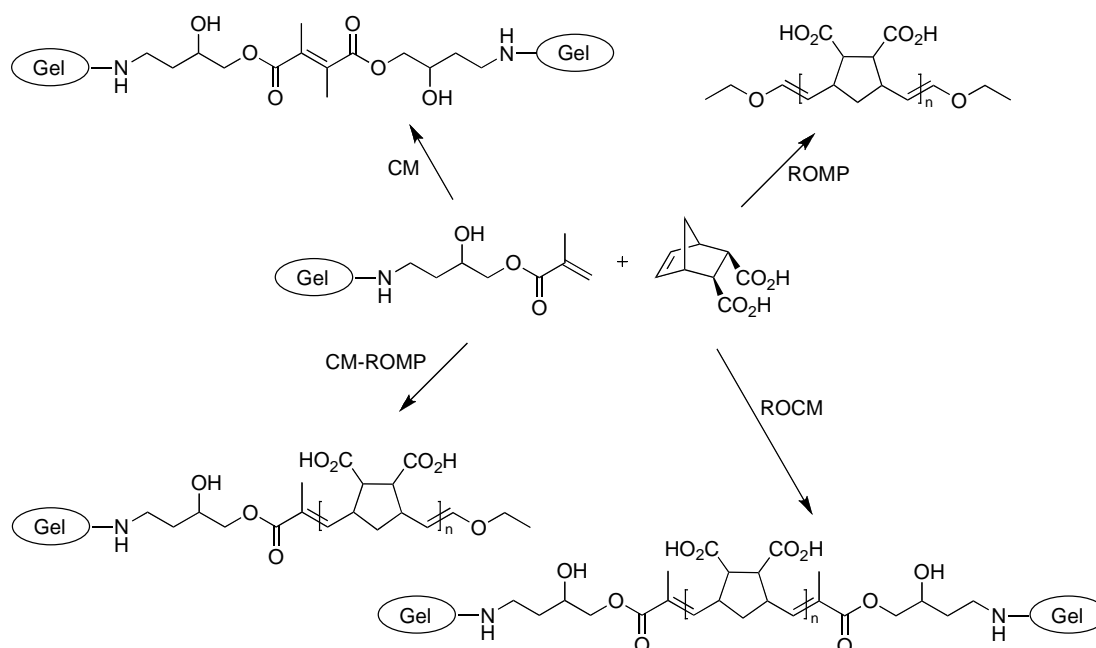
^a GI: Grubbs' 1st generation catalyst.

Figure 4.8 Summary of TMDSC analysis for polymer gels synthesized from various feed ratio of gel-GMA/NBE-OH.

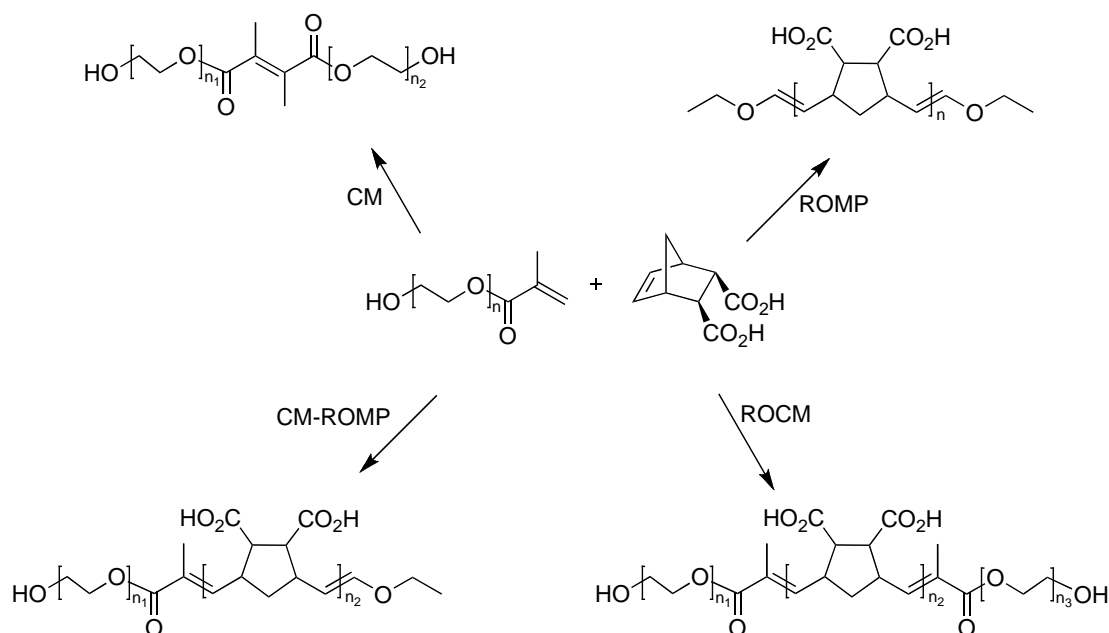
4.2.4 Mechanistic Studies of Aqueous Metathesis Reactions Using PEGMA

The metathesis of gel-GMA and NBE-OH can potentially result in the formation of four different polymers from either; i) cross-metathesis (CM) of gel-GMA, ii) ring-opening metathesis polymerization (ROMP) of NBE-OH, iii) cross metathesis-ring opening metathesis polymerization (CM-ROMP) of gel-GMA/NBE-OH and iv) ring opening cross metathesis (ROCM) of gel-GMA/NBE-OH, as shown in Scheme 4.2. However, cross-metathesis (CM) of gel-GMA and ring-opening metathesis polymerization (ROMP) of NBE-OH can be excluded, as controls reactions performed in the crosslinking validation study showed that these reactions did not occur, section 4.2.2.

In order to gain some insight into the mechanism of gel-GMA/NBE-OH polymer gel formation, a mechanistic study was conducted using a model reaction of NBE-OH and polyethylene glycol methacrylate (PEGMA), as an alternative methacrylate-tethered polymer. PEGMA was chosen for the studies as it exhibits similar physical (water soluble) and chemical (methacrylate group) properties to the original gel-GMA. Furthermore, the chosen PEGMA polymer is of known molecular weight and repeat sequence, allowing for simplistic analysis into the mode of crosslinking, Scheme 4.3.



Scheme 4.2 Possible products from the metathesis reaction of gel-GMA with NBE-OH. CM: cross metathesis; ROMP: ring opening metathesis polymerization; CM-ROMP: cross metathesis-ring opening metathesis polymerization; ROCM: ring opening cross metathesis.



Scheme 4.3 Possible products from the mechanistic studies of PEGMA with NBE-OH. CM: cross metathesis; ROMP: ring opening metathesis polymerization; CM-ROMP: cross metathesis-ring opening metathesis polymerization; ROCM: ring opening cross metathesis.

Metathesis reaction of PEGMA/NBE-OH (1:1) was conducted under the same conditions as per metathesis of gel-GMA/NBE-OH (see Table 4.1, entry 2) by dissolution of both monomers in a phosphate buffer prior to addition of GI catalyst in a toluene/hexadecane emulsion. A change in viscosity was not observed after 1 hr and thus, the solution was lyophilized and analyzed by MALDI. Commercially supplied PEGMA of greater than 8800 g/mol was utilized, where high molecular weight fragments were not observed in the MALDI analysis of the resulting polymer gels. Further investigations¹⁰⁴ confirmed that the supplier had incorrectly supplied a low molecular weight variant of PEGMA and the commercially supplied stock had an average molecular weight of 285 g/mol. As a result, PEGMA was used in 31 fold excess to NBE-OH, however, analysis of the MALDI data would not be affected by the excess PEGMA as this is removed during the extraction procedure and thus, the mechanistic studies would still be valid.

MALDI analysis of the polymer gel formed from PEGMA/NBE-OH confirmed the absence of CM and ROMP products, as evidenced by the lack of peaks due to CM and ROMP (See Table 4.4, CM: $n_1, n_2 = 1, 1 \dots 4, 1$ and ROMP: $n = 1, \dots, 7$). The major product observed was the result of ROCM reaction of PEGMA/NBE-OH, while the minor product was a result of CM-ROMP. Interestingly, there was no evidence of polymerization

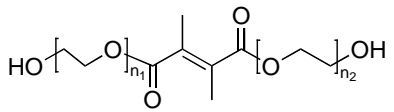
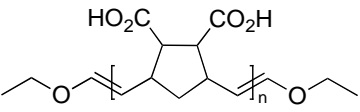
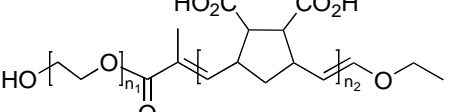
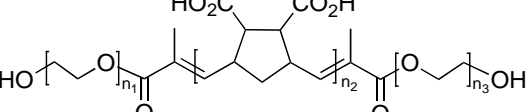
(grafting) of NBE-OH during CM-ROMP or ROCM reactions (See Table 4.4; CM-ROMP, $n_1, n_2 = 1, 2$; 2, 2; 3, 2 and ROCM $n_1, n_2, n_3 = 1, 2, 1$). However, the possibility of NBE-OH polymerization (grafting) after initial cross metathesis during CM-ROMP or ROCM reactions cannot be fully eliminated due to the 31-fold excess of PEGMA reagent with respect to NBE-OH. This preliminary insight into the mechanism suggests that the polymer gel formed from gel-GMA/NBE-OH is possibly a result of ROCM reaction between the two monomers. However, further mechanistic studies involving increasing amounts of NBE-OH with respect to PEGMA need be investigated in order to justify the differing textural properties of the polymer gels obtained with differing ratios of gel-GMA/NBE-OH, section 4.2.3.

4.2.5 Attempted Polymer Gel Film Formation.

With successful synthesis of polymer gels containing gel-GMA and NBE-OH, film formation was attempted in order to produce a uniform material for mechanical testing. Film formation of the polymer gels was performed as described in section 4.2.1. However, upon addition of catalyst (GI or HG2-S), the solution was quickly transferred between two tightly sealed glass plates, separated by a 1 mm Teflon spacer using a syringe, and the reaction was allowed to complete in a 50 °C oven. The remaining solution was transferred to a petri dish and the reaction was also allowed to complete in a 50 °C oven.

The resulting polymer gel films were dried and subjected to crosslinking validation as described in section 4.2.1. Treatment of gel-GMA/NBE-OH with HGS-2 resulted in formation of gel films that dissolved in water, indicating a lack of crosslinking. This is most likely due to exposure of the catalyst to air, in addition to the slow reactivity of HG2-S in comparison to GI or GII for polymer gel formation. Treatment of gel-GMA/NBE-OH with GI in the petri dish resulted in a gel that dissolved in water. Polymer gel crosslinking does not proceed using the petri dish formulation method as the catalyst is exposed to air, rendering the catalyst inactive over time. In contrast, polymer gel films formed between the tightly sealed glass plates were found not to dissolve in water when subjected to crosslinking analysis. This indicated successful crosslinking of gel-GMA and NBE-OH between tightly sealed glass plates due to the exclusion of air. However, the resulting material were not of uniform thickness and therefore, mechanical testing was not possible.

Table 4.4 Expected and found m/z for $M + Na^+$ specimens in the MALDI MS analysis of the reaction of PEGMA with NBE-OH. n.o.: not observed.

 Cross Metathesis			 Ring Opening Metathesis Polymerisation			 Cross Metathesis – Ring Opening Metathesis Polymerization ^a			 Ring Opening Cross Metathesis ^b		
n_1, n_2	$M_w/g \text{ mol}^{-1}$	Rel. mol %	n	$M_w/g \text{ mol}^{-1}$	Rel. mol %	n_1, n_2	$M_w/g \text{ mol}^{-1}$	Rel. mol %	n_1, n_2, n_3	$M_w/g \text{ mol}^{-1}$	Rel. mol %
1,1	255	n.o.	1	321	n.o.	1,1	379	7	1,1,1	437	9
1,2	299	n.o.	2	503	n.o.	2,1	423	3	2,1,1	481	10
2,1			3	685	n.o.	3,1	467	n.o.	1,1,2		
2,2	343	n.o.	4	867	n.o.	4,1	511	n.o.	3,1,1	525	9
1,3			5	1049	n.o.	1,2	561	n.o.	3,1,2	569	8
3,1			6	1231	n.o.	2,2	605	n.o.	3,1,3	613	8
4,1	387	n.o.	7	1413	n.o.	3,2	649	n.o.	1,2,1	619	n.o.

^a $M + H^+$ specimens were also observed for $n_1, n_2 = 2,1$ and $n_1, n_2 = 3,1$. ^b $M + Na^+$ specimens were observed up to $n_1, n_2, n_3 = 9,1,9$.

4.3 Conclusion and Future Directions.

In conclusion, polymer gels were successfully obtained from aqueous metathesis of GMA-functionalized gelatin (gel-GMA) with NBE-OH using either Grubbs' 1st generation catalyst (GI), Grubbs' 2nd generation catalyst (GII) or a new water-soluble derivative of Hoveyda-Grubbs' 2nd generation catalyst (HG2-S). All dried polymer gel samples were found to be thermally stable up to 300 °C. Polymer gels derived from GI and GII catalyst were found to have a lower T_m than that of the polymer gel derived from HG2-S, possibly due to differing extents of crosslinking. Upon successful generation of polymer gels, a series of control experiments were conducted to confirm that polymer gel formation was the result of crosslinking between gel-GMA and NBE-OH and that, in the absence of either monomer and/or catalyst, polymer gel formation does not proceed. This suggests that the formation of gel-GMA/NBE-OH polymer gel was a result of a catalytic metathesis reaction between gel-GMA and NBE-OH.

Attention was then directed to the synthesis of novel polymer gels with differing mechanical properties that could potentially be tailored for use in regenerative medicine. This was achieved by varying the concentration of NBE-OH with respect to gel-GMA, resulting in polymer gels with differing textures prior to drying. All dried polymer gels were found to be thermally stable up to 300 °C and had a T_m range of 65-85 °C.

Mechanistic studies were conducted between PEGMA and NBE-OH as a simple model as there were difficulties in characterizing the polymer gels formed between gel-GMA/NBE-OH. MALDI analysis of the model reaction between PEGMA and NBE-OH gave preliminary insights into the gel-GMA/NBE-OH polymer gel formation. The MALDI analysis suggests that formation of polymer gels between PEGMA and NBE-OH is possibly a result of ring opening cross metathesis (ROCM) reaction between the two monomers as shown in Scheme 4.3. However, due to the excess of PEGMA reagent used in this mechanistic study, the possibility of NBE-OH grafting could not be eliminated and hence, these studies are being repeated and extended in collaboration with Dr. Benjamin Pierce at Helmholtz-Zentrum Geesthacht, Centre for Materials and Coastal Research. Additionally, a similar mechanistic study should be performed with PEGMA and various

ratios of NBE-OH in order to justify the difference in texture of the polymer gels obtained when varying the ratio of NBE-OH to gel-GMA.

Uniform materials of polymer gel of gel-GMA/NBE-OH were successfully accomplished using GI catalyst, in between glass plates to give thin polymer films. Attempts at film formation in petri dishes and using HG2-S were unsuccessful due to the instability of the catalysts to air. Future film formation should be performed in a glove box in order to minimize air exposure. Upon synthesizing these films, mechanical properties of the film can then be investigated.

These studies have provided the first insight into the use of aqueous metathesis for the controlled organization of the tertiary structure of naturally occurring peptides. Novel gelatin-gels were obtained by reacting methacrylate-functionalized gelatin (gel-GMA, **4.13**) and norbornene dicarboxylic acid (NBE-OH, **4.14**) (Scheme 4.1) in the presence of multiple catalysts in aqueous media. Furthermore, these polymer gels exhibit physical and chemical properties that could potentially be utilized in regenerative medicine. However, further investigations are needed to determine the physical and mechanical properties of these gels and to evaluate their biocompatibility as medicinal tools.

4.4 References for Chapter Four

- [1] Chauvin, Y. *Adv. Synth. Catal.* **2007**, *349*, 27–33.
- [2] Grubbs, R. H. *Adv. Synth. Catal.* **2007**, *349*, 34–40.
- [3] Schrock, R. R. *Adv. Synth. Catal.* **2007**, *349*, 41–53.
- [4] Nguyen, S. T.; Johnson, L. K.; Grubbs, R. H.; Ziller, J. W. *J. Am. Chem. Soc.* **1992**, *114*, 3974–3975.
- [5] Schrock, R. R.; Murdzek, J. S.; Bazan, G. C.; Robbins, J.; DiMare, M.; O'Regan, M. *J. Am. Chem. Soc.* **1990**, *112*, 3875–3886.
- [6] Leitgeb, A.; Wappel, J.; Slugovc, C. *Polymer* **2010**, *51*, 2927–2946.
- [7] Hamilton, J. G.; Law, E. E.; Rooney, J. J. *J. Mol. Catal. A: Chem.* **1997**, *115*, 1–9.
- [8] Lipshutz, B. H.; Ghorai, S.; Aguinaldo, G. T. *Adv. Synth. Catal.* **2008**, *350*, 953–956.
- [9] Binder, J. B.; Blank, J. J.; Raines, R. T. *Org. Lett.* **2007**, *9*, 4885–4888.
- [10] Davis, K. J.; Sinou, D. *J. Mol. Catal. A: Chem.* **2002**, *177*, 173–178.
- [11] Zaman, S.; Curnow, O. J.; Abell, A. D. *Aust. J. Chem.* **2009**, *62*, 91–100.
- [12] Kemp, P. *Regen. Med.* **2006**, *1*, 653–669.
- [13] Mason, C.; Dunnill, P. *Regen. Med.* **2008**, *3*, 1–5.
- [14] Ratner, B. D.; Bryant, S. J. *Annu. Rev. Biomed. Eng.* **2004**, *6*, 41–75.
- [15] Shastri, V. P.; Lendlein, A. *MRS bulletin* **2010**, *35*, 571–575.
- [16] Shastri, V. P.; Lendlein, A. *Adv. Mater.* **2009**, *21*, 3231–3234.
- [17] Langer, R. *Acc. Chem. Res.* **2000**, *33*, 94–101.
- [18] Jagur-Grodzinski, J. *Polym. Adv. Technol.* **2006**, *17*, 395–418.
- [19] Gillette, B. M.; Jensen, J. A.; Wang, M.; Tchao, J.; Sia, S. K. *Adv. Mater.* **2010**, *22*, 686–691.
- [20] Slaughter, B. V.; Khurshid, S. S.; Fisher, O. Z.; Khademhosseini, A.; Peppas, N. A. *Adv. Mater.* **2009**, *21*, 3307–3329.
- [21] Martens, P.; Anseth, K. S. *Polymer* **2000**, *41*, 7715–7722.
- [22] Metters, A. T.; Anseth, K. S.; Bowman, C. N. *Polymer* **2000**, *41*, 3993–4004.
- [23] Bryant, S. J.; Davis-Arehart, K. A.; Luo, N.; Shoemaker, R. K.; Arthur, J. A.; Anseth, K. S. *Macromolecules* **2004**, *37*, 6726–6733.
- [24] Aamer, K. A.; Sardinha, H.; Bhatia, S. R.; Tew, G. N. *Biomaterials* **2004**, *25*, 1087–1093.

- [25] Martens, P. J.; Bryant, S. J.; Anseth, K. S. *Biomacromolecules* **2003**, *4*, 283–292.
- [26] Elisseeff, J.; McIntosh, W.; Anseth, K.; Riley, S.; Ragan, P.; Langer, R. *J. Biomed. Mater. Res.* **2000**, *51*, 164–171.
- [27] Lee, J. H.; Lee, H. B.; Andrade, J. D. *Prog. Polym. Sci.* **1995**, *20*, 1043–1079.
- [28] Pan, Y.-S.; Xiong, D.-S.; Ma, R.-Y. *Wear* **2007**, *262*, 1021–1025.
- [29] Noguchi, T.; Yamamuro, T.; Oka, M.; Kumar, P.; Kotoura, Y.; Hyon, S.; Ikada, Y. *J. Appl. Biomater.* **1991**, *2*, 101–107.
- [30] Wichterle, O.; Lim, D. *Nature* **1960**, *185*, 117–118.
- [31] Rickert, D.; Lendlein, A.; Peters, I.; Moses, M. A.; Franke, R.-P. *Eur. Arch. Otorhinolaryngol.* **2006**, *263*, 215–222.
- [32] Augst, A. D.; Kong, H.-J.; Mooney, D. J. *Macromol. Biosci.* **2006**, *6*, 623–633.
- [33] Kong, H.-J.; Lee, K. Y.; Mooney, D. J. *Polymer* **2002**, *43*, 6239–6246.
- [34] Darr, A.; Calabro, A. *J. Mater. Sci. Mater. Med.* **2009**, *20*, 33–44.
- [35] Yeh, J.; Ling, Y.; Karp, J. M.; Gantz, J.; Chandawarkar, A.; Eng, G.; Blumling, J.; Langer, R.; Khademhosseini, A. *Biomaterials* **2006**, *27*, 5391–5398.
- [36] Zhao, H.; Ma, L.; Zhou, J.; Mao, Z.; Gao, C.; Shen, J. *Biomed. Mater.* **2008**, *3*, 015001.
- [37] Ryu, J. H.; Kim, I.-K.; Cho, S.-W.; Cho, M.-C.; Hwang, K.-K.; Piao, H.; Piao, S.; Lim, S. H.; Hong, Y. S.; Choi, C. Y.; Yoo, K. J.; Kim, B.-S. *Biomaterials* **2005**, *26*, 319–326.
- [38] Hahn, M. S.; Teply, B. A.; Stevens, M. M.; Zeitels, S. M.; Langer, R. *Biomaterials* **2006**, *27*, 1104–1109.
- [39] Liao, E.; Yaszemski, M.; Krebsbach, P.; Hollister, S. *Tissue Eng.* **2007**, *13*, 537–550.
- [40] Willers, C.; Chen, J.; Wood, D.; Xu, J.; Zheng, M. H. *Tissue Eng.* **2005**, *11*, 1065–1076.
- [41] Perrimon, N.; Bernfield, M. *Semin. Cell Dev. Biol.* **2001**, *12*, 65–67.
- [42] Temenoff, J. S.; Mikos, A. G. *Biomaterials* **2000**, *21*, 431–440.
- [43] Heinegård, D.; Sommarin, Y. *Methods in Enzymology* **1987**, *144*, 305–319.
- [44] Mark, von der, K.; Park, J.; Bauer, S.; Schmuki, P. *Cell Tissue Res.* **2010**, *339*, 131–153.
- [45] Shoulders, M. D.; Raines, R. T. *Annu. Rev. Biochem.* **2009**, *78*, 929–958.
- [46] Kadler, K. E.; Holmes, D. F.; Trotter, J. A.; Chapman, J. A. *Biochem. J.* **1996**, *316*, 1–11.

- [47] Prockop, D. J.; Kivirikko, K. I. *Annu. Rev. Biochem.* **1995**, *64*, 403–434.
- [48] Raman, S. S.; Vijayaraj, R.; Parthasarathi, R.; Subramanian, V.; Ramasami, T. *J. Mol. Struct. (Theochem)* **2008**, *851*, 299–312.
- [49] Persikov, A. V.; Ramshaw, J. A. M.; Kirkpatrick, A.; Brodsky, B. *Biochemistry* **2005**, *44*, 1414–1422.
- [50] Brodsky, B.; Baum, J. *Nature* **2008**, *453*, 998–999.
- [51] Kuivaniemi, H.; Tromp, G.; Prockop, D. J. *FASEB J.* **1991**, *5*, 2052–2060.
- [52] Wu, J. J.; Woods, P. E.; Eyre, D. R. *J. Biol. Chem.* **1992**, *267*, 23007–23014.
- [53] Müller-Glauser, W.; Humbel, B.; Glatt, M.; Sträuli, P.; Winterhalter, K. H.; Bruckner, P. *J. Cell Biol.* **1986**, *102*, 1931–1939.
- [54] Joosten, E. A. J.; Veldhuis, W. B.; Hamers, F. P. T. *J. Neurosci. Res.* **2004**, *77*, 127–142.
- [55] Riesle, J.; Hollander, A. P.; Langer, R.; Freed, L. E.; Vunjak-Novakovic, G. *J. Cell. Biochem.* **1998**, *71*, 313–327.
- [56] Zioupos, P.; Currey, J. D.; Hamer, A. J. *J. Biomed. Mater. Res.* **1999**, *45*, 108–116.
- [57] Chvapil, M.; Holusa, R. *J. Biomed. Mater. Res.* **1968**, *2*, 245–264.
- [58] Lennox, F. G. *Biochim. Biophys. Acta* **1949**, *3*, 170–187.
- [59] Lynn, A. K.; Yannas, I. V.; Bonfield, W. *J. Biomed. Mater. Res. Part B Appl. Biomater.* **2004**, *71*, 343–354.
- [60] Jayakrishnan, A.; Jameela, S. R. *Biomaterials* **1996**, *17*, 471–484.
- [61] Olde Damink, L. H. H.; Dijkstra, P. J.; van Luyn, M. J.; van Wachem, P. B.; Nieuwenhuis, P.; Feijen, J. *Biomaterials* **1996**, *17*, 765–773.
- [62] Hey, K. B.; Lachs, C. M.; Raxworthy, M. J.; Wood, E. J. *Biotechnol. Appl. Biochem.* **1990**, *12*, 85–93.
- [63] Kato, Y. P.; Silver, F. H. *Biomaterials* **1990**, *11*, 169–175.
- [64] Petite, H.; Rault, I.; Huc, A.; Menasche, P.; Herbage, D. *J. Biomed. Mater. Res.* **1990**, *24*, 179–187.
- [65] Yannas, I. V.; Tobolsky, A. V. *Nature* **1967**, *215*, 509–510.
- [66] Djagny, V. B.; Wang, Z.; Xu, S. *Crit. Rev. Food. Sci. Nutr.* **2001**, *41*, 481–492.
- [67] Benguigui, L.; Busnel, J.-P.; Durand, D. *Polymer* **1991**, *32*, 2680–2685.
- [68] Gornall, J. L.; Terentjev, E. M. *Soft Matter* **2008**, *4*, 544.
- [69] Guo, L.; Colby, R. H.; Lusignan, C. P.; Howe, A. M. *Macromolecules* **2003**, *36*, 10009–10020.

- [70] Normand, V.; Muller, S.; Ravey, J. C.; Parker, A. *Macromolecules* **2000**, *33*, 1063–1071.
- [71] Choy, Y. B.; Cheng, F.; Choi, H.; Kim, K. K. *Macromol. Biosci.* **2008**, *8*, 758–765.
- [72] Yakimets, I.; Paes, S. S.; Wellner, N.; Smith, A. C.; Wilson, R. H.; Mitchell, J. R. *Biomacromolecules* **2007**, *8*, 1710–1722.
- [73] Yakimets, I.; Wellner, N.; Smith, A. C.; Wilson, R. H.; Farhat, I.; Mitchell, J. *Polymer* **2005**, *46*, 12577–12585.
- [74] Digenis, G. A.; Gold, T. B.; Shah, V. P. *J. Pharm. Sci.* **1994**, *83*, 915–921.
- [75] Zohuriaan-Mehr, M. J.; Pourjavadi, A.; Salimi, H.; Kurdtabar, M. *Polym. Adv. Technol.* **2009**, *20*, 655–671.
- [76] Liu, X.; Smith, L. A.; Hu, J.; Ma, P. X. *Biomaterials* **2009**, *30*, 2252–2258.
- [77] Draye, J. P.; Delaey, B.; Van de Voorde, A.; Van Den Bulcke, A.; De Reu, B.; Schacht, E. *Biomaterials* **1998**, *19*, 1677–1687.
- [78] Chiou, B.-S.; Avena-Bustillos, R. J.; Bechtel, P. J.; Jafri, H.; Narayan, R.; Imam, S. H.; Glenn, G. M.; Orts, W. J. *Eur. Polym. J.* **2008**, *44*, 3748–3753.
- [79] Gattás-Asfura, K. M.; Weisman, E.; Andreopoulos, F. M.; Micic, M.; Muller, B.; Sirpal, S.; Pham, S. M.; Leblanc, R. M. *Biomacromolecules* **2005**, *6*, 1503–1509.
- [80] Bigi, A.; Cojazzi, G.; Panzavolta, S.; Rubini, K.; Roveri, N. *Biomaterials* **2001**, *22*, 763–768.
- [81] Bigi, A.; Bracci, B.; Cojazzi, G.; Panzavolta, S.; Roveri, N. *Biomaterials* **1998**, *19*, 2335–2340.
- [82] Fu, Y.; Xu, K.; Zheng, X.; Giacomini, A. J.; Mix, A. W.; Kao, W. J. *Biomaterials* **2012**, *33*, 48–58.
- [83] Tonda-Turo, C.; Gentile, P.; Saracino, S.; Chiono, V.; Nandagiri, V. K.; Muzio, G.; Canuto, R. A.; Ciardelli, G. *Int. J. Biol. Macromol.* **2011**, *49*, 700–706.
- [84] Thakur, G.; Mitra, A.; Rousseau, D.; Basak, A.; Sarkar, S.; Pal, K. *J. Mater. Sci. Mater. Med.* **2011**, *22*, 115–123.
- [85] Bigi, A.; Cojazzi, G.; Panzavolta, S.; Roveri, N.; Rubini, K. *Biomaterials* **2002**, *23*, 4827–4832.
- [86] Zhang, F.; He, C.; Cao, L.; Feng, W.; Wang, H.; Mo, X.; Wang, J. *Int. J. Biol. Macromol.* **2011**, *48*, 474–481.
- [87] Kuijpers, A. J.; Engbers, G. H. M.; Feijen, J.; De Smedt, S. C.; Meyvis, T. K. L.; Demeester, J.; Krijgsveld, J.; Zaat, S. A. J.; Dankert, J. *Macromolecules* **1999**, *32*, 3325–3333.

- [88] Marois, Y.; Chakfé, N.; Deng, X.; Marois, M.; How, T.; King, M. W.; Guidoin, R. *Biomaterials* **1995**, *16*, 1131–1139.
- [89] Tronci, G.; Neffe, A. T.; Pierce, B. F.; Lendlein, A. *J. Mater. Chem.* **2010**, *20*, 8875–8884.
- [90] Bertoldo, M.; Bronco, S.; Gragnoli, T.; Ciardelli, F. *Macromol. Biosci.* **2007**, *7*, 328–338.
- [91] Hennink, W. E.; van Nostrum, C. F. *Adv. Drug Deliv. Rev.* **2002**, *54*, 13–36.
- [92] Crescenzi, V.; Francescangeli, A.; Taglienti, A. *Biomacromolecules* **2002**, *3*, 1384–1391.
- [93] Fuchsbaauer, H.-L.; Gerber, U.; Engelmann, J.; Seeger, T.; Sinks, C.; Hecht, T. *Biomaterials* **1996**, *17*, 1481–1488.
- [94] Claverie, J. P.; Viala, S.; Maurel, V.; Novat, C. *Macromolecules* **2001**, *34*, 382–388.
- [95] Lynn, D. M.; Kanaoka, S.; Grubbs, R. H. *J. Am. Chem. Soc.* **1996**, *118*, 784–790.
- [96] Zaman, S.; Chen, H.; Abell, A. D. *Tetrahedron Lett.* **2011**, *52*, 878–880.
- [97] Zaman, S.; Abell, A. D. *Tetrahedron Lett.* **2009**, *50*, 5340–5343.
- [98] Neffe, A. T.; Zuppa, A.; Pierce, B. F.; Hofmann, D.; Lendlein, A. *Macromol. Rapid Commun.* **2010**, *31*, 1534–1539.
- [99] Zaupa, A.; Neffe, A. T.; Pierce, B. F.; Nöchel, U.; Lendlein, A. *Biomacromolecules* **2011**, *12*, 75–81.
- [100] Neffe, A. T.; Loebus, A.; Zaupa, A.; Stoetzel, C.; Müller, F. A.; Lendlein, A. *Acta Biomater.* **2011**, *7*, 1693–1701.
- [101] Rohanizadeh, R.; Swain, M. V.; Mason, R. S. *J. Mater. Sci. : Mater. Med.* **2008**, *19*, 1173–1182.
- [102] Bubnis, W. A.; Ofner, C. M. *Anal. Biochem.* **1992**, *207*, 129–133.
- [103] MSDS of Hexadecane, by Sigma-Aldrich
- [104] Personal communication with Polysciences Inc. (Germany)

CHAPTER FIVE:
Experimental Procedures

5.1 General Methods and Procedures

5.1.1 General Practice

Molecular Modelling

Molecular modelling experiments in chapter 2, section 2.3.1 were conducted by Dr. Steven McNabb with the Schrödinger suite 2005. Conformational searches with MacroModel 9.1, generated an ensemble of low energy conformers for docking. The searches were conducted with the MCMM method using a GB/SA water model and the OPLS2001 force field. The minimisation was stopped with the default gradient convergence threshold of $\delta = 0.05 \text{ kJ}/(\text{mol} \cdot \text{\AA})$. The default Polak-Ribiere Conjugate Gradient method was used for all minimisations. The crystal structure of human mini calpain 1 (PDB code 1ZCM) was prepared using the protein preparation facility in GLIDE 4.0. The *in silico* ovine homology models were created by the virtual mutation of the appropriate residues (Ser₁₁₅ → Cys₁₁₅) around the active site cleft, followed by deprotonation of Cys₁₁₅, and protonation of His₂₇₂. These structures were minimised using the OPLS2005 force field with a GB/SA water model over 500 iterations. All residues within a 5 Å distance of the calcium ions, the calcium ions and the key residues Cys₁₁₅, Gly₂₀₈ and Gly₂₇₁ (o-CAPN1) or Cys₁₀₅, Gly₁₉₈ and Gly₂₆₁ (o-CAPN2) of the structures were kept frozen during this minimisation. The centre of the docking grid was defined as the centroid of the residues Cys₁₁₅, Gly₂₀₈ and Gly₂₇₁ (o-CAPN1) or Cys₁₀₅, Gly₁₉₈ and Gly₂₆₁ (o-CAPN2) and was generated using default settings. The centre of the docked ligands was defined within a 12 Å box. Docking of flexible ligands to the rigid calpain model was performed with the following parameters: OPLS2001 force field, extra precision mode, 90000 poses per ligand for the initial docking, and the best 1000 poses per ligand were kept for energy minimisation with a distance dielectric constant of 2 and a maximum of 5000 conjugate gradient steps. A representative conformer from the different clusters was used as a starting conformer in the docking studies. From each study, up to ten poses, as defined by the program default, were collected. Representative poses from these were chosen such that: i) the distance between the carbonyl carbon of the aldehyde group and the active site cysteine sulfur is less than 2.5 Å; ii) appropriate hydrogen bonds in the active site are present; and iii) the pose has a low energy GLIDE *E_{model}* score. Associated parameters of the representative poses of

compounds **2.5**, **2.7**, **2.9**, **2.11**, **2.14** and **2.15** docked with the o-CAPN1 and o-CAPN2 homology models are shown in Appendix A1.

Molecular modelling experiments in chapter 2, section 2.3.1 were conducted by Steven Ngugen and Dr. Matt Sykes with the OpenEye Scientific Software, 2010.¹ Conformational searches were carried out with OMEGA (version 2.4.3) to generate an ensemble of low energy conformers for the compounds. The searches were conducted with the default settings, and increasing the maximum conformers to 10000 to ensure all possible conformers for each compounds were generated. The crystal structure of rat mini calpain 1 (PDB code 2G8E)² was prepared using FRED Receptor (version 2.2.5), by removal of calcium ions and water molecules. The centre of the docking grid was defined as the centroid of the residues Cys₁₁₅, Gly₂₀₈ and Gly₂₇₁ (r-CAPN1), with an inner contour of 101 Å and an outer contour of 1706 Å. Custom constraints were placed to ensure that the compounds dock in the expected orientation, by increasing the docking sphere to completely encompass the carbon where the covalent bond between the thiol and co-crystallised ligand occurs (see Figure 5.1); and an additional SMARTS constraint to ensure that the aldehyde group is present within the docking sphere for successful docking of the compounds. A docking grid was generated, and inhibitors were docked to the calpain model using FRED (version 2.2.5) using the default scoring function (chemgauss3) to establish the docking of the compounds. Representative poses from these were chosen such that: i) the distance between the carbonyl carbon of the aldehyde group and the active site cysteine sulfur is less than 4.5 Å; and ii) appropriate hydrogen bonds in the active site are present.

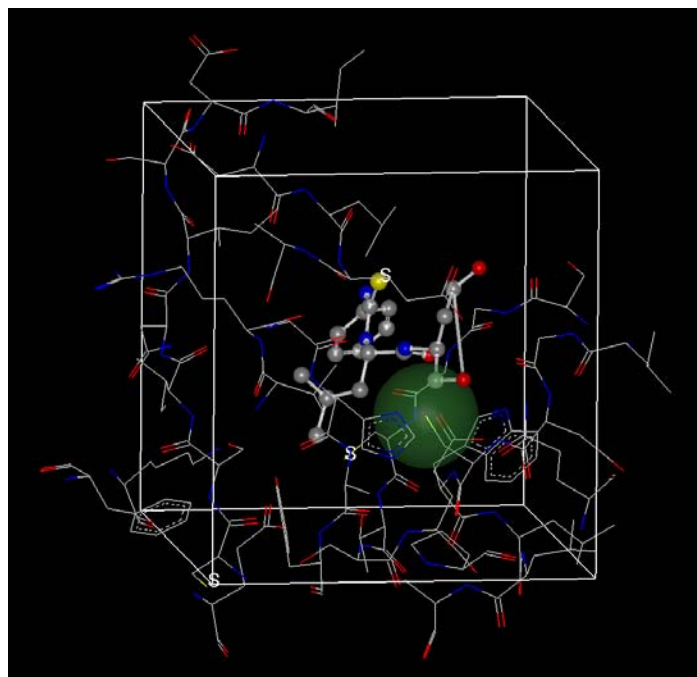


Figure 5.1 The docking sphere (in green), generated in FRED Receptor, encompassing the carbon where the covalent bond between the enzyme thiol (stick representation) and co-crystallised ligand (stick and ball representation) occurs.

NMR Spectroscopy

NMR spectra of all compounds in chapter 2 were obtained as described below.

Proton spectra were obtained on a Bruker ACP-30V spectrometer operating at 300 MHz or a Varian Inova spectrometer operating at 600 MHz. Carbon spectra were obtained on a Bruker ACP-30V 300 spectrometer operating at 75 MHz or a Varian Inova 600 spectrometer operating at 150 MHz. Two-dimensional correlation experiments (COSY, ROESY, HSQC, HMBC) were performed on a Varian Inova spectrometer operating at 600 MHz. Unless otherwise stated, all spectra were obtained at 23 °C. Chemical shifts are reported in parts per million (ppm) on a δ scale (in which trimethylsilane (TMS) is referenced to 0.00 ppm). Solvents used in NMR analysis (reference peak listed) included CDCl_3 (CHCl_3 at δ_{H} 7.26 ppm, CDCl_3 at δ_{C} 77.00 ppm); CD_3OD (CHD_2OD at δ_{H} 3.31 ppm, CD_3OD at δ_{C} 49.05 ppm); $(\text{CD}_3)_2\text{SO}$ ($(\text{CHD}_2)_2\text{SO}$ at δ_{H} 2.50 ppm, $(\text{CD}_3)_2\text{SO}$ at δ_{C} 39.70 ppm). All resonances are given in parts per million (ppm). Spin multiplicities are indicated by the following symbols: singlet (s), broad singlet (br s), doublet (d), doublet of doublet (dd), triplet (t), doublet of triplet (dt), quartet (q), quintet (quin) and multiplet (m). All coupling constants are reported in hertz (Hz).

NMR spectra for compound **4.13** and gelatin in chapter 4 were obtained on a Bruker Advance spectrometer (Karlsruhe, Germany) at 500 MHz in D₂O at Helmholtz-Zentrum, Centre for Materials and Coastal Research, Germany.

Mass Spectrometry

Electrospray ionisation (ESI) mass spectra (MS) were obtained on a Finnigan LCQ Ion Trap mass spectrometer, conditions were as follows: needle potential, 4500 V; tube lens, 60 V; heated capillary, 200 °C, 30 V; sheath gas flow, 30 psi. Electrospray ionisation (ESI) high resolution mass spectra (HRMS) were recorded on a Bruker microTOF-Q II spectrometer using a capillary voltage of 2500V, a source temperature of 200 °C and an acquisition rate of 0.5 Hz.

Melting Points

Melting points were determined on a *Reichert* ThermoVar Kofler apparatus, and are uncorrected. Melting points are not reported for oils or glassy solids.

Infrared Spectrometry

Infrared spectra were recorded on an ATI Mattson Genesis Series FTIR spectrophotometer as either nujol mulls or neat as denoted.

X-Ray Crystallography

X-Ray crystallography was performed by Daouda Traore at Monash University at the Australian Synchrotron. The data was collected on the MX2 beamline ($\lambda = 0.774917\text{\AA}$) at 100 K using Blu-Ice software. Cell refinement and data reduction were undertaken with *XDS*. The structure was solved by direct methods using *SHELXS97*, and refined by full-matrix least squares calculations on F^2 using *SHELXL97*.

Optical Rotation

Optical rotation measurements were performed on an ATAGO AP-100 polarimeter with 9.99 mm path length. Measurements were taken at 23 °C in DMSO at $\lambda = 589$ nm. $[\alpha]_D$ values are given in units of °.mL/g.dm and the sample concentration given in units of 10 mg/mL. Optical rotation measurements were not performed for diastereomeric mixtures.

Glassware

Oven-dried glassware was used in all reactions performed under an inert atmosphere (nitrogen or argon).

Reagents and Solvents

All starting materials and reagents were obtained commercially and used without further purification unless stated otherwise. Dichloromethane was dried over 4 Å molecular sieves. Anhydrous *N,N*-dimethylformamide was purchased from Sigma-Aldrich (St. Louis, MO, USA). Methanol was dried by heating to reflux with magnesium/iodine and distillation over 3 Å molecular sieves. Anhydrous tetrahydrofuran was obtained by fresh distillation from sodium/benzophenone under a nitrogen atmosphere.

Thin-layer Chromatography

Thin-layer chromatography was carried out on Merck aluminium sheets with silica gel 60 F₂₅₄. Traces were visualised using short wave UV light on Vilber Lourmat VL-6C (6W – 254 nm tube) or a suitable dip, including vanillin (general) and basic potassium permanganate (general).

Flash Chromatography

Flash column chromatography was performed using Merck or Scharlau silica gel 60, 230-400 mesh, under a positive pressure of nitrogen. The eluting solvents petroleum ether 50/70*, ethyl acetate, dichloromethane and methanol was used as received.

High Pressure Liquid Chromatography (HPLC)

Purification by reversed phased HPLC (rp-HPLC) was done using a Discovery BIOwide Pore C5, 250 x 20 mm², 5 µm column, monitored at 220 nm, 254 nm and 280 nm, using solvent A = 0.1% TFA in H₂O and solvent B = 0.08% TFA in acetonitrile; and a gradient of 20% B to 80% B over 20 min, with a flow rate of 4.0 mL/min.

Removal of volatiles *in vacuo*

Removal of volatiles *in vacuo* refers to the removal of solvents “under reduced pressure” by rotary evaporation (low vacuum pump) followed by application of high

*A mixture of hexanes with a boiling point range between 50 and 70 °C

vacuum (oil pump) for a minimum of thirty minutes. All yields reported are isolated yields determined to be homogenous by NMR spectroscopy.

Cooled Solutions

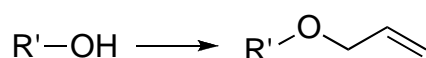
The cooled solutions comprise of the following: 0 °C refers to the reaction taking place in an ice bath; -78 °C using a mixture of CO₂(s) acetone; -18 °C using mixtures of CO₂(s) methanol.

Yields

All yields reported are isolated yields, judged to be homogeneous by TLC and NMR spectroscopy.

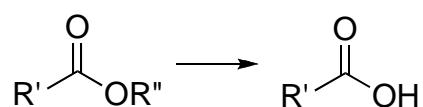
5.1.2 General Procedures

General Procedure A: *O*-Allylation



To a solution of respective alcohol (1.0 equiv) in anhydrous DMF (4.5 mL / 1 g alcohol) was added sequentially K₂CO₃ (2.0 equiv), tetrabutylammonium iodide (0.1 equiv) and allyl bromide (1.2 equiv) and the mixture was stirred at ambient temperature under a nitrogen atmosphere for 18 h. The solution was poured into ice-water and extracted with ethyl acetate (4x). Organic extracts were combined and washed with 1M aqueous HCl (2x), H₂O (2x), brine and dried over Na₂SO₄. Volatiles were removed *in vacuo* to give the desired *O*-allyl derivatives that derivatives were used without further purification.

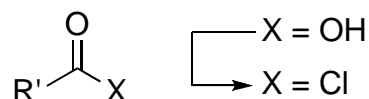
General Procedure B: Ester hydrolysis with LiOH



To a solution of respective ester (1.0 equiv) in 3:1 THF / H₂O (10 mL / 1 g ester) was added lithium hydroxide (5.0 equiv) in one portion and stirred at 40°C for 3.5 h. The

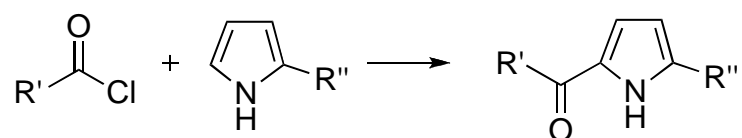
reaction mixture was cooled in an ice bath and acidified to pH 1 with 2M aqueous HCl. The resulting mixture was extracted with ethyl acetate (3x). The combined organic extracts were washed with water (2x) and brine, dried over Na₂SO₄ and volatiles were removed *in vacuo* to yield the desired carboxylic acids.

General Procedure C: Formation of acid chloride

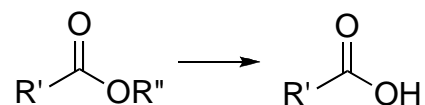


To a solution of respective carboxylic acid (1.0 equiv) in dry dichloromethane (20 mL / 1 g carboxylic acid) at 0 °C, under a nitrogen atmosphere, was added thionyl chloride (6.0 equiv). The solution was stirred for 10 min at 0 °C, heated to 40 °C and stirred for 18 h. Volatiles were removed *in vacuo* to give the desired acid chlorides, which were used without further purification.

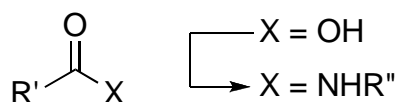
General Procedure D: Friedel-Craft's acylation



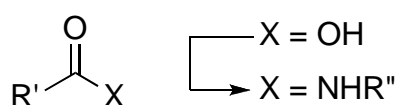
To the respective acid chloride (2.0 equiv) in nitromethane (6 mL / 1 g of acid chloride) was added the respective pyrrole (1.0 equiv) followed by the addition of ytterbium (III) trifluoromethanesulfonate (0.1 equiv). The resulting dark red solution was stirred at ambient temperature for 21 h. The reaction was quenched by addition of sat. NaHCO₃ and extracted with diethyl ether (3x). Organic layers were combined, washed with sat. NaHCO₃, H₂O (2x), brine and dried over MgSO₄. Volatiles were removed *in vacuo* and the resultant crude oil was purified via flash chromatography to give the desired pure pyrroles.

General Procedure E: Ester hydrolysis with KOH

To a solution of respective ester (1.0 equiv) in 1:1 THF / H₂O (20 mL / 1 g ester) was added potassium hydroxide (8.0 equiv) in one portion and stirred at 40-50 °C for 18 h. The reaction mixture was cooled and partitioned between diethyl ether and water. The aqueous layer was collected, cooled in an ice bath and acidified to pH 1 with conc. HCl. The precipitate was collected, washed with water (2x) and dried *in vacuo* to give the desired pure carboxylic acids.

General Procedure F: EDCI Mediated peptide coupling

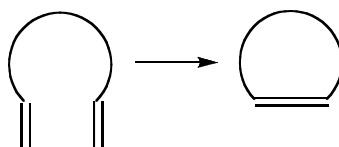
To the respective acid (1.0 equiv) in dry dichloromethane (50 mL / 1 g of carboxylic acid) at ambient temperature, under a nitrogen atmosphere, was added the appropriate amine (1.15 equiv), EDCI (1.4 equiv) and HOBt·H₂O (1.5 equiv) and the solution stirred for 5 min. To the solution was added DIPEA (2.6 equiv) and the solution stirred for 18 h. The solution was partitioned between dichloromethane and 2M aqueous HCl. The organic phase was separated and washed with 2M aqueous HCl (2x), water (2x) and brine; dried over Na₂SO₄ and volatiles removed *in vacuo*. The crude product was purified by flash chromatography to yield the desired pure amides.

General Procedure G: HATU Mediated peptide coupling

To the respective acid (1.0 equiv) in dry dichloromethane (50 mL / 1 g of carboxylic acid) at ambient temperature under a nitrogen atmosphere was added the appropriate amine

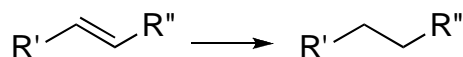
(1.15 equiv), HATU (1.2 equiv) and HOBt·H₂O (1.2 equiv) and the solution stirred for 5 min. To the solution was added DIPEA (2.6 equiv) and the solution stirred for 18 h. The solution was partitioned between dichloromethane and 1M aqueous HCl. The organic phase was separated, washed with sat. NaHCO₃ (2x), water (2x) and brine; dried over Na₂SO₄ and volatiles removed *in vacuo*. The crude product was purified by flash chromatography to yield the desired pure amides.

General Procedure H: Ring-Closing Metathesis

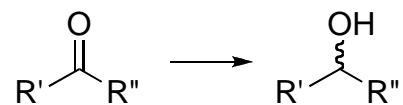


To the respective acyclic diene (1.0 equiv) in anhydrous dichloromethane (2.5 mL / 1 mg of acyclic diene) under a nitrogen atmosphere was added Grubb's 2nd generation catalyst (10 mol %) and the solution was heated to 45 °C for 30 min. An additional portion of Grubb's 2nd generation catalyst (10 mol %) was added and the solution was stirred at 45 °C for 18 h. The reaction was quenched by addition of activated charcoal and stirred for 18 h at ambient temperature. The suspension was filtered through Celite, volatiles removed *in vacuo* and the crude residue was purified by flash chromatography to give the desired *cis* and *trans* macrocycles.

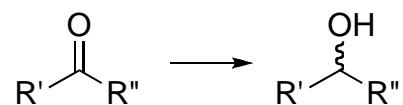
General Procedure I: Hydrogenation of a double bond



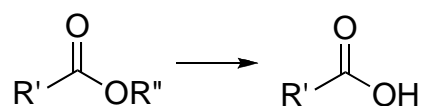
To the respective olefin (1.0 equiv) in ethyl acetate (400 mL / 1 g of olefin) was added 10% Pd/C (2.0 equiv) under a hydrogen atmosphere at ambient temperature and atmospheric pressure for 18 h. The suspension was filtered through Celite, volatiles removed *in vacuo* and the crude residue was purified by flash chromatography to give the desired pure alkanes.

General Procedure J1: Reduction with lithium borohydride

A solution of macrocyclic ester (1.0 equiv) in anhydrous THF (0.3 mL / 1 mg of macrocyclic ester), under a nitrogen atmosphere, was cooled to -78 °C. Lithium borohydride (2M in THF, 2.0 equiv) was added, and the resultant solution was stirred at -78°C for 1h, then warmed to -15 °C and stirred an additional 45 min. Solution was quenched by addition of water and extracted with ethyl acetate (3x). The combined organic extracts were washed with brine, dried over MgSO₄ and volatiles removed *in vacuo*. The crude residue was purified by flash chromatography to give the desired pure alcohols.

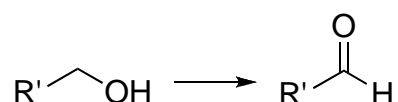
General Procedure J2: Reduction with lithium borohydride

A solution of macrocyclic ester (1.0 equiv) in anhydrous THF (0.1 mL / 1 mg of macrocyclic ester), under a nitrogen atmosphere, was cooled to -78 °C. Lithium borohydride (2M in THF, 2.0 equiv) was added, and the resultant solution was stirred at -78 °C for 1h, then warmed to rt and stirred an additional 18 h. Solution was quenched with addition of water and extracted with ethyl acetate (3x). The combined organic extracts were washed with brine, dried over MgSO₄ and volatiles removed *in vacuo*. The product was either recrystallized to give the desired pure alcohols or used without further purification.

General Procedure K: Ester hydrolysis with NaOH

To a solution of respective ester (1.0 equiv) in 1:1 THF / H₂O (20 mL / 1 g ester) was added 2M aqueous NaOH (8.0 equiv) in one portion and stirred at room temperature for 18 h. THF was removed *in vacuo*. The resulting solution was neutralized with conc. HCl and lyophilized to give the desired carboxylic acids, which was used in the next step without purification.

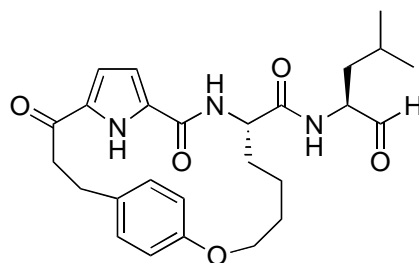
General Procedure L: Dess-Martin Oxidation of alcohols to aldehydes



To a solution of respective amino alcohol (1.0 equiv) in anhydrous dichloromethane (70 mL / 1 g amino alcohol), was added Dess-Martin Periodinane (2.0 equiv) and stirred for 1 h at ambient temperature under a nitrogen atmosphere. The reaction was quenched by addition of sat. NaHCO₃ and Na₂S₂O₅ and stirred at room temperature for 15 min. The reaction mixture was extracted with dichloromethane (2x), dried over Na₂SO₄ and volatiles were removed *in vacuo*. The resultant crude mixture was purified by rp-HPLC to give the desired pure aldehydes.

5.2 Experimental Work Described in Chapter Two

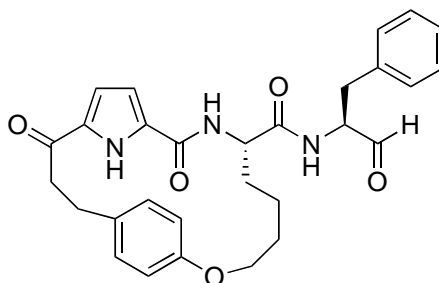
Macrocyclic aldehyde 2.21



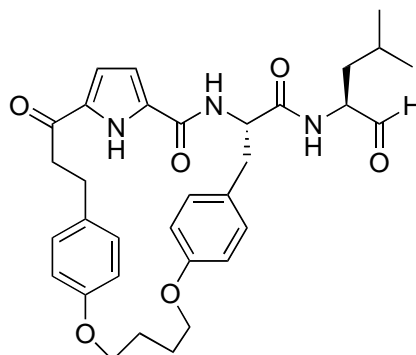
Alcohol **2.85** (15 mg, 0.032 mmol) was oxidized according to general procedure L and the crude product was purified by rp-HPLC to give aldehyde **2.21** as a clear oil (6 mg, 37%). $R_f = 0.45$ (ethyl acetate); $R_t: 9.4$ min; $[\alpha]_D = +1.8$ (c 0.1 in (CH₃)₂SO); ¹H NMR (CDCl₃, 600 MHz) δ 0.96-1.00 (m, 6H, CH₂CH(CH₃)₂), 1.41-1.55 (m, 3H, O(CH₂)₂CH₂CH₂,

$\text{CHHCH}(\text{CH}_3)_2$, 1.69-1.77 (m, 4H, $\text{CHHCH}(\text{CH}_3)_2$, $\text{OCH}_2\text{CH}_2(\text{CH}_2)_2$), 1.77-1.84 (m, 1H, $\text{O}(\text{CH}_2)_3\text{CHH}$), 2.28-2.32 (m, 1H, $\text{O}(\text{CH}_2)_3\text{CHH}$), 2.86-2.95 (m, 3H, ArCHHCH_2), 3.04-3.06 (m, 1H, ArCHHCH_2), 3.90-3.95 (m, 1H, $\text{OCHH}(\text{CH}_2)_3$), 4.02-4.07 (m, 1H, $\text{OCHH}(\text{CH}_2)_3$), 4.59-4.63 (m, 1H, NHCHCHO), 4.65-4.68 (m, 1H, NHCHCO), 6.21 (d, $J = 6.6$ Hz, 1H, NHCHCHO), 6.36-6.37 (m, 1H, pyrrole **H**), 6.41 (br s, 2H, OArH), 6.52 (d, $J = 7.2$ Hz, 1H, NHCHCO), 6.70 (br s, 2H, OArH), 6.71-6.72 (m, 1H, pyrrole **H**), 8.41 (br s, 1H, pyrrole **NH**), 9.60 (s, 1H, **CHO**); ^{13}C NMR (CDCl_3 , 150 MHz) δ 19.4, 21.9, 23.0, 24.9, 27.5, 30.4, 33.8, 37.9, 42.2, 52.5, 57.5, 65.5, 109.6, 115.7, 128.9, 131.6, 135.0, 157.2, 159.2, 171.2, 192.0, 198.6; HRMS (ES) 468.2481 (MH^+); $\text{C}_{26}\text{H}_{34}\text{N}_3\text{O}_5$ requires 468.2493.

Macrocyclic aldehyde **2.22**

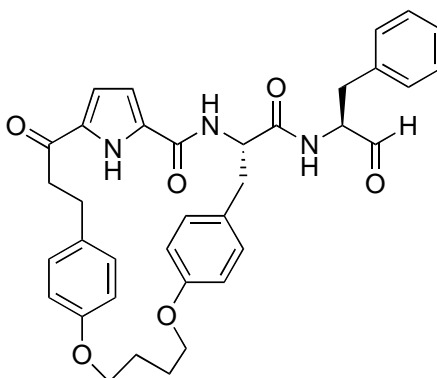


Alcohol **2.86** (26 mg, 0.05 mmol) was oxidized according to general procedure L and the crude product was purified by rp-HPLC to give aldehyde **2.22** as a clear oil (4 mg, 15%). $R_f = 0.42$ (ethyl acetate); R_t : 9.6 min; $[\alpha]_D = +2.0$ (c 0.1 in $(\text{CH}_3)_2\text{SO}$); ^1H NMR (CDCl_3 , 600 MHz) δ 1.39-1.54 (m, 2H, $\text{O}(\text{CH}_2)_2\text{CH}_2\text{CH}_2$), 1.62-1.69 (m, 2H, $\text{OCH}_2\text{CH}_2(\text{CH}_2)_2$), 1.72-1.82 (m, 1H, $\text{O}(\text{CH}_2)_3\text{CHH}$), 2.19-2.23 (m, 1H, $\text{O}(\text{CH}_2)_3\text{CHH}$), 2.85-2.98 (m, 3H, ArCH_2CHH), 3.02-3.07 (m, 1H, ArCH_2CHH), 3.13-3.21 (m, 2H, CHCH_2Ar), 3.89-3.93 (m, 1H, $\text{OCHH}(\text{CH}_2)_3$), 4.00-4.05 (m, 1H, $\text{OCHH}(\text{CH}_2)_3$), 4.61-4.62 (m, 1H, NHCHCO), 4.78 (q, $J = 6.6$ Hz, 1H, NHCHCHO), 6.33-6.35 (m, 1H, pyrrole **H**), 6.42 (br s, 2H, OArH), 6.43 (d, $J = 7.2$ Hz, 1H, NHCHCHO), 6.46 (d, $J = 7.8$ Hz, 1H, NHCHCO), 6.68 (br s, 2H, OArH), 6.71-6.73 (m, 1H, pyrrole **H**), 7.09 (d, $J = 9.0$ Hz, 1H, ArH), 7.14 (d, $J = 7.2$ Hz, 1H, ArH), 7.20-7.28 (m, 3H, ArH), 8.47 (br d, $J = 13.2$ Hz, 1H, pyrrole **NH**), 9.66 (s, 1H, **CHO**); ^{13}C NMR (CDCl_3 , 150 MHz) δ 19.6, 27.4, 30.3, 33.8, 35.0, 42.2, 52.4, 59.7, 65.5, 109.8, 112.5, 115.7, 116.5, 127.4, 128.7, 128.9, 129.0, 129.1, 129.2, 131.6, 134.9, 135.1, 157.1, 159.3, 171.1, 192.1, 198.0; HRMS (ES) 502.2325 (MH^+); $\text{C}_{29}\text{H}_{32}\text{N}_3\text{O}_5$ requires 502.2336.

Macrocyclic aldehyde **2.23**

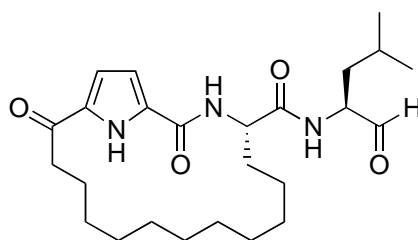
Alcohol **2.87** (24 mg, 0.04 mmol) was oxidized according to general procedure L and the crude product was purified by rp-HPLC to give aldehyde **2.23** as a white oil (10 mg, 41%). $R_f = 0.77$ (ethyl acetate); R_t : 13.0 min; $[\alpha]_D = +3.5$ (c 0.1 in $(\text{CH}_3)_2\text{SO}$); $^1\text{H NMR}$ (CDCl_3 , 600 MHz) δ 0.84, (t, $J = 5.7$ Hz, 6H, $\text{CH}_2\text{CH}(\text{CH}_3)_2$), 1.43-1.51 (m, 1H, $\text{CHHCH}(\text{CH}_3)_2$), 1.66-1.74 (m, 2H, $\text{CHHCH}(\text{CH}_3)_2$), 1.93 (br s, 4H, $\text{OCH}_2\text{CH}_2\text{CH}_2\text{CH}_2\text{O}$), 2.68-2.71 (m, 1H, ArCH_2CHH), 2.94-3.07 (m, 3H, ArCH_2CH_2 , CHCHHAr), 3.09-3.13 (m, 1H, ArCH_2CHH), 3.33 (dd, $J = 14.4$ and 4.8 Hz, 1H, CHCHHAr), 3.81-3.97 (m, 4H, $\text{OCH}_2(\text{CH}_2)_2\text{CH}_2\text{O}$), 4.52-4.60 (m, 1H, NHCHCHO), 4.74-4.79 (m, 1H, NHCHCO), 6.07-6.09 (m, 1H, pyrrole **H**), 6.14-6.15 (m, 1H, pyrrole **H**), 6.24 (d, $J = 6.0$ Hz, 1H, NHCHCHO), 6.63 (d, $J = 8.7$ Hz, 2H, OArH), 6.74 (d, $J = 9.0$ Hz, 2H, OArH), 6.91 (d, $J = 8.7$ Hz, 2H, OArH), 7.01 (d, $J = 9.0$ Hz, 2H, OArH), 7.05 (d, $J = 7.2$ Hz, 1H, NHCHCO), 9.61 (s, 1H, CHO), 10.02 (br s, 1H, pyrrole **NH**); $^{13}\text{C NMR}$ (CDCl_3 , 150 MHz) δ 21.8, 23.0, 24.8, 25.1, 25.2, 32.6, 36.1, 37.7, 40.1, 54.1, 57.5, 67.0, 67.2, 110.4, 114.3, 114.9, 117.0, 127.7, 129.5, 129.6, 130.2, 132.1, 134.7, 157.4, 158.0, 160.3, 171.4, 192.2, 199.1; HRMS (ES) 574.2900 (MH^+); $\text{C}_{33}\text{H}_{40}\text{N}_3\text{O}_6$ requires 574.2912.

Macrocyclic aldehyde **2.24**



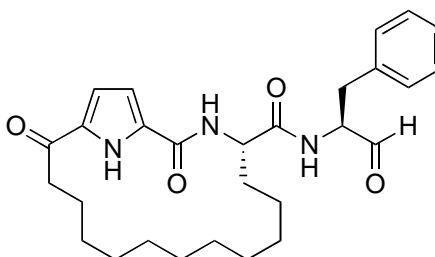
Alcohol **2.88** (18 mg, 0.03 mmol) was oxidized according to general procedure L and the crude product was purified by rp-HPLC to give aldehyde **2.24** as a white oil (12 mg, 65%). $R_f = 0.65$ (ethyl acetate); $R_t = 12.9$ min; $[\alpha]_D = +1.1$ (c 0.2 in $(\text{CH}_3)_2\text{SO}$); $^1\text{H NMR}$ (CDCl_3 , 600 MHz) δ 1.92 (br s, 4H, $\text{OCH}_2\text{CH}_2\text{CH}_2\text{CH}_2\text{O}$), 2.68-2.70 (m, 1H, ArCH_2CHH), 2.93 (dd, $J = 14.7$ and 10.5 Hz, 1H CHCHHArO), 2.96-3.04 (m, 2H, ArCH_2CH_2), 3.06-3.14 (m, 2H, CHCHHAr , ArCH_2CHH), 3.17 (dd, $J = 14.3$ and 6.3 Hz, 1H, CHCHHAr), 3.26 (dd, $J = 14.7$ and 4.5 Hz, 1H, CHCHHArO), 3.79-3.97 (m, 4H, $\text{OCH}_2(\text{CH}_2)_2\text{CH}_2\text{O}$), 4.67-4.71 (m, 1H, NHCHCO), 4.74 (q, $J = 6.8$ Hz, 1H, CHCH_2Ar), 6.00-6.02, 6.14-6.15 (m, 2H, NHCHCHO , pyrrole **H**), 6.11-6.12 (m, 1H, pyrrole **H**), 6.62 (d, $J = 8.4$ Hz, 2H, OArH), 6.74 (d, $J = 8.4$ Hz, 2H, OArH), 6.90 (d, $J = 8.4$ Hz, 2H, OArH), 6.98 (d, $J = 8.4$ Hz, 2H, OArH), 7.08-7.13 (m, 6H, ArH , NHCHCHO), 9.67 (s, 1H, CHO), 9.89 (br s, 1H, pyrrole NH); $^{13}\text{C NMR}$ (CDCl_3 , 150 MHz) δ 25.1, 32.7, 34.9, 35.7, 40.1, 53.9, 59.8, 66.9, 67.1, 110.2, 114.2, 115.0, 116.9, 127.1, 127.7, 128.7, 129.2, 129.3, 129.5, 130.1, 132.1, 134.7, 135.3, 157.3, 158.0, 160.2, 171.2, 192.2, 198.4; HRMS (ES) 608.2736 (MH^+); $\text{C}_{36}\text{H}_{38}\text{N}_3\text{O}_6$ requires 608.2755.

(*S*)-*N*-((*S*)-4-Methyl-1-oxopent-2-yl)-2,16-dioxo-3,20-diazabicyclo[15.2.1]icosa-1(19),17-diene-4-carboxamide **2.25**



Alcohol **2.89** (35 mg, 0.078 mmol) was oxidized according to general procedure L and the crude product was purified by rp-HPLC to give aldehyde **2.25** as a clear oil (13 mg, 37%). $R_f = 0.74$ (4:1 ethyl acetate / petroleum ether); $R_t = 13.0$ min; $[\alpha]_D = + 2.2$ (c 0.2 in $(\text{CH}_3)_2\text{SO}$); $^1\text{H NMR}$ (CDCl_3 , 600 MHz) δ 0.79-1.35 (m, 17H, $\text{CO}(\text{CH}_2)_2\text{CHH}(\text{CH}_2)_7$), 0.94 (t, $J = 5.4$ Hz, 6H, $\text{CH}_2\text{CH}(\text{CH}_3)_2$), 1.38-1.44 (m, 1H, $\text{CO}(\text{CH}_2)_2\text{CHH}$), 1.46-1.50 (m, 1H, $\text{CHHCH}(\text{CH}_3)_2$), 1.69-1.76 (m, 2H, $\text{CHHCH}(\text{CH}_3)_2$), 1.66-1.67 (m, 2H, $\text{COCH}_2\text{CH}_2(\text{CH}_2)_8\text{CHH}$), 2.07-2.10 (m, 1H, $\text{CO}(\text{CH}_2)_{10}\text{CHH}$), 2.69 (br s, 1H, $\text{COCHH}(\text{CH}_2)_{10}$), 2.88 (br s, 1H, $\text{COCHH}(\text{CH}_2)_{10}$), 4.52-4.55 (m, 1H, NHCHCHO), 4.89-4.90 (m, 1H, NHCHCO), 6.80 (s, 1H, pyrrole **H**), 6.93 (s, 1H, pyrrole **H**), 7.09 (br s, 2H, 2 \times **NH**), 9.59 (s, 1H, **CHO**), 10.87 (br s, 1H, pyrrole **NH**); $^{13}\text{C NMR}$ (CDCl_3 , 150 MHz) δ 21.9, 23.0, 24.5, 24.8, 26.6, 27.9, 28.1, 28.3, 28.9, 29.1, 29.3, 29.7, 30.9, 37.6, 39.1, 53.4, 57.4, 112.0, 116.6, 130.4, 134.4, 160.2, 172.4, 194.6, 199.2; HRMS (ES) 446.3001 (MH^+); $\text{C}_{25}\text{H}_{40}\text{N}_3\text{O}_4$ requires 446.3013.

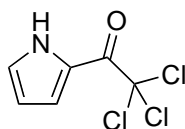
(S)-2,16-Dioxo-N-((S)-1-oxo-3-phenylpropan-2-yl)-3,20-diazabicyclo[15.2.1]icosa-1(19),17-diene-4-carboxamide 2.26



Alcohol **2.90** (58 mg, 0.12 mmol) was oxidized according to general procedure L and the crude product was purified by rp-HPLC to give aldehyde **2.26** as a clear oil (20 mg, 34%). $R_f = 0.60$ (4:1 ethyl acetate / petroleum ether); $R_t = 12.9$ min; $[\alpha]_D = + 1.8$ (c 0.2 in $(\text{CH}_3)_2\text{SO}$); $^1\text{H NMR}$ (CDCl_3 , 600 MHz) δ 0.78-1.29 (m, 15H, $\text{CO}(\text{CH}_2)_2(\text{CH}_2)_7\text{CHH}$), 1.38-1.40 (m, 1H, $\text{CO}(\text{CH}_2)_9\text{CHH}$), 1.68-1.86 (m, 3H, $\text{COCH}_2\text{CH}_2(\text{CH}_2)_8\text{CHH}$), 2.00-2.04 (m, 1H, $\text{CO}(\text{CH}_2)_{10}\text{CHH}$), 2.69 (br s, 1H, COCHH), 2.85 (br s, 1H, COCHH), 3.08-3.12 (m, 1H, **CHHAr**), 3.17-3.20 (**CHHAr**), 4.73 (q, $J = 7.0$ Hz, 1H, NHCHCHO), 4.81 (br s, 1H, NHCHCO), 6.77 (s, 1H, pyrrole **H**), 6.91 (br s, 2H, pyrrole **H**, **NHCH**), 7.06-7.22 (m, 6H, **ArH**, **NHCH**), 9.66 (s, 1H, **CHO**), 10.82 (br s, 1H, pyrrole **NH**); $^{13}\text{C NMR}$ (CDCl_3 , 150 MHz) δ 24.5, 26.7, 28.0, 28.3, 28.9, 29.2, 29.3, 29.7, 30.3, 30.9, 35.0, 39.1,

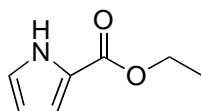
53.2, 59.8, 116.7, 127.1, 128.7, 129.2, 130.4, 134.3, 135.4, 160.1, 172.1, 194.5, 198.5; HRMS (ES) 480.2834 (MH⁺); C₂₈H₃₈N₃O₄ requires 480.2857.

2-Trichloroacetyl-1H-pyrrole **2.28**³



Pyrrole (6.72 g, 100.00 mmol) in diethyl ether (15 mL) was added dropwise over a 1 h to a solution of trichloroacetyl chloride (20.00 g, 110.00 mmol) in diethyl ether (50 mL). The resulting mixture was stirred for 3 h before the reaction was quenched with the slow addition of potassium carbonate (8.97 g) in water (35 mL). The layers were separated, and the organic phase was dried over MgSO₄. Volatiles were removed *in vacuo* to obtain a grey crystalline solid, which was dissolved in *n*-hexane (350 mL), silica gel 60 (6.00 g) was added and heated. The hot mixture was filtered and the filtrate was allowed to cool to -12°C (ice-salt bath). The white precipitate was collected by filtration and the volume of the filtrate was reduced (~50 mL) *in vacuo*. The filtrate was cooled to 4°C (fridge) and the grey crystalline solid was collected. All precipitates were separately dried *in vacuo* at ambient temperature to give pyrrole **2.28** as a white crystalline solid (17.80 g, 84%). mp 71-73 °C, lit. mp 72-74 °C³; R_f = 0.6 (4:1 petroleum ether / ethyl acetate); ¹H NMR (CDCl₃, 300 MHz) δ 6.37-6.40 (m, 1H, pyrrole **H**₄), 7.18-7.20 (m, 1H, pyrrole **H**₃), 7.39-7.42 (m, 1H, pyrrole **H**₅), 9.79 (br s, 1H, **NH**); ¹³C NMR (CDCl₃, 75 MHz) δ 94.9, 111.8, 121.3, 122.8, 127.3, 173.2. Experimental data as per literature.³

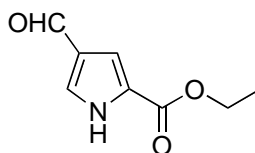
Ethyl 1H-pyrrole-2-carboxylate **2.29**³



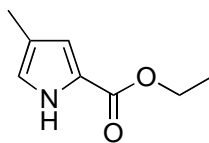
Sodium metal (0.15 g, 6.50 mmol) was added to a solution of anhydrous ethanol (20 mL) and once the sodium had dissolved, pyrrole **2.28** (10.45 g, 49.20 mmol) was added portion wise over 10 min. Upon completion, the mixture was stirred for 40 min at ambient temperature and volatiles were removed *in vacuo* to give a dark red oil, which was redissolved in diethyl ether (30 mL) and extracted with 3M aqueous hydrochloric acid

(6 mL). The organic phase was separated, and the aqueous phase was further extracted with diethyl ether (20 mL). Organic phases were combined, washed with sat. NaHCO_3 (5 mL), and dried over MgSO_4 . Volatiles were removed *in vacuo* to obtain a brown oil, which crystallised upon standing to form tan crystals (6.56 g). The tan crystals was purified by distillation under reduced pressure (130°C , 5 mm Hg) to give pyrrole **2.29** as a colourless oil, which crystallised upon standing to form white crystals (6.21 g, 91%). mp $36\text{--}37^\circ\text{C}$, lit. mp $38\text{--}39.5^\circ\text{C}$ ³; ^1H NMR (CDCl_3 , 600 MHz) δ 1.36 (t, $J = 7.2$ Hz, 3H, OCH_2CH_3), 4.33 (q, $J = 7.2$ Hz, 2H, OCH_2CH_3), 6.25–6.27 (m, 1H, pyrrole **H4**), 6.91–6.93 (m, 1H, pyrrole **H3**), 6.94–6.95 (m, 1H, pyrrole **H5**), 9.31 (br s, 1H, **NH**); ^{13}C NMR (CDCl_3 , 150 MHz) δ 14.43, 60.29, 110.35, 115.07, 122.70, 122.99, 161.25. Experimental data as per literature.³

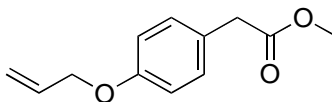
Ethyl 4-formyl-1H-pyrrole-2-carboxylate **2.30**⁴



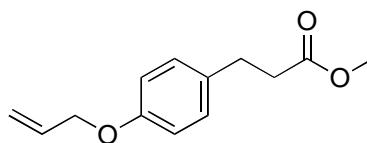
Aluminium chloride (5.03 g, 37.70 mmol) in 1:1 anhydrous dichloromethane / nitromethane (10 mL) was added to a solution of pyrrole **2.29** (2.02 g, 14.50 mmol) in 1:1 anhydrous dichloromethane / nitromethane (20 mL) and the resulting mixture was cooled to -30°C (acetone-dry ice bath). 1,1-Dichlorodimethyl ether (1.7 mL, 18.80 mmol) in anhydrous dichloromethane (2 mL) was added to the cooled solution and the mixture stored for 16 h in a -20°C freezer. The mixture was poured over crushed ice water, the aqueous layer collected and extracted with diethyl ether (2 x 25 mL). The organic layer was dried over Na_2SO_4 and volatiles were removed *in vacuo* to obtain a dark brown solid, which was recrystallized from ethanol (15 mL) to obtain pyrrole **2.30** as a tan solid (1.06 g, 44%). mp $101\text{--}105^\circ\text{C}$, lit. mp $101\text{--}102^\circ\text{C}$ ⁴; $R_f = 0.57$ (1:1 petroleum ether / ethyl acetate); ^1H NMR (CDCl_3 , 300 MHz) δ 1.38 (t, $J = 7.2$ Hz, 3H, OCH_2CH_3), 4.37 (q, $J = 7.2$ Hz, 2H, OCH_2CH_3), 7.33 (dd, $J = 2.4$ and 1.5 Hz, 1H, pyrrole **H3**), 7.58 (dd, $J = 3.3$ and 1.5 Hz, 1H, pyrrole **H5**), 9.86 (s, br s, 2H, **CHO**, **NH**); ^{13}C NMR (CDCl_3 , 75 MHz) δ 14.3, 61.2, 114.1, 125.1, 127.6, 128.3, 160.9, 185.6. Experimental data as per literature.⁴

Ethyl 4-methyl-1*H*-pyrrole-2-carboxylate 2.31⁴

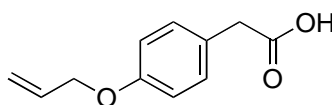
Pyrrole **2.30** (502 mg, 3.00 mmol) in ethanol (10 mL) was added 10% Pd/C (135 mg, 25% by weight) and the mixture was stirred under hydrogen atmosphere at ambient temperature for 19.5 h. Celite and ethanol (20 mL) were added to the reaction mixture, followed by filtration through a celite pad and washing with ethanol (75 mL). The filtrates were combined and volatiles were removed *in vacuo* to obtain pyrrole **2.31** as a yellowish oil, which crystallised upon standing (437 mg, 95%). mp 37-41 °C, lit. mp 37-38 °C;⁴ R_f = 0.51 (2:1 petroleum ether / ethyl acetate); ¹H NMR (CDCl₃, 300 MHz) δ 1.34 (t, J = 7.1 Hz, 3H, OCH₂CH₃), 2.11 (dd, J = 0.6 and 0.6 Hz, 3H, pyrrole CH₃), 4.30 (q, J = 7.1 Hz, 2H, OCH₂CH₃), 6.71-6.74 (m, 2H, pyrrole **H3**, pyrrole **H5**), 9.02 (br s, 1H, NH); ¹³C NMR (CDCl₃, 75 MHz) δ 11.7, 14.4, 60.1, 115.8, 121.1, 120.9, 122.5, 161.2. Experimental data as per literature.⁴

Methyl 2-(4-(allyloxy)phenyl)acetate 2.34⁵

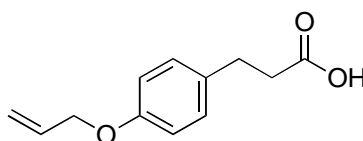
Methyl 2-(4-hydroxyphenyl)acetate (831 mg, 5.00 mmol) was subjected to *O*-allylation according to general procedure A to afford compound **2.34** as a yellow oil (1.03 g, 100%). ¹H NMR (CDCl₃, 300 MHz) δ 3.56 (s, 2H, ArCH₂), 3.68 (s, 3H, OCH₃), 4.51-4.53 (m, 2H, OCH₂CHCH₂), 5.26-5.30 (m, 1H, OCH₂CHCHH), 5.37-5.44 (m, 1H, OCH₂CHCHH), 5.99-6.11 (m, 1H, OCH₂CHCH₂), 6.87 (d, J = 8.6 Hz, 2H, OArH), 7.19 (d, J = 8.6 Hz, 2H, OArH); ¹³C NMR (CDCl₃, 75 MHz) δ 40.3, 51.9, 68.8, 114.8, 117.6, 126.2, 130.2, 133.2, 157.7, 172.3. Experimental data as per literature.⁵

Methyl 3-(4-allyloxyphenyl)propanoate 2.35^{6,7}

Methyl 3-(4-hydroxyphenyl)propanoate (9.05 g, 50.20 mmol) was subjected to *O*-allylation according to general procedure A to afford compound **2.35** as a yellow oil (11.01 g, 100%). ¹H NMR (CDCl₃, 300 MHz) δ 2.60 (t, *J* = 7.8 Hz, 2H, ArCH₂CH₂), 2.89 (t, *J* = 7.8 Hz, 2H, ArCH₂CH₂), 3.66 (s, 3H, OCH₃), 4.50-4.52 (m, 2H, OCH₂CHCH₂), 5.25-5.30 (m, 1H, OCH₂CHCHH), 5.37-5.44 (m, 1H, OCH₂CHCHH), 5.99-6.12 (m, 1H, OCH₂CHCH₂), 6.84 (d, *J* = 8.7 Hz, 2H, OArH), 7.11 (d, *J* = 8.7 Hz, 2H, OArH); ¹³C NMR (CDCl₃, 75 MHz) δ 30.1, 35.9, 51.6, 68.8, 114.7, 117.6, 129.2, 132.7, 133.4, 157.1, 173.4. Experimental data as per literature.^{6,7}

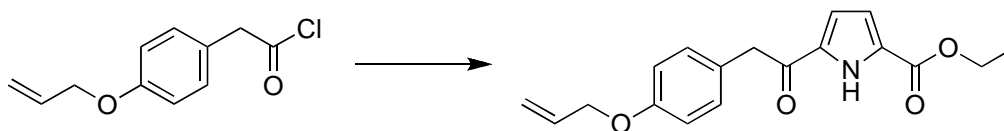
2-(4-(Allyloxy)phenyl)acetic acid 2.36⁸

Methyl 4-allyloxyphenylacetate, **2.34** (5.20 g, 25.20 mmol) was hydrolysed according to general procedure B to afford carboxylic acid **2.36** as yellowish crystals (4.77 g, 99%). mp 72-73 °C, lit. mp 69-71 °C;⁸ ¹H NMR (CDCl₃, 300 MHz) δ 3.57 (s, 2H, ArCH₂), 4.51-4.53 (m, 2H, OCH₂CHCH₂), 5.26-5.29 (m, 1H, OCH₂CHCHH), 5.37-5.43 (m, 1H, OCH₂CHCHH), 5.98-6.11 (m, 1H, OCH₂CHCH₂), 6.87 (d, *J* = 8.3 Hz, 2H, OArH), 7.18 (d, *J* = 8.3 Hz, 2H, OArH), 9.20 (br s, 1H, OH); ¹³C NMR (CDCl₃, 75 MHz) δ 40.1, 68.8, 114.9, 117.7, 125.5, 130.4, 133.2, 157.9, 178.0. Experimental data as per literature.⁸

3-(4-Allyloxyphenyl)propanoic acid 2.37⁹

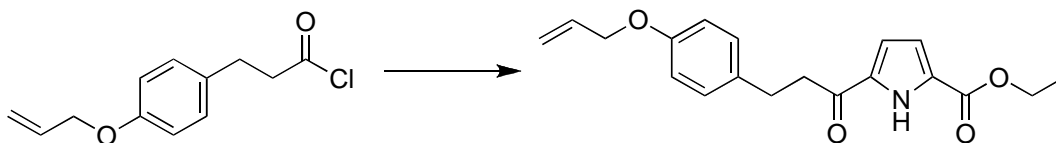
Methyl 3-(4-allyloxyphenyl)propionate, **2.35** (11.01g, 50.00 mmol) was hydrolysed according to general procedure B to afford carboxylic acid **2.37** as a yellow solid (10.31 g, 100%). mp 87-89 °C, lit. mp 89-90 °C;⁹ ¹H NMR (DMSO-*d*₆, 300 MHz) δ 2.45-2.50 (m, 2H, ArCH₂CH₂), 2.74 (t, *J* = 7.7 Hz, 2H, ArCH₂CH₂), 4.50-4.53 (m, 2H, OCH₂CHCH₂), 5.22-5.26 (m, 1H, OCH₂CHCHH), 5.34-5.41 (m, 1H, OCH₂CHCHH), 5.96-6.09 (m, 1H, OCH₂CHCH₂), 6.84 (d, *J* = 8.6 Hz, 2H, OArH), 7.12 (d, *J* = 8.6 Hz, 2H, OArH), 12.11 (br s, 1H, OH); ¹³C NMR (DMSO-*d*₆, 75 MHz) δ 29.7, 35.8, 68.3, 114.7, 117.5, 129.4, 133.1, 134.1, 156.7, 174.0. Experimental data as per literature.⁹

Ethyl 5-[2-(4-allyloxyphenyl)acetyl]-1H-pyrrole-2-carboxylate **2.45**



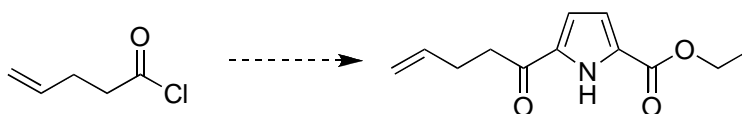
Carboxylic acid **2.36** (548 mg, 2.80 mmol) was reacted with thionyl chloride according to general procedure C to afford a dark brown oil, acid chloride **2.38** (596 mg, 100%), which was used immediately without purification. ¹H NMR (CDCl₃, 300 MHz) δ 4.05 (s, 2H, ArCH₂), 4.50-4.53 (m, 2H, OCH₂CHCH₂), 5.26-5.30 (m, 1H, OCH₂CHCHH), 5.37-5.44 (m, 1H, OCH₂CHCHH), 5.97-6.10 (m, 1H, OCH₂CHCH₂), 6.89 (d, *J* = 8.6 Hz, 2H, OArH), 7.16 (d, *J* = 8.6 Hz, 2H, OArH); ¹³C NMR (CDCl₃, 75 MHz) δ 52.2, 68.8, 115.1, 117.7, 123.4, 130.6, 133.0, 158.4, 172.1.

Ethyl 1H-pyrrole-2-carboxylate **2.29** (206 mg, 1.50 mmol) was coupled to acid chloride **2.38** (596 mg, 2.8 mmol) according to general procedure D and the crude product was purified by flash chromatography (4:1 petroleum ether / ethyl acetate) to afford compound **2.45** as a yellow oil, which crystallised upon standing (78 mg, 17 %). mp 76-88 °C; *R*_f = 0.48 (4:1 petroleum ether / ethyl acetate); ¹H NMR (CDCl₃, 300 MHz) δ 1.36 (t, *J* = 7.2 Hz, 3H, OCH₂CH₃), 4.03 (s, 2H, ArCH₂), 4.35 (q, *J* = 7.2 Hz, 2H, OCH₂CH₃), 4.50-4.52 (m, 2H, OCH₂CHCH₂), 5.26-5.29 (m, 1H, OCH₂CHCHH), 5.37-5.43 (m, 1H, OCH₂CHCHH), 5.98-6.11 (m, 1H, OCH₂CHCH₂), 6.86-6.89 (m, 4H, pyrrole H, OArH), 7.19 (d, *J* = 8.7 Hz, 2H, OArH), 9.82 (br s, 1H, NH). ¹³C NMR (CDCl₃, 75 MHz) δ 14.3, 44.5, 61.1, 68.8, 115.0, 115.5, 116.3, 117.7, 126.3, 127.5, 133.2, 133.4, 130.3, 157.7, 160.3 188.8; HRMS (ES) 314.1378 (MH⁺); C₁₈H₂₀NO₄ requires 314.1392.

Ethyl 5-[3-(4-allyloxyphenyl)propanoyl]-1H-pyrrole-2-carboxylate 2.46


Carboxylic acid **2.37** (6.60 g, 32.00 mmol) was reacted with thionyl chloride according to general procedure C to afford a dark yellow oil, acid chloride **2.39** (7.19 g, 100%), which was used immediately without purification. ^1H NMR (CDCl_3 , 300 MHz) δ 2.96 (t, $J = 7.4$ Hz, 2H, ArCH_2CH_2), 3.18 (t, $J = 7.4$ Hz, 2H, ArCH_2CH_2), 4.52-4.55 (m, 2H, $\text{OCH}_2\text{CHCH}_2$), 5.28-5.33 (m, 1H, OCH_2CHCHH), 5.39-5.46 (m, 1H, OCH_2CHCHH), 6.00-6.13 (m, 1H, $\text{OCH}_2\text{CHCH}_2$), 6.88 (d, $J = 8.6$ Hz, 2H, OArH), 7.12 (d, $J = 8.6$ Hz, 2H, OArH); ^{13}C NMR (CDCl_3 , 75 MHz) δ 30.1, 48.7, 68.7, 114.9, 117.5, 129.2, 130.7, 133.2, 157.4, 173.0.

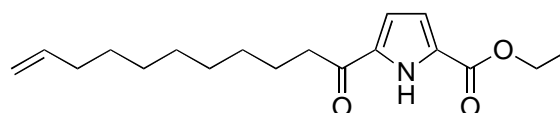
Ethyl 1H-pyrrole-2-carboxylate **2.29** (2.23 g, 16.00 mmol) was coupled to acid chloride **2.39** (7.19 g, 32.00 mmol) according to General Procedure D and the crude product was purified by flash chromatography (4:1 petroleum ether / ethyl acetate) to afford the compound **2.46** as a yellow oil, which crystallised upon standing (2.08 g, 40%). mp 69-73 °C; $R_f = 0.42$ (4:1 petroleum ether / ethyl acetate); ^1H NMR (CDCl_3 , 300 MHz) δ 1.37 (t, $J = 7.2$ Hz, 3H, OCH_2CH_3), 2.96-3.01 (m, 2H, ArCH_2CH_2), 3.07-3.13 (m, 2H, ArCH_2CH_2), 4.36 (q, $J = 7.2$ Hz, 2H, OCH_2CH_3), 4.50-4.52 (m, 2H, $\text{OCH}_2\text{CHCH}_2$), 5.26-5.30 (m, 1H, OCH_2CHCHH), 5.36-5.44 (m, 1H, OCH_2CHCHH), 5.98-6.11 (m, 1H, $\text{OCH}_2\text{CHCH}_2$), 6.80-6.88 (m, 4H, pyrrole H, OArH), 7.13 (d, $J = 8.7$ Hz, 2H, OArH), 9.83 (br s, 1H, NH); ^{13}C NMR (CDCl_3 , 50 MHz) δ 14.3, 29.6, 40.3, 61.1, 68.9, 114.9, 115.5, 117.5, 127.3, 133.1, 133.5, 133.8, 129.3, 157.2, 160.4, 190.4; HRMS (ES) 328.1541 (MH^+); $\text{C}_{19}\text{H}_{22}\text{NO}_4$ requires 328.1549.

Attempted synthesis of ethyl 5-pent-4-enoyl-1H-pyrrole-2-carboxylate 2.48


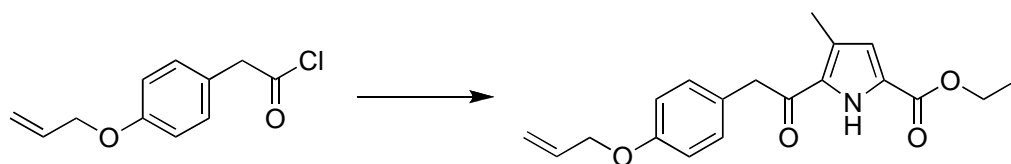
4-Pentenoic acid **2.41** (49 mg, 0.50 mmol) was reacted with thionyl chloride according to general procedure C to afford a light brown oil, acid chloride **2.43** (58 mg, 100%), which was used immediately without purification. ^1H NMR (CDCl_3 , 300 MHz) δ 2.41-2.49 (m, 2H, $\text{CH}_2\text{CH}_2\text{CHCH}_2$), 3.00 (t, $J = 7.2$ Hz, 2H, $\text{CH}_2\text{CH}_2\text{CHCH}_2$), 5.07 (dq, $J = 6.5$ and 1.3 Hz, 1H, $\text{CH}_2\text{CH}_2\text{CHCHH}$), 5.12 (dq, $J = 12.9$ and 1.3 Hz, 1H, $\text{CH}_2\text{CH}_2\text{CHCHH}$), 5.72-5.86 (m, 1H, $\text{CH}_2\text{CH}_2\text{CHCH}_2$); ^{13}C NMR (CDCl_3 , 75 MHz) δ 29.0, 46.3, 117.0, 134.8, 173.2.

Ethyl 1*H*-pyrrole-2-carboxylate **2.29** (34 mg, 0.25 mmol) was coupled to acid chloride **2.43** (58 mg, 0.50 mmol) according to General Procedure D and volatiles were removed *in vacuo*. TLC and ^1H NMR of the mixture showed that reaction had not proceeded.

Ethyl 5-undec-10-enoyl-1*H*-pyrrole-2-carboxylate **2.49**

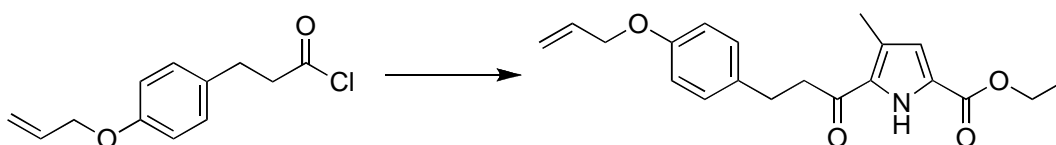


Ethyl 1*H*-pyrrole-2-carboxylate **2.29** (505 mg, 3.6 mmol) was coupled to 10-undecenoyl chloride **2.44** (1.6 mL, 7.5 mmol) according to general procedure D and the crude product was purified by flash chromatography (9:1 petroleum ether / ethyl acetate) to afford the pyrrole **2.49** as a yellow oil, which crystallised upon standing (588 mg, 53%). mp 41-43 °C; $R_f = 0.44$ (9:1 petroleum ether / ethyl acetate); ^1H NMR (CDCl_3 , 600 MHz) δ 1.25-1.39 (m, 13H, $(\text{CH}_2)_2(\text{CH}_2)_5\text{CH}_2\text{CHCH}_2$, OCH_2CH_3), 1.72 (quin, $J = 7.5$ Hz, 2H, $\text{CH}_2\text{CH}_2(\text{CH}_2)_6\text{CHCH}_2$), 2.04 (q, $J = 7.2$ Hz, 2H, $(\text{CH}_2)_2(\text{CH}_2)_5\text{CH}_2\text{CHCH}_2$), 2.79 (t, $J = 7.8$ Hz, 2H, COCH_2), 4.36 (q, $J = 7.2$ Hz, 2H, OCH_2CH_3), 4.93 (d, $J = 10.2$ Hz, 1H, $(\text{CH}_2)_8\text{CHCHH}$), 4.99 (d, $J = 17.4$ Hz, 1H, $(\text{CH}_2)_8\text{CHCHH}$), 5.78-5.84 (m, 1H, $(\text{CH}_2)_8\text{CHCH}_2$), 6.83-6.83 (m, 1H, pyrrole **H**), 6.88-6.89 (m, 1H, pyrrole **H**), 9.78 (br s, 1H, pyrrole **NH**); ^{13}C NMR (CDCl_3 , 150 MHz) δ 14.3, 24.8, 28.9, 29.0, 29.2, 29.3, 29.5, 33.8, 38.4, 61.1, 114.1, 115.3, 115.4, 127.1, 133.9, 139.2, 160.4, 191.7; HRMS (ES) 306.2052 (MH^+); $\text{C}_{18}\text{H}_{28}\text{NO}_3$ requires 306.2064.

Ethyl 5-(2-(4-allyloxyphenyl)acetyl)-4-methyl-1H-pyrrole-2-carboxylate 2.50


Carboxylic acid **2.36** (779 mg, 4.00 mmol) was reacted with thionyl chloride according to general procedure C to afford a dark brown oil, acid chloride **2.38** (847 mg, 100%), which was used immediately without purification. ^1H NMR (CDCl_3 , 300 MHz) δ 4.05 (s, 2H, ArCH_2), 4.50-4.53 (m, 2H, $\text{OCH}_2\text{CHCH}_2$), 5.26-5.30 (m, 1H, OCH_2CHCHH), 5.37-5.44 (m, 1H, OCH_2CHCHH), 5.97-6.10 (m, 1H, $\text{OCH}_2\text{CHCH}_2$), 6.89 (d, $J = 8.6$ Hz, 2H, OArH), 7.16 (d, $J = 8.6$ Hz, 2H, OArH); ^{13}C NMR (CDCl_3 , 75 MHz) δ 52.2, 68.8, 115.1, 117.7, 123.4, 130.6, 133.0, 158.4, 172.1.

Ethyl 4-methyl-1H-pyrrole-2-carboxylate **2.31** (311 mg, 2.00 mmol) was coupled to acid chloride **2.38** (847 mg, 4.00 mmol) according to general procedure D and the crude product was purified by flash chromatography (4:1 petroleum ether / ethyl acetate) to afford compound **2.50** as a yellow oil (119 mg, 18 %). $R_f = 0.49$ (4:1 petroleum ether / ethyl acetate); ^1H NMR (CDCl_3 , 300 MHz) δ 1.35 (t, $J = 7.1$ Hz, 3H, OCH_2CH_3), 2.40 (s, 3H, pyrrole CH_3), 4.04 (s, 2H, ArCH_2), 4.32 (q, $J = 7.1$ Hz, 2H, OCH_2CH_3), 4.50-4.53 (m, 2H, $\text{OCH}_2\text{CHCH}_2$), 5.25-5.30 (m, 1H, OCH_2CHCHH), 5.37-5.44 (m, 1H, OCH_2CHCHH), 5.98-6.11 (m, 1H, $\text{OCH}_2\text{CHCH}_2$), 6.69-6.70 (m, 1H, pyrrole H_3), 6.88 (d, $J = 8.4$ Hz, 2H, OArH), 7.14 (d, $J = 8.4$ Hz, 2H, OArH), 9.77 (br s, 1H, NH); ^{13}C NMR (CDCl_3 , 75 MHz) δ 14.2, 14.2, 45.7, 61.0, 68.7, 114.9, 117.6, 117.8, 125.4, 125.7, 126.8, 131.2, 133.2, 130.3, 157.6, 160.3, 188.9; HRMS (ES) 328.1573 (MH^+); $\text{C}_{19}\text{H}_{22}\text{NO}_5$ requires 328.1543.

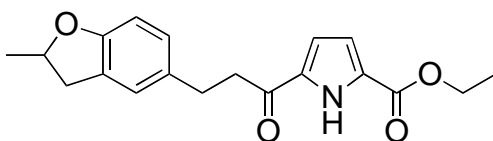
Ethyl 5-(3-(4-allyloxyphenyl)propanoyl)-4-methyl-1H-pyrrole-2-carboxylate 2.51


Carboxylic acid **2.37** (827 g, 4.00 mmol) was reacted with thionyl chloride according to general procedure C to afford a dark yellow oil, acid chloride **2.39** (902 mg, 100%), which

was used immediately without purification. ^1H NMR (CDCl_3 , 300 MHz) δ 2.96 (t, $J = 7.4$ Hz, 2H, ArCH_2CH_2), 3.18 (t, $J = 7.4$ Hz, 2H, ArCH_2CH_2), 4.52-4.55 (m, 2H, $\text{OCH}_2\text{CHCH}_2$), 5.28-5.33 (m, 1H, OCH_2CHCHH), 5.39-5.46 (m, 1H, OCH_2CHCHH), 6.00-6.13 (m, 1H, $\text{OCH}_2\text{CHCH}_2$), 6.88 (d, $J = 8.6$ Hz, 2H, OArH), 7.12 (d, $J = 8.6$ Hz, 2H, OArH); ^{13}C NMR (CDCl_3 , 75 MHz) δ 30.1, 48.7, 68.7, 114.9, 117.5, 129.2, 130.7, 133.2, 157.4, 173.0.

Ethyl 4-methyl-1*H*-pyrrole-2-carboxylate **2.31** (311 mg, 2.00 mmol) was coupled to acid chloride **2.39** (902 mg, 4.00 mmol) according to general procedure D and the crude product was purified by flash chromatography (4:1 petroleum ether / ethyl acetate) to afford compound **2.51** as a yellow oil, which crystallised upon standing (63 mg, 9%). mp 83.5-86 °C; $R_f = 0.54$ (4:1 petroleum ether / ethyl acetate); ^1H NMR (CDCl_3 , 300 MHz) δ 1.36 (t, $J = 7.2$ Hz, 3H, OCH_2CH_3), 2.37 (s, 3H, pyrrole CH_3), 2.97-3.10 (m, 4H, ArCH_2CH_2), 4.33 (q, $J = 7.2$ Hz, 2H, OCH_2CH_3), 4.50-4.53 (m, 2H, $\text{OCH}_2\text{CHCH}_2$), 5.26-5.30 (m, 1H, OCH_2CHCHH), 5.37-5.44 (m, 1H, OCH_2CHCHH), 5.99-6.12 (m, 1H, $\text{OCH}_2\text{CHCH}_2$), 6.70 (d, $J = 2.7$ Hz, 1H, pyrrole H_3), 6.86 (d, $J = 8.6$ Hz, 2H, OArH), 7.15 (d, $J = 8.6$ Hz, 2H, OArH), 9.67 (br s, 1H, NH); ^{13}C NMR (CDCl_3 , 150 MHz) δ 14.3, 14.3, 28.9, 42.4, 61.0, 68.9, 114.8, 117.6, 117.8, 125.2, 126.2, 131.3, 133.2, 133.4, 129.3, 157.1, 160.4, 190.4; HRMS (ES) 342.1722 (MH^+); $\text{C}_{20}\text{H}_{24}\text{NO}_4$ requires 342.1705.

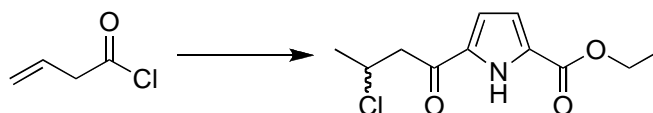
Ethyl 5-[3-(2-methyl-2,3-dihydrobenzo[*b*]furan-5-yl)propionyl]-1*H*-pyrrole-2-carboxylate **2.52**



Freshly dried zinc chloride (205 mg, 1.5 mmol) was added to acid chloride **2.39** (344 mg, 1.5 mmol) in 1,2-DCE (3 mL) to form a suspension. A solution of pyrrole **2.29** (104 mg, 0.75 mmol) in 1,2-DCE (2 mL) was added dropwise over 5 min to the stirred suspension at 0 °C under an inert atmosphere. The suspension was heated to 50 °C for 28.5 h. After cooling to room temperature, 1,2-DCE (3 mL) was added and the reaction mixture was heated to 50 °C for additional 63 h. The resulting dark reddish brown solution was cooled to room temperature, diluted with 1,2-DCE (10 mL) and poured onto a mixture of ice

(60 g) and water (20 mL). The organic phase was separated and the aqueous phase was extracted with EtOAc (3 × 20 mL). The combined organic fractions were washed with brine (30 mL), 1 M aqueous sodium hydroxide (2 × 20 mL), water (2 × 20 mL), and brine (3 × 20 mL) again. The combined organic phase was washed with water (20 mL) and brine (20 mL), dried (MgSO₄·2H₂O), and the solvent was removed *in vacuo*. The resulting dark brown oil was purified flash chromatography (4:1 petroleum ether / ethyl acetate) to give compound **2.52** as yellow oil (31 mg, 13%). ¹H NMR (CDCl₃, 300 MHz) δ 1.37 (t, *J* = 7.2 Hz, 3H, OCH₂CH₃), 1.45 (d, *J* = 6.3 Hz, 3H, CHCH₃), 2.78 (dd, *J* = 15.6 and 7.8 Hz, 1H, CHCHH), 2.94-2.99 (m, 2H, ArCH₂CH₂), 3.06-3.12 (m, 2H, ArCH₂CH₂), 3.27 (dd, *J* = 15.6 and 8.7 Hz, 1H, CHCHH), 4.36 (q, *J* = 7.2 Hz, 2H, OCH₂CH₃), 4.86-4.94 (m, 1H, CHCH₃), 6.67 (d, *J* = 8.1 Hz, 1H, OArH), 6.81-6.83 (m, 1H, pyrrole H), 6.86-6.88 (m, 1H, pyrrole H), 6.95 (d, *J* = 8.1 Hz, 1H, OArH), 7.02 (s, 1H, CH₂ArHCH₂), 9.86 (br s, 1H, NH); ¹³C NMR (CDCl₃, 75 MHz) δ 14.3, 21.7, 29.8, 37.1, 40.7, 61.1, 79.6, 109.0, 115.4, 115.5, 125.0, 127.2, 127.3, 127.7, 132.5, 133.7, 158.0, 160.4, 190.5.

rac*-Ethyl 5-(3-chlorobutanoyl)-1*H*-pyrrole-2-carboxylate **2.52*

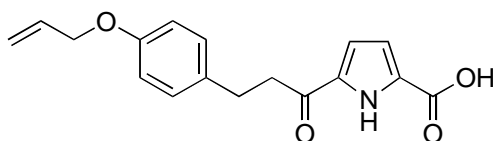


3-Butenoic acid **2.40** (211 mg, 2.50 mmol) was reacted with thionyl chloride according to general procedure C to afford a reddish oil, acid chloride **2.42** (231 mg, 88%), which was used immediately without purification. ¹H NMR (CD₂Cl₂, 300 MHz) δ 3.71 (ddd, *J* = 7.2, 1.4 and 1.4 Hz, 2H, CH₂CHCH₂), 5.30-5.39 (m, 2H, CH₂CHCH₂), 5.89-6.03 (m, 1H, CH₂CHCH₂); ¹³C NMR (CD₂Cl₂, 75 MHz) δ 51.4, 121.3, 128.5, 172.4.

Ethyl 1*H*-pyrrole-2-carboxylate **2.29** (140 mg, 1.00 mmol) was coupled to acid chloride **2.42** (231 mg, 2.20 mmol) according to general procedure D and the crude product was purified by flash chromatography (4:1 petroleum ether / ethyl acetate) to afford compound **2.52** as an off-white solid (14 mg, 6%). mp 57-61 °C; *R_f* = 0.44 (4:1 petroleum ether / ethyl acetate); ¹H NMR (CDCl₃, 600 MHz) δ 1.38 (t, *J* = 7.1 Hz, 3H, OCH₂CH₃), 1.62 (d, *J* =

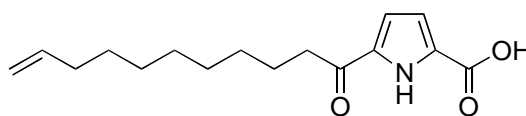
6.6 Hz, 3H, CH₂CH(Cl)CH₃), 3.08 (dd, *J* = 16 and 6.0 Hz, 1H, CHHCH(Cl)CH₃), 3.38 (dd, *J* = 16 Hz and 7.5 Hz, 1H, CHHCH(Cl)CH₃), 4.37 (q, *J* = 7.1 Hz, 2H, OCH₂CH₃), 4.59-4.64 (m, 1H, CH₂CH(Cl)CH₃), 6.87-6.92 (m, 2H, pyrrole H), 9.88 (br s, 1H, NH); ¹³C NMR (CDCl₃, 150 MHz) δ 14.3, 25.3, 48.3, 52.5, 61.2, 115.6, 116.3, 127.9, 133.6, 160.2, 187.3; MS (EI) *m/z* (rel intensity) 243.15 (M⁺, 11), 208.20 (M⁺ - Cl, 49), 166.15 (M⁺ - C₃H₆Cl, 54), 120.10 (M⁺ - C₃H₆Cl - C₂H₆O, 100).

5-[3-(4-allyloxyphenyl)propanoyl]-1*H*-pyrrole-2-carboxylic acid **2.54**



Ester **2.46** (584 mg, 1.80 mmol) was hydrolysed according to General Procedure E to afford carboxylic acid **2.54** as a yellow solid (511 mg, 96%). mp 169-172 °C; ¹H NMR (CDCl₃, 300 MHz) δ 3.01 (t, *J* = 6.9 Hz, 2H, ArCH₂CH₂), 3.16 (t, *J* = 7.2 Hz, 2H, ArCH₂CH₂), 4.51 (d, *J* = 5.1 Hz, 2H, OCH₂CHCH₂), 5.28 (d, *J* = 10.2 Hz, 1H, OCH₂CHCHH), 5.40 (d, *J* = 17.1 Hz, 1H, OCH₂CHCHH), 5.99-6.11 (m, 1H, OCH₂CHCH₂), 6.85 (d, *J* = 8.6 Hz, 2H, OArH), 6.92 (br s, 1H, pyrrole H), 7.01 (br, 1H, pyrrole H), 7.13 (d, *J* = 8.6 Hz, 2H, OArH), 10.99 (br s, 1H, NH), COOH was not observed; ¹³C NMR (CDCl₃, 75 MHz) δ 29.6, 40.7, 68.8, 114.8, 117.1, 117.4, 117.6, 127.9, 129.3, 132.8, 133.3, 134.3, 157.1, 164.1, 192.1; HRMS (ES) 300.1241 (MH⁺) C₁₇H₁₈NO₄ requires 300.1236.

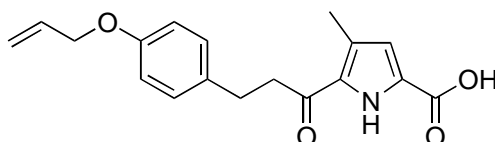
5-Undec-10-enoyl-1*H*-pyrrole-2-carboxylic acid **2.55**



Ester **2.49** (100 mg, 0.33 mmol) was hydrolysed according to general procedure E to afford carboxylic acid **2.55** as a pale yellow solid (77 mg, 85%). mp 113-115 °C. ¹H NMR (CDCl₃, 300 MHz) δ 1.24-1.42 (m, 10H, (CH₂)₂(CH₂)₅CH₂CHCH₂), 1.69-1.77 (m, 2H, CH₂CH₂(CH₂)₅CH₂CHCH₂), 2.01-2.07 (m, 2H, (CH₂)₂(CH₂)₅CH₂CHCH₂), 2.87 (t, *J* = 7.5 Hz, 2H, COCH₂), 4.92-5.02 (m, 2H, (CH₂)₈CHCH₂), 5.75-5.88 (m, 1H, (CH₂)₈CHCH₂),

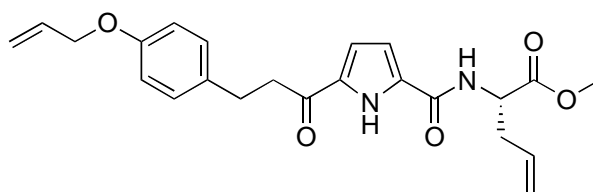
6.95-7.04 (m, 2H, pyrrole **H**), 11.18 (br s, 1H, pyrrole **NH**); ^{13}C NMR (CDCl_3 , 75 MHz) δ 24.8, 28.9, 29.0, 29.2, 29.3, 33.8, 38.7, 114.1, 117.0, 117.2, 127.8, 134.5, 139.2, 164.1, 193.4; HRMS (ES) 278.1740 (MH^+); $\text{C}_{16}\text{H}_{24}\text{NO}_3$ requires 278.1751.

5-(3-(4-(Allyloxy)phenyl)propanoyl)-4-methyl-1H-pyrrole-2-carboxylic acid 2.56



Ester **2.51** (63 mg, 0.18 mmol) was hydrolysed according to General Procedure E to afford carboxylic acid **2.56** as a white solid (58 mg, 100%). mp 177-180 °C (decomp.); ^1H NMR ($\text{DMSO}-d_6$, 300 MHz) δ 2.26 (s, 3H, pyrrole **CH**₃), 2.81 (t, $J = 7.5$ Hz, 2H, **ArCH**₂**CH**₂), 3.22 (t, $J = 7.5$ Hz, 2H, **ArCH**₂**CH**₂), 4.51-4.53 (m, 2H, **OCH**₂**CHCH**₂), 5.22-5.26 (m, 1H, **OCH**₂**CHCH****H**), 5.34-5.41 (m, 1H, **OCH**₂**CHCH****H**), 5.96-6.09 (m, 1H, **OCH**₂**CHCH**₂), 6.63 (d, $J = 2.1$ Hz, 1H, pyrrole **H**), 6.86 (d, $J = 8.6$ Hz, 2H, **OArH**), 7.17 (d, $J = 8.6$ Hz, 2H, **OArH**), 12.03 (br s, 1H, **OH**), 12.84 (br s, 1H, **NH**); ^{13}C NMR ($\text{DMSO}-d_6$, 75 MHz) δ 13.6, 28.6, 49.8, 68.3, 114.6, 117.5, 125.7, 126.9, 129.51, 131.4, 133.5, 134.1, 156.6, 161.8, 191.5; HRMS (ES) 314.1380 (MH^+); $\text{C}_{18}\text{H}_{20}\text{NO}_4$ requires 314.1392.

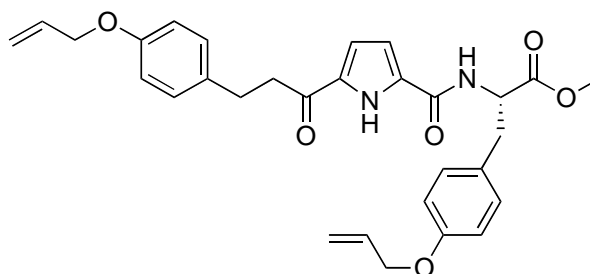
Methyl (2S)-2-[[5-[3-(4-allyloxyphenyl)propanoyl]-1H-pyrrole-2-carbonyl]amino]pent-4-enoate 2.57



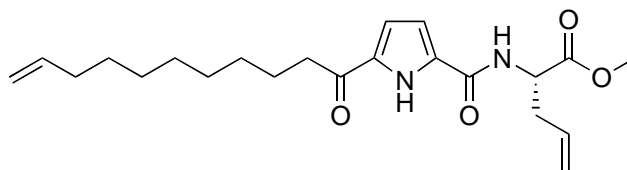
Carboxylic acid **2.54** (480 mg, 1.60 mmol) was coupled to amino acid **2.63** (297 mg, 1.80 mmol) according to General Procedure F and the crude product was purified by flash chromatography (1:1 petroleum ether / ethyl acetate) to afford the acyclic diene **2.57** as a dark yellow oil (621 mg, 94%). $R_f = 0.62$ (1:1 petroleum ether / ethyl acetate); ^1H NMR (CDCl_3 , 300 MHz) δ 2.58-2.72 (m, 2H, **CHCH**₂**CHCH**₂), 2.95-3.00 (m, 2H, **ArCH**₂**CH**₂), 3.05-3.11 (m, 2H, **ArCH**₂**CH**₂), 3.79 (s, 3H, **OCH**₃), 4.51 (dt, $J = 5.1$ and 1.5 Hz, 2H, **OCH**₂**CHCH**₂), 4.85 (dt, $J = 7.7$ and 5.6 Hz, 1H, **CHCH**₂**CHCH**₂), 5.12-5.18 (m, 2H,

CHCH₂CHCH₂), 5.28 (dq, $J = 10.4$ and 1.6 Hz, 1H, OCH₂CHCHH) 5.40 (dq, $J = 17.4$ and 1.6 Hz, 1H, OCH₂CHCHH), 5.65-5.79 (m, 1H, CHCH₂CHCH₂), 5.99-6.11 (m, 1H, OCHCH₂CHCH₂), 6.53 (d, $J = 7.7$ Hz, 1H, NHCH), 6.57 (dd, $J = 4.0$ and 2.7 Hz, 1H, pyrrole H), 6.80 (dd, $J = 4.0$ and 2.7 Hz, 1H, pyrrole H), 6.84 (dt, $J = 8.7$ and 2.3 Hz, 2H, OArH), 7.13 (dt, $J = 8.7$ and 2.3 Hz, 2H, OArH), 9.94 (br s, 1H, pyrrole NH); ¹³C NMR (CDCl₃, 75 MHz) δ 29.5, 36.6, 40.3, 51.6, 52.6, 68.8, 110.1, 114.8, 115.5, 117.6, 119.5, 129.3, 129.6, 133.1, 133.3, 133.4, 131.9, 157.0, 159.4, 172.1, 190.1; HSMS: (ES) 411.1909 (MH⁺) C₂₃H₂₇N₂O₅ requires 411.1920.

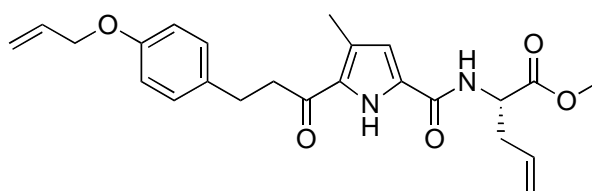
Methyl (2S)-3-(4-allyloxyphenyl)-2-[[5-[3-(4-allyloxyphenyl)propanoyl]-1H-pyrrole-2-carbonyl]amino]propanoate 2.58



Carboxylic acid **2.54** (199 mg, 0.66 mmol) was coupled to amino acid **2.66** (207 mg, 0.76 mmol) according to General Procedure G and the crude product was purified by flash chromatography (1:1 petroleum ether / ethyl acetate) to afford the acyclic diene **2.58** as a yellowish brown oil (323 mg, 94%). $R_f = 0.71$ (1:1 petroleum ether / ethyl acetate); ¹H NMR (CDCl₃, 300 MHz) δ 2.94-2.99 (m, 2H, ArCH₂CH₂), 3.04-3.10 (m, 2H, ArCH₂CH₂), 3.15 (dd, $J = 5.1$ and 5.1 Hz, 2H, NHCH), 3.76 (s, 3H, OCH₃), 4.48-4.52 (m, 4H, 2 × OCH₂CHCH₂), 5.02 (dt, $J = 7.8$ and 5.7 Hz, 1H, NHCH), 5.25-5.30 (m, 2H, 2 × OCH₂CHCHH) 5.36-5.43 (m, 2H, 2 × OCH₂CHCHH), 5.97-6.11 (m, 2H, 2 × OCH₂CHCH₂), 6.50 (dd, $J = 4.1$ and 2.6 Hz, 1H, pyrrole H), 6.59 (d, $J = 7.8$ Hz, 1H, NHCH), 6.77 (dd, $J = 4.1$ and 2.6 Hz, 1H, pyrrole H), 6.82 (d, $J = 8.7$ Hz, 2H, OArH), 6.84 (d, $J = 8.7$ Hz, 2H, OArH), 7.02 (d, $J = 8.7$ Hz, 2H, OArH), 7.13 (d, $J = 8.7$ Hz, 2H, OArH), 10.07 (br s, 1H, pyrrole NH); ¹³C NMR (CDCl₃, 75 MHz) δ 29.5, 37.1, 40.3, 52.5, 53.2, 68.7, 68.8, 110.2, 114.7, 114.8, 115.5, 117.6, 117.7, 129.3, 130.3, 127.6, 129.6, 133.1, 133.1, 133.2, 133.3, 157.0, 157.8, 159.3, 171.9, 190.1; HRMS (ES) 517.2321 (MH⁺) C₃₀H₃₃N₂O₆ requires 517.2339.

(S)-Methyl 2-(5-undec-10-enoyl-1H-pyrrole-2-carboxamido)pent-4-enoate 2.59

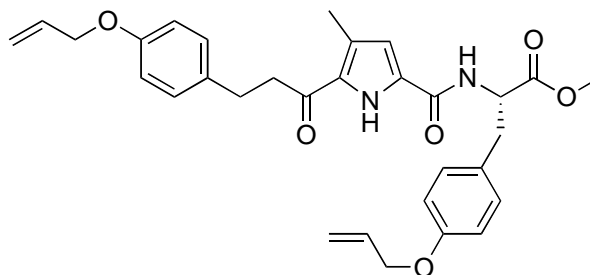
Carboxylic acid **2.55** (419 mg, 1.50 mmol) was coupled to amino acid **2.63** (314 mg, 1.80 mmol) according to general procedure F and the crude product was purified by flash chromatography (4:1 petroleum ether / ethyl acetate) to afford acyclic diene **2.59** as a pale yellow oil (280 mg, 48%). $R_f = 0.38$ (4:1 petroleum ether / ethyl acetate); $^1\text{H NMR}$ (CDCl_3 , 600 MHz) δ 1.26-1.37 (m, 10H, $(\text{CH}_2)_2(\text{CH}_2)_5\text{CH}_2\text{CHCH}_2$), 1.68-1.73 (m, 2H, $\text{CH}_2\text{CH}_2(\text{CH}_2)_5\text{CH}_2\text{CHCH}_2$), 2.03 (q, $J = 7.0$ Hz, 2H, $(\text{CH}_2)_2(\text{CH}_2)_5\text{CH}_2\text{CHCH}_2$), 2.57-2.63 (m, 1H, NHCHCHH), 2.67-2.72 (m, 1H, NHCHCHH), 2.77 (t, $J = 7.2$ Hz, 2H, COCH_2), 3.79 (s, 3H, OCH_3), 4.86 (q, $J = 6.4$ Hz, 1H, NHCH), 4.93 (d, $J = 10.2$ Hz, 1H, $(\text{CH}_2)_8\text{CHCHH}$), 4.99 (d, $J = 18.0$ Hz, 1H, $(\text{CH}_2)_8\text{CHCHH}$), 5.15 (d, $J = 13.5$ Hz, 2H, $\text{CHCH}_2\text{CHCH}_2$), 5.65-5.76 (m, 1H, $\text{CHCH}_2\text{CHCH}_2$), 5.77-5.84 (m, 1H, $(\text{CH}_2)_8\text{CHCH}_2$), 6.57 (br d, $J = 7.8$ Hz, 1H, NHCH), 6.60 (br s, 1H, pyrrole **H**), 6.83 (br s, 1H, pyrrole **H**), 9.97 (br s, 1H, pyrrole **NH**); $^{13}\text{C NMR}$ (CDCl_3 , 150 MHz) δ 24.8, 28.9, 29.0, 29.1, 29.2, 29.3, 33.8, 36.6, 38.4, 51.6, 52.6, 110.1, 114.1, 115.4, 119.5, 129.5, 132.0, 133.5, 139.2, 159.5, 172.1, 191.3; HRMS (ES) 389.2427 (MH^+); $\text{C}_{22}\text{H}_{33}\text{N}_2\text{O}_4$ requires 389.2435.

Methyl (2S)-2-[[5-[3-(4-allyloxyphenyl)propanoyl]-4-methyl-1H-pyrrole-2-carbonyl]amino]pent-4-enoate 2.60

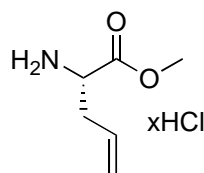
Carboxylic acid **2.56** (184 mg, 0.60 mmol) was coupled to amino acid **2.63** (112 mg, 0.68 mmol) according to general procedure F and the crude product was purified by flash chromatography (1:1 petroleum ether / ethyl acetate) to afford the acyclic diene **2.60** as a yellow oil (235 mg, 94%). $R_f = 0.67$ (1:1 petroleum ether/ethyl acetate); $^1\text{H NMR}$ (CDCl_3 , 600 MHz) δ 2.34 (s, 3H, pyrrole CH_3), 2.55-2.69 (m, 2H, $\text{CHCH}_2\text{CHCH}_2$), 2.96-2.99 (m,

2H, ArCH₂CH₂), 3.02-3.05 (m, 2H, ArCH₂CH₂), 3.76 (s, 3H, OCH₃), 4.50 (d, $J = 6.0$ Hz, 2H, OCH₂CHCH₂), 4.85 (q, $J = 6.4$ Hz, 1H, CHCH₂CHCH₂), 5.13-5.15 (m, 2H, CHCH₂CHCH₂), 5.26-5.28 (m, 1H, OCH₂CHCHH), 5.38-5.41 (m, 1H, OCH₂CHCHH), 5.69-5.76 (m, 1H, CHCH₂CHCH₂), 6.01-6.07 (m, 1H, OCH₂CHCH₂), 6.43 (s, 1H, pyrrole H), 6.74-6.78 (m, 1H, NHCH), 6.83 (d, $J = 8.4$ Hz, 2H, OArH), 7.13 (d, $J = 8.4$ Hz, 2H, OArH), 9.99 (br s, 1H, pyrrole NH); ¹³C NMR (CDCl₃, 150MHz) δ 14.2, 28.8, 36.5, 40.1, 51.6, 52.5, 68.8, 113.0, 114.7, 117.4, 119.3, 129.2, 126.5, 127.6, 130.7, 132.0, 133.2, 133.4, 156.9, 159.6, 172.2, 190.1; HRMS (ES) 425.2060 (MH⁺); C₂₄H₂₉N₂O₅ requires 425.2071.

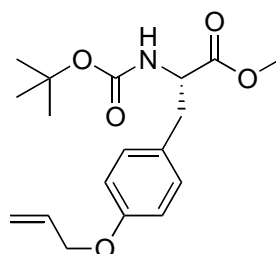
Methyl (2S)-3-(4-allyloxyphenyl)-2-[[5-[3-(4-allyloxyphenyl)propanoyl]-4-methyl-1H-pyrrole-2-carbonyl]amino]propanoate **2.61**



Carboxylic acid **2.56** (235 mg, 0.75 mmol) was coupled to amino acid **2.66** (354 mg, 0.80 mmol) according to general procedure G and the crude product was purified by flash chromatography (2:1 ethyl acetate / petroleum ether) to afford the acyclic diene **2.61** as a yellow oil (330 mg, 83%). $R_f = 0.83$ (2:1 ethyl acetate / petroleum ether); ¹H NMR (CDCl₃, 300 MHz) δ 2.31 (pyrrole CH₃), 2.91-3.19 (m, 6H, ArCH₂CH₂, ArCH₂CH), 3.72 (s, 3H, OCH₃), 4.46-4.49 (m, 4H, 2 × OCH₂CHCH₂), 5.01 (q, $J = 6.6$ Hz, 1H, NHCH), 5.24-5.27 (m, 2H, 2 × OCH₂CHCHH) 5.35-5.42 (m, 2H, 2 × OCH₂CHCHH), 5.96-6.09 (m, 2H, 2 × OCH₂CHCH₂), 6.36 (d, $J = 2.7$ Hz, 1H, pyrrole H or NHCH), 6.79-6.85 (m, 5H, pyrrole H or NHCH, OArH), 7.03 (d, $J = 8.4$ Hz, 2H, OArH), 7.11 (d, $J = 8.4$ Hz, 2H, OArH), 10.11 (br s, 1H, pyrrole NH); ¹³C NMR (CDCl₃, 75 MHz) δ 14.3, 29.0, 37.1, 42.2, 52.6, 53.4, 68.8, 68.9, 113.3, 114.8, 114.9, 117.6, 117.7, 129.4, 130.3, 126.7, 127.8, 127.9, 130.9, 133.3, 133.4, 133.5, 157.0, 157.8, 159.7, 172.4, 190.3; HRMS (ES) 553.2294 (MNa⁺); C₃₁H₃₄N₂NaO₆ requires 553.2309.

Methyl (2S)-2-aminopent-4-enoate hydrochloride, 2.63¹⁰

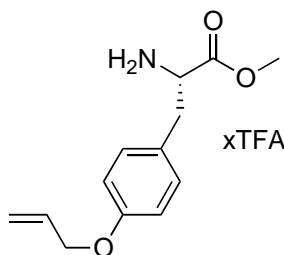
To a solution of L-allylglycine **2.62** (587 mg, 5.00 mmol) in anhydrous methanol (10 mL) at 0 °C was added thionyl chloride (1.90 g, 16.00 mmol) in portions under a nitrogen atmosphere. The resulting solution was stirred at 0 °C for 10 min, then warmed to room temperature, and stirred overnight. Volatiles were removed *in vacuo* to afford amino acid **2.63** as a white crystalline solid (847 mg, 100%). mp 88-90 °C, lit. mp 91-92 °C;¹⁰ ¹H NMR (CDCl₃, 300 MHz) δ 2.86 (br s, 2H, CHCH₂CHCH₂), 3.81 (s, 3H, OCH₃), 4.26 (br s, 1H, CHCH₂CHCH₂), 5.27 (d, *J* = 10.2 Hz, 1H, CHCH₂CHCH₂H), 5.34 (d, *J* = 17.1 Hz, 1H, CHCH₂CHCH₂H), 5.80-5.94 (m, 1H, CHCH₂CHCH₂), 8.80 (br s, 3H, N⁺H₃); ¹³C NMR (CDCl₃, 75 MHz) δ 34.5, 52.9, 53.1, 121.5, 130.1, 169.1. Experimental data as per literature.¹⁰

Methyl (2S)-3-(4-allyloxyphenyl)-2-(tert-butoxycarbonylamino)propanoate, 2.65

To a solution of *O*-allyl-*N*-tert-butyloxycarbonyl-L-tyrosine **2.64** (1.61 g, 5.00 mmol) in anhydrous DMF (20 mL) were sequentially added NaHCO₃ (555 mg, 6.60 mmol) and MeI (2.67 g, 18.80 mmol). The reaction mixture was stirred at room temperature for 50 h, then poured into ice-water (150 mL), and extracted with ethyl acetate (75 mL, 2 × 50 mL). The combined organic fractions were washed with saturated NaHCO₃ (2 × 50 mL), water (2 × 50 mL) and brine (50 mL), dried over Na₂SO₄ and volatiles were removed *in vacuo* to obtain amino acid **2.65** as yellow crystals (1.68 g, 100%). mp 38-39 °C; ¹H NMR (CDCl₃, 300 MHz) δ 1.42 (s, 9H, C(CH₃)₃), 3.00-3.04 (m, 2H, ArCH₂), 3.71 (s, 3H, OCH₃), 4.50-4.57 (m, 3H, OCH₂CHCH₂, NHCH), 4.96 (br d, *J* = 7.8 Hz, 1H, NH), 5.26-5.31 (m, 1H,

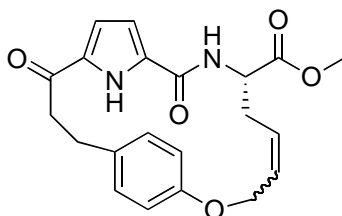
OCH₂CHCHH), 5.37-5.44 (m, 1H, OCH₂CHCHH), 5.99-6.11 (m, 1H, OCH₂CHCH₂), 6.84 (d, *J* = 8.7 Hz, 2H, OArH), 7.03 (d, *J* = 8.7 Hz, 2H, OArH); ¹³C NMR (CDCl₃, 50 MHz) δ 28.3, 37.6, 52.1, 54.6, 68.8, 79.9, 114.9, 117.6, 128.2, 130.3, 133.4, 155.1, 157.8, 172.4; HRMS (ES) 358.1652 (MNa⁺), C₁₈H₂₅NNaO₅ requires 358.1625.

Methyl (2*S*)-3-(4-allyloxyphenyl)-2-amino-propanoate trifluoroacetate, **2.66**



Trifluoroacetic acid (5 mL) was added under a stream of nitrogen to a cooled solution of amino acid **2.65** (1.01 g, 3.00 mmol) in anhydrous dichloromethane (20 mL) at 0 °C. The reaction mixture was subsequently warmed to room temperature, and then stirred for 5 h. Volatiles were removed *in vacuo* to give amino acid **2.66** as light brown crystals (1.32 g, 100%). fractionated melting, mp₁ 38-40 °C, mp₂ 87-100 °C; ¹H NMR (CDCl₃, 300 MHz) δ 3.11-3.28 (m, 2H, ArCH₂), 3.75 (s, 3H, OCH₃), 4.20-4.25 (m, 1H, ArCH), 4.48-4.50 (m, 2H, OCH₂CHCH₂), 5.28 (dd, *J* = 10.4 and 1.4 Hz, 1H, OCH₂CHCHH), 5.39 (dd, *J* = 17.4 and 1.4 Hz, 1H, OCH₂CHCHH), 5.96-6.09 (m, 1H, OCH₂CHCH₂), 6.86 (d, *J* = 8.4 Hz, 2H, OArH), 7.08 (d, *J* = 8.4 Hz, 2H, OArH), 8.35 (br s, 3H, N⁺H₃); ¹³C NMR (CDCl₃, 75 MHz) δ 35.3, 53.3, 54.3, 68.8, 115.5, 117.8, 124.7, 130.3, 133.0, 158.6, 161.6, 169.4, CF₃COOH was not found; HRMS (ES) 236.1296 (MH⁺); C₁₃H₁₈NO₃ requires 236.1287.

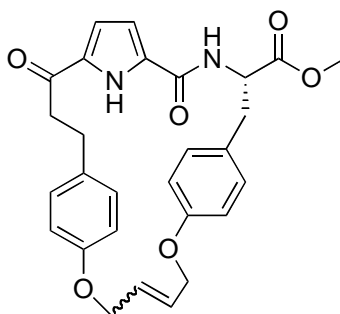
Macrocyclic ester **2.67**



Acyclic diene **2.57** (209 mg, 0.51 mmol) was subjected to RCM according to General Procedure H and purified by flash chromatography (2:1 ethyl acetate / petroleum ether) to give a mixture of *cis* and *trans* macrocycles, **2.67** as a yellow oil (103 mg, 53%). R_f = 0.42

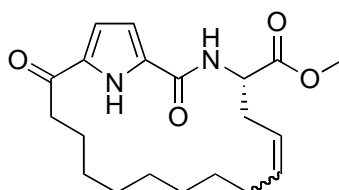
(2:1 ethyl acetate / petroleum ether); ^1H NMR (CDCl_3 , 300 MHz) δ 2.27-2.37 (m, 1H, $\text{OCH}_2\text{CHCHCHH}$), 2.87-3.06 (m, 5H, ArCH_2CH_2 , $\text{OCH}_2\text{CHCHCHH}$), 3.81 (s, 3H, OCH_3), 4.42-4.62 (m, 2H, $\text{OCH}_2\text{CHCHCH}_2$), 4.93 (dt, $J = 9.1$ and 3.9 Hz, 1H, NHCH), 5.60-5.77 (m, 2H, $\text{OCH}_2\text{CHCHCH}_2$), 6.23 (d, $J = 8.7$ Hz, 1H, NHCH), 6.34 (dd, $J = 4.1$ and 2.3 Hz, 1H, pyrrole **H**), 6.58-6.61 (m, 3H, OArH and pyrrole **H**), 6.89 (d, $J = 7.8$ Hz, 2H, OArH), 8.83 (br s, 1H, pyrrole NH); ^{13}C NMR (CDCl_3 , 75 MHz) δ 33.6, 36.2, 41.5, 50.9, 52.8, 66.0, 109.9, 114.5, 116.1, 128.1, 128.9, 129.4, 130.2, 131.5, 134.7, 156.2, 158.9, 172.0, 192.2; HRMS (ES) 383.1616 (MH^+); $\text{C}_{21}\text{H}_{23}\text{N}_2\text{O}_5$ requires 383.1601.

Macrocyclic ester **2.68**



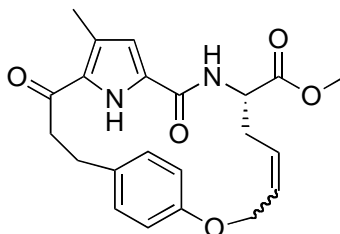
Acyclic diene **2.58** (150 mg, 0.29 mmol) was subjected to RCM according to General Procedure H and purified by flash chromatography (2:1 ethyl acetate / petroleum ether) to give a mixture of *cis* and *trans* macrocycles, **2.68** as a greenish-brown oil (88 mg, 62 %). $R_f = 0.51$ (2:1 ethyl acetate / petroleum ether); ^1H NMR (CDCl_3 , 300 MHz) δ 2.64-2.71 (m, 1H, ArCHHCH_2), 2.82 (dd, $J = 9.6$ and 13.8 Hz, 1H, NHCHCHH), 2.92-3.12 (m, 3H, ArCHHCH_2), 3.33 (dd, $J = 4.4$ and 14.0 Hz, 1H, NHCHCHH), 3.84 (s, 3H, OCH_3), 4.41-4.66 (m, 4H, $\text{OCH}_2\text{CHCHCH}_2$), 4.84-4.94 (m, 1H, NHCHCH_2), 5.82-5.84 (m, 2H, $\text{OCH}_2\text{CHCHCH}_2$), 6.07-6.13 (m, 2H, pyrrole **H**), 6.61 (d, $J = 8.6$ Hz, 2H, OArH), 6.68 (d, $J = 10.8$ Hz, 1H, NHCH), 6.75 (d, $J = 8.7$ Hz, 2H, OArH), 6.89 (d, $J = 8.6$ Hz, 2H, OArH), 7.02 (d, $J = 8.7$ Hz, 2H, OArH), 9.49 (br s, 1H, pyrrole NH); ^{13}C NMR (CDCl_3 , 75 MHz) δ 32.5, 36.6, 40.1, 52.9, 53.3, 68.3, 68.6, 110.1, 115.1, 115.9, 116.7, 128.1, 128.4, 128.8, 129.6, 130.2, 130.5, 132.7, 134.2, 157.4, 157.7, 159.8, 173.1, 191.8; HRMS (ES) 489.2009 (MH^+); $\text{C}_{28}\text{H}_{29}\text{N}_2\text{O}_6$ requires 489.2020.

(S)-Methyl 2,16-dioxo-3,20-diazabicyclo[15.2.1]icosa-1(19),6,17-triene-4-carboxylate
2.69



Acyclic diene **2.59** (308 mg, 0.79 mmol) was subjected to RCM according to general procedure H and purified by flash chromatography (2:1 petroleum ether / ethyl acetate) to give a mixture of *cis* and *trans* macrocycles **2.69** as a brown oil (100 mg, 35%). $R_f = 0.65$ (2:1 petroleum ether / ethyl acetate); $^1\text{H NMR}$ (CDCl_3 , 300 MHz) δ 0.53-0.58 (m, 1H, $\text{CO}(\text{CH}_2)_6\text{CHH}$), 0.68-0.52 (m, 1H, $\text{CO}(\text{CH}_2)_6\text{CHH}$), 0.80-0.91 (m, 3H, $\text{CO}(\text{CH}_2)_4\text{CH}_2\text{CHH}$), 0.97-1.05 (m, 1H, $\text{CO}(\text{CH}_2)_5\text{CHH}$), 1.12-1.13 (m, 1H, $\text{CO}(\text{CH}_2)_2\text{CHH}$), 1.21-1.31 (m, 2H, $\text{CO}(\text{CH}_2)_2\text{CHHCHH}$), 1.39-1.43 (m, 1H, $\text{CO}(\text{CH}_2)_3\text{CHH}$), 1.72-1.83 (m, 2H, $\text{CO}(\text{CH}_2)_7\text{CH}_2$), 1.87-1.88 (m, 1H, $\text{COCH}_2\text{CH}_2(\text{CH}_2)_6$), 2.17-2.22 (m, 1H, NHCHCHH), 2.50-2.53 (m, 1H, $\text{COCHH}(\text{CH}_2)_7$), 2.84-2.86 (m, 1H, NHCHCHH), 2.89-2.93 (m, 1H, $\text{COCHH}(\text{CH}_2)_7$), 3.81 (s, 3H, OCH_3), 4.88-4.92 (dt, $J = 9.5$ and 4.5 Hz, 1H, NHCHCO), 5.19-5.24 (m, 1H, $\text{NHCHCH}_2\text{CHCH}$), 5.30-5.35 (m, 1H, $\text{NHCHCH}_2\text{CHCH}$), 6.31 (d, $J = 7.8$ Hz, 1H, NHCHCO), 6.64-6.65 (m, 1H, pyrrole **H**), 6.88-6.89 (m, 1H, pyrrole **H**), 10.02 (br s, 1H, pyrrole **NH**); $^{13}\text{C NMR}$ (CDCl_3 , 75 MHz) δ 26.4, 28.1, 29.0, 29.4, 29.6, 29.7, 29.8, 33.4, 37.0, 38.8, 51.5, 52.7, 110.2, 115.9, 122.9, 134.2, 137.0, 159.4, 172.5, 193.6; HRMS (ES) 361.2110 (MH^+); $\text{C}_{20}\text{H}_{29}\text{N}_2\text{O}_4$ requires 361.2122.

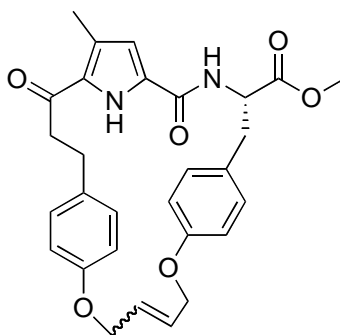
Macrocyclic ester 2.70



Acyclic diene **2.60** (31 mg, 0.07 mmol) was subjected to RCM according to General Procedure H and purified by flash chromatography (2:1 ethyl acetate / petroleum ether) to

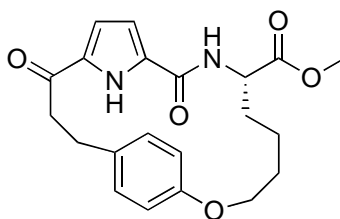
give a mixture of *cis* and *trans* macrocycles, **2.70** as a greenish-brown oil (20 mg, 71%). $R_f = 0.38$ (2:1 ethyl acetate / petroleum ether); $^1\text{H NMR}$ (CDCl_3 , 600 MHz) δ 2.22-2.29 (m, 1H, $\text{OCH}_2\text{CHCHCHH}$), 2.31 (s, 3H, pyrrole CH_3), 2.75-3.09 (m, 5H, ArCH_2CH_2 , $\text{OCH}_2\text{CHCHCHH}$), 3.79 (s, 3H, OCH_3), 4.47-4.66 (m, 2H, $\text{OCH}_2\text{CHCHCH}_2$), 4.95 (dt, $J = 9.8$ Hz, 3.6 Hz, 1H, NHCH), 5.59-5.63 (m, 1H, $\text{OCH}_2\text{CHCHCH}_2$), 5.71-5.76 (m, 1H, $\text{OCH}_2\text{CHCHCH}_2$), 6.20 (d, $J = 9.8$ Hz, 1H, CONH), 6.23 (d, $J = 1.8$ Hz, 1H, pyrrole H), 6.67 (br s, 2H, OArH), 6.96 (br s, 2H, OArH), 8.33 (br s, 1H, pyrrole NH); $^{13}\text{C NMR}$ (CDCl_3 , 150 MHz) δ 13.3, 33.4, 37.1, 42.4, 50.8, 52.9, 65.8, 111.6, 115.0, 126.8, 130.4, 128.0, 129.2, 129.3, 132.1, 156.2, 158.6, 172.1, 192.4; HRMS (ES) 397.1780 (MH^+); $\text{C}_{22}\text{H}_{25}\text{N}_2\text{O}_5$ requires 397.1758.

Macrocyclic ester **2.71**



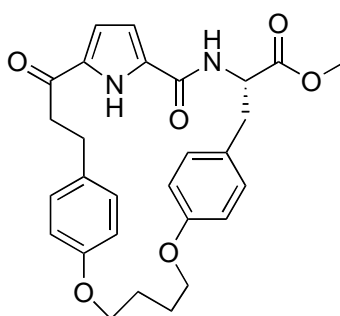
Acyclic diene **2.61** (318 mg, 0.60 mmol) was subjected to RCM according to General Procedure H and purified by flash chromatography (1:1 ethyl acetate / petroleum ether) to give a mixture of *cis* and *trans* macrocycles, **2.71** as a greenish-brown oil (45 mg, 15%). $R_f = 0.37$ (1:1 ethyl acetate / petroleum ether); $^1\text{H NMR}$ (CDCl_3 , 300 MHz) δ 2.17 (s, 3H, pyrrole CH_3), 2.75-3.09 (m, 5H, $\text{ArCCH}_2\text{CH}_2$, NHCHCHH), 3.34 (dd, $J = 4.1$ and 13.7 Hz, 1H, NHCHCHH), 3.80 (s, 3H, OCH_3), 4.47-4.59 (m, 4H, $\text{OCH}_2\text{CHCHCH}_2$), 4.93-5.03 (m, 1H, NHCH), 5.82-5.91 (m, 2H, $\text{OCH}_2\text{CHCHCH}_2$), 6.19 (d, $J = 2.7$ Hz, 1H, pyrrole H), 6.40 (d, $J = 8.7$ Hz, 1H, NHCH), 6.66 (d, $J = 8.7$ Hz, 2H, OArH), 6.72 (d, $J = 8.7$ Hz, 2H, OArH), 6.94-7.03 (m, 4H, OArH), 9.39 (br s, 1H, pyrrole NH); $^{13}\text{C NMR}$ (CDCl_3 , 75 MHz) δ 14.1, 31.1, 37.4, 40.7, 52.9, 53.1, 68.4, 68.5, 113.2, 114.4, 114.8, 115.5, 115.6, 127.0, 127.6, 128.2, 128.8, 129.7, 130.4, 131.5, 133.0, 156.9, 158.0, 159.6, 172.7, 191.6; HRMS (ES) 503.2169 (MH^+); $\text{C}_{29}\text{H}_{31}\text{N}_2\text{O}_6$ requires 503.2177.

Macrocyclic ester **2.72**



Macrocyclic **2.67** (124 mg, 0.32 mmol) was hydrogenated according to General Procedure I, purified by flash chromatography (2:1 ethyl acetate / petroleum ether) and recrystallized from ethyl acetate to give compound **2.72** as a white needle-like crystals (84 mg, 67%). mp 198-200 °C; R_f = 0.47 (2:1 ethyl acetate / petroleum ether); $^1\text{H NMR}$ (CDCl_3 , 600 MHz) δ 1.33-1.40 (m, 1H, $\text{O}(\text{CH}_2)_2\text{CHHCH}_2$), 1.45-1.52 (m, 1H, $\text{O}(\text{CH}_2)_2\text{CHHCH}_2$), 1.64-1.70 (m, 1H, $\text{OCH}_2\text{CHH}(\text{CH}_2)_2$), 1.72-1.81 (m, 2H, $\text{OCH}_2\text{CHHCH}_2\text{CHH}$), 2.31-2.37 (m, 1H, $\text{OCH}_2\text{CH}_2\text{CH}_2\text{CHH}$), 2.83-2.95 (m, 3H, ArCHHCH_2), 3.04-3.08 (m, 1H, ArCHHCH_2), 3.80 (s, 3H, OCH_3), 3.89-3.92 (m, 1H, $\text{OCHH}(\text{CH}_2)_3$), 4.03-4.06 (m, 1H, $\text{OCHH}(\text{CH}_2)_3$), 4.75-4.78 (m, 1H, NHCH), 6.37-6.40 (m, 2H, pyrrole **H**, OArH), 6.50 (d, J = 3.6 Hz, 1H, NHCH), 6.61 (br s, 1H, OArH), 6.77 (br s, 1H, pyrrole **H**), 6.81 (br s, 1H, OArH), 7.18 (br s, 1H, OArH), 8.34 (br s, 1H, pyrrole **NH**); $^{13}\text{C NMR}$ (CDCl_3 , 150 MHz, 0°C) δ 19.1, 27.3, 29.4, 33.8, 42.3, 51.9, 52.7, 65.1, 109.3, 112.0, 115.6, 116.3, 128.3, 129.1, 129.7, 131.7, 134.9, 157.3, 158.7, 172.5, 191.9; HRMS (ES) 385.1778 (MH^+); $\text{C}_{21}\text{H}_{25}\text{N}_2\text{O}_5$ requires 385.1758.

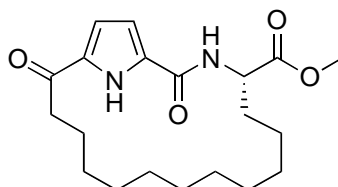
Macrocyclic ester **2.73**



Macrocyclic **2.68** (44 mg, 0.09 mmol) was hydrogenated according to General Procedure I and purified by flash chromatography (2:1 ethyl acetate / petroleum ether) to give compound **2.73** as a yellow oil (40 mg, 91 %). R_f = 0.58 (2:1 ethyl acetate / petroleum

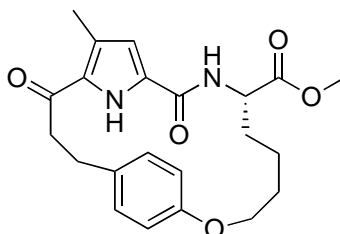
ether); ^1H NMR (CDCl_3 , 600 MHz) δ 1.88-1.98 (m, 4H, $\text{OCH}_2\text{CH}_2\text{CH}_2\text{CH}_2\text{O}$), 2.67-2.71 (m, 1H, ArCHHCH_2), 2.93-3.03 (m, 3H, ArCH_2CH_2 , NHCHCHH), 3.11 (dt, $J = 12.0$ and 5.0 Hz, 1H, ArCHHCH_2), 3.42 (dd, $J = 14.1$ and 5.0 Hz, 1H, NHCHCHH), 3.84 (s, 3H, OCH_3), 3.88 (t, $J = 5.7$ Hz, 2H, $(\text{CH}_2)_2\text{ArOCH}_2$), 3.95-4.04 (m, 2H, $\text{CH}_2\text{OArCH}_2\text{CH}$), 4.85 (q, $J = 7.2$ Hz, 1H, NHCH), 6.08-6.12 (m, 2H, pyrrole **H**), 6.16 (d, $J = 7.2$ Hz, 1H, NHCH), 6.64 (d, $J = 8.7$ Hz, 2H, OArH), 6.72 (d, $J = 8.7$ Hz, 2H, OArH), 6.88-6.92 (m, 4H, OArH), 9.71 (br s, 1H, pyrrole **NH**); ^{13}C NMR (CDCl_3 , 150 MHz) δ 25.3, 25.4, 32.8, 36.0, 40.1, 52.7, 53.1, 67.0, 67.4, 110.0, 114.0, 114.7, 116.8, 127.1, 129.6, 130.3, 129.8, 132.2, 134.4, 157.3, 158.0, 159.3, 172.0, 191.9; HRMS (ES) 491.2195 (MH^+); $\text{C}_{28}\text{H}_{32}\text{N}_2\text{O}_6$ requires 491.2177.

(S)-Methyl 2,16-dioxo-3,20-diazabicyclo[15.2.1]icosa-1(19),17-diene-4-carboxylate 2.74



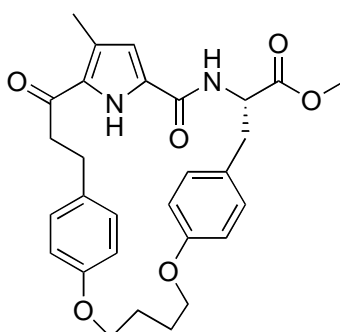
Macrocyclic **2.69** was hydrogenated according to general procedure I and purified by flash chromatography (2:1 petroleum ether / ethyl acetate) to give macrocycle **2.74** as a white oil (79 mg, 79%). $R_f = 0.29$ (2:1 petroleum ether / ethyl acetate); ^1H NMR (CDCl_3 , 600 MHz) δ 0.80-0.94 (m, 2H, $\text{CO}(\text{CH}_2)_8\text{CH}_2$), 0.96-1.13 (m, 2H, $\text{CO}(\text{CH}_2)_3\text{CH}_2$), 1.18-1.38 (m, 12H, $\text{CO}(\text{CH}_2)_2\text{CH}_2\text{CH}_2(\text{CH}_2)_4\text{CH}_2\text{CH}_2\text{CH}_2$), 1.68-1.75 (m, 1H, $\text{CO}(\text{CH}_2)_{10}\text{CHH}$), 1.78-1.88 (m, 2H, COCH_2CH_2), 2.17-2.25 (m, 1H, $\text{CO}(\text{CH}_2)_{10}\text{CHH}$), 2.60 (br s, 1H, COCHH), 2.92 (br s, 1H, COCHH), 3.80 (s, 3H, OCH_3), 4.93 (dt, $J = 8.0$ and 3.9 Hz, 1H, NHCH_3), 6.66 (br s, 1H, NHCH), 6.71 (s, 1H, pyrrole **H**), 6.91-6.92 (m, 1H, pyrrole **H**), 10.19 (br s, 1H, pyrrole **NH**); ^{13}C NMR (CDCl_3 , 150 MHz) δ 23.9, 26.5, 27.5, 28.3, 28.4, 28.8, 28.9, 29.2, 29.7, 30.1, 39.0, 52.4, 52.6, 110.6, 116.3, 130.1, 134.0, 159.4, 172.8, 194.1; HRMS (ES) 363.2274 (MH^+); $\text{C}_{20}\text{H}_{31}\text{N}_2\text{O}_4$ requires 363.2278.

Macrocyclic ester **2.75**



Macrocycle **2.70** (50 mg, 0.13 mmol) was hydrogenated according to General Procedure I, purified by flash chromatography (2:1 ethyl acetate / petroleum ether) and recrystallised from ethyl acetate to give compound **2.75** as white round crystals (51 mg, 88%). mp 193-195 °C; $R_f = 0.55$ (2:1 ethyl acetate / petroleum ether); $^1\text{H NMR}$ (CDCl_3 , 600 MHz) δ 1.33-1.40 (m, 1H, $\text{O}(\text{CH}_2)_2\text{CHHCH}_2$), 1.46-1.53 (m, 1H, $\text{O}(\text{CH}_2)_2\text{CHHCH}_2$), 1.70-1.79 (m, 1H, $\text{O}(\text{CH}_2)_3\text{CHH}$), 2.31-2.37 (m, 1H, $\text{O}(\text{CH}_2)_3\text{CHH}$), 2.35 (s, 3H, pyrrole CH_3), 2.71-2.75 (m, 1H, ArCH_2CHH), 2.85 (dt, $J = 8.4$ and 3.0 Hz, 1H, ArCHHCH_2), 2.95 (dt, $J = 8.4$ and 3.2 Hz, 1H, ArCH_2CHH), 3.06-3.09 (m, 1H, ArCHHCH_2), 3.79 (s, 3H, OCH_3), 3.92-3.95 (m, 1H, $\text{OCHH}(\text{CH}_2)_3$), 4.12-4.15 (m, 1H, $\text{OCHH}(\text{CH}_2)_3$), 4.74-4.77 (m, 1H, NHCH), 6.21 (d, $J = 1.8$ Hz, 1H, pyrrole H), 6.29 (d, $J = 7.8$ Hz, 1H, CONH), 6.36 (br s, 1H, OArH), 6.55 (br s, 1H, OArH), 6.89 (br s, 2H, OArH), 7.91 (br s, 1H, pyrrole NH); $^{13}\text{C NMR}$ (CDCl_3 , 150 MHz) δ 13.5, 19.3, 27.1, 29.6, 33.8, 43.2, 51.6, 52.7, 65.1, 110.9, 112.8, 116.3, 127.1, 128.1, 129.4, 129.7, 130.7, 132.2, 157.1, 158.6, 172.6, 192.3; HRMS (ES) 399.1906 (MH^+), $\text{C}_{22}\text{H}_{27}\text{N}_2\text{O}_5$ requires 399.1915.

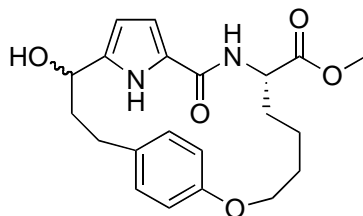
Macrocyclic ester **2.76**



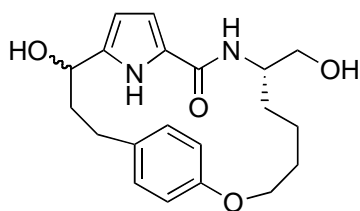
Macrocycle **2.71** (45 mg, 0.09 mmol) was hydrogenated according to General Procedure I and purified by flash chromatography (2:1 ethyl acetate / petroleum ether) to give compound **2.76** as a off white oil (44 mg, 98%). $R_f = 0.63$ (2:1 ethyl acetate / petroleum

ether); ^1H NMR (CDCl_3 , 300 MHz) δ 1.88-1.99 (m, 4H, $\text{OCH}_2\text{CH}_2\text{CH}_2\text{CH}_2\text{O}$), 2.10 (s, 3H, pyrrole CH_3), 2.78-3.16 (m, 5H, ArCH_2CH_2 , NHCHCHH), 3.40 (dd, $J = 4.8$ and 13.8 Hz, 1H, NHCHCHH), 3.81 (s, 3H, OCH_3), 3.86-3.99 (m, 4H, $2 \times \text{ArOCH}_2$), 4.89-4.95 (m, 1H, NHCH), 6.15 (d, $J = 2.7$ Hz, 1H, pyrrole H), 6.15 (d, $J = 8.1$ Hz, 1H, NHCH), 6.64 (d, $J = 8.7$ Hz, 2H, OArH), 6.71 (d, $J = 8.7$ Hz, 2H, OArH), 6.92 (d, $J = 8.7$ Hz, 2H, OArH), 6.94 (d, $J = 8.7$ Hz, 2H, OArH), 9.64 (br s, 1H, pyrrole NH); ^{13}C NMR (CDCl_3 , 75 MHz) δ 14.1, 25.4, 25.5, 32.0, 36.6, 40.4, 52.9, 53.3, 67.3, 67.5, 113.5, 114.3, 114.7, 127.0, 127.5, 127.9, 129.8, 130.5, 131.8, 132.2, 157.4, 158.1, 159.5, 172.4, 192.3; HRMS (ES) 505.2322 (MH^+); $\text{C}_{29}\text{H}_{33}\text{N}_2\text{O}_6$ requires 505.2333.

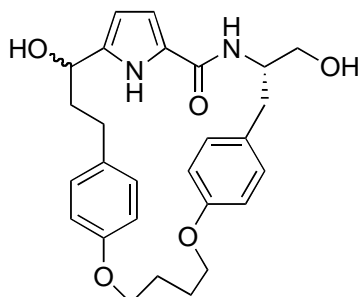
Macrocyclic ester **2.77**



Macrocyclic **2.72** (10 mg, 0.03 mmol) was reduced according to General Procedure J1 and the crude residue was purified by flash chromatography (4:1 ethyl acetate / petroleum ether) to give a white solid, alcohol **2.77** (5 mg, 50%), as a 1:1 mixture of isomers. mp 110-113 °C; $R_f = 0.28$ (4:1 ethyl acetate / petroleum ether); ^1H NMR for both isomer from mixture (CDCl_3 , 600 MHz) δ 1.32-1.42 (m, 2H, $2 \times \text{OCH}_2\text{CH}_2\text{CHHCH}_2$), 1.48-1.67 (m, 4H, $2 \times \text{OCH}_2\text{CHHCHHCH}_2$), 1.69-1.83 (m, 4H, $2 \times \text{OCH}_2\text{CHHCH}_2\text{CHH}$), 2.19-2.42 (m, 6H, $2 \times \text{OCH}_2\text{CH}_2\text{CH}_2\text{CHH}$, $2 \times \text{ArCH}_2\text{CH}_2$), 2.57-2.61 (m, 2H, $\text{ArCCH}_2\text{CH}_2$), 2.91-2.96 (m, 2H, ArCH_2CH_2), 3.80 (s, 6H, $2 \times \text{OCH}_3$), 3.92-4.03 (m, 4H, $2 \times \text{OCH}_2(\text{CH}_2)_3$), 4.67-4.75 (m, 4H, $2 \times \text{CHOH}$, $2 \times \text{NHCH}$), 5.90-5.93 (m, 1H, pyrrole H (isomer A)), 6.00-6.01 (m, 1H, pyrrole H (isomer B)), 6.19-6.20 (m, 1H, pyrrole H (isomer A)), 6.26-6.32 (m, 3H, pyrrole H (isomer B), $2 \times \text{NHCH}$), 6.49 (d, 4H, $J = 7.5$ Hz, OArH), 6.72 (d, 2H, $J = 7.5$ Hz, OArH), 6.75 (d, 2H, $J = 7.5$ Hz, OArH); ^{13}C NMR for both isomer from mixture (CDCl_3 , 150 MHz) δ 18.8, 18.9, 27.3, 27.4, 29.3, 29.4, 30.3, 30.4, 36.6, 37.4, 51.4, 51.6, 52.5, 65.1, 65.2, 68.3, 68.9, 106.1, 108.6, 108.9, 109.8, 113.7, 123.7, 124.9, 128.9, 129.0, 131.7, 132.3, 137.2, 139.5, 159.9, 160.0, 162.6, 172.9; HRMS (ES) 409.1727 (MNa^+); $\text{C}_{21}\text{H}_{26}\text{N}_2\text{NaO}_5$ requires 409.1734.

Macrocyclic diol 2.78

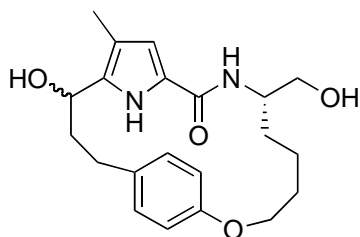
Macrocycle **2.72** (50 mg, 0.13 mmol) was reduced according to General Procedure J2 and recrystallized from ethyl acetate to give a white solid, alcohol **2.78** (38 mg, 81%), as a 1:1 mixture of isomers. mp 232-234 °C; $R_f = 0.1$ (4:1 ethyl acetate / petroleum ether); ^1H NMR for both isomer from mixture (CD_3OD , 600 MHz) δ 1.30-1.54 (m, 8H, $2 \times \text{OCH}_2\text{CHHCH}_2\text{CHH}$), 1.61-1.70 (m, 4H, $2 \times \text{OCH}_2\text{CHHCH}_2\text{CHH}$), 2.09-2.15 (m, 2H, ArCH_2CH_2 (isomer A)), 2.19-2.28 (m, 2H, ArCH_2CH_2 (isomer B)), 2.36-2.40 (m, 2H, ArCH_2CH_2 (isomer A)), 2.74-2.81 (m, 2H, ArCH_2CH_2 (isomer B)), 3.34-3.41 (m, 4H, $2 \times \text{CH}_2\text{OH}$), 3.84-4.06 (m, 6H, $2 \times \text{NHCH}$, $2 \times \text{OCH}_2(\text{CH}_2)_3$), 4.56-4.58 (m, 1H, CHOH (isomer B)), 4.61-4.63 (m, 1H, CHOH (isomer A)), 5.80 (d, $J = 3.6$ Hz, 1H pyrrole **H**), 5.85 (d, $J = 3.6$ Hz, 1H pyrrole **H**), 6.30 (d, $J = 3.6$ Hz, 1H, pyrrole **H**), 6.35-6.37 (m, 5H, pyrrole **H**, OArH), 6.60-6.62 (m, 4H, OArH). NH and OH signals not observed; ^{13}C NMR for both isomer from mixture (CD_3OD , 150 MHz) δ 23.1, 23.2, 29.1, 29.5, 31.0, 31.2, 31.8, 31.9, 38.0, 39.2, 55.9, 57.8, 66.7, 67.8, 67.9, 69.7, 70.0, 108.4, 109.9, 111.3, 112.7, 115.6, 126.1, 126.9, 130.6, 130.7, 134.2, 134.3, 138.8, 140.5, 157.0, 157.3, 163.5, 163.8; HRMS (ES) 359.1959 (MH^+); $\text{C}_{20}\text{H}_{27}\text{N}_2\text{O}_4$ requires 359.1965.

Macrocyclic diol 2.79

Macrocycle **2.73** (40 mg, 0.08 mmol) was reduced according to General Procedure J2 to give a white amorphous solid, alcohol **2.79** (33 mg, 87%), as a 3:1 mixture of isomers. mp 83-86 °C; $R_f = 0.14$ (4 : 1 ethyl acetate / petroleum ether); ^1H NMR for major isomer from

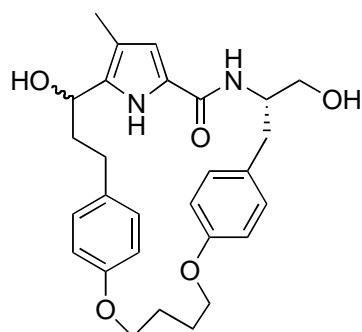
mixture (CD₃OD, 600 MHz) δ 1.77-1.96 (m, 5H, OCH₂CH₂CH₂CH₂O, ArCH₂CHH), 2.17-2.22 (m, 1H, ArCH₂CHH), 2.41-2.47 (m, 1H, ArCHHCH₂), 2.56-2.62 (m, 1H, ArCHHCH₂), 2.79 (dd, J = 7.8 and 14.3 Hz, 1H, NHCHCHHAr), 2.99 (dd, J = 3.3 and 14.3 Hz, 1H, NHCHCHHAr), 3.51-3.66 (m, 2H, CH₂OH), 3.88-4.13 (m, 4H, OCH₂(CH₂)₂CH₂O), 4.22-4.28 (m, 1H, NHCH), 4.37 (dd, J = 6.0 and 8.4 Hz, 1H, CHOH), 6.12 (d, J = 3.6 Hz, 1H, pyrrole H), 6.69 (d, J = 10.2 Hz, 2H, OArH), 6.73-6.79 (m, 5H, OArH, pyrrole H), 7.07 (d, J = 8.4 Hz, 2H, OArH). NH and OH peaks not observed; ¹³C NMR for major isomer from mixture (CD₃OD, 150 MHz) δ 26.4, 26.5, 31.7, 36.8, 40.2, 54.2, 65.1, 68.3, 68.6, 68.9, 108.9, 114.2, 115.7, 116.5, 126.9, 130.8, 131.6, 132.3, 135.8, 140.1, 158.6, 159.5, 163.8; HRMS (ES) 465.2368 (MH⁺); C₂₇H₃₃N₂O₅ requires 465.2384.

Macrocyclic diol **2.80**



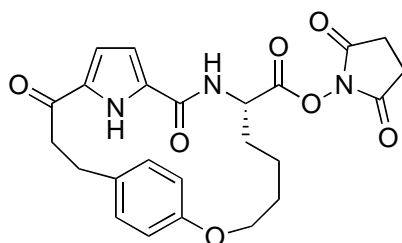
Macrocyclic **2.75** (28 mg, 0.07 mmol) was reduced according to General Procedure J2 and recrystallised from ethyl acetate to give a white round solid, alcohol **2.80** (16 mg, 62%), as a 3:1 mixture of isomers. fractionated melting, mp₁ 179-180, mp₂ 207-209 °C; R_f = 0.05 (4:1 ethyl acetate / petroleum ether); ¹H NMR for major isomer from mixture (CD₃OD, 600 MHz) δ 1.38-1.64 (m, 4H, OCH₂CHHCH₂CHH), 1.68-1.79 (m, 2H, OCH₂CHHCH₂CHH), 2.06 (s, 3H, pyrrole CH₃), 2.26-2.35 (m, 3H, ArCH₂CHH), 2.87-2.91 (m, 1H, ArCH₂CHH), 3.42-3.52 (m, 2H, CH₂OH), 3.92-3.96 (m, 1H, OCHH(CH₂)₃), 4.02-4.08 (m, 1H, NHCH), 4.14-4.17 (m, 1H, OCHH(CH₂)₃), 4.68-4.76 (m, 1H, CHOH), 6.21 (s, 1H, pyrrole H), 6.31 (s, 1H, pyrrole H), 6.35-6.49 (m, 2H, OArH), 6.72 (d, J = 7.8 Hz, 2H, OArH). NH and OH signals not observed; ¹³C NMR for major isomer from mixture (CD₃OD, 150 MHz) δ 23.3, 29.0, 31.0, 32.1, 37.6, 51.5, 66.7, 67.6, 68.0, 112.6, 115.6, 118.4, 125.3, 130.2, 134.1, 134.8, 156.9, 163.6; HRMS (ES) 371.2113 (MH⁺); C₂₁H₂₉N₂O₄ requires 371.2122.

Macrocyclic diol **2.81**



Macrocyclic **2.76** (40 mg, 0.08 mmol) was reduced according to General Procedure J2 and purified by flash chromatography (ethyl acetate) to give a white solid, alcohol **2.80** (38 mg, 100%), as a 2.3:1 mixture of isomers. mp 108-110 °C; $R_f = 0.25$ (4:1 ethyl acetate / petroleum ether); ^1H NMR for major isomer from mixture (CD_3OD , 600 MHz) δ 1.81-1.91 (m, 5H, $\text{OCH}_2\text{CH}_2\text{CH}_2\text{CH}_2\text{O}$, ArCH_2CHH), 2.05 (s, 3H, pyrrole CH_3), 2.14-2.21 (m, 1H, ArCHHCH_2), 2.24-2.33 (m, 1H, ArCH_2CHH), 2.57-2.64 (m, 1H, ArCHHCH_2), 2.71-2.77 (m, 1H, ArCHHCH), 2.99 (dd, $J = 14.1$ and 2.7 Hz, 1H, ArCHHCH), 3.58-3.66 (m, 2H, CH_2OH), 3.93-4.08 (m, 4H, $\text{OCH}_2(\text{CH}_2)_2\text{CH}_2\text{O}$), 4.21-4.25 (m, 1H, CHOH), 4.61-4.64 (m, 1H, NHCH), 6.56 (s, 1H, pyrrole H), 6.61 (s, 2H, OArH), 6.67 (d, $J = 7.8$ Hz, 1H, OArH), 6.73-6.75 (m, 2H, OArH), 6.78 (d, $J = 8.4$ Hz, 1H, OArH), 7.13 (d, $J = 8.4$ Hz, 2H, OArH), NH and OH signals not observed; ^{13}C NMR for major isomer from mixture (CD_3OD , 150 MHz) δ 11.7, 26.4, 26.5, 31.4, 37.4, 40.7, 54.6, 66.0, 67.5, 68.5, 69.0, 114.2, 115.8, 116.4, 119.0, 125.6, 130.5, 131.9, 132.4, 135.8, 136.2, 158.3, 159.4, 163.9; HRMS (ES) 479.2514 (MH^+); $\text{C}_{28}\text{H}_{35}\text{N}_2\text{O}_5$ requires 479.2540.

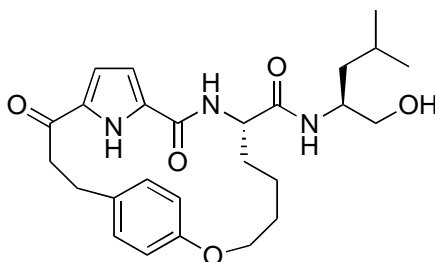
Attempted synthesis of macrocycle **2.84**



Macrocyclic ester **2.72** (30 mg, 0.08 mmol) was hydrolysed to its corresponding carboxylic acid **2.83** according to general procedure K, and was dissolved in THF (3 mL), to which *N*-hydroxysuccinimide (11 mg, 0.10 mmol) was added. The solution was cooled to 0 °C

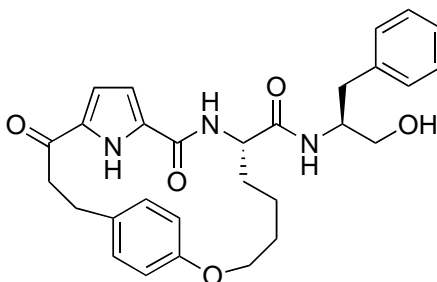
before addition of EDCI (20 mg, 0.1 mmol) or HATU (38 mg, 0.1 mmol) in dichloromethane (3 mL) and stirred for 24 h under a nitrogen atmosphere at ambient temperature. Volatiles were removed *in vacuo*, the resulting residue resuspended in dichloromethane, washed with 1M aqueous HCl (20 mL) and saturated NaHCO₃ (20 mL); dried (Na₂SO₄) and volatiles removed *in vacuo*. ¹H NMR and MS analysis of product showed reaction did not proceed. Macrocycle **2.83** recovered (5 mg, 14%).

Macrocyclic alcohol **2.85**



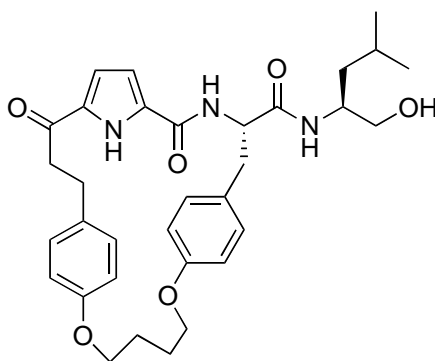
Macrocyclic ester **2.72** (29 mg, 0.08 mmol) was hydrolysed according to general procedure K to its corresponding carboxylic acid, which was coupled to (L)-Leucinol according to general procedure G and the crude product was purified by flash chromatography (ethyl acetate) to give macrocyclic alcohol **2.85** as a white oil (30 mg, 83%). $R_f = 0.24$ (ethyl acetate); $[\alpha]_D = +1.4$ (c 0.1 in (CH₃)₂SO); ¹H NMR (CDCl₃, 600 MHz) δ 0.87 (d, $J = 2.4$ Hz, 3H, CH₂CH(CH₃)₂), 0.89 (d, $J = 2.4$ Hz, 3H, CH₂CH(CH₃)₂), 1.33-1.43 (m, 2H, CH₂CH(CH₃)₂), 1.44-1.66 (m, 4H, CH₂CH(CH₃)₂, OCH₂CHHCH₂CH₂), 1.70-1.76 (m, 1H, OCH₂CHH(CH₂)₂), 1.80-1.86 (m, 1H, O(CH₂)₃CHH), 2.20-2.26 (m, 1H, O(CH₂)₃CHH), 2.89-2.95 (m, 4H, ArCHHCH₂, CH₂OH), 3.00-3.04 (m, 1H, ArCHHCH₂), 3.66-3.67 (m, 1H, CHHOH), 3.75-3.77 (m, 1H, CHHOH), 3.89-3.93 (m, 1H, OCHH(CH₂)₃), 3.96-4.00 (m, 1H, OCHH(CH₂)₃), 4.07-4.09 (m, 1H, NHCHCH₂OH), 4.79-4.80 (m, 1H, NHCHCO), 6.38-6.39 (m, 1H, pyrrole H), 6.52 (br s, 2H, OArH), 6.62 (s, 1H, pyrrole H), 6.72 (d, $J = 7.8$ Hz, 1H, NHCHCO), 6.78 (d, $J = 7.2$ Hz, 1H, NHCHCH₂OH), 6.85 (br s, 2H, OArH), 9.13 (br s, 1H, pyrrole NH); ¹³C NMR (CDCl₃, 150 MHz) δ 22.4, 22.7, 24.9, 27.9, 31.0, 33.8, 40.1, 41.8, 49.7, 52.8, 65.4, 65.8, 109.5, 112.0, 115.6, 116.5, 128.3, 129.2, 129.7, 131.2, 135.2, 157.2, 159.5, 171.3, 192.9; HRMS (ES) 470.2636 (MH⁺); C₂₆H₃₆N₃O₅ requires 470.2649.

Macrocyclic alcohol **2.86**



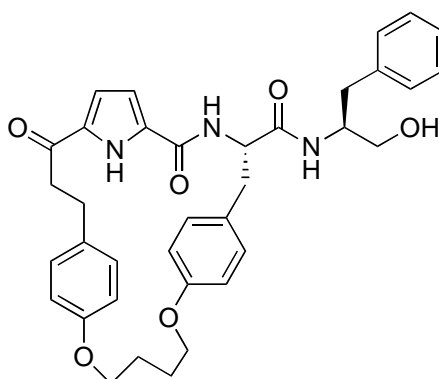
Macrocyclic ester **2.72** (69 mg, 0.18 mmol) was hydrolysed according to general procedure K to its corresponding carboxylic acid, which was coupled to (L)-Phenalaninol according to general procedure G and the crude product was purified by flash chromatography (ethyl acetate) to give macrocyclic alcohol **2.86** as a white oil (32 mg, 36%). $R_f = 0.13$ (ethyl acetate); $[\alpha]_D = +1.3$ (c 0.2 in $(\text{CH}_3)_2\text{SO}$); $^1\text{H NMR}$ (CDCl_3 , 600 MHz) δ 1.42-1.55 (O(CH₂)₂CH₂CH₂), 1.59-1.62 (OCH₂CHH(CH₂)₂), 1.72-1.82 (m, 2H, OCH₂CHHCH₂CHH), 2.19-2.22 (m, 1H, OCH₂CH₂CH₂CHH), 2.83-2.91 (m, 3H, ArCHHCH₂, CHCH₂Ar), 2.92-3.03 (m, 3H, ArCHHCH₂), 3.17 (br s, 1H, CH₂OH), 3.69-3.75 (m, 2H, CH₂OH), 3.87-3.90 (m, 1H, OCHH(CH₂)₃), 3.94-3.97 (m, 1H, OCHH(CH₂)₃), 4.20-4.21 (m, 1H, CHCH₂Ar), 4.88 (br s, 1H, NHCHCO), 6.33-6.34 (m, 1H, pyrrole H), 6.53 (br s, 2H, OArH), 6.58-6.60 (m, 2H, NHCHCO, pyrrole H), 6.82 (br s, 2H, OArH), 7.16-7.26 (m, 6H, 5 x ArH, NHCHCH₂OH), 9.43 (br s, 1H, pyrrole NH); $^{13}\text{C NMR}$ (CDCl_3 , 150 MHz) δ 19.9, 28.1, 31.1, 33.9, 37.1, 41.7, 52.6, 52.7, 63.1, 65.8, 109.8, 117.0, 126.6, 128.6, 129.2, 129.3, 129.4, 131.0, 135.3, 137.6, 157.2, 159.5, 171.1, 193.3; HRMS (ES) 504.2481 (MH^+); $\text{C}_{29}\text{H}_{34}\text{N}_3\text{O}_5$ requires 504.2493.

Macrocyclic alcohol **2.87**



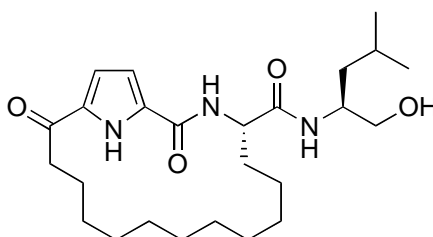
Macrocyclic ester **2.73** (40 mg, 0.08 mmol) was hydrolysed according to general procedure K to its corresponding carboxylic acid, which was coupled to (L)-Leucinol according to general procedure G and the crude product was purified by flash chromatography (4:1 ethyl acetate / petroleum ether) to give macrocyclic alcohol **2.87** as a white solid (25 mg, 54%). mp 122-125 °C; $R_f = 0.28$ (4:1 ethyl acetate / petroleum ether); $[\alpha]_D = +4.0$ (c 0.1 in $(\text{CH}_3)_2\text{SO}$); $^1\text{H NMR}$ (CDCl_3 , 600 MHz) δ 0.84, (d, $J = 3.3$ Hz, 3H, $\text{CH}_2\text{CH}(\text{CH}_3)_2$), 0.85 (d, $J = 3.3$ Hz, 3H, $\text{CH}_2\text{CH}(\text{CH}_3)_2$), 1.30-1.38 (m, 2H, $\text{CH}_2\text{CH}(\text{CH}_3)_2$), 1.53-1.58 (m, 1H, $\text{CH}_2\text{CH}(\text{CH}_3)_2$), 1.92-1.95 (m, 4H, $\text{OCH}_2\text{CH}_2\text{CH}_2\text{CH}_2\text{O}$), 2.67-2.70 (m, 1H, ArCH_2CHH), 2.91-3.04 (m, 3H, ArCH_2CH_2 , CHCHHAr), 3.13-3.18 (m, 1H, ArCH_2CHH), 3.34 (dd, $J = 14.4$ and 4.8 Hz, 1H, CHCHHAr), 3.50 (br s, 1H, CH_2OH), 3.72 (d, $J = 9.9$ Hz, 1H, CHHOH), 3.82 (d, $J = 9.9$ Hz, 1H, CHHOH), 3.85-3.98 (m, 4H, $\text{OCH}_2(\text{CH}_2)_2\text{CH}_2\text{O}$), 4.08-4.14 (m, 1H, CHCH_2OH), 4.98 (q, $J = 7.2$ Hz, 1H, CHCH_2Ar), 6.11-6.12 (m, 1H, pyrrole **H**), 6.16-6.17 (m, 1H, pyrrole **H**), 6.45 (d, $J = 7.5$ Hz, 1H, NHCHCO), 6.65 (d, $J = 8.4$ Hz, 2H, OArH), 6.73 (d, $J = 8.1$ Hz, 2H, OArH), 6.91 (d, $J = 8.4$ Hz, 2H, OArH), 7.01 (d, $J = 8.1$ Hz, 2H, OArH), 7.40 (d, $J = 9.0$ Hz, 1H, NHCHCH_2OH), 10.53 (br s, 1H, pyrrole **NH**); $^{13}\text{C NMR}$ (CDCl_3 , 150 MHz) δ 22.4, 22.7, 24.9, 25.2, 25.3, 32.7, 37.2, 40.1, 40.2, 49.2, 53.9, 64.6, 67.1, 67.3, 110.2, 114.2, 114.6, 117.7, 127.9, 129.5, 130.1, 130.4, 132.0, 134.5, 157.4, 157.9, 160.0, 171.2, 192.7; HRMS (ES) 576.30682 (MH^+); $\text{C}_{33}\text{H}_{42}\text{N}_3\text{O}_6$ requires 576.30681.

Macrocyclic alcohol **2.88**



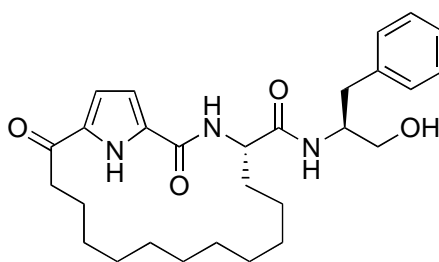
Macrocyclic ester **2.73** (40 mg, 0.08 mmol) was hydrolysed according to general procedure K to its corresponding carboxylic acid, which was coupled to (L)-Phenalaninol according to general procedure G and the crude product was purified by flash chromatography (4:1 ethyl acetate / petroleum ether) to give macrocyclic alcohol **2.88** as a white solid (28 mg, 55%). mp 118-120 °C; $R_f = 0.28$ (4:1 ethyl acetate / petroleum ether); $[\alpha]_D = +1.4$ (c 0.2 in $(\text{CH}_3)_2\text{SO}$); $^1\text{H NMR}$ (CDCl_3 , 600 MHz) δ 1.92-1.99 (m, 4H, $\text{OCH}_2\text{CH}_2\text{CH}_2\text{CH}_2\text{O}$), 2.70-2.73 (m, 1H, ArCH_2CHH), 2.84 (d, $J = 7.8$ Hz, 2H, CHCH_2Ar), 2.95-3.05 (m, 3H, ArCH_2CH_2 , CHCHHArO), 3.17-3.21 (m, 1H, ArCH_2CHH), 3.34 (dd, $J = 14.4$ and 6 Hz, 1H, CHCHHArO), 3.76-3.85 (m, 3H, CH_2OH), 3.90-4.02 (m, 4H, $\text{OCH}_2(\text{CH}_2)_2\text{CH}_2\text{O}$), 4.22-4.26 (m, 1H, CHCH_2Ar), 5.15 (q, $J = 7$ Hz, 1H, CHCH_2ArO), 6.07-6.08, 6.14-6.15 (m, 2H, 2 \times pyrrole **H**), 6.32 (d, $J = 7$ Hz, 1H, NHCHCO), 6.66 (d, $J = 8.4$ Hz, 2H, OArH), 6.73 (d, $J = 8.4$ Hz, 2H, OArH), 6.92 (d, $J = 8.4$ Hz, 2H, OArH), 6.97 (d, $J = 8.4$ Hz, 2H, OArH), 7.10-7.12 (m, 1H, ArH), 7.16-7.19 (m, 4H, ArH), 7.78 (d, $J = 7.8$ Hz, 1H, NHCHCH_2OH), 10.78 (br s, 1H, pyrrole **NH**); $^{13}\text{C NMR}$ (CDCl_3 , 150 MHz) δ 25.3, 25.4, 32.9, 37.1, 37.2, 40.5, 52.5, 53.3, 62.9, 67.0, 67.4, 110.0, 114.1, 114.5, 118.2, 126.4, 127.7, 128.4, 129.3, 129.6, 130.3, 130.6, 132.0, 134.4, 138.0, 157.4, 157.9, 159.8, 171.1, 183.0; HRMS (ES) 610.29114 (MH^+); $\text{C}_{36}\text{H}_{40}\text{N}_3\text{O}_6$ requires 610.29116.

(S)-N-((S)-1-Hydroxy-4-methylpentan-2-yl)-2,16-dioxo-3,20-diazabicyclo[15.2.1]icosa-1(19),17-diene-4-carboxamide **2.89**

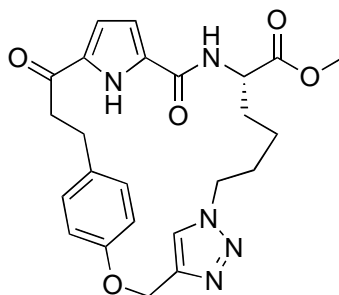


Macrocyclic ester **2.74** (61 mg, 0.17 mmol) was hydrolysed according to general procedure K to its corresponding carboxylic acid, which was coupled to (L)-Leucinol according to general procedure G and the crude product was purified by flash chromatography (4:1 ethyl acetate / petroleum ether) to give macrocyclic alcohol **2.89** as a white oil (42 mg, 62%). $R_f = 0.30$ (4:1 ethyl acetate / petroleum ether); $[\alpha]_D = +1.3$ (c 0.2 in $(\text{CH}_3)_2\text{SO}$); ^1H NMR (CDCl_3 , 600 MHz) δ 0.84 (d, $J = 6.0$ Hz, 3H, $\text{CH}_2\text{CH}(\text{CH}_3)_2$), 0.88 (d, $J = 7.2$ Hz, 3H, $\text{CH}_2\text{CH}(\text{CH}_3)_2$), 0.85-1.35 (m, 18H, $\text{CO}(\text{CH}_2)_2(\text{CH}_2)_8$, $\text{CH}_2\text{CH}(\text{CH}_3)_2$), 1.58-1.59 (m, 2H, $\text{CO}(\text{CH}_2)_{10}\text{CHH}$, $\text{CH}_2\text{CH}(\text{CH}_3)_2$), 1.66-1.67 (m, 2H, COCH_2CH_2), 1.77-1.79 (m, 1H, $\text{CO}(\text{CH}_2)_{10}\text{CHH}$), 2.61-2.62 (m, 1H, COCHH), 2.88-2.90 (m, 1H, COCHH), 3.20-3.24 (m, 1H, CHHOH), 3.28-3.33 (m, 1H, CHHOH), 3.81 (br d, $J = 4.2$ Hz, 1H, NHCHCH_2OH), 4.48 (t, $J = 8.7$ Hz, 1H, NHCHCO), 4.62 (t, $J = 5.1$ Hz, 1H, CH_2OH), 6.81 (s, 1H, pyrrole **H**), 6.91 (s, 1H, pyrrole **H**), 7.66 (d, $J = 8.4$ Hz, 1H, NHCHCH_2OH), 8.41 (d, $J = 8.4$ Hz, 1H, NHCHCO), 12.16 (br s, 1H, pyrrole **NH**); ^{13}C NMR (CDCl_3 , 150 MHz) δ 21.8, 23.4, 24.2, 25.9, 26.9, 27.3, 27.5, 27.7, 27.9, 28.1, 28.6, 31.5, 38.2, 48.7, 52.6, 63.7, 114.0, 115.0, 131.0, 134.0, 159.1, 171.5, 193.0; HRMS (ES) 448.3149 (MH^+); $\text{C}_{25}\text{H}_{42}\text{N}_3\text{O}_4$ requires 448.3170.

(S)-N-((S)-1-hydroxy-3-phenylpropan-2-yl)-2,16-dioxo-3,20-diazabicyclo[15.2.1]icosa-1(19),17-diene-4-carboxamide **2.90**



Macrocyclic ester **2.74** (79 mg, 0.22 mmol) was hydrolysed according to general procedure K to its corresponding carboxylic acid, which was coupled to (L)-Phenalaninol according to general procedure G and the crude product was purified by flash chromatography (ethyl acetate) to give macrocyclic alcohol **2.90** as a white oil (62 mg, 58%). $R_f = 0.60$ (ethyl acetate); $[\alpha]_D = +1.6$ (c 0.2 in $(\text{CH}_3)_2\text{SO}$); $^1\text{H NMR}$ (CDCl_3 , 600 MHz) δ 0.64-1.47 (m, 16H, $\text{CO}(\text{CH}_2)_2(\text{CH}_2)_8$), 1.74-1.80 (m, 1H, $\text{CO}(\text{CH}_2)_{10}\text{CHH}$), 1.81-1.86(m, 2H, COCH_2CH_2), 2.12 (br s, 1H, $\text{CO}(\text{CH}_2)_{10}\text{CHH}$), 2.51 (br s, 1H, COCHH), 2.88-2.92(m, 2H, CH_2Ar), 3.08 (br s, 1H, COCHH), 3.77 (s, 2H, CH_2OH), 4.10-4.18 (m, 1H, CH_2OH), 4.24 (q, $J = 8.0$ Hz, 1H, NHCHCH_2OH), 5.36 (br s, 1H, NHCHCO), 6.74 (s, 1H, pyrrole **H**), 6.95-6.98 (m, 2H, pyrrole **H**, NHCH), 7.14-7.26 (m, 5H, ArH), 8.19 (br s, 1H, NHCH), 11.42 (br s, 1H, pyrrole NH); $^{13}\text{C NMR}$ (CDCl_3 , 150 MHz) δ 24.8, 26.7, 27.2, 28.1, 28.8, 29.1, 29.3, 29.4, 29.6, 31.8, 37.3, 38.9, 52.3, 53.5, 62.5, 110.4, 117.9, 126.4, 128.4, 129.4, 131.0, 134.0, 138.2, 159.7, 171.7, 195.4; HRMS (ES) 482.2991 (MH^+); $\text{C}_{28}\text{H}_{40}\text{N}_3\text{O}_4$ requires 482.3013.

Macrocyclic ester 2.91

Method 1: To a solution of tripeptide **2.93** (16 mg, 0.03 mmol) in acetonitrile (10 mL) and H₂O (1 mL), was added a small piece of Cu wire and stirred at 35 °C for 120 h. The solution was filtered through Celite and volatiles removed *in vacuo*. TLC and ¹H NMR of the mixture showed that the reaction had not proceeded.

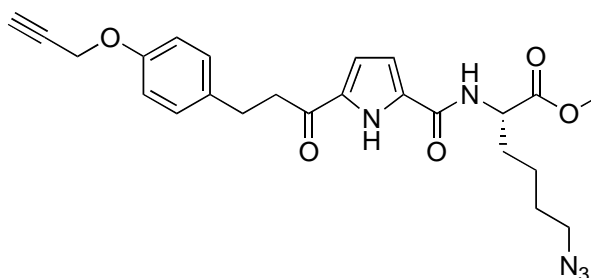
Method 2: To a solution of tripeptide **2.93** (12 mg, 0.03 mmol) in 1:1 THF / H₂O (12 mL), was added sequentially CuSO₄·5H₂O (6 mg, 0.03 mmol) and sodium ascorbate (5 mg, 0.03 mmol) in H₂O (0.7 mL). The reaction was stirred vigorously at ambient temperature for 20 h, filtered through Celite and volatiles removed *in vacuo*. TLC and ¹H NMR of the mixture showed that the reaction had not proceeded.

Method 3: To a solution of tripeptide **2.93** (12 mg, 0.03 mmol) in 2:1 *t*-BuOH / H₂O (27 mL), was added sequentially Cu nanopowder (1.6 mg, 0.03 mmol) and Et₃N·HCl (3.5 mg, 0.03 mmol). The reaction was stirred vigorously at ambient temperature for 72 h, filtered through Celite and volatiles removed *in vacuo*. TLC and ¹H NMR of the mixture showed that the reaction had not proceeded.

Method 4: To a solution of tripeptide **2.93** (12 mg, 0.03 mmol) in toluene (26 mL) was added DBU (12 mg, 0.08 mmol) and the solution was degassed under nitrogen atmosphere for 30 min. The solution was then heated to 110 °C before addition of CuBr (33 mg, 0.03 mmol) and stirred for 20 h at 110 °C under nitrogen atmosphere. The resulting mixture was cooled, filtered through Celite, volatiles removed *in vacuo* and the crude residue was purified by preparative TLC (4:1 ethyl acetate / petroleum ether) to give macrocycle **2.91** as a yellow gum (3.1 mg, 25%). *R_f* = 0.21 (4:1 ethyl acetate / petroleum ether); ¹H NMR (CDCl₃, 600 MHz) δ 1.36-1.50 (m, 2H, CHCH₂CH₂(CH₂)₂N), 1.78-1.84 (m, 1H,

CHCHH(CH₂)₃N), 1.89-1.94 (m, 1H, CH(CH₂)₂CHHCH₂N), 2.02-2.06 (m, 1H, CH(CH₂)₂CHHCH₂N), 2.10-2.15 (m, 1H, CHCHH(CH₂)₂CH₂N), 2.66-2.68 (m, 1H, ArCHHCH₂), 2.96 (dt, *J* = 12.9 and 4.2 Hz, 1H, ArCH₂CHH), 3.02-3.04 (m, 1H, ArCHHCH₂), 3.18 (dt, *J* = 12.0 and 4.2 Hz, 1H, ArCH₂CHH), 3.78 (s, 3H, OCH₃), 4.20-4.25 (m, 1H, CHHN), 4.35-4.39 (m, 1H, CHHN), 4.78-4.81 (m, 1H, CHNH), 5.14 (d, *J* = 14.4 Hz, 1H, OCHH), 5.22 (d, *J* = 14.4 Hz, 1H, OCHH), 6.22-6.23 (m, 1H, pyrrole H), 6.31-6.32 (m, 1H, pyrrole H), 6.41 (d, *J* = 7.8 Hz, CHNH), 6.74 (d, *J* = 7.8 Hz, 2H, OArH), 6.93 (d, *J* = 8.4 Hz, 2H, OArH), 7.33 (s, 1H, triazole CH), 9.60 (br s, 1H, pyrrole NH); ¹³C NMR (CDCl₃, 150 MHz) δ 22.0, 29.4, 30.7, 33.1, 39.9, 49.8, 52.0, 52.8, 62.3, 110.1, 115.0, 117.2, 122.1, 129.7, 132.3, 134.6, 135.2, 144.5, 157.0, 159.4, 172.2, 192.1; HRMS (ES) 488.1928 (MNa⁺), C₂₄H₂₇N₅NaO₅ requires 488.1904.

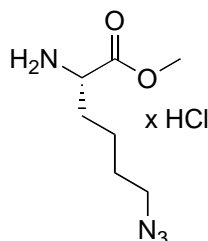
(S)-Methyl 6-azido-2-(5-(3-(4-(prop-2-ynoxy)phenyl)propanoyl)-1H-pyrrole-2-carboxamido)hexanoate 2.93



Carboxylic acid **2.96** (31 mg, 0.10 mmol) was coupled to amino acid **2.95** (27 mg, 0.12 mmol) according to general procedure F and the crude product purified by flash chromatography (1:1 petroleum ether / ethyl acetate) to afford tripeptide **2.93** as a pale yellow oil (16 mg, 33%). *R_f* = 0.47 (1:1 petroleum ether / ethyl acetate); ¹H NMR (CDCl₃, 600 MHz) δ 1.41-1.51 (m, 2H, CHCH₂CH₂(CH₂)₂N), 1.57-1.67 (m, 2H, CH(CH₂)₂CH₂CH₂N), 1.75-1.84 (m, 1H, CHCHH(CH₂)₃N), 1.91-2.05 (m, 1H, CHCHH(CH₂)₃N), 2.52 (t, *J* = 2.3 Hz, 1H, OCH₂CCH), 2.95-3.00 (m, 2H, ArCH₂CH₂), 3.05-3.11 (m, 2H, ArCH₂CH₂), 3.27 (dt, 2H, *J* = 6.6 and 1.2 Hz, CH₂N), 3.79 (s, 3H, OCH₃), 4.66 (d, *J* = 1.8 Hz, 2H, OCH₂CCH), 4.78-4.85 (m, 1H, CHNH), 6.61-6.63 (m, 1H, pyrrole H), 6.78-6.80 (m, 1H, pyrrole H), 6.88-6.92 (m, 3H, CHNH, OArH), 7.15 (d, *J* = 8.7 Hz, 2H, OArH), 10.08 (br s, 1H, pyrrole NH); ¹³C NMR (CDCl₃, 150 MHz) δ 22.5, 28.4, 29.5, 32.1, 40.2, 51.0, 52.1, 52.7, 55.9, 75.4, 78.7, 110.4, 115.0, 115.6, 129.4, 129.9,

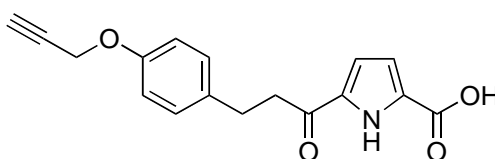
133.3, 133.9, 156.0, 159.6, 172.9, 190.1; HRMS (ES) 466.2074 (MH^+), $C_{24}H_{28}N_5O_5$ requires 466.2085.

(S)-Methyl 2-amino-6-azidohexanoate 2.95

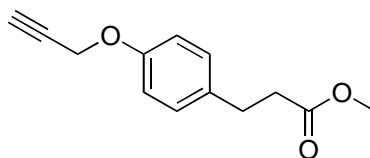


Thionyl chloride (0.2 mL, 2.60 mmol) was added drop wise to anhydrous methanol (5 mL) at 0 °C. A solution of the azide **2.104** (0.15 g, 0.60 mmol) in anhydrous methanol (10 mL) was added to the mixture, stirred at 0 °C for 1 h before warming to ambient temperature and stirred for a further 16 h. The mixture was concentrated *in vacuo*, resuspended in toluene (15 mL) and volatiles removed *in vacuo* to afford azide **21** as a yellow oil (0.15 g, 100%). 1H NMR (300 MHz, $CDCl_3$) δ 1.65 (br s, 4H, $N_3CH_2(CH_2)_3$), 2.10 (br s, 2H, $N_3CH_2(CH_2)_3$), 3.32 (br s, 2H, N_3CH_2), 3.83 (s, 3H, OCH_3), 4.15 (br s, 1H, $NHCH$), 8.57 (br s, 2H, NH); ^{13}C NMR (300 MHz, $CDCl_3$): δ 22.7, 28.5, 30.3, 46.8, 53.7, 53.9, 170.2; HRMS (ES) 187.1196 (MH^+), $C_7H_{15}N_4O_2$ requires 187.1190.

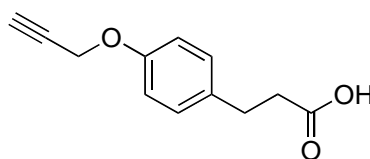
5-(3-(4-(Prop-2-ynoxy)phenyl)propanoyl)-1H-pyrrole-2-carboxylic acid 2.96



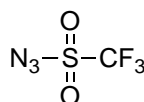
Ester **2.105** (63 mg, 0.20 mmol) was hydrolysed according to general procedure E to afford carboxylic acid **2.96** as a white solid (55 mg, 94%). mp 165-167 °C; 1H NMR ($CDCl_3$, 300 MHz) δ 2.51 (t, $J = 2.4$ Hz, 1H, OCH_2CCH), 2.99-3.04 (m, 2H, $ArCH_2CH_2$), 3.13-3.18 (m, 2H, $ArCH_2CH_2$), 4.67 (d, $J = 2.4$, 2H, OCH_2CCH), 6.88-6.93 (m, 3H, pyrrole **H**, $OArH$), 6.98-7.01 (m, 1H, pyrrole **H**), 7.16 (d, $J = 8.7$ Hz, 2H, $OArH$), 10.69 (br s, 1H, NH); ^{13}C NMR ($CDCl_3$, 75 MHz) δ 29.7, 40.7, 56.1, 75.7, 78.9, 115.2, 116.7, 117.3, 129.6, 133.9, 134.6, 139.1, 156.3, 163.7; HRMS (ES) 298.1074 (MH^+), $C_{17}H_{16}NO_4$ requires 298.1074.

Methyl 3-(4-(prop-2-ynyloxy)phenyl)propanoate 2.99^{11,12}

Methyl 3-(4-hydroxyphenyl)propanoate **2.33** (1.89 g, 10.40 mmol) was subjected to *O*-allylation according to general procedure A to afford compound **2.99** as a orange-yellow oil (2.28 g, 99%). ¹H NMR (CDCl₃, 300 MHz) δ 2.52 (t, *J* = 3.5 Hz, 1H, OCH₂CCH), 2.60 (t, *J* = 8.1 Hz, 2H, ArCH₂CH₂), 2.90 (t, *J* = 8.1 Hz, 2H, ArCH₂CH₂), 3.67 (s, 3H, OCH₃), 4.67 (d, *J* = 2.1 Hz, 2H, OCH₂CCH), 6.90 (d, *J* = 8.1 Hz, 2H, OArH), 7.13 (d, *J* = 8.1 Hz, 2H, OArH); ¹³C NMR (CDCl₃, 75 MHz) δ 30.3, 36.1, 51.8, 56.0, 75.6, 78.9, 115.1, 129.4, 133.8, 156.2, 173.5; HRMS (ES) 241.0867 (MNa⁺), C₁₃H₁₄NaO₃ requires 241.0835.

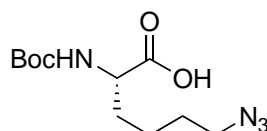
3-(4-(Prop-2-ynyloxy)phenyl)propanoic acid 2.100^{11,12}

Methyl 3-(4-(prop-2-ynyloxy)phenyl)propanoate, **2.99** (2.28 g, 10.00 mmol) was hydrolysed according to general procedure B to afford carboxylic acid **2.100** as an off-white solid (2.09 g, 98%). m.p. 80-82 °C; ¹H NMR (CDCl₃, 300 MHz) δ 2.51 (t, *J* = 2.3 Hz, 1H, OCH₂CCH), 2.63 (t, *J* = 7.8 Hz, 2H, ArCH₂CH₂), 2.89 (t, *J* = 7.8 Hz, 2H, ArCH₂CH₂), 4.66 (d, *J* = 2.4 Hz, 2H, OCH₂CCH), 6.90 (d, *J* = 8.7 Hz, 2H, OArH), 7.13 (d, *J* = 8.7 Hz, 2H, OArH), 10.08 (br s, 1H, COOH); ¹³C NMR (CDCl₃, 75 MHz) δ 30.0, 36.2, 56.0, 75.7, 78.9, 115.2, 129.5, 133.5, 156.3, 179.4; HRMS (ES) 227.0704 (MNa⁺), C₁₂H₁₂NaO₃ requires 227.0679.

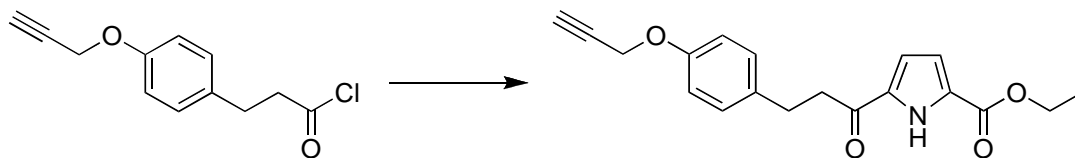
Trifluoromethanesulfonyl azide 2.102¹³

A solution of sodium azide **2.101** (3.80 g, 58.40 mmol) in anhydrous acetonitrile (60 mL) was stirred at 0 °C for 15 min and triflic anhydride (8.1 mL, 48.70 mmol) was added dropwise. The solution was stirred vigorously for 1 h at 0 °C to afford an orange solution of trifluoromethanesulfonyl azide **2.102**, which was subsequently used without further purification.¹³

(S)-6-Azido-2-(tert-butoxycarbonylamino)hexanoic acid 2.104

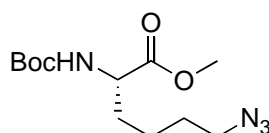


*N*_t-Boc-L-lysine **2.103** (9.92 g, 40 mmol) was dissolved in 4:1 acetonitrile / water (135 mL) and stirred for 40 min at ambient temperature. Triethylamine (17 mL, 121.80 mmol) and CuSO₄·5H₂O (0.10 g, 0.40 mmol) were added to the solution, cooled in an ice-bath and freshly prepared trifluoromethanesulfonyl azide (8.43 g, 48.00 mmol) **2.102**, was added dropwise. The solution was stirred at 0° C for 3 h, warmed to ambient temperature and stirred for a further 16 h. The resulting green solution was concentrated *in vacuo* and extracted with ethyl acetate (3 x 200 mL). The combined organic layers was washed with brine (100 mL), dried (Na₂SO₄) and concentrated *in vacuo* to give a green gum which was purified by flash chromatography (4:1 chloroform / methanol) to afford carboxylic acid **2.104** as a yellow foamy solid (4.98 g, 48%). ν_{\max} (film)/cm⁻¹ 1594, 1693, 2098, 3453; ¹H NMR (600 MHz, CDCl₃) δ 1.42 (s, 9H, *t*-butyl CH₃), 1.60-1.55 (m, 4H, N₃CH₂CH₂CH₂CH₂), 1.80 (br s, 2H, CH₂CH₂CH), 3.26 (t, 2H, *J* = 6.9 Hz, N₃CH₂), 3.92 (m, 1H, NHCH), 5.67 (br s, 1H, NH), COOH signal was not observed; ¹³C NMR (150 MHz, CDCl₃): δ 23.1, 28.4, 28.5, 31.9, 45.0, 51.3, 79.8, 156.7, 158.4; HRMS (ES) 295.1394 (MNa⁺), C₁₁H₂₀N₄NaO₄ requires 295.1277.

Methyl 5-(3-(4-(prop-2-ynoxy)phenyl)propanoyl)-1H-pyrrole-2-carboxylate 2.105

Carboxylic acid **2.100** (378 mg, 1.85 mmol) was reacted with thionyl chloride according to general procedure C to afford a dark brown oil, acid chloride **2.98** (412 mg, 100%), which was used immediately without purification. ^1H NMR (CDCl_3 , 300 MHz) δ 2.52 (t, $J = 2.4$ Hz, 1H, OCH_2CCH), 2.96 (t, $J = 7.4$ Hz, 2H, ArCH_2CH_2), 3.17 (t, $J = 7.4$ Hz, 2H, ArCH_2CH_2), 4.67 (d, $J = 2.4$ Hz, 2H, OCH_2CCH), 6.92 (d, $J = 8.7$ Hz, 2H, OArH), 7.13 (d, $J = 8.7$ Hz, 2H, OArH); ^{13}C NMR (CDCl_3 , 75 MHz) δ 30.4, 48.9, 56.0, 75.8, 78.7, 115.3, 129.5, 131.8, 156.6, 173.3.

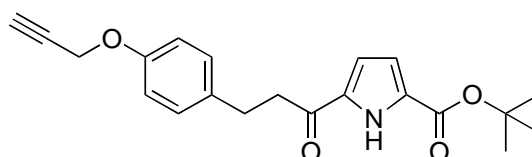
Ethyl 1H-pyrrole-2-carboxylate **2.29** (134 mg, 0.96 mmol) was coupled to acid chloride **2.98** (412 mg, 1.85 mmol) according to general procedure D and the crude product was purified by flash chromatography (4:1 petroleum ether / ethyl acetate) to afford compound **2.105** as a off-white solid (84 mg, 27%). mp 99-101 °C; $R_f = 0.37$ (4:1 petroleum ether / ethyl acetate); ^1H NMR (CDCl_3 , 300 MHz) δ 1.37 (t, $J = 7.2$ Hz, 3H, OCH_2CH_3), 2.51 (t, $J = 2.2$ Hz, 1H, OCH_2CCH), 2.97-3.02 (m, 2H, ArCH_2CH_2), 3.08-3.13 (m, 2H, ArCH_2CH_2), 4.35 (q, $J = 7.2$ Hz, 2H, OCH_2CH_3), 4.66 (d, $J = 2.2$, 2H, OCH_2CCH), 6.80-6.92 (m, 4H, pyrrole **H**, OArH), 7.16 (d, $J = 8.7$ Hz, 2H, OArH), 9.81 (br s, 1H, **NH**); ^{13}C NMR (CDCl_3 , 75 MHz) δ 14.3, 29.4, 40.2, 55.8, 61.1, 75.4, 78.6, 114.9, 115.4, 115.5, 127.2, 129.3, 133.7, 133.8, 156.0, 160.3, 190.3; HRMS (ES) 326.1409 (MH^+), $\text{C}_{19}\text{H}_{20}\text{NO}_4$ requires 326.1387.

(S)-Methyl 6-azido-2-(tert-butoxycarbonylamino)hexanoate 2.106

To a solution of carboxylic acid **2.104** (286 mg, 1.05 mmol) in anhydrous DMF (5 mL) was added sequentially NaHCO_3 (176 mg, 2.10 mmol), TBAI (38 mg, 0.10 mmol) and methyl iodide (0.45 mL, 7.20 mmol) and stirred at ambient temperature for 4 h under a

nitrogen atmosphere. The reaction mixture was poured into ice water (20 mL) and extracted with ethyl acetate (3 × 10 mL). Organic phases were combined, washed with saturated NaHCO₃ (2 × 10 mL), water (2 × 10 mL) and brine (10 mL); dried (Na₂SO₄) and concentrated *in vacuo* to give ester **2.106** as a yellow oil (172 mg, 57%). ν_{\max} (film)/cm⁻¹ 1643, 1713, 2097, 2953, 3376; ¹H NMR (CDCl₃, 300 MHz) δ 1.38-1.51 (m, 11H, *t*-butyl CH₃, CHCH₂CH₂(CH₂)₂N₃), 1.57-1.72 (m, 3H, CHCH₂CH₂CH₂CH₂N₃), 1.78-1.87 (m, 1H, CHCH₂(CH₂)₃N₃), 3.28 (t, *J* = 6.8 Hz, 2H, CH₂N₃), 3.75 (s, 3H, OCH₃), 4.31 (q, *J* = 5.4 Hz, 1H, NHCH), 5.14 (d, *J* = 7.8 Hz, 1H, NHCH), COOH signal was not observed; ¹³C NMR (CDCl₃, 75 MHz) δ 22.6, 28.4, 28.5, 32.3, 51.2, 52.4, 53.3, 80.0, 155.5, 173.2; HRMS (ES) 309.1557 (MNa⁺), C₁₂H₂₂N₄NaO₄ requires 309.1533.

Tert-butyl 5-(3-(4-(prop-2-ynoxy)phenyl)propanoyl)-1H-pyrrole-2-carboxylate
2.107

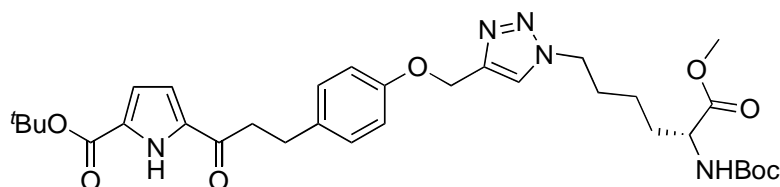


Method 1: To a solution of carboxylic acid **2.96** (48 mg, 0.16 mmol) in anhydrous dichloromethane (2 mL) and catalytic amount of DMF (70 μ L) was added oxalyl chloride (43 μ L, 0.5 mmol) in anhydrous dichloromethane (3 mL) and stirred at ambient temperature for 1 h. Volatiles were removed *in vacuo* and the resulting oil resuspended in anhydrous *t*-BuOH (6 mL), before heating the solution to 40 °C. Potassium *t*-butylate (32 mg, 0.25 mmol) was added, stirred at 40 °C for 2 h and volatiles removed *in vacuo*. The resulting oil was redissolved in dichloromethane (25 mL), washed with saturated NaHCO₃ (3 x 20 mL) and H₂O (20 mL); dried (Na₂SO₄) and volatiles removed *in vacuo* to obtain the crude product, which was purified by flash chromatography (4:1 petroleum ether / ethyl acetate) to give ester **2.107** as a yellow oil (5 mg, 9%).

Method 2: Carboxylic acid **2.96** (9.3 mg, 0.03 mmol) was converted to the acid chloride, according to General Procedure C. The acid chloride in anhydrous *t*-BuOH (2.3 mL) was heated to 40 °C before addition of potassium *t*-butoxide (6.3 mg, 0.06 mmol) and stirred for 3 h at 40 °C. The reaction was cooled, volatiles removed *in vacuo* and the resulting residue was dissolved in dichloromethane, which was washed with saturated NaHCO₃ (2 x

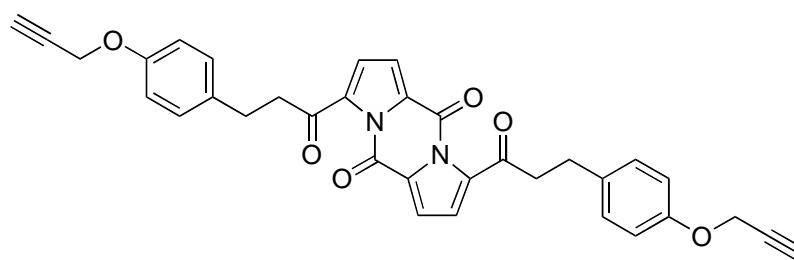
10 mL) and H₂O (2 x 10 mL); dried (Na₂SO₄) and volatiles removed *in vacuo* to give ester **2.107** as an orange-yellow oil (12 mg, 100%), which was used without further purification. ¹H NMR (CDCl₃, 300 MHz) δ 1.57 (s, 9H, OC(CH₃)₃), 2.51 (t, *J* = 2.4 Hz, 1H, OCH₂CCH), 2.96-3.02 (m, 2H, ArCH₂CH₂), 3.07-3.12 (m, 2H, ArCH₂CH₂), 4.67 (d, *J* = 2.4, 2H, OCH₂CCH), 6.79 (d, *J* = 2.7 Hz, 2H, pyrrole **H**), 6.91 (d, *J* = 8.7 Hz, 2H, OAr**H**), 7.16 (d, *J* = 8.7 Hz, 2H, OAr**H**), 9.68 (br s, 1H, NH); ¹³C NMR (CDCl₃, 75 MHz) δ 28.4, 29.7, 40.4, 56.1, 75.6, 78.9, 82.4, 115.2, 115.3, 115.7, 128.9, 129.6, 133.4, 134.1, 156.2, 159.8, 190.6; HRMS (ES) 376.1503 (MNa⁺), C₂₁H₂₃NNaO₄ requires 376.1520.

(S)-Tert-butyl 5-(3-(4-((1-(5-(tert-butoxycarbonylamino)-6-methoxy-6-oxohexyl)-1H-1,2,3-triazol-4-yl)methoxy)phenyl)propanoyl)-1H-pyrrole-2-carboxylate 2.108



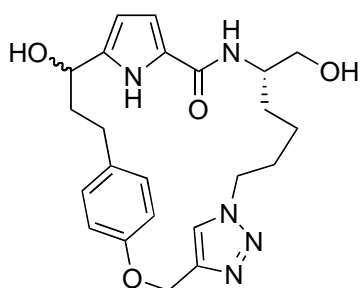
To a solution of alkyne **2.107** (33 mg, 0.1 mmol) in *t*-BuOH (1.9 mL) and H₂O (1 mL) was added sequentially azide **2.106** (29 mg, 0.1 mmol) in *t*-BuOH (0.1 mL), Cu nanopowder (1.2 mg, 0.02 mmol) and Et₃N.HCl (2.6 mg, 0.02 mmol), and stirred vigorously at ambient temperature for 144 h. The reaction was diluted with H₂O (15 mL) and extracted with dichloromethane (2 x 15 mL, 1 x 10 mL). The combined organic layers was dried over Na₂SO₄, volatiles removed *in vacuo* and purified by flash chromatography (4:1 ethyl acetate / petroleum ether) to give triazole **2.108** as a yellow oil (10 mg, 16%). R_f = 0.68 (4:1 ethyl acetate / petroleum ether); ¹H NMR (CDCl₃, 600 MHz) δ 1.31-1.44 (m, 20H, CHCH₂CH₂(CH₂)₂N, 2 x OC(CH₃)₃), 1.64-1.70 (m, 1H, CHCHH(CH₂)₃N), 1.83 (br s, 1H, CHCHH(CH₂)₃N), 1.92-1.99 (m, 2H, CH(CH₂)₂CH₂CH₂N), 2.99 (t, *J* = 7.7 Hz, 2H, ArCH₂CH₂), 3.10 (t, *J* = 7.7 Hz, 2H, ArCH₂CH₂), 3.73 (s, 3H, OCH₃), 4.30-4.39 (m, 3H, CH(CH₂)₃CH₂N), 5.08 (br d, *J* = 7.2 Hz, 1H, CHNH), 5.17 (s, 2H, OCH₂), 6.81-6.87 (m, 2H, pyrrole **H**), 6.91 (d, *J* = 8.4 Hz, 2H, OAr**H**), 7.14 (d, *J* = 8.4 Hz, 2H, OAr**H**), 7.58 (s, 1H, triazole **CH**), 9.85 (br s, 1H, pyrrole **NH**); ¹³C NMR (CDCl₃, 150 MHz) δ 22.3, 28.4, 28.7, 29.4, 29.6, 32.2, 40.2, 50.0, 52.4, 53.0, 62.1, 80.0, 81.7, 114.8, 115.4, 115.5, 122.4, 127.2, 129.4, 133.5, 133.7, 144.3, 156.7, 160.3, 173.0, 190.4; HRMS (ES) 662.3181 (MNa⁺), C₃₃H₄₅N₅NaO₈ requires 662.3160.

3,8-Bis(3-(4-(prop-2-ynoxy)phenyl)propanoyl)dipyrrolo[1,2-*a*:1',2'-*d*]pyrazine-5,10-dione **2.110**



To a solution of carboxylic acid **2.96** (9.5 mg, 0.03 mmol) in anhydrous dichloromethane (1 mL) was sequentially added DMAP (3.8 mg, 0.03 mmol) and *t*-BuOH (6 μ L, 0.06 mmol). The solution was cooled to 0 °C before addition of EDCI (8.9 mg, 0.05 mmol), stirred at 0 °C for 2 h, warmed to room temperature and stirred for a further 16 h. Volatiles were removed *in vacuo* and the resulting oil was partitioned between ethyl acetate (10 mL) and H₂O (5 mL). The organic layer was washed with saturated NaHCO₃ (2 x 10 mL) and H₂O (2 x 10 mL); dried (Na₂SO₄) and volatiles removed *in vacuo* to give dimer **2.110** as an orange solid (11 mg, 100 %). mp 117-119 °C; ¹H NMR (CDCl₃, 600 MHz) δ 2.51 (t, *J* = 2.4 Hz, 2H, 2 x OCH₂CCH), 3.02 (t, *J* = 7.6 Hz, 4H, 2 x ArCH₂CH₂), 3.17 (t, *J* = 7.6 Hz, 4H, 2 x ArCH₂CH₂), 4.65 (d, *J* = 2.4, 4H, 2 x OCH₂CCH), 6.65 (d, *J* = 3.6 Hz, 2H, 2 x pyrrole **H**), 6.88 (d, *J* = 8.9 Hz, 4H, 2 x OAr**H**), 7.14 (d, *J* = 8.9 Hz, 4H, 2 x OAr**H**), 7.29 (d, *J* = 3.6 Hz, 2H, 2 x pyrrole **H**); ¹³C NMR (CDCl₃, 150 MHz) δ 29.5, 44.3, 55.8, 75.4, 78.6, 115.0, 118.3, 122.4, 126.2, 129.3, 138.2, 133.4, 150.7, 156.1, 190.3; HRMS (ES) 581.1656 (MNa⁺), C₃₄H₂₆N₂NaO₆ requires 581.1683.

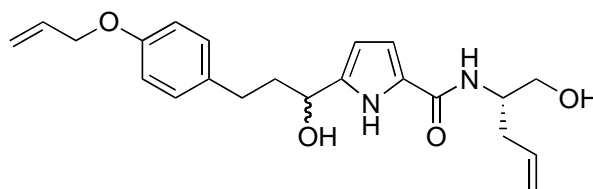
Macrocyclic diol 2.111



Macrocycle **2.91** (10 mg, 0.02 mmol) was reduced according to General Procedure J2 and recrystallized from ethyl acetate to give a off-white solid, alcohol **2.111** (10 mg, 10%), as a

1:1 mixture of isomers. mp 122-124 °C; $R_f = 0.1$ (4:1 ethyl acetate / petroleum ether); ^1H NMR for both isomer from mixture (CD_3OD , 600 MHz) δ 1.36-1.50 (m, 4H, $2 \times \text{CHCH}_2\text{CH}_2(\text{CH}_2)_2\text{N}$), 1.80-1.86 (m, 2H, $2 \times \text{CHCHH}(\text{CH}_2)_3\text{N}$), 1.90-1.94 (m, 2H, $2 \times \text{CH}(\text{CH}_2)_2\text{CHHCH}_2\text{N}$), 2.02-2.06 (m, 2H, $2 \times \text{CH}(\text{CH}_2)_2\text{CHHCH}_2\text{N}$), 2.10-2.15 (m, 2H, $2 \times \text{CHCHH}(\text{CH}_2)_2\text{CH}_2\text{N}$), 2.66-2.68 (m, 2H, $2 \times \text{ArCHHCH}_2$), 2.96 (dt, $J = 12.9$ and 4.2 Hz, 1H, ArCH_2CHH), 3.02-3.04 (m, 2H, $2 \times \text{ArCHHCH}_2$), 3.18 (dt, $J = 12.0$ and 4.2 Hz, 1H, ArCH_2CHH), 3.44-3.61 (m, 4H, $2 \times \text{CH}_2\text{OH}$), 4.20-4.25 (m, 2H, $2 \times \text{CHHN}$), 4.35-4.39 (m, 2H, $2 \times \text{CHHN}$), 4.78-4.81 (m, 2H, $2 \times \text{CHNH}$), 4.85-4.88 (m, 1H, CHOH (isomer B)), 4.91-4.93 (m, 1H, CHOH (isomer A)), 5.14 (d, $J = 14.4$ Hz, 1H, OCHH), 5.22 (d, $J = 14.4$ Hz, 1H, OCHH), 6.18-6.23 (m, 2H, pyrrole **H**), 6.31-6.35 (m, 2H, pyrrole **H**), 6.70-6.74 (m, 4H, OArH), 6.92-6.95 (m, 4H, OArH), 7.33 (s, 1H, triazole **CH**), **NH** and **OH** signals not observed; ^{13}C NMR for both isomer from mixture (CD_3OD , 150 MHz) δ 22.0, 29.4, 30.7, 33.1, 39.9, 49.8, 52.8, 62.3, 63.9, 64.0, 73.5, 74.7, 110.1, 115.0, 117.2, 122.1, 129.7, 132.3, 134.6, 135.2, 144.5, 157.0, 159.4, 172.2, 192.1; HRMS (ES) 462.2189 (MNa^+); $\text{C}_{23}\text{H}_{29}\text{N}_5\text{NaO}_4$ requires 462.2220.

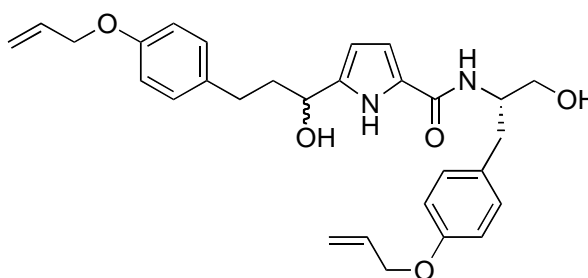
(S)-5-(3-(4-(Allyloxy)phenyl)-1-hydroxypropyl)-N-(1-hydroxypent-4-en-2-yl)-1H-pyrrole-2-carboxamide 2.112



Acyclic tripeptide **2.57** (52 mg, 0.13 mmol) was reduced according to general procedure J2 and purified by flash chromatography (4:1 ethyl acetate / petroleum ether) to give a yellow oil, alcohol **2.112** (38 mg, 78%), as a 1:1 mixture of isomers. $R_f = 0.21$ (4:1 ethyl acetate / petroleum ether); ^1H NMR (CDCl_3 , 600 MHz) δ 2.07-2.15 (m, 4H, $2 \times \text{ArCH}_2\text{CH}_2$), 2.33-2.46 (m, 4H, $2 \times \text{CHCH}_2\text{CHCH}_2$), 2.61-2.73 (m, 4H, $2 \times \text{ArCH}_2\text{CH}_2$), 3.04 (br s, 2H, $2 \times \text{CH}_2\text{OH}$), 3.68 (br s, 4H, $2 \times \text{CH}_2\text{OH}$), 3.91 (d, $J = 4.8$ Hz, 1H, CHOH), 3.93 (d, $J = 4.8$ Hz, 1H, CHOH), 4.10-4.14 (m, 2H, $2 \times \text{CHCH}_2\text{CHCH}_2$), 4.50 (dd, $J = 5.4$ and 1.2 Hz, 2H, $2 \times \text{OCH}_2\text{CHCH}_2$), 4.68-4.74 (m, 2H, $2 \times \text{CHOH}$), 5.13-5.18 (m, 4H, $2 \times \text{CHCH}_2\text{CHCH}_2$), 5.27 (d, $J = 10.2$ Hz, 2H, $2 \times \text{OCH}_2\text{CHCHH}$), 5.40 (d, $J = 17.1$ Hz, 2H, $2 \times \text{OCH}_2\text{CHCHH}$), 5.77-5.85 (m, 2H, $2 \times \text{CHCH}_2\text{CHCH}_2$), 6.02-6.08 (m, 4H, $2 \times$ pyrrole

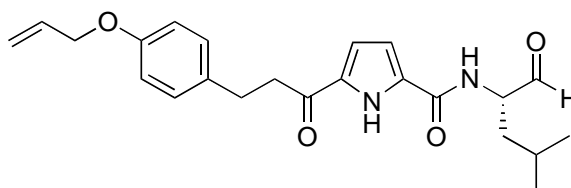
H, 2 × OCH₂CHCH₂), 6.11 (br d, $J = 7.8$ Hz, 2H, 2 × CONH), 6.48 (t, $J = 3.3$ Hz, 2H, 2 × pyrrole **H**), 6.83 (d, $J = 9.0$ Hz, 4H, 2 × OAr**H**), 7.09 (d, $J = 9.0$ Hz, 4H, 2 × OAr**H**), 10.58 (br s, 2H, 2 × pyrrole NH); ¹³C NMR (CDCl₃, 150 MHz) δ 30.9, 31.0, 35.8, 38.5, 38.9, 51.2, 64.9, 67.0, 67.3, 68.9, 106.5, 106.7, 109.8, 109.9, 114.7, 117.5, 118.6, 124.4, 124.5, 129.3, 133.5, 133.7, 134.0, 139.7, 139.8, 156.9, 162.1; HRMS (ES) 385.2112 (MH⁺); C₂₂H₂₉N₂O₄ requires 385.2122.

(S)-5-(3-(4-(Allyloxy)phenyl)-1-hydroxypropyl)-N-(1-(4-(allyloxy)phenyl)-3-hydroxypropan-2-yl)-1H-pyrrole-2-carboxamide 2.113



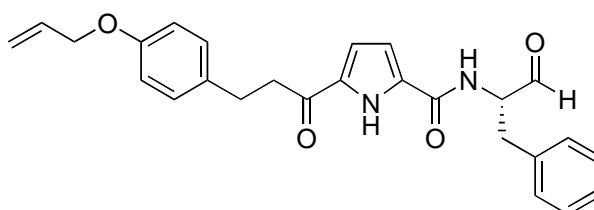
Acyclic tripeptide **2.58** (52 mg, 0.1 mmol) was reduced according to general procedure J2 and purified by flash chromatography (4:1 ethyl acetate / petroleum ether) to give a yellow oil, alcohol **2.113** (38 mg, 78%), as a 1:1 mixture of isomers. $R_f = 0.36$ (4:1 ethyl acetate / petroleum ether); ¹H NMR (CDCl₃, 600 MHz) δ 2.06-2.17 (m, 4H, 2 × ArCH₂CH₂), 2.59-2.73 (m, 4H, 2 × ArCH₂CH₂), 2.82-2.91 (m, 4H, 2 × NHCHCH₂), 3.01 (br s, 2H, 2 × CH₂OH), 3.61 (br s, 2H, CH₂OH), 3.65 (br s, 2H, CH₂OH), 3.93 (br s, 1H, CHOH), 3.97 (br s, 1H, CHOH), 4.24 (s, 1H, NHCHCH₂), 4.26 (s, 1H, NHCHCH₂), 4.48-4.50 (m, 8H, 4 × OCH₂CHCH₂), 4.68 (br s, 1H, CHOH), 4.72 (br s, 1H, CHOH), 5.26 (d, $J = 10.2$ Hz, 2H, 4 × OCH₂CHCH₂), 5.39 (d, $J = 17.1$ Hz, 4H, 4 × OCH₂CHCH₂), 5.98-6.07 (m, 6H, 4 × OCH₂CHCH₂, 2 × pyrrole **H**), 6.13 (d, $J = 8.1$ Hz, 2H, 2 × NHCH), 6.39-6.40 (m, 2H, 2 × pyrrole **H**), 6.81-6.84 (m, 8H, OAr**H**), 7.07 (d, $J = 8.4$ Hz, 4H, OAr**H**), 7.13 (d, $J = 9$ Hz, 4H, OAr**H**), 10.53 (br s, 1H, pyrrole NH), 10.55 (br s, 1H, pyrrole NH); ¹³C NMR (CDCl₃, 150 MHz) δ 30.9, 30.1, 36.3, 38.4, 38.8, 52.7, 64.0, 67.0, 67.3, 68.8, 68.9, 106.5, 106.7, 109.9, 110.0, 114.7, 115.0, 117.5, 117.6, 124.5, 124.6, 129.3, 130.2, 133.3, 133.5, 133.7, 139.7, 156.9, 157.5, 161.9; HRMS (ES) 491.2528 (MH⁺); C₂₉H₃₅N₂O₅ requires 491.2541.

(S)-5-(3-(4-(Allyloxy)phenyl)propanoyl)-N-(4-methyl-1-oxopentan-2-yl)-1H-pyrrole-2-carboxamide 2.114



Alcohol **2.122** (30 mg, 0.08 mmol) was oxidized according to general procedure L and the crude product purified by rp-HPLC to give aldehyde **2.114** as a yellow oil (10 mg, 33%). $R_f = 0.48$ (96:4 dichloromethane / methanol); $R_t = 12.9$ min; $[\alpha]_D = + 1.8$ (c 0.1 in $(\text{CH}_3)_2\text{SO}$); $^1\text{H NMR}$ (CDCl_3 , 600 MHz) δ 0.99 (d, $J = 6.6$ Hz, 3H, $\text{CH}(\text{CH}_3)_2$), 1.02 (d, $J = 6.6$ Hz, 3H, $\text{CH}(\text{CH}_3)_2$), 1.67-1.72 (m, 1H, $\text{CHHCH}(\text{CH}_3)_2$), 1.74-1.79 (m, 1H, $\text{CHHCH}(\text{CH}_3)_2$), 1.80-1.87 (m, 1H, $\text{CH}(\text{CH}_3)_2$), 2.99 (t, $J = 7.2$ Hz, 2H, ArCH_2CH_2), 3.13-3.22 (m, 2H, ArCH_2CH_2), 3.90-3.93 (m, 1H, NHCH), 4.51 (d, $J = 4.8$ Hz, 2H, $\text{OCH}_2\text{CHCH}_2$), 5.28 (d, $J = 10.8$ Hz, 1H, OCH_2CHCHH), 5.40 (d, $J = 17.1$ Hz, 1H, OCH_2CHCHH), 6.01-6.08 (m, 1H, $\text{OCH}_2\text{CHCH}_2$), 6.17 (br s, 1H, NHCH), 6.85 (d, $J = 7.8$ Hz, 2H, OArH), 6.93 (d, $J = 4.2$ Hz, 1H, pyrrole **H**), 6.97 (d, $J = 4.2$ Hz, 1H, pyrrole **H**), 7.13 (d, $J = 9.0$ Hz, 2H, OArH), 9.66 (s, 1H, CHO), 10.30 (br s, 1H, pyrrole **NH**); $^{13}\text{C NMR}$ (CDCl_3 , 150 MHz) δ 22.3, 22.8, 24.2, 29.6, 38.8, 41.4, 52.7, 68.9, 113.3, 114.9, 117.6, 118.9, 128.6, 129.2, 131.5, 132.7, 133.3, 157.2, 160.4, 193.0, 199.1; HRMS (ES) 397.21219 (MH^+); $\text{C}_{23}\text{H}_{29}\text{N}_2\text{O}_4$ requires 397.21218.

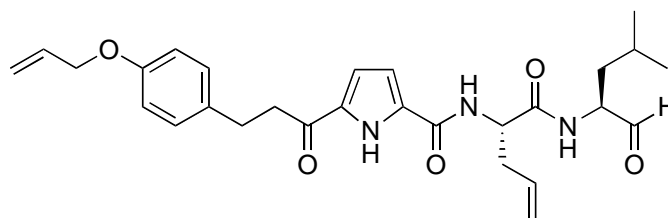
(S)-5-(3-(4-(Allyloxy)phenyl)propanoyl)-N-(1-oxo-3-phenylpropan-2-yl)-1H-pyrrole-2-carboxamide 2.115



Alcohol **2.123** (56 mg, 0.13 mmol) was oxidized according to general procedure L and the crude product purified by rp-HPLC to give aldehyde **2.115** as a yellow amorphous solid (22 mg, 39%). mp 63-65 °C; $R_f = 0.40$ (96:4 dichloromethane/methanol); $R_t = 13.3$ min; $[\alpha]_D = - 1.6$ (c 0.2 in $(\text{CH}_3)_2\text{SO}$); $^1\text{H NMR}$ (CDCl_3 , 600 MHz) δ 2.68 (dd, $J = 14.4$ and 9.3

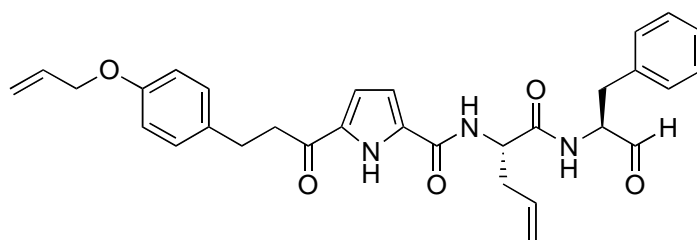
Hz, 1H, CHCHHAr), 2.95-3.05 (m, 3H, ArCH₂CH₂, CHCHHAr), 3.19 (t, $J = 7.8$ Hz, 2H, ArCH₂CH₂), 4.01-4.05 (m, 1H, NHCH), 4.51 (d, $J = 5.4$ Hz, 2H, OCH₂CHCH₂), 5.27 (d, $J = 10.2$ Hz, 1H, OCH₂CHCHH), 5.40 (d, $J = 17.1$ Hz, 1H, OCH₂CHCHH), 5.89 (br s, 1H, CONH), 5.98-6.07 (m, 1H, OCH₂CHCH₂), 6.86 (d, $J = 8.4$ Hz, 2H, OArH), 6.93 (d, $J = 4.8$ Hz, 1H, pyrrole H), 7.02 (d, $J = 4.2$ Hz, 1H, pyrrole H), 7.11-7.15 (m, 4H, OArH, ArH), 7.24-7.28 (m, 1H, ArCH), 7.30-7.32 (m, 2H, ArH), 9.70 (s, 1H, CHO), 10.01 (br s, 1H, pyrrole NH); ¹³C NMR (CDCl₃, 150 MHz) δ 29.8, 40.7, 41.4, 58.0, 68.9, 113.4, 114.9, 117.6, 119.7, 127.4, 128.5, 129.1, 129.2, 129.3, 131.9, 132.6, 133.3, 135.4, 157.2, 159.0, 193.3, 198.2; HRMS (ES) 431.1961 (MH⁺); C₂₆H₂₇N₂O₄ requires 431.1965.

5-(3-(4-(Allyloxy)phenyl)propanoyl)-N-((S)-1-((S)-4-methyl-1-oxopentan-2-ylamino)-1-oxopent-4-en-2-yl)-1H-pyrrole-2-carboxamide 2.116



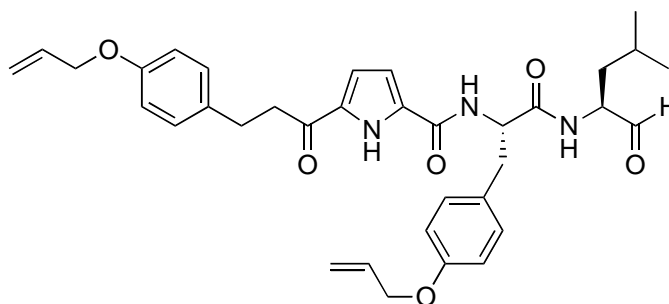
Alcohol **2.127** (34 mg, 0.07 mmol) was oxidized using general procedure L and the crude product purified by rp-HPLC to give aldehyde **2.116** as a off-white amorphous solid (7.5 mg, 21%). mp 56-60 °C; $R_f = 0.52$ (2:1 ethyl acetate / petroleum ether); $R_t = 13.3$ min; $[\alpha]_D = +1.4$ (c 0.1 in (CH₃)₂SO); ¹H NMR (CDCl₃, 600 MHz) δ 0.92 (d, $J = 5.4$ Hz, 3H, CH₂CH(CH₃)₂), 0.97 (d, $J = 6.0$ Hz, 3H, CH₂CH(CH₃)₂), 1.42-1.48 (m, 1H, CHHCH(CH₃)₂), 1.57-1.76 (m, 2H, CHHCH(CH₃)₂), 2.60-2.63 (m, 2H, CHCH₂CHCH₂), 2.97 (br d, $J = 3$ Hz, 2H, ArCH₂CH₂), 3.08 (br d, $J = 3.6$ Hz, 2H, ArCH₂CH₂), 4.50 (br d, $J = 4.8$ Hz, 2H, OCH₂CHCH₂), 4.54-4.56 (m, 1H, CHCH₂CH(CH₃)₂), 4.76-4.77 (m, 1H, CHCH₂CHCH₂), 5.16-5.21 (m, 2H, CHCH₂CHCH₂), 5.27 (d, $J = 10.2$ Hz, 1H, OCH₂CHCHH), 5.40 (d, $J = 16.8$ Hz, 1H, OCH₂CHCHH), 5.80-5.86 (m, 1H, CHCH₂CHCH₂), 6.01-6.07 (m, 1H, OCH₂CHCH₂), 6.59-6.63 (m, 2H, pyrrole H, NHCHCHO), 6.77-6.84 (m, 4H, pyrrole H, NHCHCO, OArH), 7.12 (d, $J = 7.2$ Hz, 2H, OArH), 9.56 (d, $J = 10.8$ Hz, 1H, CHO), 10.31 (br s, 1H, pyrrole NH); ¹³C NMR (CDCl₃, 150 MHz) δ 21.8, 23.0, 24.8, 36.7, 37.7, 40.3, 52.4, 57.6, 68.9, 110.7, 114.8, 115.8, 117.6, 119.5, 129.2, 129.7, 132.6, 133.1, 133.4, 133.5, 157.1, 159.9, 171.2, 190.4, 199.0; HRMS (ES) 494.2649 (MH⁺); C₂₈H₃₆N₃O₅ requires 494.2650.

5-(3-(4-(Allyloxy)phenyl)propanoyl)-*N*-((*S*)-1-oxo-1-((*S*)-1-oxo-3-phenylpropan-2-ylamino)pent-4-en-2-yl)-1*H*-pyrrole-2-carboxamide 2.117



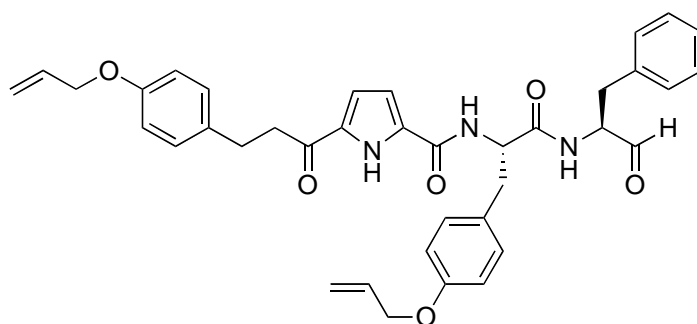
Alcohol **2.128** (26 mg, 0.05 mmol) was oxidized using general procedure L and the crude product purified by rp-HPLC to give aldehyde **2.117** as a colourless oil (7.5 mg, 29%). mp 56-60 °C; $R_f = 0.64$ (2:1 ethyl acetate / petroleum ether); $R_t = 14.6$ min; $[\alpha]_D = +2.3$ (c 0.1 in $(\text{CH}_3)_2\text{SO}$); $^1\text{H NMR}$ (CDCl_3 , 600 MHz) δ 2.48-2.64 (m, 2H, $\text{CHCH}_2\text{CHCH}_2$), 2.98 (t, $J = 7.2$ Hz, 2H, ArCH_2CH_2), 3.07-3.17 (m, 4H, ArCH_2CH_2 , CHCH_2Ar), 4.50 (d, $J = 5.4$ Hz, 2H, $\text{OCH}_2\text{CHCH}_2$), 4.67-4.75 (m, 2H, $\text{CHCH}_2\text{CHCH}_2$, CHCH_2Ar), 5.07-5.15 (m, 2H, $\text{CHCH}_2\text{CHCH}_2$), 5.27 (d, $J = 9.3$ Hz, 1H, OCH_2CHCHH), 5.40 (d, $J = 17.1$ Hz, 1H, OCH_2CHCHH), 5.72-5.79 (m, 1H, $\text{CHCH}_2\text{CHCH}_2$), 6.01-6.07 (m, 1H, $\text{OCH}_2\text{CHCH}_2$), 6.55-6.56 (m, 1H, pyrrole **H**), 6.62 (br d, $J = 7.8$ Hz, 1H, NHCHCHO), 6.80-6.82 (m, 2H, pyrrole **H**, NHCHCO), 6.84 (d, $J = 9.0$ Hz, 2H, OArH), 7.09-7.18 (m, 7H, OArH , ArH), 9.64 (2, 1H, CHO), 10.22 (br s, 1H, pyrrole **NH**); $^{13}\text{C NMR}$ (CDCl_3 , 150 MHz) δ 29.6, 35.0, 36.4, 40.3, 52.1, 59.8, 68.9, 110.5, 114.8, 115.7, 117.6, 119.5, 127.2, 128.7, 129.2, 129.3, 129.6, 132.6, 133.1, 133.4, 133.5, 135.2, 157.1, 159.8, 170.9, 190.4, 198.3; HRMS (ES) 528.24933 (MH^+); $\text{C}_{31}\text{H}_{34}\text{N}_3\text{O}_5$ requires 528.2493.

***N*-((*S*)-3-(4-(Allyloxy)phenyl)-1-((*S*)-4-methyl-1-oxopentan-2-ylamino)-1-oxopropan-2-yl)-5-(3-(4-(allyloxy)phenyl)propanoyl)-1*H*-pyrrole-2-carboxamide 2.118**



Alcohol **2.129** (44 mg, 0.07 mmol) was oxidized using general procedure L and the crude product purified by rp-HPLC to give aldehyde **2.118** as a yellow amorphous solid (23 mg, 53%). mp 57-60 °C; R_f = 0.45 (96:4 dichloromethane / methanol); R_t = 15.2 min; $[\alpha]_D = +1.9$ (c 0.1 in $(\text{CH}_3)_2\text{SO}$); $^1\text{H NMR}$ (CDCl_3 , 600 MHz) δ 0.84-0.86 (m, 6H, $\text{CH}_2\text{CH}(\text{CH}_3)_2$), 1.27-1.37 (m, 1H, $\text{CHHCH}(\text{CH}_3)_2$), 1.50-1.61 (m, 2H, $\text{CHHCH}(\text{CH}_3)_2$), 2.94-2.96 (m, 2H, ArCH_2CH_2), 3.05-3.11 (m, 3H, ArCH_2CH_2 , CHCHHArO), 3.13-3.16 (m, 1H, CHCHHArO), 4.35-4.42 (m, 1H, $\text{CHCH}_2(\text{CH}_3)_2$), 4.47 (d, $J = 5.4$ Hz, 2H, $\text{OCH}_2\text{CHCH}_2$), 4.50 (d, $J = 4.8$ Hz, 2H, $\text{OCH}_2\text{CHCH}_2$), 4.99 (q, $J = 7.2$ Hz, 1H, CHCH_2ArO), 5.25-5.28 (m, 2H, $2 \times \text{OCH}_2\text{CHCHH}$), 5.36-5.43 (m, 2H, $2 \times \text{OCH}_2\text{CHCHH}$), 5.98-6.08 (m, 2H, $2 \times \text{OCH}_2\text{CHCH}_2$), 6.56-6.57 (m, 1H, pyrrole **H**), 6.66 (br d, $J = 6.0$ Hz, 1H, CONH), 6.79-6.84 (m, 5H, pyrrole **H**, $2 \times \text{OArH}$), 6.97 (br d, $J = 7.2$ Hz, 1H, CONH), 7.12 (d, $J = 7.8$ Hz, 2H, OArH), 7.16 (d, $J = 7.8$ Hz, 2H, OArH), 9.35 (s, 1H, CHO), 10.52 (br s, 1H, pyrrole **NH**); $^{13}\text{C NMR}$ (CDCl_3 , 150 MHz) δ 21.8, 22.9, 24.6, 29.5, 37.6, 37.7, 40.3, 54.5, 57.4, 68.8, 68.9, 110.7, 114.8, 115.0, 115.9, 117.6, 117.7, 128.2, 129.2, 129.9, 130.3, 133.0, 133.2, 133.4, 133.5, 157.1, 157.8, 159.8, 171.4, 190.5, 199.1; HRMS (ES) 601.3072 (MH^+); $\text{C}_{35}\text{H}_{42}\text{N}_3\text{O}_6$ requires 601.3068.

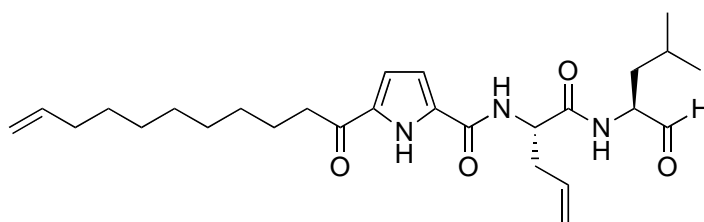
N*-((*S*)-3-(4-(Allyloxy)phenyl)-1-oxo-1-((*S*)-1-oxo-3-phenylpropan-2-ylamino)propan-2-yl)-5-(3-(4-(allyloxy)phenyl)propanoyl)-1*H*-pyrrole-2-carboxamide **2.119*



Alcohol **2.130** (13 mg, 0.02 mmol) was oxidized using general Procedure L and the crude product purified by rp-HPLC to give aldehyde **2.119** as a colorless oil (6 mg, 48%). R_f = 0.62 (2:1 ethyl acetate / petroleum ether); R_t = 15.0 min; $[\alpha]_D = +1.6$ (c 0.2 in $(\text{CH}_3)_2\text{SO}$); $^1\text{H NMR}$ (CDCl_3 , 600 MHz) δ 2.94-3.14 (m, 8H, CHCH_2Ar , ArCH_2CH_2 , CHCH_2ArO), 4.48 (d, $J = 6.0$ Hz, 2H, $\text{OCH}_2\text{CHCH}_2$), 4.50 (d, $J = 5.4$ Hz, 2H, $\text{OCH}_2\text{CHCH}_2$), 4.60 (q, $J = 6.8$ Hz, 1H, CHCH_2Ar), 4.85 (q, $J = 7.4$ Hz, 1H, CHCH_2ArO), 5.27 (d, $J = 10.2$ Hz, 2H, OCH_2CHCHH), 5.37-5.41 (m, 2H, OCH_2CHCHH), 5.99-6.07 (m, 2H, $\text{OCH}_2\text{CHCH}_2$),

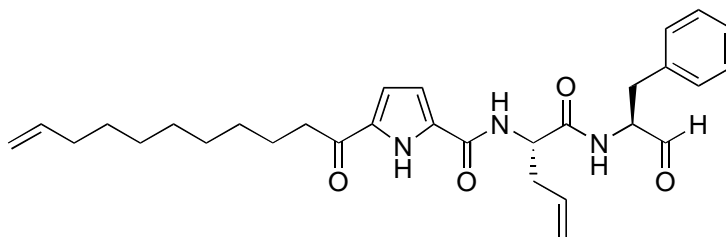
6.47-6.49 (m, 2H, pyrrole **H**, NHCH), 6.59 (br d, $J = 7.8$ Hz, 1H, NHCH), 6.78-6.85 (m, 5H, pyrrole **H**, 2 × OAr**H**), 7.00 (d, $J = 7.5$ Hz, Ar**H**), 7.10-7.16 (m, 7H, 2 × OAr**H**, Ar**H**), 9.48 (s, 1H, CHO), 10.20 (br s, 1H, pyrrole NH); ^{13}C NMR (CDCl_3 , 150 MHz) δ 29.5, 34.9, 37.4, 40.3, 54.3, 59.7, 68.8, 68.9, 110.3, 114.8, 115.0, 115.7, 117.6, 117.7, 127.2, 128.1, 128.7, 129.1, 129.3, 129.6, 130.3, 133.1, 133.2, 133.4, 133.5, 135.2, 157.1, 157.8, 159.6, 170.8, 190.3, 198.1; HRMS (ES) 634.2903 (MH^+); $\text{C}_{38}\text{H}_{40}\text{N}_3\text{O}_6$ requires 634.2912.

N*-((*S*)-1-((*S*)-4-methyl-1-oxopentan-2-ylamino)-1-oxopent-4-en-2-yl)-5-undec-10-enoyl-1*H*-pyrrole-2-carboxamide **2.120*



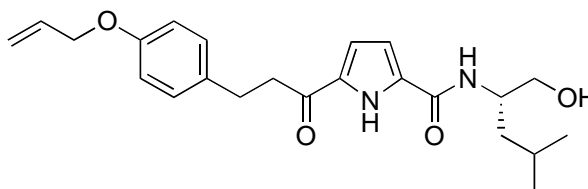
Alcohol **2.131** (41 mg, 0.09 mmol) was oxidized using general procedure L and the crude product purified by rp-HPLC to give aldehyde **2.120** as a colourless oil (13 mg, 31%). $R_f = 0.77$ (2:1 ethyl acetate / petroleum); $R_t = 15.8$ min; $[\alpha]_D = +2.7$ (c 0.1 in $(\text{CH}_3)_2\text{SO}$); ^1H NMR (CDCl_3 , 600 MHz) δ 0.91 (d, $J = 5.7$ Hz, 3H, $\text{CH}_2\text{CH}(\text{CH}_3)_2$), 0.96 (dd, $J = 6.0$ and 3.0 Hz, 3H, $\text{CH}_2\text{CH}(\text{CH}_3)_2$), 1.23-1.37 (m, 11H, $\text{COCH}_2\text{CH}_2(\text{CH}_2)_5$, $\text{CH}_2\text{CH}(\text{CH}_3)_2$), 1.43-1.49 (m, 1H, $\text{CHHCH}(\text{CH}_3)_2$), 1.68-1.71 (m, 3H, $\text{CHHCH}(\text{CH}_3)_2$, COCH_2CH_2), 2.03 (q, $J = 7.0$ Hz, 2H, $\text{COCH}_2\text{CH}_2(\text{CH}_2)_5\text{CH}_2$), 2.58-2.68 (m, 2H, $\text{CHCH}_2\text{CHCH}_2$), 2.75-2.81 (m, 2H, COCH_2), 4.49-4.54 (m, 1H, NHCHCHO), 4.86 (q, $J = 6.8$ Hz, 1H, NHCHCO), 4.93 (d, $J = 10.2$ Hz, 1H, $(\text{CH}_2)_8\text{CHCHH}$), 4.99 (d, $J = 17.4$ Hz, 1H, $(\text{CH}_2)_8\text{CHCHH}$), 5.15-5.20 (m, 2H, $\text{CHCH}_2\text{CHCH}_2$), 5.77-5.85 (m, 2H, $\text{CHCH}_2\text{CHCH}_2$, $(\text{CH}_2)_8\text{CHCH}_2$), 6.63-6.64 (m, 1H, pyrrole **H**), 6.84-6.85 (m, 1H, pyrrole **H**), 6.91 (d, $J = 7.2$ Hz, 1H, NHCHCO), 7.02 (d, $J = 7.2$ Hz, 1H, NHCHCHO), 9.57 (s, 1H, CHO), 10.53 (br s, 1H, pyrrole NH); ^{13}C NMR (CDCl_3 , 150 MHz) δ 21.8, 22.9, 24.8, 28.9, 29.1, 29.2, 29.3, 29.4, 33.8, 36.8, 37.6, 38.5, 52.4, 57.5, 110.8, 114.1, 115.8, 119.4, 129.7, 132.6, 133.7, 139.2, 160.0, 171.4, 191.8, 199.1; HRMS (ES) 472.3151 (MH^+); $\text{C}_{27}\text{H}_{42}\text{N}_3\text{O}_4$ requires 472.3170.

N*-((*S*)-1-Oxo-1-((*S*)-1-oxo-3-phenylpropan-2-ylamino)pent-4-en-2-yl)-5-undec-10-enoyl-1*H*-pyrrole-2-carboxamide **2.121*



Alcohol **2.132** (61 mg, 0.12 mmol) was oxidized using general procedure L and the crude product purified by rp-HPLC to give aldehyde **2.121** as a white oil (13 mg, 22%). $R_f = 0.65$ (2:1 ethyl acetate / petroleum ether); $R_t = 15.6$ min; $[\alpha]_D = +1.3$ (c 0.1 in $(\text{CH}_3)_2\text{SO}$); ^1H NMR (CDCl_3 , 600 MHz) δ 1.26-1.37 (m, 10H, $\text{COCH}_2\text{CH}_2(\text{CH}_2)_5$), 1.63-1.72 (m, 2H, COCH_2CH_2), 2.03 (q, $J = 7.0$ Hz, 2H, $\text{COCH}_2\text{CH}_2(\text{CH}_2)_5\text{CH}_2$), 2.52-2.61 (m, 2H, $\text{CHCH}_2\text{CHCH}_2$), 2.78 (t, $J = 4.8$ Hz, 2H, COCH_2), 3.06-3.18 (m, 2H, CHCH_2Ar), 4.73 (q, $J = 7.0$ Hz, 1H, CHCH_2Ar), 4.78 (q, $J = 7.0$ Hz, 1H, $\text{CHCH}_2\text{CHCH}_2$), 4.93 (d, $J = 9.6$ Hz, 1H, $(\text{CH}_2)_8\text{CHCHH}$), 4.99 (d, $J = 17.4$ Hz, 1H, $(\text{CH}_2)_8\text{CHCHH}$), 5.11-5.15 (m, 2H, $\text{CHCH}_2\text{CHCH}_2$), 5.73-5.84 (m, 2H, $\text{CHCH}_2\text{CHCH}_2$, $(\text{CH}_2)_8\text{CHCH}_2$), 6.58-6.59 (m, 1H, pyrrole **H**), 6.70 (d, $J = 8.4$ Hz, NHCHCO), 6.85-6.86 (m, 1H, pyrrole **H**), 7.07-7.17 (m, 6H, NHCHCHO , ArH), 9.64 (s, 1H, CHO), 10.39 (br s, 1H, pyrrole **NH**); ^{13}C NMR (CDCl_3 , 150 MHz) δ 24.9, 28.9, 29.1, 29.2, 29.3, 29.4, 33.8, 35.0, 36.4, 38.5, 52.1, 59.8, 110.6, 114.1, 115.7, 119.4, 127.1, 128.7, 129.2, 129.6, 132.6, 133.7, 135.3, 139.2, 159.9, 171.1, 191.7, 198.4; HRMS (ES) 506.3006 (MH^+); $\text{C}_{30}\text{H}_{40}\text{N}_3\text{O}_4$ requires 506.3013.

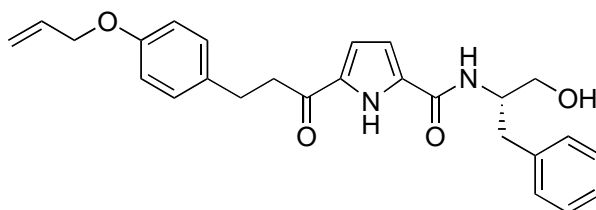
(S)*-5-(3-(4-(Allyloxy)phenyl)propanoyl)-*N*-(1-hydroxy-4-methylpentan-2-yl)-1*H*-pyrrole-2-carboxamide **2.122*



Carboxylic acid **2.54** (50 mg, 0.17 mmol) was coupled to (L)-Leucinol (25 mg, 0.21 mmol) according to general procedure G and the crude product was purified by flash chromatography (4:1 ethyl acetate / petroleum ether) to give alcohol **2.122** as a yellow oil

(42 mg, 62%). $R_f = 0.52$ (4:1 ethyl acetate / petroleum ether); $[\alpha]_D = + 1.1$ (c 0.1 in $(\text{CH}_3)_2\text{SO}$); $^1\text{H NMR}$ (CDCl_3 , 300 MHz) δ 0.95 (d, $J = 6.6$ Hz, 6H, $\text{CH}(\text{CH}_3)_2$), 1.40-1.45 (m, 1H, $\text{CHHCH}(\text{CH}_3)_2$), 1.50-1.65 (m, 1H, $\text{CHHCH}(\text{CH}_3)_2$), 1.67-1.70 (m, 1H, $\text{CH}(\text{CH}_3)_2$), 2.76 (br s, 1H, CH_2OH), 2.95-2.98 (m, 2H, ArCH_2CH_2), 3.05-3.08 (m, 2H, ArCH_2CH_2), 3.66-3.87 (m, 1H, CHHOH), 3.80-3.82 (m, 1H, CHHOH), 4.24-4.29 (m, 1H, NHCH), 4.55 (d, $J = 5.4$ Hz, 2H, $\text{OCH}_2\text{CHCH}_2$), 5.27 (d, $J = 10.2$ Hz, 1H, OCH_2CHCHH), 5.40 (d, $J = 17.1$ Hz, 1H, OCH_2CHCHH), 6.01-6.07 (m, 1H, $\text{OCH}_2\text{CHCH}_2$), 6.32 (br d, $J = 8.4$ Hz, 1H, NHCH), 6.54-6.55 (m, 1H, pyrrole **H**), 6.77-6.78 (m, 1H, pyrrole **H**), 6.83 (d, $J = 8.7$ Hz, 2H, OArH), 7.12 (d, $J = 8.7$ Hz, 2H, OArH), 10.34 (br s, 1H, pyrrole NH); $^{13}\text{C NMR}$ (CDCl_3 , 75 MHz) δ 22.2, 23.0, 25.0, 40.2, 40.3, 49.9, 65.7, 68.9, 110.1, 114.8, 115.7, 117.6, 129.3, 130.5, 133.1, 133.2, 133.4, 157.0, 169.5, 190.3; HRMS (ES) 399.22781 (MH^+); $\text{C}_{23}\text{H}_{31}\text{N}_2\text{O}_4$ requires 399.22783.

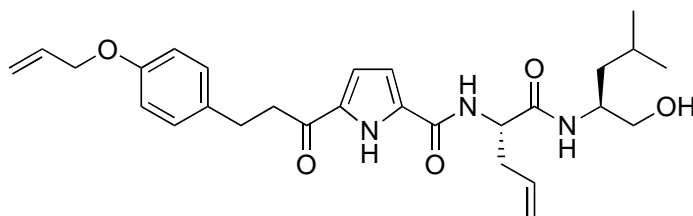
(S)-5-(3-(4-(Allyloxy)phenyl)propanoyl)-N-(1-hydroxy-3-phenylpropan-2-yl)-1H-pyrrole-2-carboxamide 1.123



Carboxylic acid **2.54** (48 mg, 0.16 mmol) was coupled to (L)-Phenalaninol (35 mg, 0.23 mmol) according to general procedure G and the crude product purified by flash chromatography (4:1 ethyl acetate / petroleum ether) to give alcohol **2.123** as a yellow solid (57 mg, 82%). mp 132-135 °C; $R_f = 0.52$ (4:1 ethyl acetate / petroleum ether); $[\alpha]_D = - 1.2$ (c 0.1 in $(\text{CH}_3)_2\text{SO}$); $^1\text{H NMR}$ (CDCl_3 , 600 MHz) δ 2.83 (br s, 1H, CH_2OH), 2.95-2.99 (m, 4H, ArCH_2CH_2 , CHCH_2Ar), 3.05-3.08 (m, 2H, ArCH_2CH_2), 3.67-3.71 (m, 1H, CHHOH), 3.78-3.80 (m, 1H, CHHOH), 4.36-4.40 (m, 1H, NHCH), 4.50 (d, $J = 5.4$ Hz, 2H, $\text{OCH}_2\text{CHCH}_2$), 5.21 (d, $J = 9.9$ Hz, 1H, OCH_2CHCHH), 5.39 (d, $J = 17.1$ Hz, 1H, OCH_2CHCHH), 6.01-6.07 (m, 1H, $\text{OCH}_2\text{CHCH}_2$), 6.47-6.48 (m, 1H, pyrrole **H**), 6.53 (br d, 1H, CONH), 6.75-6.76 (m, 1H, pyrrole **H**), 6.83 (d, $J = 8.4$ Hz, 2H, OArH), 7.11 (d, $J = 8.4$ Hz, 2H, OArH), 7.22-7.26 (m, 3H, ArH), 7.29-7.31 (m, 2H, ArH), 10.37 (br s, 1H, pyrrole NH); $^{13}\text{C NMR}$ (CDCl_3 , 150 MHz) δ 29.6, 37.0, 40.3, 52.7, 63.6, 68.9, 110.2,

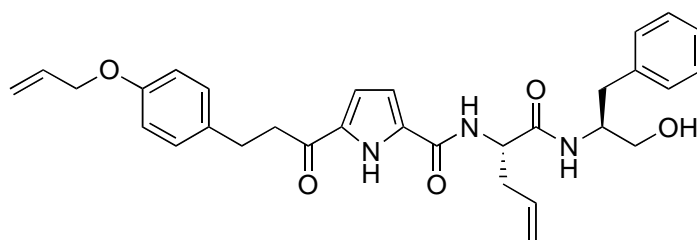
114.8, 115.8, 117.6, 126.8, 128.7, 129.3, 130.4, 133.1, 133.2, 133.4, 137.4, 157.1, 160.3, 190.4; HRMS (ES) 433.2119 (MH^+); $C_{26}H_{29}N_2O_4$ requires 433.2122.

5-(3-(4-(Allyloxy)phenyl)propanoyl)-*N*-((*S*)-1-((*S*)-1-hydroxy-4-methylpentan-2-ylamino)-1-oxopent-4-en-2-yl)-1*H*-pyrrole-2-carboxamide **2.127**



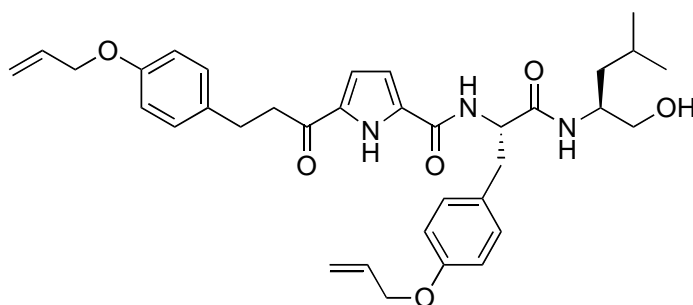
Acyclic ester **2.57** (50 mg, 0.12 mmol) was hydrolysed using general procedure K to its corresponding carboxylic acid **2.124**, which was coupled to (L)-Leucinol (46 mg, 0.39 mmol) via general procedure G and the crude product was purified by flash chromatography (4:1 ethyl acetate / petroleum ether) to give alcohol **2.127** as a off-white amorphous solid (34 mg, 57%). mp 62-65 °C; $R_f = 0.30$ (4:1 ethyl acetate / petroleum ether); $[\alpha]_D = +1.8$ (c 0.1 in $(CH_3)_2SO$); 1H NMR ($CDCl_3$, 600 MHz) δ 0.87 (d, $J = 6.6$ Hz, 6H, $CH_2CH(CH_3)_2$), 1.36-1.45 (m, 2H, $CH_2CH(CH_3)_2$), 1.56-1.61 (m, 1H, $CH_2CH(CH_3)_2$), 2.62 (t, $J = 6.9$ Hz, 2H, $CHCH_2CHCH_2$), 2.95-2.98 (m, 2H, $ArCH_2CH_2$), 3.08-3.15 (m, 2H, $ArCH_2CH_2$), 3.79-3.88 (m, 2H, CH_2OH), 4.08 (br s, 1H, CH_2OH), 4.10-4.14 (m, 1H, $CHCH_2CH(CH_3)_2$), 4.50-4.51 (m, 2H, OCH_2CHCH_2), 5.08-5.14 (m, 2H, $CHCH_2CHCH_2$), 5.21-5.25 (m, 1H, $CHCH_2CHCH_2$), 5.28 (d, $J = 10.8$ Hz, 1H, OCH_2CHCHH), 5.40 (d, $J = 17.1$ Hz, 1H, OCH_2CHCHH), 5.82-5.89 (m, 1H, $CHCH_2CHCH_2$), 6.01-6.08 (m, 1H, OCH_2CHCH_2), 6.62-6.63 (m, 1H, pyrrole **H**), 6.83-6.86 (m, 3H, pyrrole **H**, $OArH$), 7.11-7.13 (m, 3H, $NHCHCO$, $OArH$), 7.92 (d, $J = 8.4$ Hz, 1H, $NHCHCH_2OH$), 11.24 (br s, 1H, pyrrole **NH**); ^{13}C NMR ($CDCl_3$, 150 MHz) δ 22.5, 22.9, 24.9, 29.7, 38.5, 40.2, 40.4, 48.9, 52.5, 64.7, 68.9, 110.3, 114.8, 117.1, 117.6, 118.5, 129.2, 130.7, 133.0, 133.1, 133.4, 157.1, 159.5, 170.6, 191.5; HRMS (ES) 496.28058 (MH^+); $C_{28}H_{38}N_3O_5$ requires 496.2806.

5-(3-(4-(Allyloxy)phenyl)propanoyl)-*N*-((*S*)-1-((*S*)-1-hydroxy-3-phenylpropan-2-ylamino)-1-oxopent-4-en-2-yl)-1*H*-pyrrole-2-carboxamide **2.128**



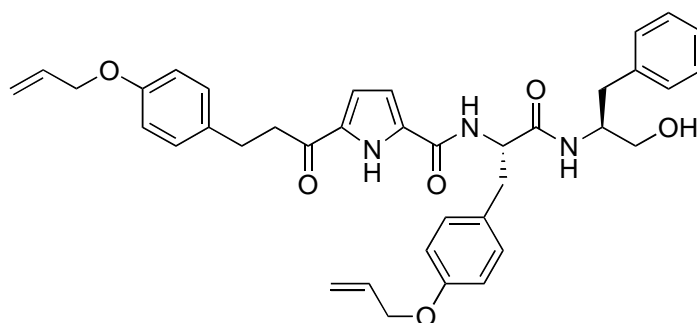
Acyclic ester **2.57** (50 mg, 0.12 mmol) was hydrolysed using general procedure K to its corresponding carboxylic acid **2.124**, which was coupled to (L)-Phenalaninol (31 mg, 0.21 mmol) via general procedure G and the crude product was purified by flash chromatography (4:1 ethyl acetate / petroleum ether) to give alcohol **2.128** as a white amorphous solid (39 mg, 60%). mp 48-50 °C; $R_f = 0.47$ (4:1 ethyl acetate / petroleum ether); $[\alpha]_D = +2.0$ (c 0.1 in $(\text{CH}_3)_2\text{SO}$); $^1\text{H NMR}$ (CDCl_3 , 600 MHz) δ 2.63 (t, $J = 6.9$ Hz, 2H, $\text{CHCH}_2\text{CHCH}_2$), 2.85-2.93 (m, 2H, CHCH_2Ar), 2.96-3.02 (m, 2H, ArCH_2CH_2), 3.06-3.15 (m, 2H, ArCH_2CH_2), 3.75-3.83 (m, 2H, CH_2OH), 4.22-4.26 (m, 1H, CHCH_2Ar), 4.39 (br s, 1H, CH_2OH), 4.50 (d, $J = 5.4$ Hz, 2H, $\text{OCH}_2\text{CHCH}_2$), 5.03-5.17 (m, 2H, $\text{CHCH}_2\text{CHCH}_2$), 5.27 (d, $J = 10.2$ Hz, 1H, OCH_2CHCHH), 5.35-5.41 (m, 2H, $\text{CHCH}_2\text{CHCH}_2$, OCH_2CHCHH), 5.81-5.88 (m, 1H, $\text{CHCH}_2\text{CHCH}_2$), 6.00-6.07 (m, 1H, $\text{OCH}_2\text{CHCH}_2$), 6.63-6.64 (m, 1H, pyrrole **H**), 6.85 (d, $J = 8.4$ Hz, 2H, OArH), 6.90-6.91 (m, 1H, pyrrole **H**), 6.98 (br d, $J = 7.8$ Hz, 1H, NHCHCO), 7.11-7.15 (m, 4H, OArH , ArH), 7.21-7.24 (m, 3H, ArH), 8.30 (br d, $J = 9.0$ Hz, 1H, NHCHCH_2OH), 11.52 (br s, 1H, pyrrole **NH**); $^{13}\text{C NMR}$ (CDCl_3 , 150 MHz) δ 29.8, 37.3, 38.7, 40.5, 52.2, 52.3, 62.4, 68.9, 110.2, 114.9, 117.5, 117.6, 118.6, 126.4, 128.5, 129.3, 129.4, 130.8, 132.9, 133.2, 133.4, 138.2, 157.1, 159.4, 170.6, 191.8; HRMS (ES) 530.2651 (MH^+); $\text{C}_{31}\text{H}_{36}\text{N}_3\text{O}_5$ requires 530.2650.

***N*-((*S*)-3-(4-(Allyloxy)phenyl)-1-((*S*)-1-hydroxy-4-methylpentan-2-ylamino)-1-oxopropan-2-yl)-5-(3-(4-(allyloxy)phenyl)propanoyl)-1*H*-pyrrole-2-carboxamide
2.129**



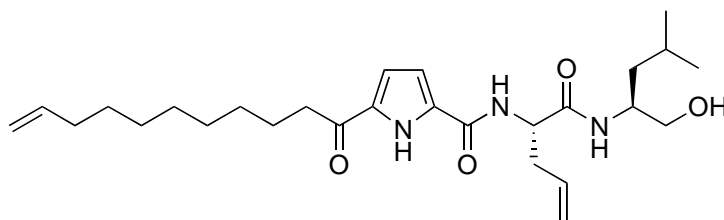
Acyclic ester **2.58** (30 mg, 0.06 mmol) was hydrolysed using general procedure K to its corresponding carboxylic acid **2.125**, which was coupled to (L)-Leucinol (8.2 mg, 0.07 mmol) via general procedure G and the crude product was purified by flash chromatography (4:1 petroleum ether / ethyl acetate) to give alcohol **2.129** as a off-white solid (25 mg, 71%). mp 155-158 °C; $R_f = 0.43$ (4:1 petroleum ether / ethyl acetate); $[\alpha]_D = + 2.0$ (c 0.1 in $(\text{CH}_3)_2\text{SO}$); $^1\text{H NMR}$ (CDCl_3 , 600 MHz) δ 0.86 (t, $J = 7.2$ Hz, 6H, $\text{CH}_2\text{CH}(\text{CH}_3)_2$), 1.36 (t, $J = 7.2$ Hz, 2H, $\text{CH}_2\text{CH}(\text{CH}_3)_2$), 1.47-1.51 (quin, $J = 6.6$ Hz, 1H, $\text{CH}_2\text{CH}(\text{CH}_3)_2$), 2.91-3.17 (m, 6H, ArCH_2CH_2 , CHCH_2Ar), 3.50 (d, $J = 7.8$ Hz, 1H, CHHOH), 3.62 (d, $J = 10.2$ Hz, 1H, CHHOH), 3.73 (br s, 1H, CH_2OH), 4.10 (d, $J = 7.2$ Hz, 1H, $\text{CHCH}_2(\text{CH}_3)_2$), 4.27 (d, $J = 4.2$ Hz, 2H, $\text{OCH}_2\text{CHCH}_2$), 4.52 (d, $J = 5.4$ Hz, 2H, $\text{OCH}_2\text{CHCH}_2$), 5.13 (q, $J = 7.8$ Hz, 1H, CHCH_2Ar), 5.18 (d, $J = 10.2$ Hz, 2H, $\text{OCH}_2\text{CHCH}_2$), 5.25-5.30 (m, 2H, $\text{OCH}_2\text{CHCH}_2$, $\text{OCH}_2\text{CHCH}_2$), 5.41 (d, $J = 17.4$ Hz, 2H, $\text{OCH}_2\text{CHCH}_2$), 5.87-5.94 (m, 1H, $\text{OCH}_2\text{CHCH}_2$), 6.02-6.09 (m, 1H, $\text{OCH}_2\text{CHCH}_2$), 6.56-6.68 (m, 3H, pyrrole **H**, OArH), 6.77 (br s, 1H, pyrrole **H**), 6.82 (d, $J = 8.4$ Hz, 2H, OArH), 6.98 (br s, 2H, OArH), 7.15 (d, $J = 8.4$ Hz, 2H, OArH), 7.70 (br s, 1H, NHCH), 10.74 (br s, 1H, pyrrole **NH**); $^{13}\text{C NMR}$ (CDCl_3 , 150 MHz) δ 22.7, 22.8, 29.3, 38.6, 40.2, 40.3, 48.3, 55.2, 64.5, 68.6, 68.9, 110.2, 114.4, 114.8, 116.7, 117.3, 117.6, 129.3, 130.5, 130.8, 132.7, 133.3, 133.4, 157.1, 157.5, 159.5, 191.2; HRMS (ES) 602.3212 (MH^+); $\text{C}_{35}\text{H}_{44}\text{N}_3\text{O}_6$ requires 602.3225.

***N*-((*S*)-3-(4-(allyloxy)phenyl)-1-((*S*)-1-hydroxy-3-phenylpropan-2-ylamino)-1-oxopropan-2-yl)-5-(3-(4-(allyloxy)phenyl)propanoyl)-1*H*-pyrrole-2-carboxamide
2.130**



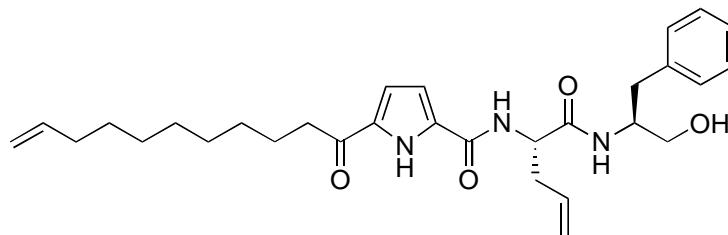
Acyclic ester **2.58** (31 mg, 0.06 mmol) was hydrolysed using general procedure K to its corresponding carboxylic acid **2.125**, which was coupled to (L)-Phenalaninol (13.8 mg, 0.09 mmol) via general procedure G and the crude product was purified by flash chromatography (4:1 petroleum ether / ethyl acetate) to give alcohol **2.130** as a yellow solid (23 mg, 62%). mp 154-156 °C; $R_f = 0.57$ (4:1 petroleum ether / ethyl acetate); $[\alpha]_D = +1.6$ (c 0.3 in $(\text{CH}_3)_2\text{SO}$); $^1\text{H NMR}$ (CDCl_3 , 600 MHz) δ 2.89 (d, $J = 7.8$ Hz, 2H, CHCH_2Ar), 2.92-3.19 (m, 6H, ArCH_2CH_2 , CHCH_2ArO), 3.50 (d, $J = 9.6$ Hz, 1H, CHHOH), 3.68 (d, $J = 9.6$ Hz, 1H, CHHOH), 4.19-4.22 (m, 1H, CHCH_2Ar), 4.25 (d, $J = 4.8$ Hz, 2H, $\text{OCH}_2\text{CHCH}_2$), 4.31 (br s, 1H, CH_2OH), 4.50 (d, $J = 5.4$ Hz, 2H, $\text{OCH}_2\text{CHCH}_2$), 5.14 (d, $J = 9.6$ Hz, 1H, OCH_2CHCHH), 5.24 (d, $J = 17.7$ Hz, 1H, OCH_2CHCHH), 5.27 (d, $J = 10.5$ Hz, 1H, OCH_2CHCHH), 5.36 (q, $J = 7.8$ Hz, 1H, CHCH_2ArO), 5.40 (d, $J = 16.8$ Hz, 1H, OCH_2CHCHH), 5.84-5.90 (m, 1H, $\text{OCH}_2\text{CHCH}_2$), 6.01-6.08 (m, 1H, $\text{OCH}_2\text{CHCH}_2$), 6.58 (d, $J = 8.4$ Hz, 2H, OArH), 6.61-6.63 (m, 1H, pyrrole **H**), 6.82-6.86 (m, 3H, pyrrole **H**, OArH), 6.97 (d, $J = 8.4$ Hz, 2H, OArH), 7.06 (t, $J = 6.9$ Hz, 1H, ArH), 7.14-7.26 (m, 6H, OArH , ArH), 7.60 (br s, 1H, NHCH), 8.19 (br s, 1H, NHCH), 11.14 (br s, 1H, pyrrole **NH**); $^{13}\text{C NMR}$ (CDCl_3 , 150 MHz) δ 29.6, 37.4, 38.8, 40.4, 51.9, 54.7, 62.5, 68.6, 68.9, 110.2, 114.5, 114.8, 117.3, 117.6, 126.2, 128.3, 129.0, 129.3, 129.4, 130.4, 131.1, 132.8, 133.1, 133.3, 133.4, 138.4, 157.1, 157.5, 159.6, 171.4, 191.6; HRMS (ES) 636.3058 (MH^+); $\text{C}_{38}\text{H}_{42}\text{N}_3\text{O}_6$ requires 636.3068.

N*-((*S*)-1-((*S*)-1-Hydroxy-4-methylpentan-2-ylamino)-1-oxopent-4-en-2-yl)-5-undec-10-enoyl-1*H*-pyrrole-2-carboxamide **2.131*



Acyclic ester **2.59** (100 mg, 0.26 mmol) was hydrolysed using general procedure K to its corresponding carboxylic acid **2.126**, which was coupled to (L)-Leucinol (47 mg, 0.40 mmol) via general procedure G and the crude product was purified by flash chromatography (4:1 petroleum ether / ethyl acetate) to give alcohol **2.131** as a yellow oil (96 mg, 79%). $R_f = 0.56$ (4:1 petroleum ether / ethyl acetate); $[\alpha]_D = +1.7$ (c 0.2 in $(\text{CH}_3)_2\text{SO}$); $^1\text{H NMR}$ (CDCl_3 , 600 MHz) δ 0.87 (d, $J = 1.8$ Hz, 3H, $\text{CH}_2\text{CH}(\text{CH}_3)_2$), 0.88 (d, $J = 2.4$ Hz, 3H, $\text{CH}_2\text{CH}(\text{CH}_3)_2$), 1.25-1.45 (m, 12H, $\text{COCH}_2\text{CH}_2(\text{CH}_2)_5$, $\text{CH}_2\text{CH}(\text{CH}_3)_2$), 1.58-1.62 (m, 1H, $\text{CH}_2\text{CH}(\text{CH}_3)_2$), 1.70 (quin, $J = 7.4$ Hz, 2H, COCH_2CH_2), 2.03 (q, $J = 7.0$ Hz, 2H, $\text{COCH}_2\text{CH}_2(\text{CH}_2)_5\text{CH}_2$), 2.62 (t, $J = 6.9$ Hz, 2H, $\text{CHCH}_2\text{CHCH}_2$), 2.78-2.81 (m, 2H, COCH_2), 3.78-3.81 (m, 1H, CHHOH), 3.87-3.90 (m, 1H, CHHOH), 4.10-4.15 (m, 2H, $\text{CHCH}_2\text{CH}(\text{CH}_3)_2$, CH_2OH), 4.93 (d, $J = 10.2$ Hz, 1H, $(\text{CH}_2)_8\text{CHCHH}$), 4.99 (d, $J = 17.4$ Hz, 1H, $(\text{CH}_2)_8\text{CHCHH}$), 5.07-5.14 (m, 2H, $\text{CHCH}_2\text{CHCH}_2$), 5.25 (q, $J = 7.0$ Hz, 1H, $\text{CHCH}_2\text{CHCH}_2$), 5.75-5.90 (m, 2H, $\text{CHCH}_2\text{CHCH}_2$, $(\text{CH}_2)_8\text{CHCH}_2$), 6.64-6.65 (m, 1H, pyrrole **H**), 6.88-6.90 (m, 1H, pyrrole **H**), 7.04 (d, $J = 7.8$ Hz, 1H, NHCHCO), 7.95 (d, $J = 9.0$ Hz, 1H, NHCHCH_2OH), 11.29 (br s, 1H, pyrrole **NH**); $^{13}\text{C NMR}$ (CDCl_3 , 150 MHz) δ 22.4, 22.9, 24.9, 25.0, 28.9, 29.0, 29.2, 29.3, 29.4, 33.8, 38.5, 38.6, 40.2, 49.0, 52.4, 64.6, 110.2, 114.2, 117.1, 118.5, 130.6, 133.0, 133.3, 139.1, 159.5, 170.5, 192.9; HRMS (ES) 474.3323 (MH^+); $\text{C}_{27}\text{H}_{44}\text{N}_3\text{O}_4$ requires 474.3326.

N*-((*S*)-1-((*S*)-1-Hydroxy-3-phenylpropan-2-ylamino)-1-oxopent-4-en-2-yl)-5-undec-10-enoyl-1*H*-pyrrole-2-carboxamide **2.132*



Acyclic ester **2.59** (100 mg, 0.26 mmol) was hydrolysed using general procedure K to its corresponding carboxylic acid **2.126**, which was coupled to (L)-Phenalaninol (65 mg, 0.43 mmol) via general procedure G and the crude product was purified by flash chromatography (4:1 petroleum ether / ethyl acetate) to give alcohol **2.132** as a colourless oil (122 mg, 92%). $R_f = 0.51$ (4:1 petroleum ether / ethyl acetate); $[\alpha]_D = +1.6$ (c 0.1 in $(\text{CH}_3)_2\text{SO}$); $^1\text{H NMR}$ (CDCl_3 , 600 MHz) δ 1.26-1.39 (m, 10H, $\text{COCH}_2\text{CH}_2(\text{CH}_2)_5$), 1.66-1.76 (m, 2H, COCH_2CH_2), 2.03 (q, $J = 7.0$ Hz, 2H, $\text{COCH}_2\text{CH}_2(\text{CH}_2)_5\text{CH}_2$), 2.63 (t, $J = 6.9$ Hz, 2H, $\text{CHCH}_2\text{CHCH}_2$), 2.79-2.98 (m, 4H, COCH_2 , CHCH_2Ar), 3.75 (d, $J = 10.8$ Hz, 1H, CHHOH), 3.81 (d, $J = 9.0$ Hz, 1H, CHHOH), 4.23 (q, $J = 8.0$ Hz, 1H, CHCH_2Ar), 4.45 (br s, 1H, CH_2OH), 4.92 (d, $J = 10.2$ Hz, 1H, $(\text{CH}_2)_8\text{CHCHH}$), 4.99 (d, $J = 17.4$ Hz, 1H, $(\text{CH}_2)_8\text{CHCHH}$), 5.03-5.12 (m, 2H, $\text{CHCH}_2\text{CHCH}_2$), 5.38 (q, $J = 7.0$ Hz, 1H, $\text{CHCH}_2\text{CHCH}_2$), 5.77-5.89 (m, 2H, $\text{CHCH}_2\text{CHCH}_2$, $(\text{CH}_2)_8\text{CHCH}_2$), 6.65-6.66 (m, 1H, pyrrole **H**), 6.93-6.94 (m, 1H, pyrrole **H**), 6.98 (d, $J = 8.4$ Hz, 1H, NHCHCO), 7.12-7.15 (m, 1H, **ArH**), 7.21-7.24 (m, 3H, **ArH**), 7.31-7.32 (m, 1H, **ArCH**), 8.33 (d, $J = 8.4$ Hz, 1H, NHCHCH_2OH), 11.53 (br s, 1H, pyrrole **NH**); $^{13}\text{C NMR}$ (CDCl_3 , 150 MHz) δ 25.0, 28.9, 29.1, 29.3, 29.4, 33.8, 37.3, 38.6, 38.8, 52.2, 52.3, 62.3, 110.1, 114.2, 117.3, 118.5, 126.3, 128.4, 129.4, 130.7, 132.9, 133.3, 138.2, 139.1, 159.4, 170.6, 193.1; HRMS (ES) 508.3152 (MH^+); $\text{C}_{30}\text{H}_{42}\text{N}_3\text{O}_4$ requires 508.3170.

5.3 Experimental Work Described in Chapter Three

Assay of Ovine Calpain Activity

Fluorometric assays (excitation: 485 nm, emission: 520 nm) with ovine calpains 1 and 2 were done with a (BMG Labtech) Fluostar Optima plate reader at 37.0 ± 0.2 °C in 96-well black (Greiner Bio-one) microassay plates. Calpains 1 and 2 partially purified from sheep lung by hydrophobic interaction and ion-exchange chromatography were diluted in 20 mM MOPS, pH 7.5, containing 2 mM EGTA, 2 mM EDTA and 0.035% v/v 2-mercaptoethanol to give a linear response over the course of the assay. The substrate BODIPY-Fl casein was prepared as reported.¹⁴ A 0.0005% solution of the substrate in 10 mM MOPS, pH 7.5, 10 mM CaCl₂, 0.1 mM NaN₃, 0.1% v/v 2-mercaptoethanol was prepared freshly before each experiment. Stock solutions of inhibitors (5 mM) were freshly prepared in DMSO and diluted in DMSO/water mixtures to obtain a total DMSO concentration of 4% v/v.

Inhibition studies were performed in the presence of 187.5 µg/mL calpain 1 or 14 µg/mL calpain 2, seven different inhibitor concentrations and 1% v/v DMSO in a volume of 200 µL: 50 µl of inhibitor solution was added to a microassay well followed by 50 µl of calpain-containing solution. The reaction was initiated by adding 100 µl of BODIPY-Fl casein solution to each well and progress curves were monitored every 30 s over 570 s. Uninhibited enzyme activity was determined by adding 4% v/v DMSO in water instead of inhibitor solution. Every experiment included two blanks, a Ca²⁺ blank and an EDTA blank. The Ca²⁺ blank contained 50 µl water and 50 µl 20 mM MOPS, pH 7.5, 2 mM EGTA, 2 mM EDTA and 0.035% v/v 2-mercaptoethanol instead of inhibitor and enzyme solution, respectively. For the EDTA blank, 50 µl 50 mM EDTA/NaOH, pH 7.5, was added instead of inhibitor solution to the well.

The rate of enzyme-catalyzed substrate hydrolysis was obtained by linear regression of the progress curves over the time course. If slow-binding inhibition occurred,¹⁵ only those data points representing the steady state of enzyme-inhibitor interaction were taken into account, i.e. data points between 390 s and 570 s. The rate of the enzymatic reaction was corrected by the average value of the rates obtained for the two blanks, and the rate in the absence of inhibitor was set to 100%.

The average value of rates obtained in two or three separate experiments, each in triplicate, was plotted versus the inhibitor concentration and IC_{50} values were calculated with the following equation:

$$v_i = \frac{v_0}{1 + \frac{[I]}{IC_{50}}}$$

where $[I]$ is the inhibitor concentration, and v_0 and v are the enzyme activities in the absence and presence of inhibitor. All analyses was done with the program GraphPad Prism version 5.02 for Windows.¹⁶

Reference values:

Inhibitor	IC_{50} on Calpain 1	IC_{50} on Calpain 2
CAT-0811	336 ± 36 nM	209 ± 31 nM
SJA-6017	81.7 ± 9.3 nM	54.3 ± 3.9 nM

Assay of Bovine α -Chymotrypsin Activity

The activity of bovine α -chymotrypsin (bCT) was assayed spectrophotometrically with a Varian Cary 500 UV-VIS-NIR spectrophotometer equipped with a thermostated muticell holder at 25.0 ± 0.1 °C. The assay buffer used was Tris-HCl (77 mM), $CaCl_2$ (20 mM), pH 7.8 (optimum pH for α -chymotrypsin¹⁷). A solution of bCT (21.9 μ g/mL) in aq. HCl (1 mM) was prepared daily by a 1:40 dilution of a stock solution (874 μ g/mL) in aq. HCl (1 mM) and kept at 0 °C. A 1:100 dilution in ice-cold aq. HCl (1 mM) was prepared immediately before starting each measurement. Stock solutions of the substrate Suc-Ala-Ala-Pro-Phe-pNA

(10 mM) and all inhibitors (0.001-1 mM) were freshly prepared in DMSO and stored at r.t. All compounds were analyzed at five different inhibitor concentrations, $[I]$. Progress curves were monitored at 405 nm over 6 min and characterized by a linear steady-state turnover of the substrate.

Inhibition studies were performed in the presence of 6% v/v DMSO in a volume of 1 mL containing 0.011 $\mu\text{g/mL}$ bCT, different concentrations of Suc-Ala-Ala-Pro-Phe-pNA (10-100 μM) and inhibitor (0.001-1 mM). In each cuvette containing 890 μL assay buffer, 10 μL of substrate solution (1-10 mM), inhibitor stock, and DMSO were added to give a total volume of 950 μL . After thoroughly mixing of the contents of the cuvette, the enzymatic reaction was initiated by adding 50 μL of bCT solution. Uninhibited enzyme activity was determined by adding DMSO instead of inhibitor solution. Non-enzymatic hydrolysis of Suc-Ala-Ala-Pro-Phe-pNA was analyzed by adding DMSO and 1 mM aq. HCl instead of inhibitor and enzyme solution, respectively, and found to be negligible. The rate of enzyme-catalyzed hydrolysis of substrate was determined without inhibitor in each experiment and was set to 100%. K_i values of all inhibitors were determined graphically according to Dixon¹⁸ using mean values of percentage rates obtained in three separate experiments at two different substrate concentrations, [S]. The mode of inhibition was concluded from Dixon plots.¹⁸

Assay of Human Cathepsin L¹⁹

The *in vitro* enzyme inhibition assay against human cathepsin L was conducted by Prof. Michael Gütschow at the University of Bonn, Germany.

Human isolated cathepsin L (Enzo Life Sciences, Lörrach, Germany) was assayed spectrophotometrically (Cary 50 Bio, Varian) at 405 nm and at 37 °C. The reactions were followed over 10 min. Assay buffer was 100 mM sodium phosphate buffer pH 6.0, 100 mM NaCl, 5 mM EDTA, and 0.01% Brij 35. An enzyme stock solution of 135 $\mu\text{g/mL}$ in 20 mM malonate buffer pH 5.5, 400 mM NaCl, and 1 mM EDTA was diluted 1:100 with assay buffer containing 5 mM DTT and incubated for 30 min at 37 °C. Inhibitor stock solutions were prepared in DMSO. A 10 mM stock solution of the chromogenic substrate Z-Phe-Arg-pNA was prepared with DMSO. The final concentration of DMSO was 5%, and the final concentration of the substrate was 100 μM . Assays were performed with a final concentration of 54 ng/mL of cathepsin L. Into a cuvette containing 910 μL assay buffer, inhibitor solution and DMSO in a total volume of 40 μL , and 10 μL of the substrate solution were added and thoroughly mixed. The reaction was initiated by adding 40 μL of the cathepsin L solution.

Assay of Human Cathepsin S¹⁹

The in vitro enzyme inhibition assay against human cathepsin L was conducted by Prof. Michael Gütschow at the University of Bonn, Germany.

Human recombinant (*E. coli*) cathepsin S (Calbiochem, Darmstadt, Germany) was assayed spectrophotometrically (Cary 50 Bio, Cary 100 Bio; Varian) at 405 nm and at 37 °C. The reactions were followed over 10 min. Assay buffer was 50 mM sodium phosphate buffer pH 6.5, 50 mM NaCl, 2 mM EDTA, and 0.01% Triton X-100. An enzyme stock solution of 375 µg/mL in 35 mM potassium phosphate, 35 mM sodium acetate pH 6.5, 2 mM DTT, 2 mM EDTA, and 50% ethylene glycol was diluted 1:200 with assay buffer containing 5 mM DTT and incubated for 30 min at 37 °C. Inhibitor stock solutions were prepared in DMSO. A 10 mM stock solution of the chromogenic substrate Z-Phe-Arg-pNA was prepared with DMSO. The final concentration of DMSO was 5%, and the final concentration of the substrate was 100 µM. Assays were performed with a final concentration of 94 ng/mL of cathepsin S. Into a cuvette containing 900 µL assay buffer, inhibitor solution and DMSO in a total volume of 40 µL, and 10 µL of the substrate solution were added and thoroughly mixed. The reaction was initiated by adding 50 µL of the cathepsin S solution.

Assay of Human Leukocyte Elastase²⁰

The in vitro enzyme inhibition assay against human leukocyte elastase was conducted by Prof. Michael Gütschow at the University of Bonn, Germany.

Human leukocyte elastase (Calbiochem, Darmstadt, Germany) was assayed spectrophotometrically (Cary 50 Bio, Varian) at 405 nm at 25°C. Assay buffer was 50 mM sodium phosphate buffer, 500 mM NaCl, pH 7.8. A stock solution of the chromogenic substrate MeOSuc-Ala-Ala-Pro-Val-*para*-nitroanilide was prepared in DMSO and diluted with assay buffer. The inhibitor stock solutions were prepared in DMSO. Final concentration of DMSO was 5.5%, the final concentration of the substrate was 100 µM. Assays were performed with a final HLE concentration of 50 ng mL⁻¹. An inhibitor solution (50 µL) and the substrate solution (50 µL) were added to a cuvette that contained

the assay buffer (850 μL), and the solution was thoroughly mixed. The reaction was initiated by adding the HLE solution (50 μL) and was followed over 10 min. IC₅₀ values were calculated from the linear steady-state turnover of the substrate. HLE inhibition was determined in duplicate experiments with five different inhibitor concentrations.

Assay of Bovine Trypsin²¹

The in vitro enzyme inhibition assay against human leukocyte elastase was conducted by Prof. Michael Gütschow at the University of Bonn, Germany.

Bovine trypsin (Sigma, Steinheim Germany) was assayed spectrophotometrically (Cary 50 Bio, Cary 100 Bio; Varian) at 405 nm and at 25 °C. Assay buffer was 20 mM Tris HCl buffer and 150 mM NaCl (pH 8.4). An enzyme stock solution of 10 $\mu\text{g}/\text{mL}$ was prepared in 1 mM HCl and diluted with assay buffer. A 40 mM stock solution of the chromogenic substrate Suc-Ala-Ala-Pro-Arg-pNA in DMSO was diluted with assay buffer. Final concentrations were as follows: substrate, 200 μM ; DMSO, 6%; trypsin, 12.5 $\mu\text{g}/\text{mL}$. Inhibitor solution (55 μL) and substrate solution (50 μL) were added to a cuvette containing 845 μL assay buffer and thoroughly mixed. The reaction was initiated by adding 50 μL of a trypsin solution.

5.4 Experimental Work Described in Chapter Four

Materials

Gelatin (Type A, 200 Bloom) was purchased from Fluka (Germany). PEGMA ($M_n = 8800 \text{ g}\cdot\text{mol}^{-1}$) was purchased from Polysciences, Inc. (Germany). Glycidyl methacrylate (GMA), *cis*-5-norbornene-*endo*-2,3-dicarboxylic acid (NBE-OH), Grubb's 1st generation (GI) catalyst, Grubb's 2nd generation (GII) catalyst, ethyl vinyl ether, and all other chemicals were purchased from Sigma Aldrich (Germany).

Materials Characterization

Thermal analysis was performed using the Gerätebau TGA 209 (Netzsch) thermogravimetric analyzer and Gerätebau DSC 204 F1 (Netzsch) differential scanning calorimeter.

Samples analyzed by mass spectrometry were dissolved in 1 mL of water containing 0.2% formic acid and subjected to ESI-Q-TOF analysis on a Micromass Q-TOF Ultima with a source temperature of 120 °C, desolvation temperature of 150 °C, and capillary voltage of 2.5 kV (positive ion mode).

Gelatin Functionalization

A 10 wt% solution of gelatin in pH 9.6 carbonate/bicarbonate buffer (50 mM: 1.59 g sodium carbonate and 2.93 g sodium bicarbonate in 1L water, pH 9.6) was stirred at 50 °C until complete dissolution (ca. 1 h). GMA (25 g, 0.18 mmol) was added and the solution stirred at 50 °C for 3 h. The product was precipitated in 5-fold volume excess ethanol, with gentle stirring, and soaked overnight for further extraction of unreacted GMA. The functionalized gelatin (gel-GMA) was cut into smaller pieces and dried at 50 °C under reduced pressure.

¹H NMR (500 MHz) spectra of functionalized gelatin was recorded on a Bruker Advance spectrometer (Karlsruhe, Germany) in D₂O. A 2,4,6-trinitrobenzenesulfonic (TNBS) colorimetric assay was performed to determine the degree of substitution of GMA.²² Samples of gel-GMA (11 mg, six replicates) were dissolved in 4% NaHCO₃ (1 mL, pH 8.5) at 40 °C for 10 min. Three replicates of each material were treated with 0.5% TNBS (1 mL) while the other three replicates were used as blanks, which were treated with 6N HCl (3 mL) before adding 0.5% TNBS (1 mL). The samples and blanks were heated at 40 °C for 4 h, prior to addition of 6N HCl (3 mL) and heating at 120 °C for 1h. Distilled water (5 mL) was added to the samples and blanks, washed with diethyl ether (15 mL) and the light absorbance at 346 nm for the samples and blanks were detected using Varian Cary 50 Bio UV-Visible Spectrophotometer (Agilent Technologies, Waldbronn, Germany).

Percentage Functionalization of Gelatin:

Batch 1: 2.2428×10^{-4} mol GMA/1 g of Gel-GMA

Batch 2: 1.861×10^{-4} mol GMA/1 g of Gel-GMA

Aqueous Metathesis Reaction***GI and GII Emulsion***

A 10 wt% solution of gel-GMA (2.54 g, 0.57 mmol) in aqueous phosphate buffer pH 7.4 (21.00 g) was stirred at 50 °C under nitrogen flow until complete dissolution (ca. 5 h). 1 wt% SDS (0.24 g) was added and stirred until dissolution at 50 °C under Argon (30 min). NBE-OH (varying amounts) was added and stirred at 50 °C under nitrogen atmosphere for a further 30 min. 1 wt% SDS (0.02 g) in aqueous phosphate buffer pH 7.4 (2.00 g) was added to a solution of 1 mol% of GI or GII in toluene (0.2 mL) and 1 wt% hexadecane and purged under nitrogen. The catalyst mixture was sonicated and cannula transferred under nitrogen into the reaction mixture. The solution became viscous within 3-10 min (depending on the amount of catalyst used). Ethyl vinyl ether (2 mL) was added and sonicated at room temperature for 30 min. The gel was washed with DCM (50 mL) and soaked in DCM (50 mL) for 1 h, before sequential washing with MeOH (100 mL) and water (100 mL). The gel was soaked in water (100 mL) over night (16 h), and dried in a 37 °C oven in a petri dish. The resulting gel was tested for crosslinking using the crosslinking analysis procedure.

HG2S (2 mol%)

A 10 wt% solution of gel-GMA (2.60 g, 0.58 mmol) in aqueous phosphate buffer pH 7.4 (22.50 g) was stirred at 50 °C under nitrogen flow until dissolution (ca. 5 h). NBE-OH (0.11g, 0.60 mmol) was added and stirred at 50°C under nitrogen atmosphere for a further 30 min. 1 mol% HG2-S (0.01 g, 0.012 mmol) in aqueous phosphate buffer pH 7.4 (3.50 g) was added to the reaction mixture, and stirred at 50 °C under nitrogen for 1 h. An additional 1 mol% HG2-S (0.01 g, 0.012 mmol) was added to the reaction mixture and stirred under nitrogen at 50 °C for 16 h. The reaction was quenched by addition of ethyl vinyl ether (4 mL) and stirred at room temperature for 30 min. 5 mL and 10 mL aliquots were transferred onto petri dish or foil dishes and dried at room temperature over night (16 h) in the fumehood. The resulting gel was tested for crosslinking using the crosslinking analysis procedure.

HG2S (5 mol%)

A 10 wt% solution of gel-GMA (3.03 g, 0.58 mmol) in aqueous phosphate buffer pH 7.4 (25.50 g) was stirred at 50°C under nitrogen flow until dissolution (ca. 5h). NBE-OH (0.11 g, 0.60 mmol) was added and stirred at 50°C under nitrogen atmosphere for a further 1.5 h. 5 mol% HG2-S (43 mg, 0.06 mmol) in aqueous phosphate buffer pH 7.4 (2.50 g) was transferred into the reaction mixture and stirred overnight (17 h) at 50 °C under nitrogen. Reaction was quenched with ethyl vinyl ether (4 mL) and sonicated at room temperature for 30 min. The gel was washed with DCM (50 mL) and soaked in DCM (50 mL) for 30 min, before extracting with MeOH (2 x 50 mL). The gel was sequentially soaked in MeOH (100 mL) for 30 min and water (100 mL) overnight (16 h), and dried in a 37 °C oven in a petri dish. The resulting gel was tested for crosslinking using the crosslinking analysis procedure.

Crosslinking Analysis

A dried sample of gel (ca. 100 mg) was added to water (25 mL) and heated at 50 °C for 5 h. The dissolution or non-dissolution of the sample was recorded.

Controls Reactions with GI***Gel-GMA-Catalyst Control***

A 10 wt% solution of gel-GMA (2.60 g, 0.58 mmol) in aqueous phosphate buffer pH 7.4 (22.50 g) was stirred at 50°C under nitrogen flow until dissolution (ca. 5 h). 1 wt % SDS (0.24 g) was added and stirred until dissolution at 50 °C under nitrogen atmosphere (30 min). 1 wt/v% SDS (0.02 g) in aqueous phosphate buffer pH 7.4 (2.00 g) was added to a solution of 1 mol% GI (0.01 g, 0.01 mmol) in toluene (0.2 mL) and 1 wt % (0.3 mL) hexadecane and purged under nitrogen. The catalyst mixture was sonicated and cannula transferred under nitrogen into the reaction mixture. Ethyl vinyl ether (2 mL) was added after 1 h and stirred at room temperature for 25 min. 10 mL aliquots were transferred onto petri dish and dried at room temperature over night (16 h) in the fumehood. The gel was washed with DCM (50 mL) and soaked in DCM (50 mL) for 1 h, before sequential washing with MeOH (100 mL) and water (100 mL). The gel was soaked in water (100 mL)

over night (16 h), and dried in a 37 °C oven in a petri dish. The resulting gel was tested for crosslinking using the crosslinking analysis procedure.

NBE-OH-Catalyst Control

NBE-OH (220 mg, 1.20 mmol) in aqueous phosphate buffer pH 7.4 (25.00 g) was stirred at 50 °C under nitrogen flow until dissolution (20 min). 1 wt/v% SDS (0.28g) was added and stirred until dissolution at 50 °C under nitrogen atmosphere (30 min). 1 wt % SDS (0.02 g) in aqueous phosphate buffer pH 7.4 (2.00 g) was added to a solution of 1 mol% GI (10 mg, 0.01 mmol) in toluene (0.2 mL) and 1 wt % hexadecane (0.3 mL) and purged under nitrogen. The catalyst mixture was sonicated and cannula transferred under nitrogen into the reaction mixture. The reaction was quenched with ethyl vinyl ether (2 mL) after 1 h and stirred at room temperature for 30 min, before extraction with diethyl ether (50 mL). The aqueous layer was lyophilized to obtain a fluffy white solid.

Gel-GMA-NBE-OH Control

A 10 wt% solution of gel-GMA (3.01 g, 0.58 mmol) in aqueous phosphate buffer pH 7.4 (27.20 g) was stirred at 50 °C under nitrogen flow until dissolution (ca. 5 h). NBE-OH (0.11 g, 0.60 mmol) was added and stirred at 50 °C under nitrogen overnight (17 h). 10 mL aliquots were transferred onto petri dish, dried at room temperature over night (16 h) in the fumehood and further dried in the a 37 °C oven. The resulting gel was tested for crosslinking using the crosslinking analysis procedure.

Film Formation

HG2-S (5 mol%)

A 10 wt% solution of gel-GMA (3.02 g, 0.56 mmol) in aqueous phosphate buffer pH 7.4 (25.90 g) was stirred at 50 °C under nitrogen flow until dissolution (ca. 5 h). NBE-OH (0.11 g, 0.60 mmol) was added and stirred at 50 °C under nitrogen for a further 1.5 h. 5 mol% HG2-S (42 mg, 0.06 mmol) in aqueous phosphate buffer pH 7.4 (1.60 g) was transferred into the reaction mixture and stirred at 50 °C under nitrogen for 1 h. An aliquot the solution (9 mL) was quickly transferred between two tightly sealed glass plates (10 cm x 10 cm), separated by a 1 mm Teflon spacer using a syringe. The remainder of the solution was transferred into a petri dish. The petri dish and glass plates were placed in a 50 °C oven for 72 h, before drying in a 37 °C oven. The film produced was soaked in ethyl

vinyl ether (30 min), washed and soaked in DCM (50 mL, 30 min), washed with MeOH (100 mL, 1 h) and soaked in H₂O (100 mL) overnight (16 h). The resulting film was tested for crosslinking using the crosslinking analysis procedure.

GI (1 mol%)

A 10 wt% solution of GMA-functionalized gelatin (3.06 g, 0.57 mmol) in aqueous phosphate buffer pH 7.4 (25.60 g) was stirred at 50 °C under nitrogen flow (ca. 4 h). 1 wt% SDS (0.28 g) was added and stirred at 50 °C under nitrogen (10 min). NBE-OH (0.11 g, 0.60 mmol) was added and stirred at 50 °C under nitrogen atmosphere for 1.5 h. 1 wt% SDS (0.02 g) in aqueous phosphate buffer pH 7.4 (2.00 g) was added to 1 mol% of GI (9.7 mg, 0.01 mmol) in toluene (0.2 mL) and 1 wt% hexadecane (0.3 mL) and purged under nitrogen. The catalyst mixture was sonicated and cannula transferred under nitrogen into the reaction mixture.

An aliquot of the solution (8 mL) was quickly transferred between two tightly sealed glass plates (10 cm x 10 cm), separated by a 1 mm Teflon spacer using a syringe. The remainder of the solution was poured into a petri dish. The petri dish and glass plates were placed in a 50 °C oven for 1 h, before drying in a 37 °C oven. The film produced was soaked in ethyl vinyl ether (30 min), washed and soaked in DCM (50 mL, 30 min), washed with MeOH (100 mL, 1 h) and soaked in H₂O (100 mL) overnight (16 h). The resulting film was tested for crosslinking using the crosslinking analysis procedure.

Mechanistic Model

A 10 wt% solution of PEGMA (4.98 g, 0.56 mmol) in aqueous phosphate buffer pH 7.4 (42.90 g) was added 1 wt% SDS (0.47 g) and stirred at 50 °C under nitrogen for 10 min. NBE-OH (0.11 g, 0.60 mmol) was added and stirred at 50 °C under nitrogen for a further 10 min. 1 wt% SDS (0.02 g) in aqueous phosphate buffer pH 7.4 (1.90 g) was added to 1 mol% GI (9.6 mg, 0.01 mmol) in toluene (0.2 mL) and 1 wt% hexadecane (0.3 mL) and purged under nitrogen. The catalyst mixture was sonicated and cannula transferred under nitrogen into the reaction mixture. The reaction was quenched with ethyl vinyl ether (2 mL) for 1 h and stirred at room temperature for 30 min. The mixture was extracted with DCM (3 x 50 mL). The aqueous phase was lyophilized to obtain fluffy white solid and subjected to analysis by MALDI (MS).

5.5 References for Chapter Five

- [1] OEChem, version 1.7.4, OpenEye Scientific Software, Inc., Santa Fe, NM, USA, www.eyesopen.com, **2010**.
- [2] Cuerrier, D.; Moldoveanu, T.; Inoue, J.; Davies, P. L.; Campbell, R. L. *Biochemistry* **2006**, *45*, 7446-7452.
- [3] Wallace, D. M.; Leung, S. H.; Senge, M. O.; Smith, K. M. *J. Org. Chem.* **1993**, *58*, 7245–7257.
- [4] Garrido, D. O. A.; Buldain, G.; Ojea, M. I.; Frydman, B. *J. Org. Chem.* **1988**, *53*, 403–407.
- [5] Bose, D. S.; Narsaiah, A. V. *Bioorg. Med. Chem.* **2005**, *13*, 627–630.
- [6] Xia, Y.; Li, Q. X.; Gong, S.; Li, Y.; Cao, Y.; Liu, X.; Li, J. *Food Chem* **2010**, *120*, 1178–1184.
- [7] Bressy, C.; Piva, O. *Synlett* **2003**, 87–90.
- [8] Breukelman, S. P.; Meakins, G. D.; Roe, A. M. *J. Chem. Soc., Perkin Trans. 1* **1985**, 1627–1635.
- [9] Stoessl, A. *Tetrahedron Lett.* **1966**, *7*, 2287–2292.
- [10] Kaul, R.; Surprenant, S.; Lubell, W. D. *J. Org. Chem.* **2005**, *70*, 3838–3844.
- [11] Mullen, D. G.; Desai, A. M.; Waddell, J. N.; Cheng, X.-M.; Kelly, C. V.; McNerny, D. Q.; Majoros, I. J.; Baker, J. R. J.; Sander, L. M.; Orr, B. G.; Holl, M. M. B. *Bioconjug. Chem.* **2008**, *19*, 1748–1752.
- [12] Mullen, D. G.; McNerny, D. Q.; Desai, A.; Cheng, X.-M.; Dimaggio, S. C.; Kotlyar, A.; Zhong, Y.; Qin, S.; Kelly, C. V.; Thomas, T. P.; Majoros, I.; Orr, B. G.; Baker, J. R.; Banaszak Holl, M. M. *Bioconjug. Chem.* **2011**, *22*, 679–689.
- [13] Yan, R. B.; Yang, F.; Wu, Y. F.; Zhang, L. H.; Ye, X. S. *Tetrahedron Lett.* **2005**, *46*, 8993–8995.
- [14] Thompson, V. F.; Saldaña, S.; Cong, J.; Goll, D. E. *Anal. Biochem.* **2000**, *279*, 170–178.
- [15] Morrison, J. F. *Trends Biochem. Sci.* **1982**, *7*, 102-105.
- [16] GraphPad Prism version 5.02 for Windows, GraphPad Software, San Diego California USA, www.graphpad.com.
- [17] Liljelblad, A.; Kanerva, L. T. *Tetrahedron* **2006**, *62*, 5831–5854.
- [18] Dixon, M. *Biochem. J.* **1953**, *55*, 170.

- [19] Frizler, M.; Lohr, F.; Lülldorff, M.; Gütschow, M. *Chem. Eur. J.* **2011**, *17*, 11419–11423.
- [20] Gütschow, M.; Pietsch, M.; Themann, A.; Fahrig, J.; Schulze, B. *J. Enz. Inhib. Med. Chem.* **2005**, *20*, 341–347.
- [21] Sisay, M. T.; Hautmann, S.; Mehner, C.; König, G. M.; Bajorath, J.; Gütschow, M. *ChemMedChem* **2009**, *4*, 1425–1429.
- [22] Bubnis, W. A.; Ofner, C. M. *Anal. Biochem.* **1992**, *207*, 129–133.

APPENDIX

Appendix A1: Raw Data for Molecular Modelling

Table A1: Docking results and parameters for **2.10**, **2.12**, **2.14**, **2.16**, **2.19** and **2.20**.

Comp.	Grid	No. poses with WHD < 4.5 ^a	Most Representative Pose		
			H-bonds ^{b,c}	WHD ^a	<i>Emodel</i> ^d
2.10	o-CAPN1	17	A,B,C,Ser ₂₅₁	3.96	-53.70
	o-CAPN2	11	B,C	4.33	-54.86
2.12	o-CAPN1	6	A,B,C	3.28	-45.24
	o-CAPN2	4	A,B,C	3.61	-43.10
2.14	o-CAPN1	2	A,B,C,Ser ₂₅₁	3.77	-59.01
	o-CAPN2	4	B,C,Ser ₂₄₁	3.59	-51.06
2.16	o-CAPN1	4	B,C	3.80	-46.96
	o-CAPN2	4	A,B,C,Ser ₂₅₀	3.56	-47.30
2.19	o-CAPN1	3	Gly ₂₀₈	3.48	-43.48
	o-CAPN2	4	A,B,C,Ser ₂₄₁	3.92	-66.56
2.20	o-CAPN1	4	B,C	3.31	-51.33
	o-CAPN2	6	A,B,C	3.60	-45.58

^a Warhead distance (WHD) is the distance between the carbonyl carbon of the aldehyde and the active site cysteine sulfur in Å

^b Hydrogen bonds from the carbonyl group of Gly₂₀₈, the NH group of Gly₂₀₈ and the carbonyl group of Gly₂₇₁ of the Ovine I homology model are labelled A, B and C, respectively.

^c The analogous hydrogen bonds from the carbonyl group of Gly₁₉₈, the NH group of Gly₁₉₈ and the carbonyl group of Gly₂₆₁ of the Ovine II homology model are also labelled A, B and C, respectively.

^d GLIDE Emodel combines the energy grid score, the binding affinity predicted by the GlideScore, and the internal strain energy of the ligand for the model potential used to direct the conformational-search algorithm.

Appendix A2: Raw Assay Data and IC₅₀ Calculation Example for Calpain Assay

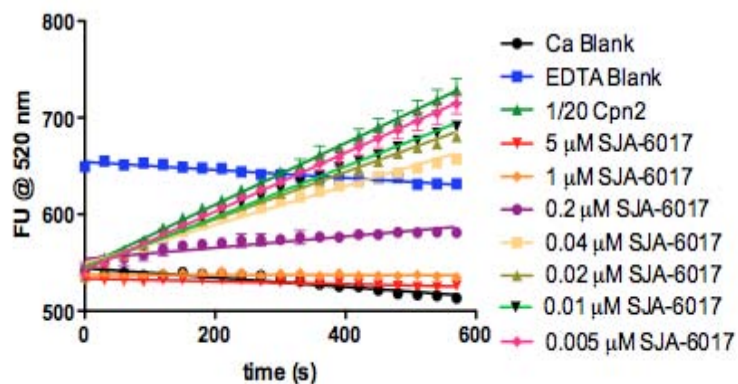
The data in Table A2 was collected for one assay run for SJA6017. Rows 1-3 correspond to the calcium blank; 4-6 EDTA Blank; 7-9 m-calpain; 10-12 SJA6017 at 5 μ M; 13-15 SJA6017 at 1 μ M; 16-18 SJA6017 at 0.2 μ M; 19-21 SJA6017 at 0.04 μ M; 22-24 SJA6017 at 0.02 μ M; 25-27 SJA6017 at 0.01 μ M; 28-30 SJA6017 at 0.005 μ M. The columns correspond to the amount of fluorescence (in fluorescence units) recorded at 30 s intervals for a total of 10 min. The fluorescence over time for the blanks and inhibitor concentration was plotted and analysed using GraphPad Prism version 5.02 for Windows {GraphPad Software, San Diego California USA, www.graphpad.com} (Figure A1).

time (s)	0	30	60	90	120	150	180	210	240	270	300	330	360	390	420	450	480	510	540	570
Ca Blank	540	534	538	536	534	537	538	534	535	534	529	529	527	521	523	518	514	513	514	510
	537	540	543	538	537	543	538	540	537	539	536	529	529	529	525	524	521	518	516	515
	542	540	538	536	539	540	539	541	539	537	536	535	527	526	527	522	519	519	517	515
EDTA Blank	651	651	649	650	652	647	648	641	640	640	639	637	636	637	634	636	634	627	629	631
	647	658	653	655	650	648	647	649	644	640	640	638	640	637	635	640	640	630	635	634
	650	656	599	654	653	652	649	652	648	644	644	643	639	635	636	637	640	636	631	630
m-calpain (calpain 2)	543	559	565	575	589	600	607	619	628	639	650	656	671	674	687	699	707	717	728	740
	541	556	564	573	586	596	609	613	628	632	643	652	661	669	682	690	696	709	720	729
	540	550	560	572	584	594	604	613	621	629	639	643	652	663	671	681	686	696	706	715
SJA 5 μM	535	534	534	534	531	532	533	534	534	530	530	530	527	530	531	528	526	528	525	529
	528	528	525	526	533	531	530	530	530	529	529	527	527	526	528	526	522	522	521	525

	534	534	534	532	532	534	534	533	533	533	530	528	531	531	526	526	528	523	527	525
SJA 1 μM	534	535	534	536	539	539	538	542	538	536	539	538	538	539	536	534	535	538	535	533
	533	538	533	537	538	538	539	540	540	535	540	541	535	538	538	535	536	537	535	535
	537	536	536	535	539	540	540	541	540	538	537	539	536	540	535	540	537	537	537	537
SJA 0.2 μM	540	548	548	553	559	563	564	567	569	570	571	569	455	573	576	575	575	576	576	576
	539	544	551	557	561	567	568	568	569	570	571	576	573	576	579	578	584	581	582	581
	551	557	563	565	571	572	575	576	581	581	580	583	580	580	582	584	585	586	587	586
SJA 0.04 μM	539	549	555	564	579	584	591	598	604	609	615	620	624	633	637	640	645	651	658	659
	538	547	562	568	579	584	592	600	602	609	615	619	625	629	635	641	644	648	654	657
	538	547	556	566	574	579	586	597	601	602	613	615	623	626	628	636	640	644	648	655
SJA 0.02 μM	532	544	556	566	578	583	590	598	606	613	620	626	630	638	642	651	661	669	667	677
	538	549	561	572	579	591	597	604	611	619	623	635	641	647	650	656	664	669	677	683
	538	546	557	569	578	588	595	603	613	619	623	634	635	642	648	657	664	669	675	681
SJA 0.01 μM	540	548	556	570	580	586	596	605	612	619	626	630	642	647	656	661	671	677	686	690
	536	548	557	568	580	585	597	602	613	620	627	634	639	650	658	663	671	677	684	692
	535	547	557	565	578	583	596	602	611	614	624	636	638	648	653	659	667	674	681	691
SJA 0.005 μM	535	548	559	570	584	591	601	606	616	624	631	640	648	656	667	673	681	690	696	710
	539	547	557	568	580	589	599	606	615	624	631	641	648	652	662	673	683	691	699	707
	539	549	556	570	582	590	601	611	624	628	639	648	661	668	679	690	698	707	718	726

Table A2 Raw calpain inhibition assay data for SJA6017.

Inhibition of Calpain 2 by SJA-6017 (MOPS substrate buffer)



**Inhibition of Calpain 2 by SJA-6017 (MOPS substrate buffer):
steady state of slow-binding inhibitor
(linear fit: 390-570 s)**

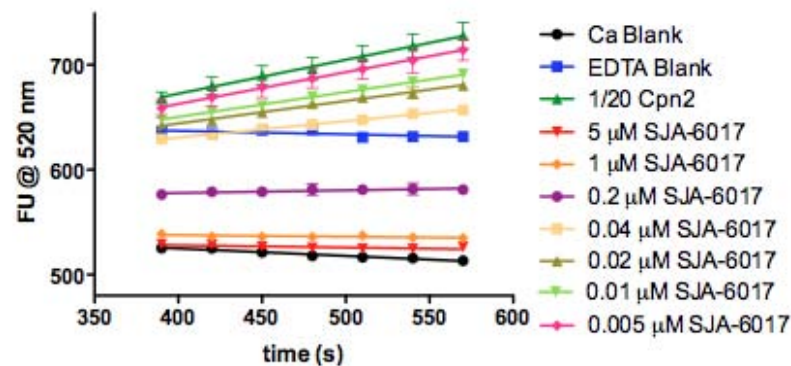


Figure A1 Graph of a the calpain inhibition assay for SJA6017

The average enzyme activity was obtained from the slope of the linear regression over data points 390-570 s (corresponding to the steady state rate of slow binding inhibition); and the corrected enzyme activity average values were obtained using **equation A1** for the inhibitor samples or using **equation A2** for the uninhibited enzyme, which represent the baseline corrected fluorescence.

$$FU_{\text{avg. inhibitor}} = FU_{\text{avg. sample}} - (FU_{\text{Ca blank}} + FU_{\text{EDTA blank}})/2$$

Equation A1

$$FU_{\text{uninhibited}} = FU_{\text{enzyme}} - (A_{\text{Ca blank}} + A_{\text{EDTA blank}})/2$$

Equation A2

Where FU corresponds to the change in fluorescence over 390-570 s.

The corrected enzyme activity in the absence of inhibitor (m-calpain) was set to 100%. Enzyme activities in the presence of inhibitors were calculated in relation to the activity in the absence of inhibitor using **equation A3**:

$$\% \text{ Inhibition} = [(FU_{\text{avg. Inhibitor}} - FU_{\text{uninhibited}}) / FU_{\text{uninhibited}}] \times 100$$

Equation A3

	Average (FU/s)	Std. error (FU/s)	Corrected average (FU/s)	Inhibition (FU/min)	Inhibition (%)
Ca Blank	-0.07063	0.006117			
EDTA Blank	-0.03254	0.01478			
m-calpain	0.323	0.00807	0.3746	22.4751	100.00
SJA-6017 5 μM	-0.02183	0.008076	0.0298	1.7853	7.94
SJA-6017 1 μM	-0.01468	0.006145	0.0369	2.2143	9.85
SJA-6017 0.2 μM	0.0254	0.006716	0.0770	4.6191	20.55
SJA-6017 0.04 μM	0.1567	0.00313	0.2083	12.4971	55.60
SJA-6017 0.02 μM	0.2155	0.008531	0.2671	16.0251	71.30
SJA-6017 0.01 μM	0.2369	0.004314	0.2885	17.3091	77.01
SJA-6017 0.005 μM	0.3028	0.004705	0.3544	21.2631	94.61

Table A3 Calculations for SJA6017

The average values of percentage inhibition obtained in two separate experiments, each in triplicate, were plotted against the inhibitor concentration (logarithmic scale, value for [I] = 0 is not depicted), and analysed using **equation A4** to obtain the IC₅₀ value (Figure A2).

$$v_i = \frac{v_0}{1 + \frac{[I]}{IC_{50}}} \quad \text{Equation A4}$$

Where [I] is the inhibitor concentration, and v_0 and v are the percentage enzyme activities in the absence and presence of inhibitor.

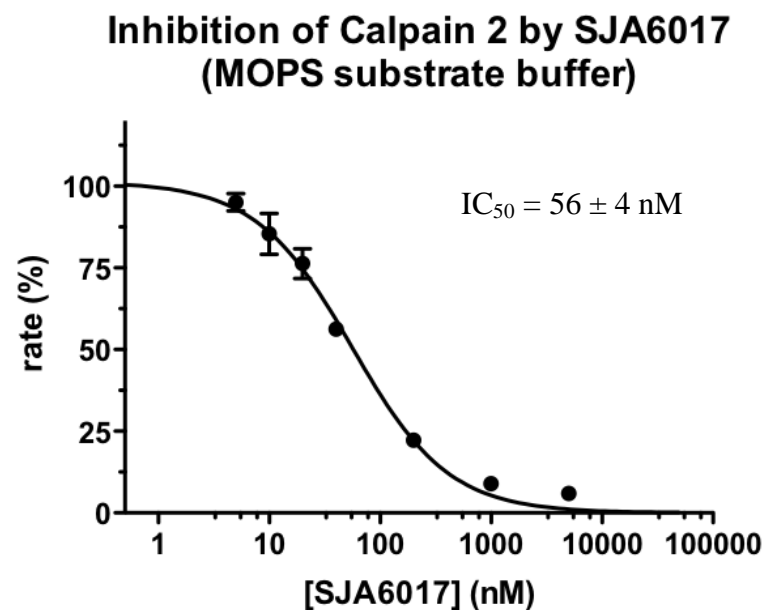


Figure A2 IC₅₀ analysis for SJA6017

Appendix A3: Raw Assay Data and K_i Calculation Example for α -Chymotrypsin Assay

The data in Table A4 are the slopes obtained from three assay runs for inhibitor **2.86** at two different substrate concentrations. The slope values are the raw data, as given by the Varian Cary 5000 UV-VIS-NIR spectrophotometer, after automatic analysis over 6 min at zero order. The columns correspond to the rates of substrate hydrolysis over 6 minutes in the absence of inhibitor (row 1) and in the presence of 5 different inhibitor concentrations (rows 2-6). The rates in the absence of inhibitor, v_0 , and the rates in the presence of inhibitor, v_i , were used for the determination of IC_{50} and K_i .

Table A4 Raw data for the α -chymotrypsin inhibition assay data of macrocyclic inhibitor **2.86**.

50 μM Suc-Ala-Ala-Pro-Phe-PNA				20 μM Suc-Ala-Ala-Pro-Phe-PNA			
	Run 1, v_i	Run 2, v_i	Run 3, v_i		Run 1, v_i	Run 2, v_i	Run 3, v_i
no inhibitor, v_0	0.0053	0.0049	0.005	no inhibitor, v_0	0.0026	0.0023	0.0029
0.6 μ M 2.86	0.0016	0.0019	0.0014	0.6 μ M 2.86	0.0005	0.0005	0.0003
0.3 μ M 2.86	0.0026	0.0029	0.0024	0.3 μ M 2.86	0.001	0.0009	0.0009
0.15 μ M 2.86	0.0033	0.0039	0.003	0.15 μ M 2.86	0.0016	0.0012	0.0012
0.075 μ M 2.86	0.0045	0.0049	0.0039	0.075 μ M 2.86	0.0017	0.0017	0.0021
0.0375 μ M 2.86	0.0045	0.0052	0.0045	0.0375 μ M 2.86	0.0025	0.0022	0.0028

The IC_{50} for inhibitor **2.86** was determined graphically using GraphPad Prism version 5.02 for Windows {GraphPad Software, San Diego California USA, www.graphpad.com} at two substrate concentration (50 mM and 20 mM) were determined using **equation A4**. By rearranging **equation A4** to obtain **equation A5**, the IC_{50} for **2.86** was obtained from the reciprocal of the slope, $\frac{1}{IC_{50}}$, by plotting $\frac{v_0}{v_i}$ against inhibitor concentration, [I] (Figure A3).

$$v_i = \frac{v_0}{\left(1 + \frac{[I]}{IC_{50}}\right)} \quad \text{Equation A4}$$

$$\frac{v_0}{v_i} = \frac{1}{IC_{50}}[I] + 1 \quad \text{Equation A5}$$

where v_0 and v_i are the rates in the absence and presence of inhibitor, and [I] is the inhibitor concentration.

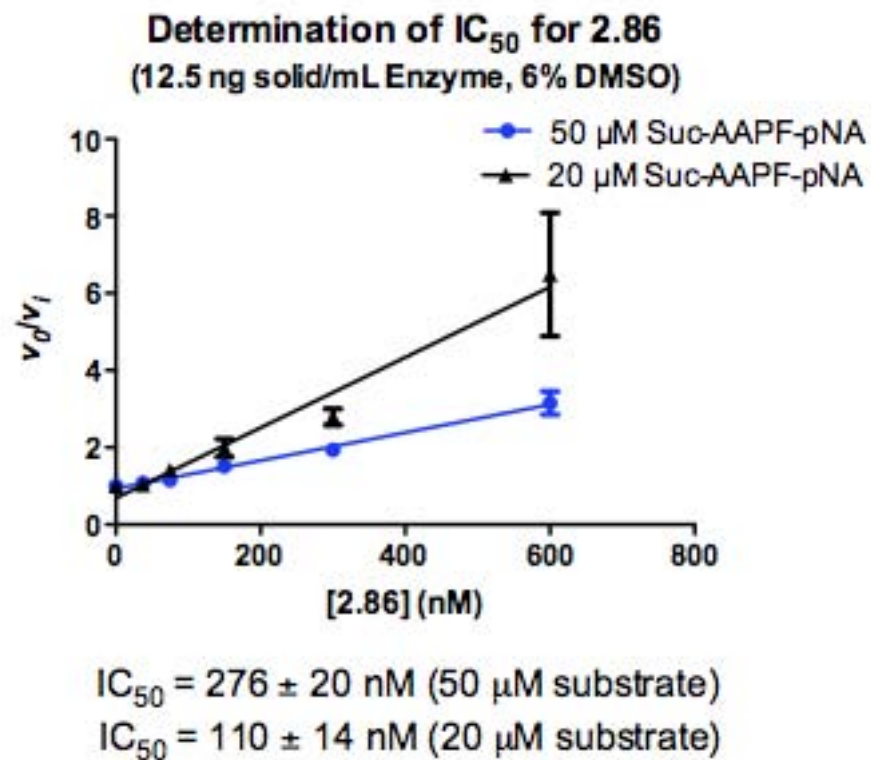


Figure A3 IC₅₀ determination for **2.86** at 50 mM and 20 mM substrate.

The inhibition constant, K_i , for inhibitor **2.86** was determined graphically using the Dixon plot {Dixon, M. *Biochem. J.* **1974**, 137, 143}. The Dixon plot is derived from the Michaelis-Menton equation (**equation A6**), which relates the rate of reaction, v_0 to the concentration of inhibitor, [I]. This equation can be transformed to the Lineweaver-Burk equation (**equation A7**) to obtain a linear plot, by plotting the inverse of the relative

rates, $\frac{1}{v_i}$, against inhibitor concentration, [I], at a constant substrate concentration, [S]. The intersect of the two lines determined at 50 mM and 20 mM substrate concentration intersects at $-K_i$ (Figure A4).

$$v_i = \frac{V_{\max} [S]}{[S] + K_m \left(1 + \frac{[I]}{K_i} \right)} \quad \text{Equation A6}$$

$$\frac{1}{v_i} = \frac{[S] + K_m}{V_{\max} [S]} + \frac{K_m}{V_{\max} [S] K_i} [I] \quad \text{Equation A7}$$

where v_i is the rate, K_m is the Michaelis constant, and [I] is the inhibitor concentration.

Dixon Plot for 2.86 (To determine K_i)
(12.5 ng solid/mL Enzyme, 6% DMSO)

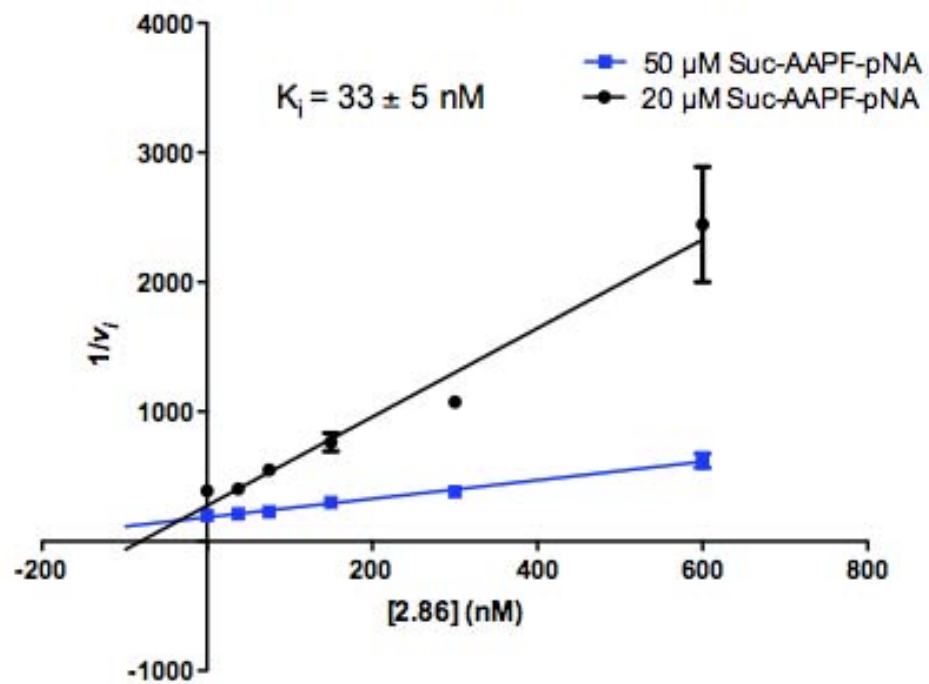
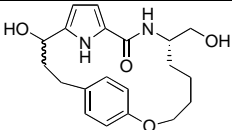
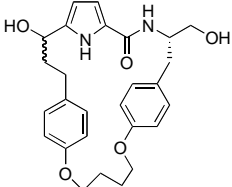
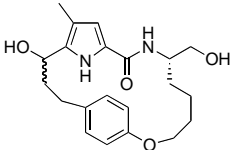
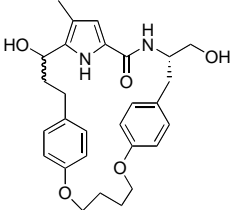
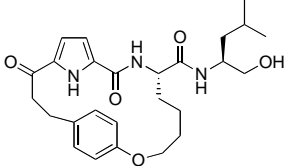
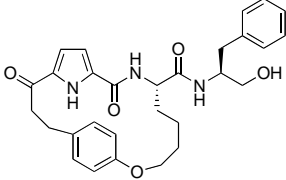
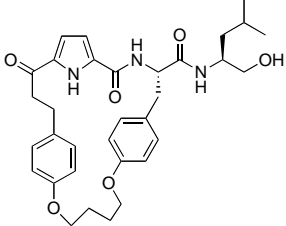


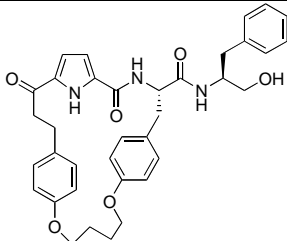
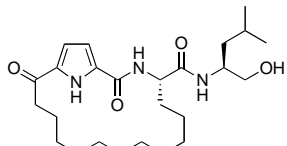
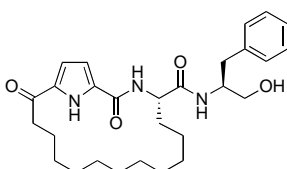
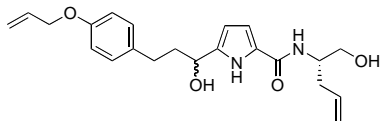
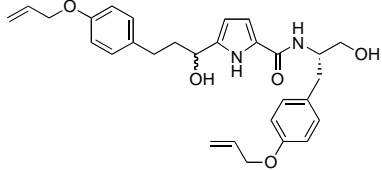
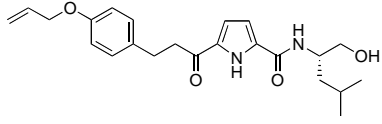
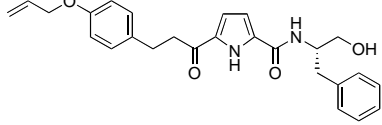
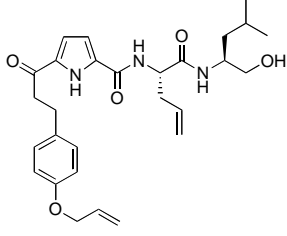
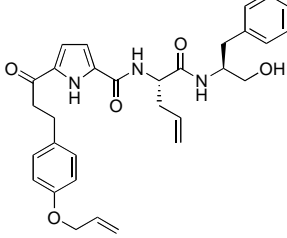
Figure A4 K_i determination for 2.86 using the Dixon plot.

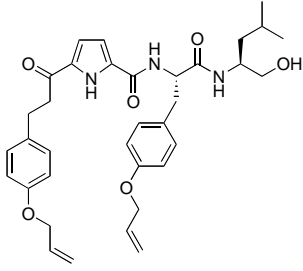
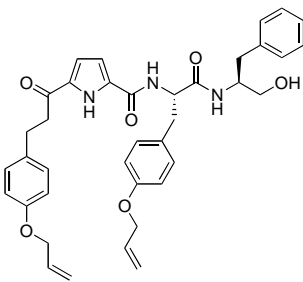
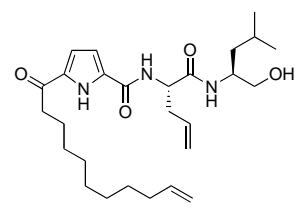
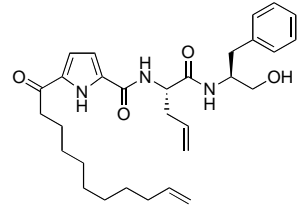
Appendix A4: Percentage Inhibition of Alcohols Synthesized in Chapter 2

Table A5 below outlines all the alcohols compounds assayed against m-calpain and α -chymotrypsin using the assay protocols in Chapter Three. Values given are the percentage inhibition for each compound at their highest possible concentration.

Table A5 Percentage inhibition of alcohols against m-calpain and α -chymotrypsin.

Compound	% Inhibition	
	m-calpain (CAPN2)	α -chymotrypsin
2.78 	0% @ 50 mM	0% @ 250 mM
2.79 	0% @ 50 mM	0% @ 250 mM
2.80 	0% @ 50 mM	0% @ 250 mM
2.81 	0% @ 50 mM	0% @ 250 mM
2.85 	0% @ 50 mM	0% @ 50 mM
2.86 	10% @ 50 mM	0% @ 125 mM
2.87 	10% @ 25 mM	0% @ 125 mM

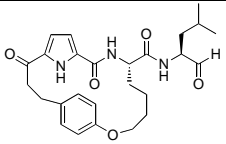
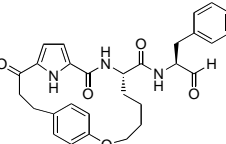
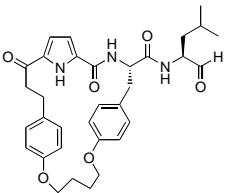
Compound	% Inhibition	
	m-calpain (CAPN2)	α -chymotrypsin
2.88 	12% @ 25 mM	0% @ 50 mM
2.89 	0% @ 25 mM	25% @ 50 mM
2.90 	10% @ 25 mM	0% @ 125 mM
2.122 	0% @ 50 mM	0% @ 50 mM
2.123 	0% @ 50 mM	0% @ 250 mM
2.127 	0% @ 25 mM	0% @ 125 mM
2.128 	0% @ 10 mM	0% @ 50 mM
2.129 	6% @ 25 mM	0% @ 50 mM
2.130 	17% @ 25 mM	0% @ 50 mM

Compound	% Inhibition	
	m-calpain (CAPN2)	α -chymotrypsin
2.131 	43% @ 50 mM	0% @ 50 mM
2.132 	26% @ 25 mM	0% @ 25 mM
2.133 	0% @ 50 mM	25% @ 125 mM
2.134 	0% @ 10 mM	0% @ 25 mM

Appendix A5: Enzyme Assays Data

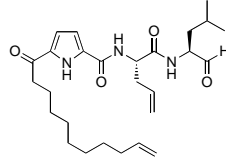
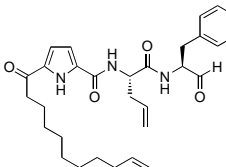
Table A6 below outlines assay data for all the aldehyde compounds assayed against cysteine proteases and serine proteases using the assay protocols in Chapter Three.

Table A6 Enzyme inhibition assay data for aldehyde compounds.

Compound	Cysteine Protease (IC ₅₀ (μM))				Serine Protease (IC ₅₀ (μM))		
	Ovine μ-calpain (CAPN1) ^a	Ovine m-calpain (CAPN2) ^a	Human Cathepsin L ^c	Human Cathepsin S ^g	Bovine α-Chymotrypsin (K _i (μM)) ⁱ	Human Leukocyte Elastase ^l	Bovine Trypsin
2.21 	0.324 ± 0.08	0.249 ± 0.05	0.0470 ± 0.0012	0.0217 ± 0.0043	37% residual activity @ 125 μM ^j	n.i. @ 10 μM ^m	n.i. @ 10 μM ^m
2.22 	n.d. ^b	0.153 ± 0.02	n.d. ^e	n.d. ^e	0.431 ± 0.0028	n.i. @ 10 μM ^m	n.i. @ 10 μM ^m
2.23 	n.d. ^b	0.203 ± 0.04	0.0207 ± 0.0023	0.00137 ± 0.00015	1.917 ± 0.167	1.82 ± 0.43	n.i. @ 10 μM ^m

Compound	Cysteine Protease (IC ₅₀ (μM))				Serine Protease (IC ₅₀ (μM))		
	Ovine μ-calpain (CAPN1) ^a	Ovine m-calpain (CAPN2) ^a	Human Cathepsin L ^c	Human Cathepsin S ^g	Bovine α-Chymotrypsin (K _i (μM)) ⁱ	Human Leukocyte Elastase ^l	Bovine Trypsin
2.24	n.d. ^b	0.246 ± 0.06	0.206 ± 0.014	0.0066 ± 0.0019	0.033 ± 0.005	1.72 ± 0.68	n.i. @ 10 μM ^m
2.25	0.042 ± 0.005	0.066 ± 0.008	0.00300 ± 0.00036d	0.00171 ± 0.00035	34% residual activity @ 50 μM ^j	52.6% residual activity @ 10 μM ^f	n.i. @ 10 μM ^m
2.26	n.d. ^b	0.156 ± 0.027	0.0115 ± 0.0018d	0.00169 ± 0.00033	2.525 ± 0.248	54.6% residual activity @ 10 μM ^f	n.i. @ 10 μM ^m
2.114	n.d. ^b	3.11 ± 0.5	IC ₅₀ > 100 μM @ 10 μM ^f	5.6h	n.i. @ 125 μM ^k	54.4% residual activity @ 10 μM ^f	n.i. @ 10 μM ^m
2.115	n.d. ^b	8.9 ± 0.5	IC ₅₀ > 300 μM @ 10 μM ^f	14h	n.i. @ 50 μM ^k	82.1% residual activity @ 5 μM ^f	n.i. @ 10 μM ^m

Compound	Cysteine Protease (IC ₅₀ (μM))				Serine Protease (IC ₅₀ (μM))		
	Ovine μ-calpain (CAPN1) ^a	Ovine m-calpain (CAPN2) ^a	Human Cathepsin L ^c	Human Cathepsin S ^g	Bovine α-Chymotrypsin (K _i (μM)) ⁱ	Human Leukocyte Elastase ^l	Bovine Trypsin
	2.116	n.d. ^b	0.067 ± 0.005	0.0931 ± 0.0008	0.00185 ± 0.00015	0.939 ± 0.19	0.859 ± 0.432
2.117	n.d. ^b	0.823 ± 0.28	1.72 ± 0.13	0.0563 ± 0.00203	0.056 ± 0.015	1.46 ± 0.40	n.i. @ 10 μM ^m
2.118	n.d. ^b	7.76 ± 1.08	0.0115 ± 0.0018d	0.00141 ± 0.00028	n.i. @ 50 μM ^k	0.465 ± 0.154	n.i. @ 10 μM ^m
2.119	n.d. ^b	1.3 ± 0.2	0.366 ± 0.05d	0.0214 ± 0.00198	0.688 ± 0.08	0.524 ± 0.030	n.i. @ 10 μM ^m

Compound	Cysteine Protease (IC ₅₀ (μM))				Serine Protease (IC ₅₀ (μM))		
	Ovine μ-calpain (CAPN1) ^a	Ovine m-calpain (CAPN2) ^a	Human Cathepsin L ^c	Human Cathepsin S ^g	Bovine α-Chymotrypsin (K _i (μM)) ⁱ	Human Leukocyte Elastase ^l	Bovine Trypsin
2.120 	0.055 ± 0.011	0.04 ± 0.006	0.921 ± 0.072	0.0105 ± 0.0008	40% residual activity @ 25 μM ^j	0.148 ± 0.029	n.i. @ 10 μM ^m
2.121 	n.d. ^b	0.072 ± 0.014	1.39 ± 0.07	0.176 ± 0.038	2.474 ± 0.118	0.520 ± 0.206	n.i. @ 10 μM ^m

^a Triplicate measurement @ seven inhibitor concentration

^b Not determined due to insufficient enzyme for assay

^c Duplicate measurements @ 2 days @ five inhibitor concentrations, the first 10 min of the progress curves were analysed

^d Progress curve analysed between 2 and 10 min.

^e Not determined due to insufficient compound for assay

^f Quadruplicate measurement @ single inhibitor concentration

^g Single measurements @ 2 days @ five inhibitor concentrations, the first 10 min of the progress curves were analysed

^h Duplicate measurement @ single inhibitor concentration

ⁱ Triplicate measurement @ five inhibitor concentration at 20 and 50 μM substrate concentrations.

^j Triplicate measurement @ single inhibitor concentration, 50 μM substrate concentration.

^k No inhibition; > 80% residual activity; triplicate measurement

^l Duplicate measurement @ five inhibitor concentration

^m No inhibition; > 80% residual activity; duplicate measurement